STRUCTURAL ASSOCIATIONS OF SYMPTOMATIC KNEE OSTEOARTHRITIS

Laura Angela Wyatt (Stoppiello), BSc. (Hons)

Thesis submitted to the University Of Nottingham for the degree of Doctor of Philosophy

December 2015

ABSTRACT

Background: Osteoarthritis (OA) is a major source of pain and disability. Pain is the major symptom of OA, and is usually the reason why patients seek medical assistance. However, the link between OA knee pain and structural change is incompletely understood. Furthermore, the earliest pathological changes in an osteoarthritic joint are difficult to characterise as structural pathology may develop in the absence of symptoms, which limits investigation into the earliest changes of preclinical knee OA.

Aim and objectives: The major aim of this thesis was to better understand the role of knee joint pathology in OA pain. Further objectives were to determine the earliest features of knee OA and to classify subgroups of patients based on histological characteristics. This thesis also describes method development and validation for histopathological assessment of OA changes in the joint.

Hypothesis: Specific pathological, biochemical and molecular changes within the OA knee contribute to OA pain, whereas other changes may be coincidental or even protective.

Methods: Medial tibial plateaux and synovium samples were obtained at the time of total knee replacement (TKR) surgery for OA, or obtained post-mortem (PM). To identify features associated with symptoms, tissue was compared from 29 patients undergoing TKR for OA pain (symptomatic chondropathy) and from 29 PM cases with similar severity of chondropathy who did not report symptoms during the last year of life (asymptomatic chondropathy). Immunohistochemical and microarray techniques were employed to determine molecular changes in synovium that are associated with OA knee pain.

To determine early features of OA, PM cases were classified as non-arthritic controls based on history and macroscopic examination of joint surfaces. The remaining PM cases were classified as early OA. Histological severity scores for cartilage pathology, subchondral bone marrow replacement and synovial inflammation (synovitis) were compared between non-arthritic controls (n=48),

early OA (n=295) and TKR (end-stage OA, n=143) cases. Latent class analysis classified subgroups of PM and TKR cases based on histopathological criteria.

Results: Symptomatic OA was associated with synovitis, increase in synovial nerve growth factor (NGF), loss of cartilage surface integrity and chondrocyte changes (all $P< 0.05$ for each comparison). Microarray analysis of the synovium revealed an up-regulation of various inflammatory mediators (including monocyte chemoattractant protein-1 [increased 1.65 fold, $P =0.013$]) in the symptomatic chondropathy group, which may explain an association between synovitis and pain.

Tidemark breaching was more common in early knee OA compared to non-arthritic controls (55% vs. 30%, $P <0.05$), whereas synovitis and subchondral bone marrow replacement were more common in end-stage OA compared to early OA cases (67% vs. 18% and 42% vs. 16% respectively, $P<0.01$). Latent class analysis identified a subgroup of people with mild chondropathy and absence of synovitis, and for 2 subgroups with established chondropathy distinguished by the severity of synovitis.

Discussion: In support of the hypothesis, a range of histopathological features in the medial tibial plateaux and synovium were associated with OA, but not all features were associated with symptoms. Symptomatic OA was associated with histological synovitis. Within the synovium, up-regulation of pro-nociceptive molecules such as NGF and chemokines might mediate the association between synovitis and pain. Furthermore, the severity of synovitis defines subgroups of patients with established chondropathy. Different pathologic features of OA typically coincide, and better understanding of the structural features that are associated with symptomatic OA may help develop structure-modifying treatments (disease-modifying OA drugs) by focusing on those which are most likely to improve symptoms.

DECLARATION

This is to certify that the work submitted in this thesis is the result of original research. The work presented has been conducted by myself unless otherwise stated.

All tissue biopsy samples were processed on site at King's Mill Hospital by an experienced research technician, Roger Hill. Articular surfaces of the medial and lateral tibial plateaux and femoral condyles were macroscopically scored by Roger Hill. Deborah Wilson compiled the clinical database for the tissue repository, and obtained patient consent for tissue donations. Supervision of this thesis was undertaken by Professor David Walsh and Professor Brigitte Scammell.

PUBLICATIONS

- Stoppiello LA, Mapp PI, Wilson D, Hill R, Scammell BE, Walsh DA. Structural associations of symptomatic knee osteoarthritis. Arthritis Rheumatol. 2014;66(11):3018-3027.

- Stoppiello LA, Doherty M, Morphological aspects of pathology. Oxford textbook of Osteoarthritis and crystal anthropology 3e (in press).

- Stoppiello LA, Moreton BJ, Mapp PI, Wilson D, Hill R, Ferguson E, Scammell BE, Walsh DA. Histological subgroups in knee osteoarthritis (in preparation).

- Stoppiello LA, Mapp PI, Wilson D, Hill R, Bennett A, Scammell BE, Walsh DA. Gene expression patterns in the synovium and their association with symptomatic knee osteoarthritis (in preparation).

PRESENTATIONS

ORAL

- Stoppiello LA, Mapp PI, Wilson D, Hill R, Scammell BE, Walsh DA. Increased synovial nerve growth factor in the synovium of people with painful knee osteoarthritis. The European League Against Rheumatism (EULAR) congress, Madrid, Spain 2013. Ann Rheum Dis, 72, supplement 3. 153-153.

- Stoppiello LA, Mapp PI, Wilson D, Hill R, Scammell BE, Walsh DA. Structural associations of pain in human knee osteoarthritis. Lunchtime seminar. Division of Rheumatology, Orthopaedics and Dermatology, University of Nottingham, 2013.

POSTER

- Stoppiello LA, Moreton BJ, Mapp PI, Wilson D, Hill R, Ferguson E, Scammell BE, Walsh DA. Histopathological classification of osteoarthritis as a multi-tissue disease. World Congress of the Osteoarthritis Research Society International (OARSI), Seattle, USA, May 2015. Abstract: Osteoarthritis and Cartilage, 23, supplement 2, Page A314.

- Stoppiello LA, Mapp PI, Wilson D, Hill R, Scammell BE, Walsh DA. Identifying the earliest histopathological changes in knee osteoarthritis. OARSI, Paris, France, April 2014. Abstract: Osteoarthritis and Cartilage, 22, supplement S362-S363.

- Stoppiello LA, Mapp PI, Ashraf S, Wilson D, Hill R, Scammell BE, Walsh DA. Structural associations of pain in human knee osteoarthritis. British Society of Rheumatology (BSR) congress, Birmingham, UK, 2013. Abstract: Rheumatology. Vol:52:Supplement 1. 153-153.

- Stoppiello LA, Mapp PI, Ashraf S, Wilson D, Hill R, Scammell BE, Walsh DA. Structural associations of pain in human knee osteoarthritis. Postgraduate research forum at University of Nottingham 2012. Awarded 1st prize.

ACKNOWLEDGEMENTS

First of all I am extremely thankful to the Arthritis Research UK Pain Centre for funding this research project. I would also like to express my sincere gratitude to my supervisors Professor David Walsh, Professor Brigitte Scammell and Dr Paul Mapp for their excellent supervision, guidance and continued support throughout my PhD research project. I am particularly grateful to David for always giving his time so freely to help me with my work.

I am thankful to Professor Eamonn Ferguson for his help with latent class analysis, Dr. Andrew Bennett and Monika Owen for their support and guidance with the molecular work. I am also thankful to Dr. Bryan Moreton for teaching me Rasch analysis.

I would like to thank my colleagues in Academic Rheumatology past and present for their friendship and support; Sadaf, Zena, Ivan, Chen, Kun, Sophie, Sanjay, Hollie, Aliya, Gwen, Fran and Mohsen. In particular I would like to thank Lilian Nwosu for always being there for me, for making me smile and for making my time in Academic Rheumatology so enjoyable, thanks pal!

I am grateful to the patients, relatives, orthopaedic surgeons and Bereavement Centre colleagues at Sherwood Forest Hospitals NHS Foundation Trust for providing the clinical material. Many thanks to Roger Hill, Deborah Wilson and colleagues for processing the tissues and compiling the clinical data for the tissue repository.

Finally I'd like to thank my family (in particular mum, dad, Craig and Joe), my friends and fiancé Dave Wyatt for their constant love and support.

"It always seems impossible until it's done" Nelson Mandela

TABLE OF CONTENTS

ABSTRACT i
DECLARATION iii
PUBLICATIONS iv
PRESENTATIONS v
ACKNOWLEDGEMENTS vi
TABLE OF CONTENTS vii
LIST OF FIGURES xiv
LIST OF TABLES xvi
ABBREVIATIONS xviii
CHAPTER 1: INTRODUCTION 1
1.1 Anatomy of the human knee joint 1
1.1.1 Articular cartilage 3
1.1.2 Subchondral bone 6
1.1.3 Synovium 6
1.1.4 Meniscus 8
1.1.5 Nerve supply to the knee joint 8
1.2 Osteoarthritis 9
1.2.1 Classification 11
1.2.2 Risk factors 11
1.2.3 Signs and symptoms 14
1.2.4 Pathological characteristics 15
1.2.5 Diagnosis 16
1.2.6 Treatment 18
1.2.6.1 Non-pharmacological management 18
1.2.6.2 Pharmacological interventions 20
1.2.6.3 Surgical interventions 21
1.2.7 Phenotypes 22
1.3 Early and late osteoarthritis 23
1.3.1 Articular cartilage changes 24
1.3.2 Subchondral bone modifications 28
1.3.2.1 Bone marrow lesions 29
1.3.2.2 Bone remodelling and osteophyte formation 30
1.3.3 Synovial inflammation 32
1.4 Pain 33
1.4.1 Peripheral nociception 34
1.4.2 Central sensitisation 35

1.5 Peripherally mediated pain in osteoarthritis 37
1.5.1 Structural associations of pain 37
1.5.2 Synovitis and pain 38
1.5.3 Subchondral pathology and pain 39
1.5.4 Meniscal pathology and pain 40
1.6 Inflammatory mediators in osteoarthritis 41
1.6.1 Nerve growth factor 42
1.6.2 Cytokines 46
1.6.3 Chemokines 47
1.6.4 Matrix metalloproteases 49
1.6.5 Protease-activated receptors 50
1.6.6 Cyclo-oxygenases 51
1.6.7 Damage associated molecular patterns 51
1.6.8 Nitric oxide 51
1.6.9 Bradykinin 52
1.6.10 Resolvins 52
1.7 Signalling pathways 52
1.7.1 Nuclear factor-kappa B 52
1.7.2 Janus activated kinase/signal transducers and activators of transcription (JAK/STAT) 54
1.7.3 Mitogen activated protein kinase (MAPK) 54
1.8 Conclusions 56
1.9 Aims, Objectives and Hypotheses 57
CHAPTER 2: MATERIALS AND METHODS 58
INTRODUCTION 58
2.1 Patient Selection 58
2.1.1 Histological features of osteoarthritis 59
2.1.2 Histological associations with symptomatic osteoarthritis 61
2.1.3 Gene patterns in the synovium and their association with symptomatic osteoarthritis 62
2.1.4 Cellular source of synovial NGF 63
2.1.5 Early and mild osteoarthritis and histopathological subgroups 63
2.1.6 Rasch analysis and development of a weighted histopathological OA score 66
2.1.7 Effects of post mortem delay in surgical tissue 66
2.2 Tissue collection and processing 67
2.2.1 Medial tibial plateaux 67
2.2.2 Synovium 68

2.3 Histological staining 69
2.3.1 Haematoxylin and eosin 69
2.3.2 Safranin-O and Fast green 70
2.4 Immunohistochemistry 70
2.4.1 Introduction 70
2.4.2 Indirect immunohistochemistry 72
2.4.3 Optimising conditions for immunohistochemistry 75
2.4.4 Principles of fluorescence microscopy 76
2.4.5 Double immunofluorescence 78
2.4.6 Auto fluorescence 80
2.4.7 Immunofluorescence protocol 81
2.5 Histological scoring 82
2.5.1 Medial tibial plateau 82
2.5.2 Synovitis histological score 89
2.5.3 Meniscus histological classification 92
2.6 Image analysis and quantification 93
2.7 Macroscopic chondropathy scoring 94
2.8 Radiographic osteoarthritis score 96
2.9 Clinical characteristics of total knee replacement cases 97
2.10 Body mass index 97
2.11 Simulating the effects of post-mortem decay in surgical tissue 98
2.12 Gene expression patterns in the synovium 99
2.12.1 Extraction of total RNA from synovia 99
2.12.2 Spectrophotometric analysis of RNA 102
2.12.3 Reverse transcription 102
2.12.4 Real-time polymerase chain reaction 103
2.12.5 TaqMan® 104
2.12.5.1 Gene expression analysis: standard curve method 107
2.12.6 384-well microfluidic cards 109
2.12.6.1 Assay selection criteria 109
2.12.6.2 Protocol 110
2.12.7 Selecting the most stable reference genes for normalisation 111
2.12.8 Determining fold change in gene expression between the groups 112
2.13 Statistical analysis 112
2.13.1 Univariate and regression analyses 112
2.13.2 Intra and inter-observer reliability 113

2.13.3 Ingenuity Pathway analysis 115
2.13.4 Rasch analysis 115
2.13.5 Principle components analysis 117
2.13.6 Receiver operator characteristic (ROC) curves 118
2.13.7 Latent class analysis 120
2.14 Reagents 122
CHAPTER 3: HISTOLOGICAL FEATURES ASSOCIATED WITH SYMPTOMATIC OSTEOARTHRITIS 123
INTRODUCTION 123
3.1 Objectives 125
3.2 Hypothesis 125
METHODS 126
3.3 Study subgroups 126
RESULTS 127
3.4 Histopathological features of knee osteoarthritis 127
3.5 Histological features associated with symptomatic osteoarthritis 133
3.6 Association of BMI with histological outcomes 135
3.7 Determining the cellular localisation of synovial nerve growth factor 137
3.8 Effect of post-mortem delay on nerve growth factor and macrophage immunoreactivity in the human synovium. 142
3.8.1 Associations between post-mortem delay and immunohistochemical outcomes 142
3.8.2 Mimicking the effects of post-mortem delay in synovial tissue obtained at TKR 143
3.9 Summary of results 145
DISCUSSION 146
3.10 Conclusions 150
CHAPTER 4: IDENTIFICATION OF GENE EXPRESSION PATTERNS IN THE SYNOVIUM AND THEIR RELATIONSHIP WITH SYMPTOMATIC OSTEOARTHRITIS 151
INTRODUCTION 151
4.1 Objectives 153
METHODS 153
4.2 Patient subgroups 153
4.2.1 Preliminary study; assessing RNA integrity. 153
4.2.2 Main study 155
4.3 Microfluidic cards 156
4.3.1 Gene selection criteria 156

4.3.2 Gene expression analysis 170
RESULTS 170
4.4 Patient demographics 170
4.5 RNA purity and concentration 173
4.5.1 Taqman: Beta actin expression 173
4.6 Microfluidic cards 175
4.6.1 Reference gene stability 175
4.6.2 Gene expression patterns in the synovium associated with symptomatic OA 178
4.6.3 Nerve growth factor signalling pathway in symptomatic OA. . 188
4.6.4 Associations of gene expression patterns with post-mortem delay 190
4.6.5 Associations with age 193
4.6.6 Associations with synovitis 193
4.6.7 Correlations between genes 199
4.6.8 Pathway analysis 201
4.7 SUMMARY OF RESULTS 202
DISCUSSION 202
4.8 Conclusions 209
CHAPTER 5: OSTEOARTHRITIS AS A MULTI-TISSUE DISEASE AND FEATURES OF EARLY KNEE OSTEOARTHRITIS 211
INTRODUCTION 211
5.1 What is early knee osteoarthritis? 211
5.2 Models of OA progression 212
5.3 Osteoarthritic changes in the articular cartilage 213
5.4 Osteoarthritic changes in the subchondral bone 214
5.5 Synovial inflammation in knee osteoarthritis 214
5.6 Histological grading of OA pathology 215
5.7 Histological phenotypes in knee OA 218
5.8 Objectives 219
METHODS 219
5.9 Study subgroups 219
5.10 Histological scoring methods 222
5.11 Statistical analysis 222
5.11.1 Rasch analysis of the Mankin scoring system 222
5.11.2 Principle components analysis 223
5.11.3 Receiver operating characteristic (ROC) analysis 224
5.11.4 Latent class analysis 225

RESULTS 225
5.12 Histological features of osteoarthritis 225
5.13 Rasch analysis of the Mankin scoring system 230
5.13.1 Test group; early or mild OA 230
5.13.2 Test group; normal to end-stage OA 230
5.13.3 Validation group 231
5.13.4 Spearman-Brown Prophecy formula 231
5.14 Principle components analysis 236
5.15 Rasch analysis 239
5.16 Discriminative abilities of the Mankin and weighted score 239
5.16.1 Distinguishing cases with end-stage OA from post-mortem cases 239
5.16.2 Distinguishing between knees with or without osteophytes 239
5.16.3 Mankin vs uncompressed weighted score 240
5.16.4 Distinguishing between cases with or without pain 243
5.16.5 The use of the weighted score in mild/early OA 244
5.16.6 Correlations between histopathological and macroscopic scores 246
5.17 Identifying the earliest features of knee osteoarthritis 246
5.18 Latent class analysis 249
5.18.1 Whole dataset 249
5.18.2 Class 1: No synovitis, mild structural change 251
5.18.3 Class 2: Mild synovitis and moderate structural change 251
5.18.4 Class 3: Moderate or severe synovitis, severe structural change 251
5.18.5 Clinical characteristics of TKR cases 253
5.18.6 Analgesic use 253
5.18.7 Mild/Early OA 256
5.18.8 End-stage OA 256
5.19 Summary of results 258
DISCUSSION 259
5.20 Conclusions 265
CHAPTER 6: CONCLUSIONS AND FUTURE DIRECTIONS 267
6.1 KEY FINDINGS FROM THIS THESIS 268
6.1.1 Histological and molecular features associated with symptomatic osteoarthritis 268
6.1.2 Histological features of early and mild osteoarthritis and subgroups 270

6.2 LIMITATIONS 272
6.2.1 Histological and molecular associations of symptomatic OA 272
6.2.2 Osteoarthritis as a multi-tissue disease and features of early knee osteoarthritis 274
6.3 FUTURE DIRECTIONS 275
6.4 CONCLUDING REMARKS 278
CHAPTER 7: REFERENCES 280
CHAPTER 8 : APPENDIX 313
8.1 PATIENT CONSENT FORMS 313
8.1.1 Post-mortem tissue 313
8.1.2 Surgical tissue 314
8.1 PATIENT INFORMATION SHEET 315
8.1.1 Post-mortem tissue 315
8.1.2 Surgical tissue 319
8.2 Antibodies 325
8.2.1 Primary antibodies 325
8.2.2 Secondary antibodies 326
8.3 RNA CONCENTRATIONS 327
8.4 MICROFLUIDIC CARD ASSAY SELECTION 330
8.5 LATENT CLASS ANALYSIS 338
8.5.1 Input syntax 338
8.6 MATERIALS AND REAGENTS 339
8.7 SOLUTIONS AND BUFFERS 341

LIST OF FIGURES

Figure 1.1: Anatomy of the right knee joint (anterior view). 3
Figure 1.2: Structure of protein aggregates. 4
Figure 1.3: Organisation of the articular cartilage and subchondral bone layers. 5
Figure 1.4: Venn diagram illustrating the link between intrinsic and extrinsic risk factors in driving OA susceptibility. 12
Figure 1.5: Comparison of a normal and osteoarthritic knee joint. 16
Figure 1.6: Therapeutic approach for knee OA. 19
Figure 1.7: Histopathological features of osteoarthritic articular cartilage. 27
Figure 1.8: Schematic diagram showing the modulation and up-regulation of pro-inflammatory mediators in the dorsal root ganglion by NGF following inflammation or tissue damage. 45
Figure 1.9: Classical NF-κB signalling pathway. 53
Figure 1.10: Simplified mitogen activated protein kinase (MAPK) pathway. . 55
Figure 2.1: Overview of the strategy undertaken to select non-arthritic control post-mortem cases and age-matched total knee replacement cases. 60
Figure 2.2: Overview of the strategy undertaken to select post-mortem and total knee replacement cases with similar macroscopic chondropathy scores cases and age-matched total knee replacement cases. 62
Figure 2.3: Overview of the strategy undertaken to select characterise post-mortem cases as non-arthritic controls or early OA cases. 65
Figure 2.4: A schematic illustration of the "Y-shaped" structure of an IgG antibody molecule. 72
Figure 2.5: Illustrative representation of the ABC method in indirect immunohistochemistry. 74
Figure 2.6: Graphical representation of the Stokes shift. 77
Figure 2.7: Schematic representation of a fluorescent microscope. 79
Figure 2.8: Histological assessment of cartilage surface integrity 85
Figure 2.9: Chondrocyte morphology in the medial tibial plateau. 86
Figure 2.10: Histological assessment of proteoglycan scoring in the medial tibial plateaux of PM (A-B) and TKR (C-D) cases. 87
Figure 2.11: Histological assessment of tidemark integrity. 88
Figure 2.12: Histological assessment of the subchondral bone marrow in human tibial plateau. 89
Figure 2.13: Histological scoring of synovial inflammation according to Haywood et al criteria. 91
Figure 2.14: Histological appearance of human menisci 93
Figure 2.15: Severity of macroscopic chondropathy at the articular surface of tibiofemoral joints obtained at post-mortem. 96
Figure 2.16: Flowchart illustrating steps undertaken to isolate total RNA and quantify gene expression in human synovial samples. 101
Figure 2.17: Primer design for quantitative polymerase chain reaction. 104
Figure 2.18: TaqMan® chemistry. 106
Figure 2.19: Graphical representation of TaqMan® real-time PCR data. 107
Figure 2.20: ROC curve illustrating the Youden Index (J) and (0,1) method for determining optimal cut-offs on ROC curves. 119

Figure 3.1: Histopathological features of non-arthritic (A,C,E,G) and OA ((B,D,F,H,I,J) knees..... 130
Figure 3.2: Histopathological features of OA. 133
Figure 3.3: Histological associations of symptomatic OA. 135
Figure 3.4: Scatterplots illustrating the relationship between histological scores and body mass index (BMI) from TKR cases. 136
Figure 3.5: Cellular localisation of nerve growth factor (NGF) with Hsp47 immunoreactivity in osteoarthritic human synovium. 138
Figure 3.6: Cellular localisation of nerve growth factor (NGF) with CD68 immunoreactivity in osteoarthritic human synovium. 139
Figure 3.7: Cellular localisation of nerve growth factor (NGF) with Hsp47 immunoreactivity in non-arthritic control synovium. 140
Figure 3.8: Cellular localisation of nerve growth factor (NGF) with CD68 immunoreactivity in non-arthritic control synovium sublining. 141
Figure 3.9: Associations between PM delay and CD68 and NGF immunoreactivity. 143
Figure 3.10: Comparison of NGF-immunoreactivity in osteoarthritic synovial tissue left to 'decay' for 24h, 48hr and 72 hours following tissue collection. 144
Figure 4.1: RNA integrity assessments using micro-chip based electrophoresis (Agilent RNA 6000 Nano kit). 155
Figure 4.2: Taqman quantitative real time polymerase chain reactions for beta actin expression. 174
Figure 4.3: Reference gene stability. 177
Figure 4.4: Molecular associations with symptomatic OA. 189
Figure 4.5: Scatterplot illustrating the relationship between NGF immunoreactivity and NGF gene expression. 190
Figure 4.6: Scatterplots illustrating the relationship between gene expression and age. 194
Figure 5.1: Models of OA progression. 213
Figure 5.2: Flowchart detailing the overall study designs including numbers of PM and TKR cases that were required at each step. 220
Figure 5.3: Person item-threshold distributions for the Rasch transformed Mankin score. 232
Figure 5.4: Category probability curves for chondrocyte morphology scores. 233
Figure 5.5 Comparison of area under receiver operating characteristic (ROC) curves for the Mankin and weighted scores (compressed and original/uncompressed chondrocyte morphology scores). 241
Figure 5.6: Comparison of area under receiver operating characteristic (ROC) curves for the Mankin and weighted score. 244
Figure 5.7: Comparison of area under receiver operating characteristic (ROC) curves for the Mankin and weighted score in mild/early OA. 245
Figure 5.8: Histogram of the commonest pathological features observed in knee tissue collected from 343 post-mortem cases. 247
Figure 5.9: Histograms illustrating histopathological differences between non-arthritic controls, mild/early OA and end-stage OA cases. 248
Figure 5.10: Analgesic uses of TKR cases within each latent class. 255

LIST OF TABLES

Table 1.1: Sensory fibre classification..... 9
Table 1.2: The ACR criteria for classification of idiopathic osteoarthritis of the knee (Altman et al., 1986). 17
Table 1.3: The four chemokine groups, and examples of family members. 48
Table 1.4: Classification of matrix metalloproteases 49
Table 2.1: Spectral properties of fluorophores used to determine localisation of synovial NGF. 80
Table 2.2: The histological-histochemical grading system for osteoarthritic articular cartilage developed by Mankin et al..... 84
Table 2.3: Classification system for histologically assessing synovial tissue inflammation in haematoxylin and eosin tissue sections..... 90
Table 2.4: Modified Copenhaver classification system for histologically assessing meniscal degeneration in haematoxylin and eosin tissue sections. .. 92
Table 2.5: BMI Classification..... 98
Table 2.6: Intra- and inter-observer reliability kappa and weighted kappa statistics for histological scores. 114
Table 3.1: Clinical details and pathological characteristics of study groups*. 128
Table 4.1: Selection of references genes included in the microfluidic card.. 157
Table 4.2: Selection of target genes included in the microfluidic card. 158
Table 4.3: Clinical and pathological characteristics of the study groups* 171
Table 4.4: Comparison of reference gene Ct values in asymptomatic and symptomatic chondropathy cases. 175
Table 4.5: Summary table of differentially expressed genes*..... 179
Table 4.6: Synovial gene expression analysis (mean, 95% C.I) for asymptomatic and symptomatic chondropathy cases. 181
Table 4.7: Correlations between gene expression and PM delay. 191
Table 4.8: Associations between gene expression and age. 195
Table 4.9: Associations between gene expression and synovitis. 197
Table 4.10: Correlations between suppressors of cytokine signalling (SOCS)-1 and 3, with chemokines and cytokines. 200
Table 4.11: Top three networks revealed by Ingenuity Pathway Analysis. ... 201
Table 5.1: Clinical demographics of study groups. 226
Table 5.2: Histological characteristics of PM and TKR cases 228
Table 5.3: Associations between macroscopic chondropathy scores, histologic score, ages and gender. 229
Table 5.4: Rasch analysis of the Mankin scoring system on initial test group. 234
Table 5.5: Rasch analysis of the Mankin scoring system on validation group. 235
Table 5.6: Weightings for each histological variable derived from principle components analysis using Rasch transformed* chondrocyte morphology scoring..... 237
Table 5.7: Weightings for each histological variable derived from principle components analysis using uncompressed original chondrocyte scoring..... 238
Table 5.8: Comparison of the abilities of the original Mankin scoring system and weighted OA score to distinguish between cases with end-stage OA and PM cases, and between those with or without osteophytes. 242

Table 5.9: Associations of the Mankin and weighted score with macroscopic chondropathy score. 246
Table 5.10: Latent class models fit indices in whole dataset. 250
Table 5.11: Clinical characteristics of the 3 latent classes. 252
Table 5.12: Clinical characteristics defining the 3 latent classes in total knee replacement cases. 254
Table 5.13: Classification of analgesic medications used by TKR patients... 256
Table 5.14: Latent class models fit indices in PM cases and TKR cases, separately only 257

ABBREVIATIONS

5-HT	Serotonin
ABC	Avidin-biotin complex
ACL	Anterior cruciate ligament
ACR	American College of Rheumatology
ACTB	Beta actin
ADAM	A disintegrin and metalloproteinase domain
AIC	Akaike Information Criteria
ALL	Anterolateral ligament
ASIC	Acid sensing ion channel
AUC	Area under the curve
BCP	1-bromo-3-chloro-propane
BDNF	Brain derived neurotrophic factor
BLRT	Bootstrapped likelihood ratio test
BMD	Bone mineral density
BME	Bone marrow oedema
BMI	Body mass index
BML	Bone marrow lesions
BMP	Bone morphogenic protein
BSA	Bovine serum albumin
CC	Calcified cartilage
CCL	Chemokine ligand
CD68	Macrophage
cDNA	Complementary deoxyribonucleic acid
CGRP	Calcitonin gene-related peptide
CI	Confidence interval
CILP	Cartilage intermediate layer protein, nucleotide pyrophosphohydrolase
C_t	Cycle threshold
CX3CL1	Fractalkine
COX	Cyclo-oxygenase
DAB	Diaminobenzidine
DAMPS	Damage associated molecular patterns
DAPI	4’-6’-diamidino-2-phenylindole hydrochloride
DIF	Differential item functioning
DMOADs	Disease modifying osteoarthritis drugs
DNA	Deoxyribonucleic acid
ECM	Extracellular matrix
EDTA	Ethylenediaminetetraacetic acid
eNOS	Endothelial nitric oxide synthase
EULAR	European League Against Rheumatism
FDA	US Drug and Food Administration

FITC	Fluorescein isothiocyanate
FLS	Fibroblast like synoviocytes
FRET	Fluorescence resonance energy transfer
GAGs	Glycosaminoglycans
GAPDH	Glyceraldehyde 3-phosphate dehydrogenase
gDNA	Genomic deoxyribonucleic acid
HA	Hyaluronic acid
HIER	Heat-induced epitope retrieval
HMBS	Hydroxymethylbilane synthase
HPLC	High performance liquid chromatography
HSANs	Hereditary sensory autonomic neuropathies
HSP47	Heat shock protein
ICOAP	Intermittent and constant arthritis pain scale
IHC	Immunohistochemistry
IFN-γ	Interferon gamma
IL	Interleukin
IMS	Industrial methylated spirits
iNOS	Inducible nitric oxide synthase
IQR	Inter quartile range
JSN	Joint space narrowing
LCA	Latent class analysis
LCL	Lateral collateral ligament
LMR	Vuong-Lo-Mendell-Rubin
MAPK	Mitogen activated protein kinase
MCL	Medial collateral ligament
MCP	Monocyte chemotactic protein
MIA	Monosodium iodoacetate
MIP	Macrophage inflammatory protein
MRI	Magnetic resonance imaging
MRP	Myeloid-related protein
mRNA	Messenger ribonucleic acid
MMP	Metalloproteinase
NCC	Non calcified cartilage
NF-kB	Nuclear factor kappa-B
NGF	Nerve growth factor
NMDA	*N*-methyl-$_{D}$-aspartate
NO	Nitric oxide
nNOS	Neuronal nitric oxide synthase
NSAIDs	Non-steroidal anti-inflammatory drugs
NT	Neurotrophin
OA	Osteoarthritis
OARSI	Osteoarthritis Research Society International
OCT	Optimum cutting temperature
OKS	Oxford knee score

OPG	Osteoprotegrin
OST	Osteophytes
PAR	Protease-activated receptors
PBS	Phosphate buffered saline
PCA	Principle component analysis
PCS	Photographic chondropathy score
PCL	Posterior cruciate ligament
PCR	Polymerase chain reaction
PFA	Paraformaldehyde
PGE	Prostaglandin
PIER	Proteolytic-induced epitope retrieval
PM	Post-mortem
PSI	Person Separation Index
PVP	Polyvinylpyrrolidone
QST	Quantitative sensory testing
RA	Rheumatoid arthritis
RNA	Ribonucleic acid
ROC	Receiver operating characteristic
RT	Room temperature
RTr	Reverse transcriptase
RT-PCR	Real time-polymerase chain reaction
SD	Standard deviation
SFA	Systeme Francaise D'Athroscoprie
SS.Adj BIC	Sample size adjusted Bayesian Information criteria
SP	Substance P
TGF-β	Transforming growth factor-beta
TIMP	Tissue inhibitors of metalloproteases
TKR	Total knee replacement
TNF	Tumour necrosis factor
TRITC	Tetramethylrhodamine isothiocyanate
TrkA	Tyrosine kinase receptor A
TRPV1	Transient receptor potential vallinoid 1
UBC	Ubiquitin C
VEGF	Vascular endothelial growth factor
WOMAC	Western Ontario McMaster Index

CHAPTER 1: INTRODUCTION

Arthritic disease is a major source of pain and disability throughout the world and it places a major burden on society (Bitton, 2009) due to expensive treatment and an increasing life expectancy in developed countries. More than 69,000 total knee replacement (TKR) operations were carried out by the NHS in 2014 (Njr, 2015). Osteoarthritis (OA) is the most common form of arthritis and can affect any synovial joint. The knee joint is one of the most commonly affected sites, and all tissues within the knee joint are affected by OA.

Pain is the major symptom of OA, and is usually the reason OA sufferers seek medical assistance; however the role of joint pathology in mediating pain is not entirely understood. Furthermore, the earliest pathological alterations in OA are difficult to characterise as structural pathology may develop in the absence of symptoms. Consequently this limits investigation into the earliest changes of preclinical knee OA.

Better understanding of the structural features that are associated with both early and symptomatic OA would help to refine strategies for developing structure-modifying treatments by focussing on those which are most likely to improve symptoms.

1.1 Anatomy of the human knee joint

The knee joint is the largest synovial joint in the body, connecting the upper and lower bones of the leg; the femur and tibia, respectively. The joint is formed by the articulation of the medial and lateral condyles of the distal femur with the medial and lateral tibial plateaux of the proximal tibia. The patella (knee cap) is the most anterior aspect of the joint. The anatomy of the knee joint is illustrated in figure 1.1.

The synovial joint is enclosed within the synovial capsule, and is stabilised by ligaments and menisci. The four major ligaments supporting the joint are characterised by their anatomical location. The anterior and posterior cruciate

ligaments (ACL and PCL, respectively) are intra-articular (within the capsule), whereas the medial and lateral collateral ligaments (MCL and LCL, respectively) are classified as extracapsular (outside of the capsule). More recently the anterolateral ligament (ALL) of the knee has been identified (Claes et al., 2013).

The ACL arises from the posteromedial corner of medial aspect of lateral femoral condyle in the intercondylar notch and inserts into the interspinous area of the tibia. The PCL originates from the antero-lateral aspect of medial femoral condyle in the area of intercondylar notch; its origin is much more anterior than that of ACL and its tibial attachment is not intra articular, but over back of tibial plateau, it is approximately 1 cm distal to the joint line. The cruciate ligaments prevent posterior and anterior excessive movements, respectively. The MCL extends from the medial femoral epicondyle to the medial tibia. The LCL extends from the lateral femoral epicondyle to the fibular head. The collateral ligaments prevent sideways movement of the joint. The fibula is the second bone of the lower leg, located lateral to the tibia. Anterior to the LCL is the ALL, originating on the lateral femoral epicondyle and extending to the anterolateral tibia (Claes et al., 2013).

The arterial supply to the knee joint is derived from the genicular branches of the popliteal and femoral arteries, the lateral circumflex femoral and fibular artery (Shim and Leung, 1986). The majority of the structures within the knee joint have a rich blood supply; subchondral bone, articular capsule, synovial membrane, outer third of the meniscus and cruciate ligaments (Davies and Edwards, 1948). The articular cartilage and inner two thirds of meniscus are usually avascular (Franses et al., 2010, Ashraf et al., 2011, Mapp and Walsh, 2012) except when diseased.

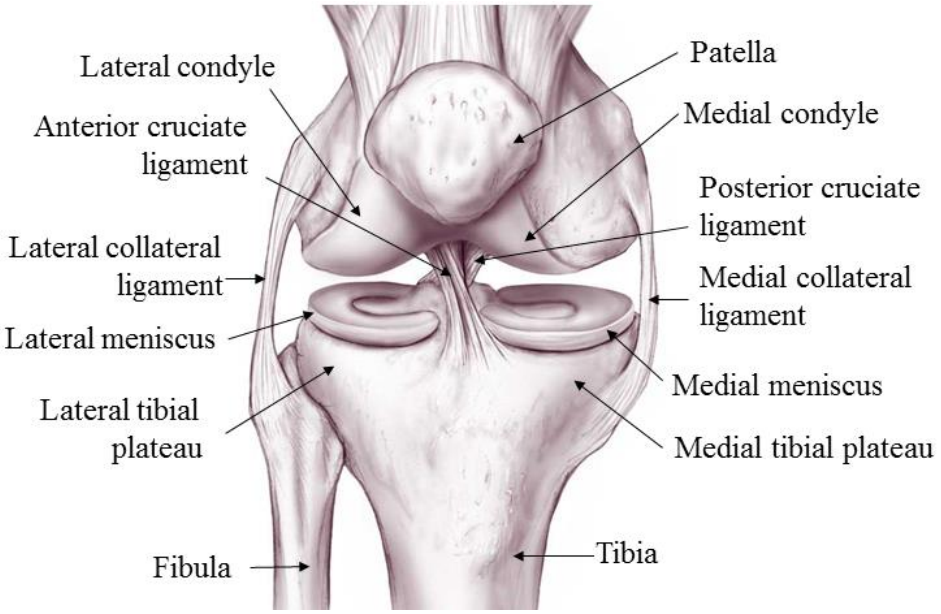


Figure 1.1: Anatomy of the right knee joint (anterior view).

Figure adapted from http://mywwwzone.heckyeahllc.netdna-cdn.com/wp-content/uploads/2010/06/Knee-anatomy-570.jpg. Webpage accessed 01.06.15.

1.1.1 Articular cartilage

Articular cartilage is the protective connective tissue lining the articulating bony ends of the knee joint. The articular cartilage possesses unique biomechanical properties which enable weight bearing and dissipation of compressive and tensile loads imposed onto the joint. Furthermore articular cartilage, in addition to the viscous synovial fluid, is essential for providing a low-friction joint movement. These highly specialised functions are attributed to the structural organisation and composition of the tissue.

Chondrocytes are specialised cells of the cartilage, responsible for synthesis of a highly organised extracellular matrix (ECM). The ECM is comprised of tissue fluid and structural macromolecules; collagen (type II), proteoglycan and non-collagenous proteins and glycoproteins, see references in (Heijink et al., 2012). A highly organised collagenous network provides the strength needed to withstand sheer and tensile forces. Compressive resistance of the articular cartilage is provided by proteoglycans within the collagen matrix (Goldring and Marcu, 2009).

Aggrecan is the major aggregating proteoglycan; it consists of a protein core, to which sulphated glycosaminoglycan (GAG) chains (chondroitin sulphate and keratan sulphate) are attached, see references in (Buckwalter et al., 2005, Madry et al., 2012). The core protein associates with hyaluronic acid, via link proteins to form a large macromolecular complex. The basic structure is illustrated in figure 1.2.

Articular cartilage is normally avascular and aneural. Avascularity is maintained by the synthesis of angiogenesis inhibitors by chondrocytes (Moses et al., 1990). Oxygen and nutrients are supplied by diffusion from the synovial vasculature, or from subchondral bone vessels (Haywood and Walsh, 2001). Normally proteoglycan (aggrecan) acts to inhibit neurite growth to maintain aneurality of the articular cartilage (Binch et al., 2014).

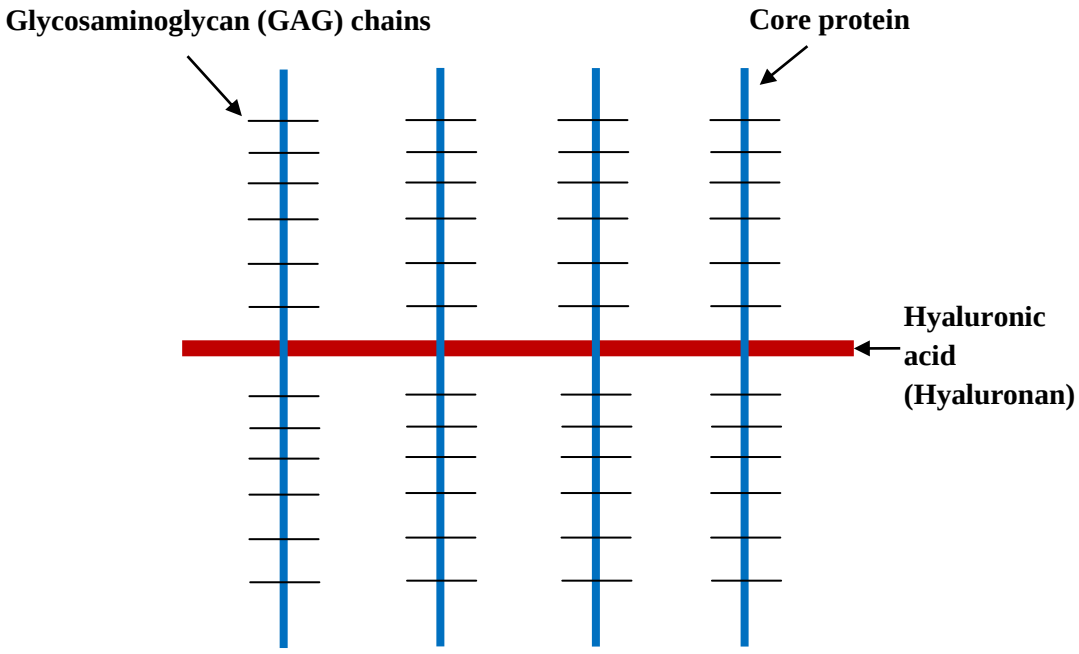


Figure 1.2: Structure of protein aggregates.

Aggrecan consists of a protein core, to which sulphated glycosaminoglycan (GAG) chains (chondroitin sulphate and keratan sulphate) are attached. The aggrecan core protein associates with hyaluronic acid, via link proteins to form a large macromolecular complex.

Articular cartilage is composed of four separate layers (figure 1.3); the superficial (tangenital), middle (transitional), deep (radial) and the calcified layers (Poole, 1997). The former three layers are non-calcified cartilage. Each layer is differentiated by chondrocyte shape, proteoglycan content and arrangement of collagen fibres. The superficial layer is in contact with the synovial cavity, whereas the calcified layer is adjacent to the subchondral bone.

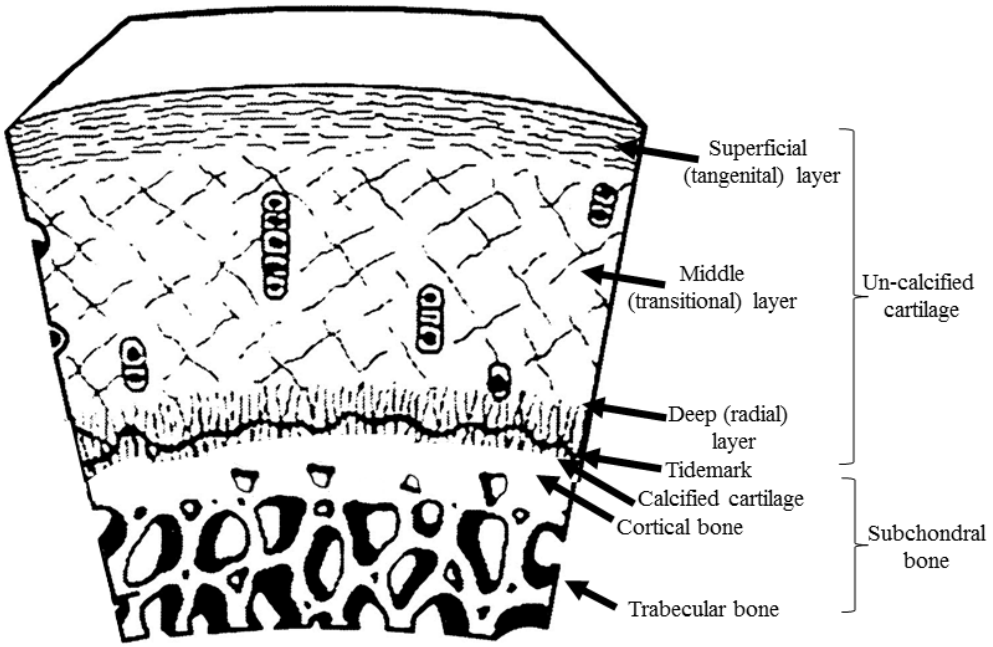


Figure 1.3: Organisation of the articular cartilage and subchondral bone layers.

Figure adapted from (Mandelbaum et al., 1998).

The superficial layer provides a gliding surface, making up 10-20% of the normal cartilage volume. This layer has a low proteoglycan content, but is rich in collagen fibrils which are orientated parallel to the articular surface (Buckwalter et al., 2005). Chondrocytes are of an elongated appearance (Pearle et al., 2005). Approximately half of the articular cartilage is comprised of the middle layer. Here, the collagen fibres are thicker in diameter and are obliquely orientated and the chondrocytes are rounded (Martel-Pelletier et al., 2008). The deep layer is characterised by abundant proteoglycan content, in addition to large collagen fibrils aligned perpendicular to the articular surface.

Chondrocytes are typically aligned in a column orientation (Pearle et al., 2005). The calcified layer is separated from the deep layer by a 2-5 μm thick mineralising front referred to as the tidemark (Pesesse et al., 2011). The junction between the calcified cartilage and subchondral bone is defined by the cement line (Madry et al., 2010).

1.1.2 Subchondral bone

The subchondral bone is located immediately below the calcified layer of articular cartilage. The subchondral bone has essential roles in providing support to the articular cartilage through absorption of mechanical forces to the joint (Radin and Rose, 1986).

Both the calcified cartilage layer and subchondral bone region are mineralised tissues (Burr, 2004). The subchondral bone consists of subchondral bone plate which is normally 1-3mm in thickness (Milz and Putz, 1994). Beneath the cortical bone is the subchondral trabecular (or cancellous) bone, which is characterised by a porous appearance (figure. 1.3). Subchondral bone marrow spaces typically contain fatty marrow; however during pathology fatty spaces may be replaced by fibrovascular tissue (Milgram, 1983, Walsh et al., 2010).

Channels originating in the subchondral bone have been observed to breach the tidemark and enter the deep layer of non-calcified cartilage (Clark, 1990, Suri et al., 2007, Walsh et al., 2010).The channels are approximately 10-30 μm in diameter (Clark, 1990). They can be characterised as open or closed, depending on whether there is direct contact between channel contents and non-calcified cartilage, or if channel is enclosed within a bony sheaf, respectively (Clark, 1990).

1.1.3 Synovium

The synovial joint is enclosed within the synovial capsule which forms a stabilising seal around the femur and tibia. The capsule is comprised of two layers; an external fibrous connective tissue membrane and a more delicate internal synovial membrane layer (Ralphs and Benjamin, 1994).

The anatomy of the synovium in the knee joint is complex. The synovium lines both the non-articular compartment of the joint cavity in addition to the intra-

articular ligaments. Different compartments of the synovial lining can be identified. The central portion is located posterior to the patella; it extends medially and laterally across the cruciate ligaments, and continues below the patella where it is replaced by the infrapatellar fat pad. The suprapatellar pouch is formed above the patella (Fenn et al., 2009).

The synovial lining is responsible for the secretion of synovial fluid. Normal synovial fluid is a viscous ultrafiltrate of plasma containing hyaluronic acid, glycoproteins and albumin (Adamopoulos et al., 2006) secreted by fibroblast-like synoviocytes. One of the most important functions of synovial fluid is to provide joint lubrication (Swann et al., 1984). The synovium is highly vascularised; the synovial fluid transports nutrients and oxygen from the synovial vasculature to the chondrocytes in the normally avascular articular cartilage (Haywood and Walsh, 2001). Moreover, the synovial fluid facilitates the removal of metabolites and waste products from the synovial cavity (Sellam and Berenbaum, 2010).

The synovium is comprised of two layers; the intima (lining) and subintima (sublining). The synovial lining contains two distinct types of synovial cells (synoviocytes) which have been identified and characterised using electron microscopy (Barland et al., 1962). Type A cells, are of macrophage lineage, and type B are fibroblast-like synoviocytes (FLS) (Athanasou, 1995). Normal synovial lining is usually 1-4 cells in thickness (Haywood et al., 2003, Smith, 2011). The normal sublining has a relatively sparse cellular distribution, in addition to dispersed distribution of blood vessels, lymphatic vessels, adipocytes, and few or no inflammatory cells, such as macrophages. (Levi-Montalcini, 1990, Haywood et al., 2003, Smith, 2011).

Synovial histological changes during inflammation are characterised by a marked increase in synovial cell lining layer thickness (hypertrophy) which may be deeper than 7 cells in thickness and increase in the size of synovial cells (hyperplasia). Furthermore there may be recruitment of inflammatory cells such as macrophages, and in severe inflammation perivascular lymphoid aggregates may be observed (Haywood et al., 2003).

The normal synovium is richly innervated with neuronal fibres (Mapp et al., 1990). Various cell types exist within the synovium, these include macrophages, fibroblasts, mast cells, T and B cells and plasma cells (De Lange-Brokaar et al., 2012).

1.1.4 Meniscus

The medial and lateral menisci are two cresenteric shaped fibrocartilage discs situated between the femoral condyles and tibial plateaux. The meniscal periphery is thick and convex, whereas the unattached borders are thin and concave (Standring, 2005). The meniscal horns are attached to the superficial surface of the tibia by insertional ligaments (Messner and Gao, 1998). The menisci are important in absorbing shock transmitted to the joint, dissipating the weight placed on the joint, in addition to proprioception (Seedhom et al., 1974, Van Der Esch et al., 2013).

The menisci are comprised of approximately 70% water. The dry weight of the menisci consists mainly of a collagenous (predominantly type I) extra cellular matrix (ECM) and other non-collagenous proteins. Two distinct regions of the menisci are identified histologically. Two thirds of the menisci are occupied by the aneural and avascular inner region; collagen fibrils are orientated in an organised manner, with chondrocyte-like cells (Makris et al., 2011). In contrast, the outer region which makes up one third of the meniscus is richly innervated with blood vessels and nerves, cells are fibroblast-like in appearance (Makris et al., 2011). Collagen fibrils are arranged in a more disordered manner (Ashraf et al., 2011).

1.1.5 Nerve supply to the knee joint

The knee joint is innervated by sensory and sympathetic branches of the obturator, femoral, tibial and common peroneal nerves (Gardner, 1948). The majority of structures within the knee joint are richly innervated, these include; synovium, joint capsule, subchondral bone, periosteum, outer region of the menisci, tendons, ligaments and surrounding muscle. Articular cartilage, and the inner region of menisci are however aneural (Hunter et al., 2008, Ashraf et al., 2011).

Sensory nerves function to convey mechanical information from the joint (periphery) to the higher processing centres (central nervous system). Sensory fibres are characterised according to morphological characteristics as detailed in Table 1.1. A-delta (Aδ) fibres have a fast conduction velocity of 12-30 m/sec and are responsible for the sharp acute pain experienced immediately in injury. In contrast C fibres are more abundant and have a slower conduction velocity of approximately 0.4 -1.4 m/sec and mediate the dull persistent ache experienced in chronic pain states. Both Aδ and C fibres are activated by thermal and mechanical stimulation (Voscopoulos and Lema, 2010). C fibres are polymodal and are also activated by chemical stimuli and have higher thresholds for activation than Aδ or Aβ fibres (Voscopoulos and Lema, 2010).

Table 1.1: Sensory fibre classification.

Neuron type	Function	Myelinated	Diameter	Innervates
Aβ	Proprioception	Yes	Thick	Capsule, fat pad, ligaments, menisci and periosteum
Aδ	Nociception	Yes	<5µm	Capsule ligament, menisci, periosteum and bone
C	Nociception	No	<2µm	

References: (Mcdougall, 2006, Hunter et al., 2008).

1.2 Osteoarthritis

OA is the most common form of arthritic disease. It is a chronic, disabling condition that can affect any synovial joint, and is highly prevalent amongst the middle aged to elderly population. Although OA is strongly associated with ageing, it is not an inevitable consequence of ageing. Globally, 18% of women and 10% of men (over 60 years old), approximately are affected by the disease (Woolf, 2003). However, this is likely to be an underestimation as many suffers may not be aware they have the disease as it can often be asymptomatic.

OA has been long regarded as a ‘wear and tear’ disease of the cartilage, however it is becoming increasingly recognised that the pathophysiology of OA is more complex than previously thought. Certainly, all tissue types within the joint are involved in the pathogenesis (Loeser et al., 2012), and OA is often considered as joint failure.

Determining the earliest intrinsic tissue changes in OA is extremely challenging, since structural change may develop in the absence of symptoms. Furthermore OA is a heterogeneous disease, and the sequence of disease progression is widely debated. Traditional models of OA progression conceptualise OA as a disease originating in one tissue type (e.g., the articular cartilage or subchondral bone) and progressing to secondary structures. In contrast more recent models suggest that pathology can arise in several tissue types in parallel in the early stages of disease and progress in severity to facilitate joint failure in the later stages of diseases. Different subgroups of OA patients might exist since OA patients have varied clinical presentations.

Pain is the major clinical symptom of OA (Hunter et al., 2013). Painful disabling knee OA has been reported in 10% of people over the age of 55 years old, a quarter of these were severely disabled as a result (Peat et al., 2001). Other clinical symptoms of OA include joint stiffness resolving in less than 30 minutes, crepitus and bony tenderness or enlargement (Altman et al., 1986). Pathological features include focal articular cartilage degradation, subchondral bone remodelling, synovial inflammation, bone marrow lesions, marginal osteophyte formation and meniscal damage.

Diagnosis of OA is based on clinical, pathological and radiographic features. The associations between clinical symptoms and pathology are not entirely clear (Dieppe et al., 1997, Bedson and Croft, 2008). Some patients with symptomatic OA do not have significant radiographic changes, whereas other patients may have severe radiographic changes in the absence of joint pain. However in one study, radiographic OA was present in 68% of individuals over the age of 50 years old who had reported knee pain within the last year (Peat et al., 2006). This suggests that some aspects of joint pain are correlated

with radiographic change, but radiographic evidence alone does not fully associate with symptomatic OA.

Cases of OA are expected to increase in the future due to increasing life expectancy, obesity and increased sports injuries. By 2020 OA is estimated to be the fourth leading cause of disability (Woolf, 2003). Despite efforts to comprehend the aetiology of the disease, the definitive cause of the condition remains to be fully elucidated. The development of disease-modifying osteoarthritic drugs (DMOADs) is vital to revolutionise the management of both clinical and pathological outcomes of OA.

1.2.1 Classification

The aetiology of OA is specified as primary (or idiopathic), where there is no obvious cause of the disease, or as secondary OA. Secondary OA occurs as a consequence of previous joint trauma (Gelber et al., 2000), or medical conditions including inflammatory arthritis, such as rheumatoid arthritis (Altman et al., 1986) and Paget's disease (Altman, 1980). OA can be monoarticular (affecting 1 joint), or generalised (affecting at least 3 joints).

1.2.2 Risk factors

OA is a complex pathological process; it remains to be determined whether OA exists as a single disease, or is the common final endpoint of numerous disorders. The association between risk factors and OA have been well documented in epidemiological studies. Risk factors are classified as those which may predispose the individual to OA (intrinsic), or external factors (extrinsic) that may dictate the severity of the disease. Examples of common intrinsic and extrinsic risk factors are detailed in figure 1.4. The exact contribution of these factors to both the incidence and progression of the disorder remains relatively unclear. OA is a multifactorial disease, which is driven by the interplay of both intrinsic and extrinsic factors. In reality, the majority of people with OA fall into several risk factor categories.

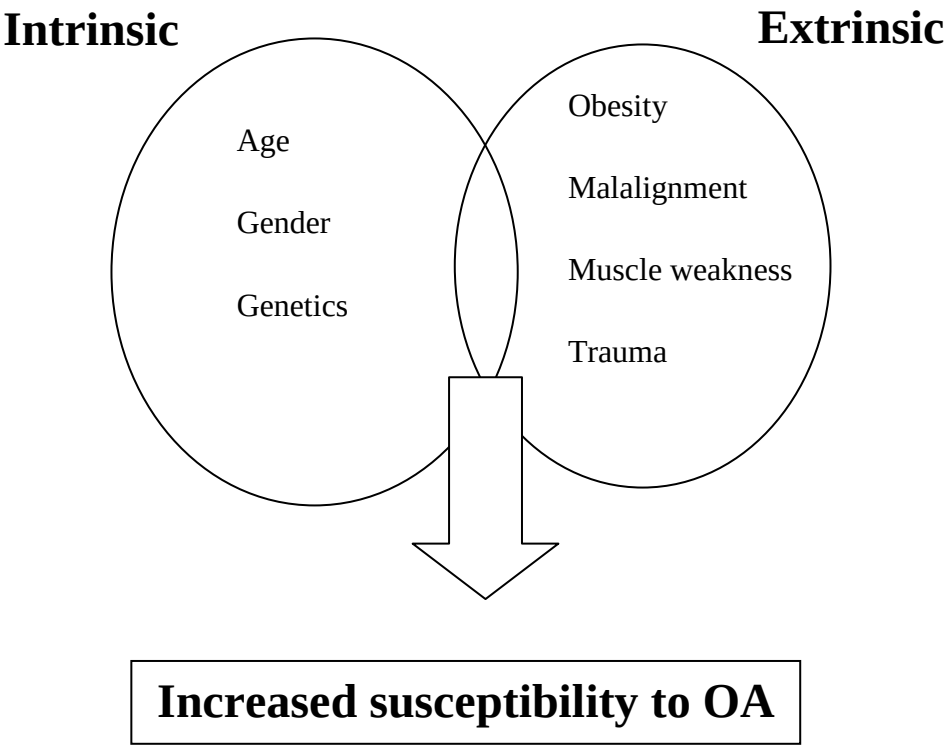


Figure 1.4: Venn diagram illustrating the link between intrinsic and extrinsic risk factors in driving OA susceptibility.

OA is most prevalent in the middle aged to elderly population; nevertheless OA can occur at any age. Age is a major risk factor for OA; however OA is not a normal consequence of ageing (Shane Anderson and Loeser, 2010). Accordingly, dissecting normal age related changes within the knee joint from pathological osteoarthritic changes is extremely challenging. The Framingham Osteoarthritis study showed the annual incidence of OA in individuals over 80 was 17% higher than in those under 70 years old (Felson et al., 1987).

Obesity is believed to have a strong influence on the development of OA (Ackerman and Osborne, 2012, Jiang et al., 2012), and is the main modifiable risk factor for OA (Felson et al., 1988). Obesity has been shown to be associated with both pain (Goulston et al., 2011), and cartilage loss in OA (Roemer et al., 2009a, Antony et al., 2011). The mechanism by which obesity increases propensity to OA remains to be fully determined. Increased

mechanical loading on the joint and local inflammatory cytokines derived from adipose tissue are postulated to be involved in the pathogenesis (Sowers and Karvonen-Gutierrez, 2010).

Post-menopausal woman are at an increased risk of OA (Felson et al., 2000, Grotle et al., 2008), implying a role for reduced oestrogen levels in OA pathogenesis. This is further evidenced by studies which show a possible protective effect of hormone replacement therapy in preventing radiographic progression (Spector et al., 1997).

Twin studies have been fundamental in demonstrating the important role of genetics in the incidence of OA. Studies of monozygotic (identical genes) and dizygotic twins (share half of genes), found a 65% and 38% correlation, respectively (Spector et al., 1996), strongly implying genetic susceptibility to hand and knee OA. Furthermore, familial aggregation of OA is demonstrated by sibling studies. Siblings of patients with symptomatic knee OA are 3 times more likely to have OA than the general population (Neame et al., 2004).

Various candidate genes may be associated with the prevalence and progression of OA. Genetic polymorphisms in several genes from cartilage and synovial tissue have been associated with OA susceptibility, which was assessed by OA radiographic modifications. The genes included A disintegrin and metalloproteinase domain 12 (ADAM12), bone morphogenic protein 2 (BMP2), CD36, cyclooxygenase 2 (COX2) and nuclear receptor co-repressor 2 (NCOR2). OA progression was associated with polymorphisms in ADAM12, cartilage intermediate layer protein, nucleotide pyrophosphohydrolase (CILP), osteoprotegrin (OPG) and tetranecton (TNA) (Valdes et al., 2004). Furthermore a variant in the transient receptor potential vallinoid 1 (TRPV1) heat-gated ion channel may be associated with the risk symptomatic OA (Valdes et al., 2011). Nevertheless genetic susceptibility to OA is complex and not completely understood. It is likely to be multigenic in nature.

Previous knee injury is a significant risk factor for OA (Muthuri et al., 2011). Trauma may arise through sporting injury or other means. Injury of the ACL increases the likelihood of developing knee OA (Lohmander et al., 2004). Furthermore valgus or varus knee malalignment is a risk factor for OA

(Tanamas et al., 2009). Valgus malalignment describes the angulation of the distal component away from the midline (knock-kneed), whereas varus malalignment is towards the midline, or bow legged.

1.2.3 Signs and symptoms

OA can affect any synovial joint, but is more common in the interphalangeal joints of the hand and in weight bearing joints such as the knee and hip. Clinical symptoms in OA are often unilateral, however can occur bilaterally.

- **Pain** is the major clinical symptom in OA, and is usually the reason sufferers first seek clinical assistance. Pain may be described as an intermittent, persistent, dull ache, accompanied by intense pain flares which appear to be unpredictable in nature (Hawker et al., 2008).

- **Joint stiffness and weakness** is a common complaint in patients with OA, stiffness of the joint usually occurs after period of inactivity. Stiffness is usually short-lived (less than 30 minutes). Weakness of the quadriceps muscle is associated with knee OA, which may be attributed to gradual disuse due to pain and reflex inhibition.

- **Swelling** of the joint may be attributed to osteophyte formation at the joint margin, or synovitis and effusion. Swelling is often accompanied by warmth and tenderness of the affected joint.

- **Gait alterations**; pain and discomfort in the arthritic joint alters gait. Weight is shifted onto the contralateral side to reduce pressure and protect the affected joint. Gait alterations include instability, loss of proprioception and reduced range of movement.

- **Crepitus** is defined as a creaking or crunching sound in the knee upon flexion or extension and is common in osteoarthritic knees.

- **Limitation of movement and loss of function.** The range of movement may be limited and associated with pain as a consequence additional stress is placed on the contralateral joint.

- **Psychological and emotional impact** OA is associated with alteration in mood, depression, anxiety, sleep disturbance and ability to cope with daily life events (Wise et al., 2010)**.**

Pain is the major symptom of OA, and is believed to originate from a variety of tissues including the subchondral bone, synovium, menisci, ligaments and muscles (Hunter et al., 2008). Pain in OA is discussed further in section 1.5.

1.2.4 Pathological characteristics

OA is a metabolically active, slow, reparative disease that attempts to compensate for initial joint insult. Joint destruction eventually outweighs the repair process, which eventually results in morphological alterations in the joint. The pathophysiology of OA involves all tissue types within the joint. The main pathological characteristics are focal cartilage loss with accompanying bone remodelling and osteophyte formation. Localised synovial inflammation, remodelling and thickening of the synovial capsule, muscle atrophy and meniscal degeneration and extrusion are also associated with OA. The formation of osteophytes and thickening of the joint capsule are believed to be adaptive protective mechanisms to stabilise the joint to prevent further trauma (Pottenger et al., 1990). Comparison of an osteoarthritic knee joint with a normal joint is depicted in figure 1.5. Morphological alterations in both early and late-stage OA are discussed in more detail in section 1.3.

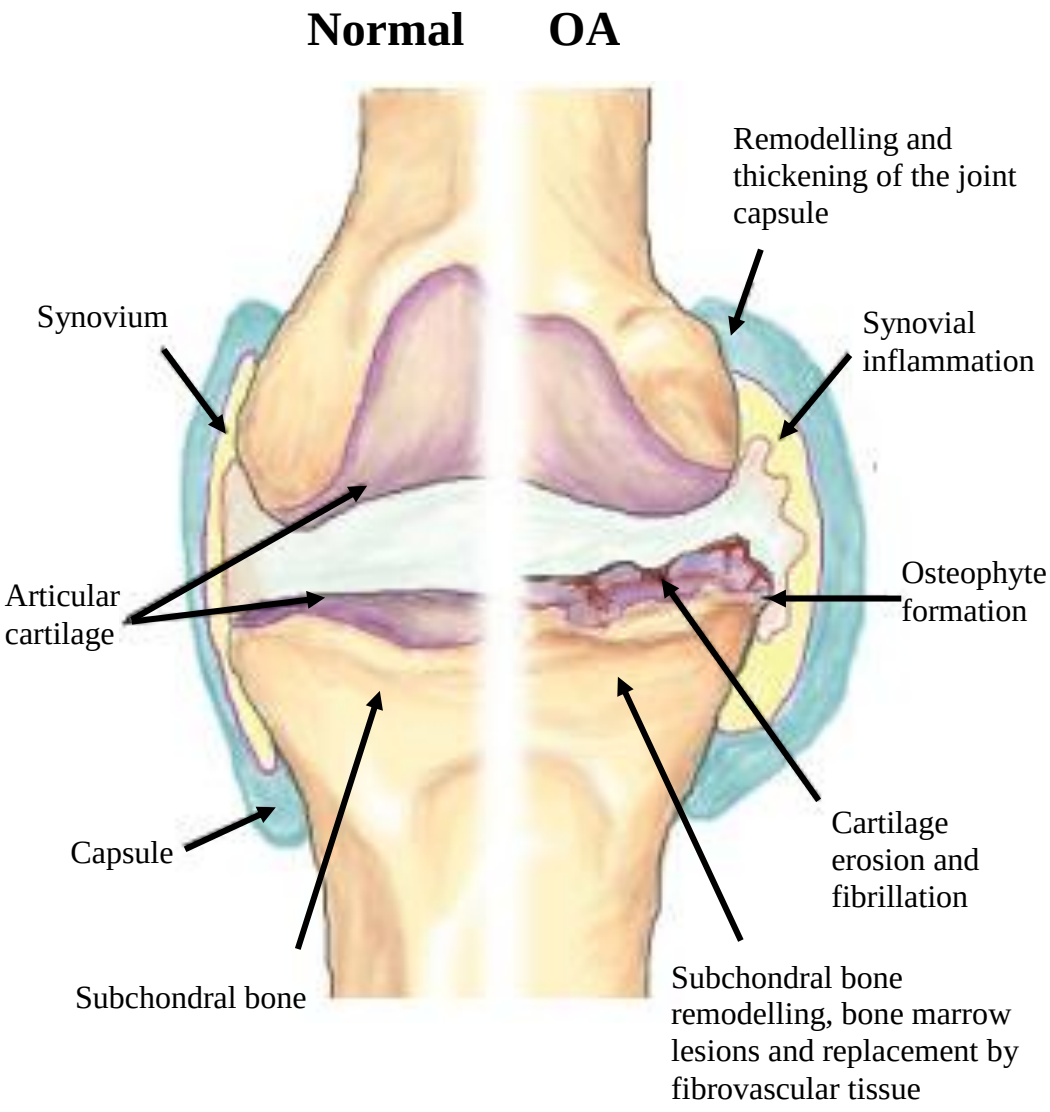


Figure 1.5: Comparison of a normal and osteoarthritic knee joint.

Pathological changes in knee OA are characterised by articular cartilage fibrillation and erosion, subchondral bone remodelling, bone marrow lesions and replacement by fibrovascular tissue, synovial inflammation and thickened joint capsule. Figure adapted from http://communiqiacupuncture.com/2013/04/04/knee-pain/. Webpage accessed 29/07/14.

1.2.5 Diagnosis

OA is a heterogeneous disease, where different clinical and pathological phenotypes exist. The association between knee pain and pathological characteristics is not completely understood. Classification is based on the on the American College of Rheumatology (ACR) criteria outlined in 1986 by

Altman and colleagues (Altman et al., 1986), and illustrated in table 1.2. Diagnosis is based on a combination of clinical, pathological and radiographic features. Knee pain is the main clinical criteria.

The recent European League Against Rheumatism (EULAR) evidence-based recommendations for diagnosing knee OA have highlighted the importance of six clinical signs and symptoms which are the most useful in OA diagnosis. These included persistent knee pain, limited morning stiffness, reduced function, crepitus and bony enlargement (Zhang et al., 2010).

Table 1.2: The ACR criteria for classification of idiopathic osteoarthritis of the knee (Altman et al., 1986).

Clinical and laboratory	**Clinical and radiographic**	**Clinical**
Knee pain	Knee pain	Knee pain
At least 5 of:	Osteophytes	*At least 3 of:*
Age > 50 years	*At least 1 of:*	Age > 50 years
Stiffness < 30 minutes	Age > 50 years	Stiffness < 30 minutes
Crepitus	Stiffness < 30 minutes	Crepitus
Bony tenderness		Bony tenderness
Bony enlargement		Bony enlargement
No palpable warmth		No palpable warmth
ESR < 40mm/hour		
Rheumatoid factor < 1:40		
Synovial fluid signs of OA		

Abbreviations: ESR = erythrocyte sedimentation rate. Synovial fluid signs of OA (viscous, clear or white blood cell count <2,000/mm3).

1.2.6 Treatment

Currently, there is no known cure for OA. OA is a complex disease process; therefore management of the disease comprises of a holistic approach and is tailored individually to the patient. Combinations of non-pharmacological and pharmacological modalities are optimal to alleviate symptoms, inflammation, increase joint function and improve quality of life of the patient. The aims of treatment in OA are to educate the patient, alleviate pain, maintain function and slow or prevent disease progression. In patients where non-pharmacological and pharmacological therapies are no longer sufficient in relieving pain, surgical intervention may be beneficial. A brief flow chart of treatment strategies is outlined in figure 1.6.

1.2.6.1 Non-pharmacological management

Initially, core treatment is managed by a non-pharmacological approach. Patient education is a fundamental first step in order to implement life-style modifications. Exercise is encouraged in moderation to enhance aerobic fitness, build muscle strength, maintain range of articular motion and increase joint motility. Obesity is a risk factor for OA, therefore weight loss is recommended for overweight patients. Furthermore randomised controlled trials have shown weight loss to be of benefit in knee OA (Christensen et al., 2005). A combination of exercise and weight loss is most effective in reducing pain and improving function in overweight and obese people with symptomatic knee OA (Messier et al., 2004). Orthopaedic aids and devices such as supports, insoles, braces and canes may aid the management. Physical therapy may improve symptoms through increasing muscle stability.

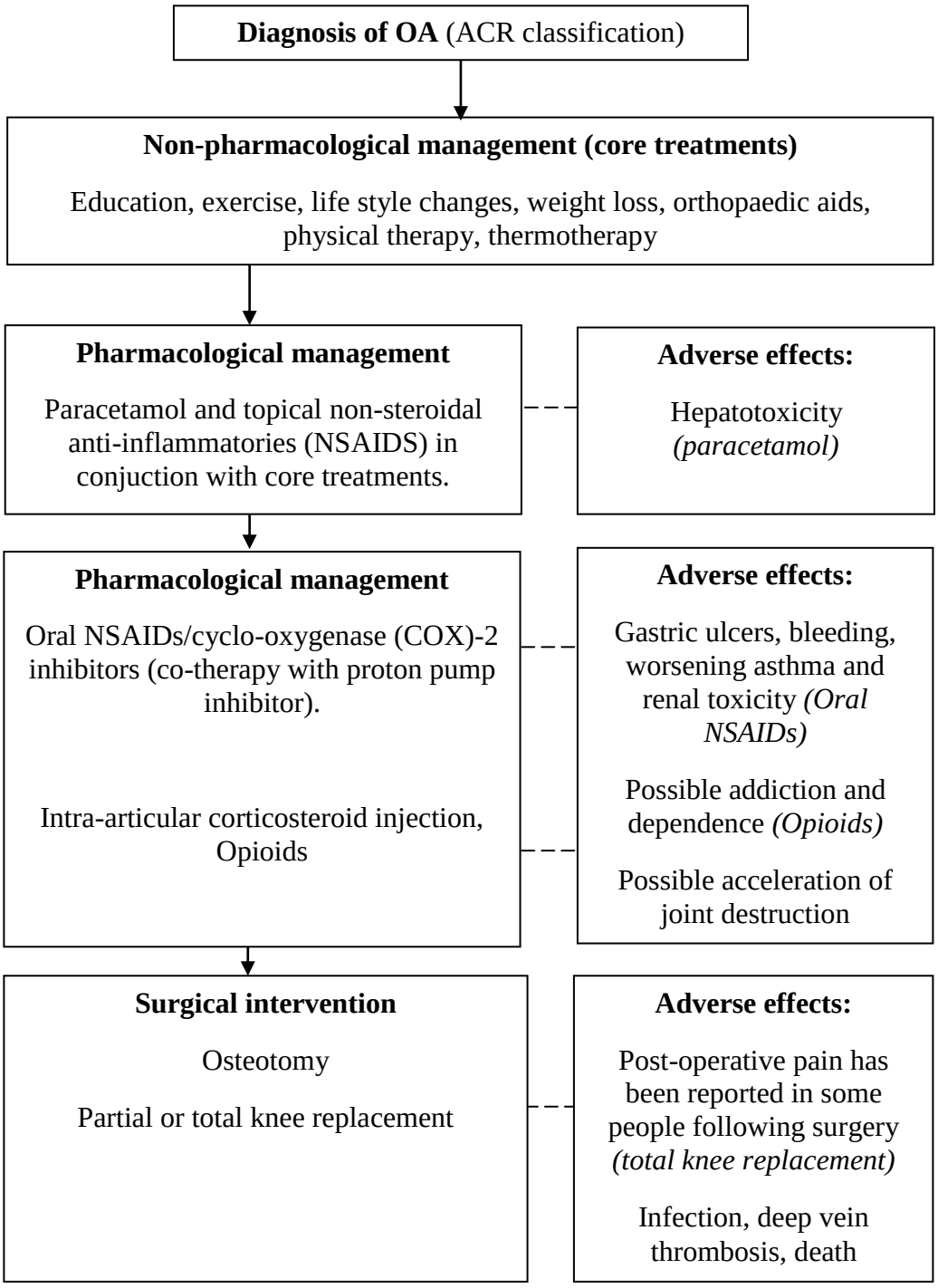


Figure 1.6: Therapeutic approach for knee OA.

Following diagnosis of OA the core treatment strategy using non-pharmacological modalities is first followed. If this is insufficient to alleviate pain and improve function, pharmacological treatments are employed. Finally, in patients who are refractory to both non-pharmacological and pharmacological modalities, orthopaedic intervention is sought. The therapies are accompanied by adverse effects as described in the right hand panel.

1.2.6.2 Pharmacological interventions

Drug therapy is considered in addition to core treatment strategy. Paracetamol is usually considered as the first line of treatment. The analgesic properties of paracetamol are effective for mild to moderate OA pain relief. However the recent OARSI guidelines advise clinicians to be cautious in prescribing paracetamol due to toxicity effects of long term use, especially in patients with comorbidities (Mcalindon et al., 2014).

Paracetamol in combination with topical non-steroidal anti-inflammatory drugs (NSAIDs) should first be considered. NSAIDs are used to alleviate inflammation and associated symptoms in the affected joint. The anti-inflammatory properties of classic NSAIDs, such as ibuprofen and naproxen are mediated through reducing the synthesis of prostaglandins by inhibiting cyclo-oxygenase (COX)-1 and COX-2 enzymes. Prostaglandins not only induce inflammation and pain, but also have a key role in the gastric mucosal defence. Long term uses of NSAIDs are therefore associated with adverse effects in the gastrointestinal tract in addition to nephrotoxicity (Ofman et al., 2002, Harirforoosh and Jamali, 2009). Chronic use of these drugs therefore can promote peptic ulceration and bleeds.

If paracetamol and topical NSAIDs are unable to provide sufficient pain relief, oral NSAIDs or COX-2 inhibitors should be considered, co-therapy with a proton pump inhibitor should be considered to protect against gastrointestinal ulcers associated with oral NSAID use (Scheiman, 2013).

Other pharmacological options include centrally acting analgesics such as opioids, although these drugs are associated with the risk of addiction and dependence. In patients with moderate to severe pain intra-articular corticosteroid injections should be considered. Steroid injections may be beneficial in improving pain and stiffness in OA patients who have previously not benefited from paracetamol or NSAID use (Raynauld et al., 2003). Injections may be given up to three to four times a year. Long term use of corticosteroids use may promote joint destruction, but this may be explained by natural OA progression.

The role of cytokines in OA pathophysiology has been widely reported (Fernandes et al., 2002). Anti-cytokine therapy therefore may be beneficial in preventing structural progression. Interleukin (IL)-1 and tumour necrosis factor (TNF)-α are major cytokines involved in OA pathophysiology (Bondeson et al., 2006). Evidence in animal models of OA reports favourable benefits of IL-1 receptor antagonist therapy (Fernandes et al., 1999, Pelletier et al., 1997); however clinical trial data in human studies reported no improvement in pain (Chevalier et al., 2009). Antibodies directed against nerve growth factor (NGF) are showing promising potential in reducing pain in patients with OA (Lane et al., 2010, Sanga et al., 2013), although clinical trials have been associated with rapidly progressing OA.

Hyaluronic acid (HA) is a natural component of the synovial fluid. Injection of HA has similar efficacy to oral NSAIDs and a lower risk of adverse effects (Ishijima et al., 2014). However the latest OARSI guidelines remain uncertain about the appropriateness of HA in OA (Mcalindon et al., 2014) therefore do not recommend it.

Recent OARSI guidelines recommend stratification of treatment dependent upon clinical sub-phenotypes (knee OA only, or multi-joint OA), in the presence or absence of comorbidities (Mcalindon et al., 2014). Co-morbidities include diabetes, hypertension, renal and cardiovascular disease, gastrointestinal bleeding, depression and obesity. For knee OA patients with co-morbidities topical NSAIDs and intra-articular corticosteroids in addition assistance with a walking cane should be considered (Mcalindon et al., 2014).

Ultimately targeted therapeutics to delay or halt the disease process and provide symptomatic relief, rest on the therapeutic potential of disease modifying OA drugs (DMOADs).

1.2.6.3 Surgical interventions

End-stage OA is characterised by severe chronic pain, stiffness, disability, loss of function, and reduction in quality of life. When non-pharmacological and pharmacological therapies are no longer effective in managing the symptoms, surgical intervention is considered.

Patients with unicompartmental tibio-femoral knee OA may benefit from a knee osteotomy correction. This is a realignment procedure which involves shifting the weight from the diseased area of the knee to the normal compartment.

Eventually patients with severe OA may be eligible for joint replacement surgery, to replace part of (unicompartmental knee replacement), or all of (TKR) the disease joint. Although TKR is associated with favourable outcome in the majority of patients, in one study 44% patients experienced post-surgical pain 3-4 years after athroplasty, which in 6% may be severe or neuropathic in nature (Wylde et al., 2011).

1.2.7 Phenotypes

Phenotype is defined as " The sum total of the observable characteristics of an individual, regarded as the consequence of the interaction of the individual's genotype with the environment; a variety of an organism distinguished by observable characteristics rather than underlying genetic features" (Oxford English Dictionary).

OA is a heterogeneous disease (Driban et al., 2010); not all patients experience the same clinical and pathological manifestations of the disease, which is demonstrated by the varied clinical presentations of OA patients. For example around half of patients with radiographic evidence of OA are asymptomatic (Hannan et al., 2000).

OA pathophysiology is extremely complex; there appear to be many distinct clinical phenotypes, or subgroups that constantly evolve leading to the common final end-point of OA. Classification of OA phenotypes may be based on many different variables. For example, developmental aetiologies, structural appearance, mechanism of onset, response to treatment, genetics, or pain type (centrally or peripherally mediated). The disease may be primarily mediated in the cartilage, subchondral bone, synovium or indeed any other tissue within the knee joint.

Identifying homogenous subgroups of patients is important to allow for stratification of treatments, by focusing on those which are most likely to

modify disease progression and improve outcomes. For example anti-inflammatory NSAIDs are administered to all patients with OA, if there is a sub-group of patients where subchondral bone remodelling, but not the synovium, might be playing a major role in the pathogenesis then NSAIDs are unlikely to have a major beneficial effect. As mentioned previously, the recent OARSI treatment guidelines are based on a stratified approach according to clinical subgroup (Mcalindon et al., 2014). In the future, stratified treatment may reduce referrals for surgical intervention, which would be of benefit to the patient and be beneficial in reducing the economic burden of the disease.

One approach to classifying patient phenotypes according to clinical or pathological characteristics is by statistical modelling. Latent class analysis (LCA) uses statistical methods to classify subtypes of related classes. Cases are assigned to their most highly probable latent class. LCA attempts to identify the smallest number of classes that group associated cases together (Muthen and Muthen, 2000). Cluster analysis uses a similar concept to latent class analysis. Cluster analysis has previously identified 5 OA phenotypes based on radiographic OA severity, lower extremity muscle strength and depression, and their associations with pain were determined using regression analysis (Knoop et al., 2011). Moreover homogeneous psychological phenotypes of patients with knee OA have been identified (Cruz-Almeida et al., 2013). However classifications based on histopathological characteristics are yet to be identified.

1.3 Early and late osteoarthritis

The exact pathogenesis of OA is difficult to determine, therefore defining the earliest pathological events which lead to OA is extremely challenging. There is no clear correlation between structural and symptomatic features of the disease (Dieppe et al., 1997). Structural changes may precede or follow symptoms in OA. The presence of pain is usually the reason patients first seek medical attention, by which time pathology may have been well established. Radiographs, magnetic resonance imaging (MRI) and arthroscopic examinations are extremely useful for detecting macroscopic abnormalities in the affected joint. However these imaging modalities are limited by their

insensitivity to detect discrete pathological alterations occurring at the molecular and cellular level in people with newly diagnosed OA. For the reasons outlined above, it is very difficult to reach a universally accepted consensus of the definition of 'early' OA.

Some research groups classify patients with knee pain with mild structural changes (Scanzello et al., 2009) or knee pain in the absence of radiographic change (Smith et al., 1997, Benito et al., 2005) as 'early' OA. Most work to date focuses on patients with mid-to end-stage OA. The earliest pathological events in OA are relatively unexplored.

An unmet need exists to identify pathological features which may be occurring earlier in the disease process which then may be driving secondary pathology in surrounding joint tissues. It is not clear which lesions occur first or if they develop in a temporal sequence. It is possible that multiple pathologies may occur in parallel and eventually converge to facilitate total joint failure. Or, different phenotypes of OA patients may exist. The primary source of pathology may be initiated in different tissues types in different people, which may be influenced by intrinsic or extrinsic risk factors.

Currently there is a limited access to study joint tissue from people with 'early OA' whose pain is less than that which would lead them to undergo joint replacement. Alternatively animal models of OA are extensively used and have been developed to mimic aspects of the disease process and provide a useful insight into pathological mechanisms. Although useful they may not model all aspects of the disease process.

1.3.1 Articular cartilage changes

The earliest morphological changes in the osteoarthritic cartilage have been proposed by various research groups to include; fibrillation, chondromalacia, necrosis and alteration of macromolecule composition. There are various hypotheses regarding the earliest pathological changes, however the initial structural and biochemical sequence of events leading to disease onset is yet to be determined. Defining early OA is challenging, as the disease is diagnosed when symptoms (such as pain) first appear, which can vary amongst suffers. At

the point of diagnosis the general features of early OA can be detected through radiographs, however the initial structural and biochemical features specific to the disease onset cannot be easily determined. Additionally, when studying human OA it is very difficult to define a normal aged-matched control group as the disease can be asymptomatic which can mask pathological changes.

Concepts of OA pathophysiology have proposed cartilage as the key mediator of pain and pathology, however since cartilage is normally aneural and avascular it cannot be the direct cause of pain (Swales and Athanasou, 2010).

In healthy cartilage, homeostasis is maintained through the controlled balance of catabolism and synthesis of extracellular matrix (ECM) by chondrocytes. Early OA is characterised by overexpression of collagen type II (Swales and Athanasou, 2010) and aggrecan synthesis by chondrocytes in medial and deep layers (Aigner et al., 1997). Furthermore there is a focal increase in cartilage volume during the earliest stages of the disease, see references in (Calvo et al., 2001, Swales and Athanasou, 2010, Cotofana et al., 2012). In contrast, as the disease progresses the balance is shifted in favour of degradation, promoting release of proteolytic enzymes, matrix metalloproteases (MMPs) from chondrocytes (Reboul et al., 1996). The exact mechanism regarding the trigger of MMP activity is still unknown; however evidence has suggested a role for various inflammatory cytokines, including IL-1 and TNF-α (Fernandes et al., 2002). Additionally, chondrocytes are subjected to phenotypic modulation, which is altered throughout the progression of the disease and may be induced by subchondral osteoblasts (Sanchez et al., 2005).

Hypertrophy and clustering of chondrocytes (figure.1.7A, inset) is a characteristic feature of the disease (Sandell and Aigner, 2001), the former is associated with elevated expression of alkaline phosphatase, MMP13 (James et al., 2005) and expression of collagen type X (Reichenberger et al., 1991). Chondrocyte hypertrophy is a normal feature of embryonic endochondral ossification; however it is a pathological process in OA. Other characteristic changes include loss of cartilage, calcification of articular cartilage and duplication of the tidemark (Oegema et al., 1997). Tidemark abnormality has been shown to precede cartilage surface lesions (Pesesse et al., 2011).

Chondromalacia (cartilage softening) is detected at arthroscopy and is believed to be due to elevated non-aggregated proteoglycan content; a major pathological feature in early OA. Normally, the low permeability of the matrix and hydraulic pressure maintains the stiffness of the cartilage which is essential for distributing compressive and tensile stresses over the bone.

Proteoglycan loss is a key feature in OA (Mankin et al., 1971) (figure. 1.7B), but occurs also in inflammatory arthritis without OA (Mitchell and Shepard, 1978) and is reversible (Malfait et al., 2009). Furthermore, there are changes in the molecular structure of proteoglycans; from the normal aggregated form to non-aggregated form. Subsequently, aberrant breakdown of the non-aggregated form increases hydraulic permeability, reducing the fluid pressure thus resulting in loss of stiffness and chondromalacia (Setton et al., 1994). Post-mortem studies have confirmed loss of cartilage stiffness is primarily due to loss of integrity of the extracellular matrix (Franz et al., 2001).

Cartilage degradation is a hallmark pathological feature of OA. In experimental studies histological cartilage surface integrity is evaluated (0 [normal] to 6 [complete disorganisation]) using the scoring system described by Mankin (Mankin et al., 1971). Fibrillation is a feature of OA and is histologically identified as clefts perpendicular to the articular surface (figure 1.7B), in early OA these irregularities originate at the superficial surface. As the disease severity progresses the lesions penetrate further into the cartilage and are identified in the middle, deep, and eventually the calcified layer in advanced OA. Fibrillation is a consequence of impaired integrity of the collagen network due to reduced fluid pressure as described above. Additionally, evidence suggests that fibrillation may be due to the reduced adhesion of chondrocytes to fibronectin, a large molecular weight glycoprotein (Piperno et al., 1998). In relation to fibrillation, water content in the cartilage is significantly increased in OA (Berberat et al., 2009). These features, along with the altered proteoglycan composition all contribute to increased permeability and decreased stiffness of the extracellular matrix.

Advanced OA is characterised clinically by chronic pain, loss of function, and joint deformity. Pathological features more commonly found in later OA

include the loss of proteoglycan content, in addition to pronounced fibrillation extending to the calcified layer. End-stage OA may result in complete loss of articular cartilage.

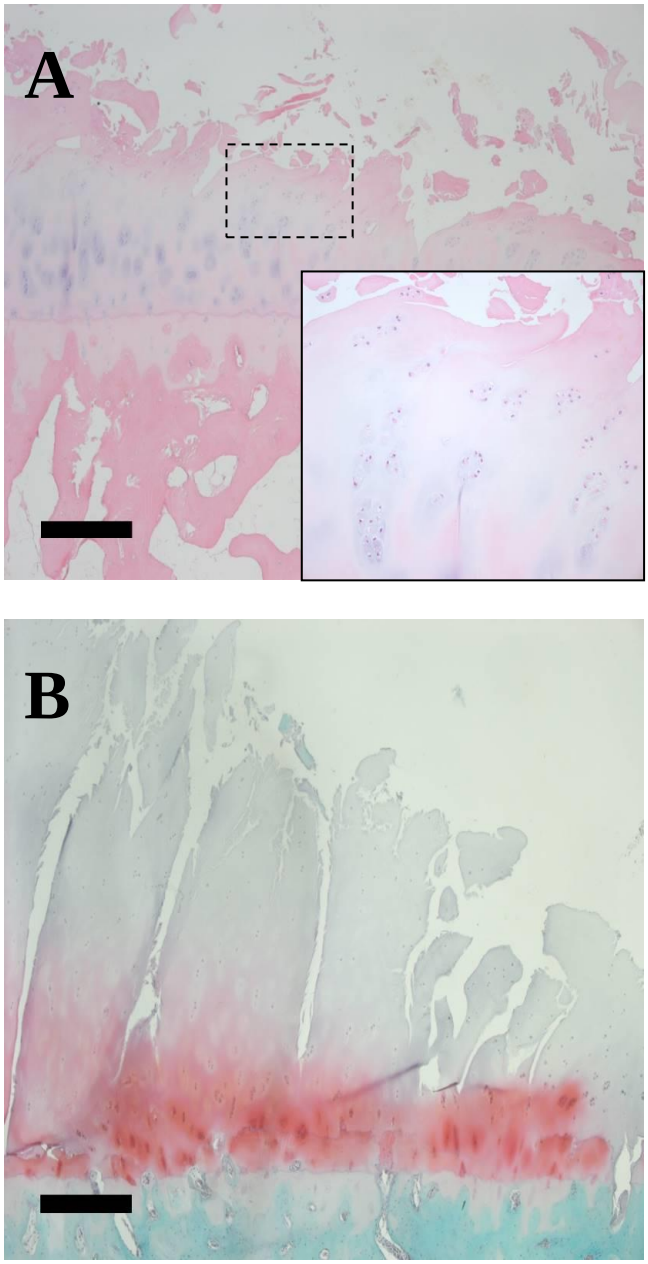


Figure 1.7: Histopathological features of osteoarthritic articular cartilage.

Cartilage fibrillation at the articular surface from the medial tibial plateau is shown. Inset: chondrocyte cloning within the articular cartilage **(A)**. Deep vertical clefts and proteoglycan loss are shown in **(B)**. Tissue morphometry is revealed by haematoxylin and eosin (H&E) staining **(A)** and Safranin-O staining **(B)**.

Chondrocytes in normal non-calcified articular cartilage maintain avascularity through secretion of anti-angiogenic mediators such as tissue inhibitors of metalloproteinases (Rundhaug, 2005) and troponin -1 (Moses et al., 1999). Vascular and neural invasion of articular cartilage might be a feature of OA joints, since tidemark breaching was found in 43% (16/37) TKR cases compared with 11% (1/9) PM cases (Suri et al., 2007). Phenotypic modification of chondrocytes to express angiogenic factors, such as vascular endothelial growth factor (VEGF) may play a crucial role in vascular invasion (Murata et al., 2008). Innervations by unmyelinated sensory nerves have been shown to accompany blood vessel invasion in late OA, mediated by NGF production (Nico et al., 2008).

Difficulty arises when trying to definitively separate OA induced cartilage changes from normal age-related changes. A study by Hudelmaier's group aimed to determine age-related changes in the articular cartilage (Hudelmaier et al., 2001). Their study showed that in 'healthy' asymptomatic knees of individuals between 50 – 78 years old femoral articular cartilage had undergone significant thinning (21% and 13% in women and men, respectively). However, these results cannot conclusively rule out the presence of asymptomatic preclinical OA.

1.3.2 Subchondral bone modifications

Alternative theories of OA initiation postulate morphological changes in subchondral bone advance before the degradation of articular cartilage. Early evidence clearly showed bone rigidity precedes cartilage damage in experimental models of OA in Guinea pigs (Simon et al., 1972). In support, Radin and colleagues (Radin and Rose, 1986) suggested that architectural changes in bone density and rigidity are increased due to pressure induced microfractures in the trabecular bone. Consequently there is an impaired ability for the stiffened bone to act as a shock absorber, which potentiates stress induced lesions in the cartilage.

Throughout the course of OA remodelling in the subchondral bone is observed. These include; changes in bone mineral density (BMD), bone marrow lesions (BML), sclerosis and osteophyte formation (protrusions of bony spurs).

1.3.2.1 Bone marrow lesions

Bone marrow lesions (BML) in the subchondral bone can be observed on magnetic resonance imaging (MRI) in patients with OA. These lesions are represented both as a hypointense or hyperintense signal in T1 or T2 weighted MRIs, respectively (Bassiouni, 2010). Histologically, BML have been reported as manifestations of necrosis, fibrosis, bone marrow bleeding, trabecular microfractures and bone marrow oedema (BME) with areas of enhanced vascularisation (Zanetti et al., 2000, Eriksen and Ringe, 2011).

Malalignment of the knee appears to be involved in determining the onset and anatomical location of BML. Medial lesions are associated with varus knee; in contrast valgus knee is related to lateral lesions (Felson et al., 2003). BML have also been shown to be located centrally, which are related to anterior cruciate ligament pathology (Hernandez-Molina et al., 2008a). Mechanical loading has also been shown to predispose BML. Local bone mineral density (BMD) is strongly related to increased mechanical loading where the difference in BMD in the medial and lateral tibial plateau (M:L BMD ratio) reflects the difference in loading across the knee. Increased loading of the medial tibial plateau (high M:L ratio) is associated with increased medial BMD and the occurrence of medial BML, a lower M:L ratio is associated with lateral lesion formation (Lo et al., 2005).

Longitudinal MRI studies have found a positively correlated relationship between size of BMLs and subsequent cartilage degeneration (Hunter et al., 2006a, Roemer et al., 2009b). Additional evidence has shown BMLs are strongly associated with OA severity. When comparing mild and severe OA (assessed by Kellgren-Lawrence scale) BML were found in 41% of mild OA, compared to 94% in advanced OA at baseline (Phan et al., 2006). Furthermore, subchondral cysts are a characteristic feature of advanced OA and may be associated with the development of BMLs (Kornaat et al., 2007). However it is possible that BMLs and cysts may just be present in the same arthritic knee, rather than being a direct consequence of each other.

The natural progression of BMLs has been explored in a recent study of individuals with no clinical diagnosis of OA. Within two years 14% of the

knees developed BMLs, which were strongly associated with an increase in body mass index (BMI). Interestingly just less than half (46%) of lesions present at the beginning of the study had decreased after two years (Davies-Tuck et al., 2009). When assessing the stability of BMLs in symptomatic OA, there have been several conflicting findings in the literature. Garnero showed there was both a decrease (9.8%) and increase (18.8%) in BML score in patients with OA, although these measurements were only collected after 3 months (Garnero et al., 2005). In contrast, Hunter et al. reported that in 99% of patients BMLs increased or remained the same, after a 30 month follow up study (Hunter et al., 2006a). In conclusion, BML formation appears to be a dynamic process, this may account for disparities within the literature.

1.3.2.2 Bone remodelling and osteophyte formation

Bone anabolic and catabolic activity is normally balanced to maintain bone homeostasis. In OA these processes are shifted in favour of increased bone formation and deposition manifesting as osteophytes, sclerosis and bone remodelling. This can be detected by measuring biomarkers of bone formation such as osteocalcin, which have been shown to be 47% greater in patients with severe OA compared with less severe OA (Sharif et al., 1995). Moreover, collagen breakdown, hence bone remodelling, is found to be higher in OA sufferers compared to healthy controls (Seibel et al., 1989).

Bone remodelling refers to the progressive change in structural architecture through anabolic activity, which may be attributed to mechanical loading. As the severity of OA advances, cartilage loss exposes the subchondral bone which is then more prone to sclerosis, these polished bone areas are referred to as eburnation (Shepstone et al., 2000).

Radioisotope studies have been important in monitoring the changes of bone in early OA and predicting the nature of progression. In knee OA, measureable sclerosis of the subchondral cortical plate and trabeculae may sometimes occur before joint space narrowing (JSN). However, further sclerosis did not progress until JSN was smaller than 1.5 mm in one study (Buckland-Wright, 2004). A recent Framingham OA study used MRI imaging and radiographs to determine the extent of bone attrition in the tibiofemoral joint. Bone attrition refers to the

remodelling of the subchondral bone in OA which causes changes in the bone shape. Bone attrition was evident in 14.8% of patients classified as having mild OA, in the absence of JSN (Reichenbach et al., 2008).

Furthermore, retrospective studies assessing the earliest bone alternations in OA have examined patients with ligament ruptures, as the pathology has been shown to lead to early OA (Lohmander et al., 2004). After 3 to 4 years following the trauma, the injured knees showed evidence of subchondral trabeculae sclerosis, with osteophytes in 50% of these knees, in the absence of JSN (Buckland-Wright et al., 2000). Nevertheless the time course of the changes may be different to those observed in primary OA. Subchondral sclerosis appears to be site specific and dependent on the time course of the disease. Thickening of the bone plate is a feature associated with late OA; as sclerosis was not detected after two years in one study (Buckland-Wright et al., 1995) but was associated with joint space width smaller than 1.5 mm, which is indicative of advanced OA (Buckland-Wright et al., 1994). In comparison, early sclerotic changes have been reported in cancellous bone and horizontal trabeculae (Buckland-Wright et al., 1996).

Osteophytes are a common feature of OA and are identified through radiographic imaging. The aetiology and pathogenesis of osteophytes is not entirely clear. It is postulated that osteophytes may develop as a homeostatic response to stabilise the OA joint (Pottenger et al., 1990), to maintain the normal joint shape in addition to support areas of cartilage under stress (Swales and Athanasou, 2010). Osteophytes are cartilaginous and osseous protrusions within the joint capsule and synovial envelope which develop pathologically through endochondral ossification. Various endogenous growth factors have been linked to osteophyte formation, including transforming growth factor-beta (TGF-β) (Uchino et al., 2000). In addition to bone morphogenic proteins (BMP) which are usually observed during embryogenesis; which further supports the role of endochondral ossification in the developmental process of osteophyte formation (Zoricic et al., 2003). Similar to BML, the medial and lateral location of osteophytes appears to be determined by varus and valgus alignment, respectively (Felson et al., 2001).

1.3.3 Synovial inflammation

Synovial inflammation is not exclusive to rheumatoid arthritis (RA), but is a well recognised feature of both early and late stage-OA (Smith et al., 1997). Synovial pathology is characterised as synovitis, which manifests clinically as local inflammation. Synovitis may be persistent or, episodic, and varying degrees of inflammation are detected in patients with OA. Imaging techniques, such as MRI and ultrasound in addition to histology are useful in identifying and quantifying synovial inflammation.

Biopsies of synovial tissue are most commonly obtained at arthroscopy or the time of TKR in patients with symptomatic OA. Various key characteristics are observed in the synovium throughout the disease process. Pathologically, histological hypertrophy and hyperplasia of the synovial membrane in addition to lymphocyte and macrophage infiltration, are a key feature throughout disease progression (Myers et al., 1990, Haywood et al., 2003).

Synovial inflammation is observed in early OA. Benito et al aimed to compare immunohistochemical features of inflammation in patients with early and end-stage OA. Early OA was associated with increased inflammatory cell infiltration (CD4+; T helper cells and CD68+; pan macrophages), angiogenic factors (VEGF), and blood vessel formation compared to patients with end-stage OA (Benito et al., 2005). Patients with knee pain, in the absence of radiographic manifestations of OA but with arthroscopic evidence of chondropathy were classified as having early knee OA.

Synovitis is also a feature of end-stage OA. A third of patients who had undergone TKR or arthroscopy for symptomatic OA showed histological evidence of severe synovial inflammation (Haywood et al., 2003). Synovitis is associated with thickening of the synovial capsule (Hunter et al., 2013).

Synovial angiogenesis is associated with end-stage OA, and is positively correlated with histological synovitis grading (Walsh et al., 2007). VEGF release from macrophages and from some fibroblasts in the inflamed synovium may be associated with synovial angiogenesis (Ben-Av et al., 1995, Haywood et al., 2003).

Synovitis is not only caused by OA, other causes of synovitis include chondrocalcinosis and amyloid deposits. Chondrocalcinosis is characterised by the deposition of calcium pyrophosphate dehydrate (CPPD) or basic calcium phosphate (BCP) in joint tissues, and can be associated with histological synovitis (Swan et al., 1995). Synovial amyloid deposition may cause synovitis through synovial macrophage phagocytosis which may initiate and perpetuate local inflammation (Pessler et al., 2014).

1.4 Pain

Pain is defined as "an unpleasant sensory and emotional experience associated with actual or potential tissue damage or described in terms of such damage" (Merskey and Bogduk, 1994). Pain is a protective evolutionary drive to prompt us to avoid damaging stimuli in the environment. It is a complex multimodal phenomenon that may comprise physiological, inflammatory and neuropathic elements. Minor tissue damage elicits a brief excitation of sensory nociceptors which usually subsides. Occasionally pain can persist beyond the usual recovery period and can become chronic and debilitating. Chronic pain presents significant challenges and is associated with major social and economic impacts.

The "gate control theory" of pain was first proposed by Melzack and Wall in 1965. The theory alludes to a gated mechanism within the dorsal horn of the spinal cord which modulates afferent input via the spinothalamic tract to the higher brain centres (Melzack and Wall, 1965). This theory underpins modern principles of pain pathway physiology.

Under normal situations peripheral nociceptors are not responsive to normal ranges of movement and are only activated by extreme mechanical, physical or chemical noxious stimuli. Signal transduction generates action potentials which are transmitted through sensory Aδ and C-nociceptive fibres which terminate in laminar IV and II, respectively of the spinal cord dorsal horn, see references in (Hunter et al., 2008). Signals are then transmitted along ascending pain pathways to higher brain centres (hypothalamus, thalamus and cortex) where the sensation is perceived as pain. Pain signalling is modulated by facilitatory

and inhibitory feedback loops in both the spinal cord and higher brain centres, see references in (Hassan and Walsh, 2014).

The transition between acute and chronic pain is mediated through remodelling of the highly plastic neuronal architecture in response to repeated or intense stimulation of peripheral or central nociceptive pathways. Over time nociceptor threshold activation is reduced and pain processing altered, leading to phenotypic alterations in both the dorsal horn and higher brain centres. Furthermore nerve damage may induce neuropathic pain see references in (Dickenson, 2002). Neuropathic pain like symptoms (eg lowered pain thresholds) may be prevalent in patients with severe OA, and may be associated with damage sustained at previous knee surgery (Valdes et al., 2014).

Accordingly, pain can be generated spontaneously and in response to usually non-painful (innocuous) stimuli such as increased physical activity, which is clinically defined as allodynia. There may also be an amplified response to stimuli that normally cause pain (hyperalgesia).

1.4.1 Peripheral nociception

The capsule, menisci, ligaments, periosteum and bone are richly innervated by sensory Aδ and C nociceptive fibres see references in (Mcdougall, 2006, Hunter et al., 2008). During inflammation or tissue damage noxious pro-inflammatory mediators including NGF, substance P (SP), bradykinin, 5-(HT) hydroxytryptamin (serotonin) and histamine are released from inflammatory cells into the joint see references in (Rang et al., 1991). Inflammation is amplified by the paracrine action of mediators inducing further release of inflammatory cytokines from inflammatory cells, thus perpetuating the inflammatory process.

Eventually these inflammatory substances, directly or indirectly (through other cells) sensitise primary afferent joint receptors through reducing Aδ and C-fibre, activation thresholds see references in (Hunter et al., 2008) which act to increase responsiveness. Furthermore silent (or ‘sleeping’) nociceptors which are usually quiescent become active during inflammation which further

contributes nociceptive input to the spinal cord (Schaible and Grubb, 1993, Schmidt et al., 1995).

The highly plastic nature of the nociceptive system is demonstrated by a phenotypic switch of proprioceptive Aβ fibres to possess characteristics of C fibres following prolonged inflammation (Neumann et al., 1996). Aβ fibres may contribute to pain under some conditions, and can contribute to peripheral and central hypersensitivity by expressing and releasing the pro-inflammatory mediator SP (Neumann et al., 1996).

1.4.2 Central sensitisation

The International Association of the study of Pain (IASP) define central sensitisation as "increased responsiveness of nociceptive neurons in the central nervous system to their normal or subthreshold afferent input". Prolonged and enhanced peripheral nociceptive function and input induced by neural injury or inflammation to the spinal cord leads to an increase in the excitability of spinal cord neurons and subsequently maladaptive modifications in central pain processing (Woolf, 1983). Central sensitisation is characterised clinically as hypersensitivity to pain; allodynia (pain to innocuous stimuli, i.e., reduction in threshold), hyperalgesia (heightened pain sensitivity) and increased temporal summation. Physiologically, there is an increased membrane excitability, synaptic efficacy and reduced activation threshold of second order spinal cord neurons to peripheral input (Woolf, 2011).

Synapses are subject to activity-dependent plasticity. Repeated low frequency stimulation of dorsal horn C-fibres (>0.3 Hz) elicits a progressive increase in the magnitude of C-fibre evoked action potentials (Mendell, 1966). 'Wind up' can lead to a facilitation of spinal processing of sensory neurons (homosynaptic potentiation), and sustained firing of C-fibres causes the release of the excitatory neurotransmitter glutamate. Heterosynaptic potentiation refers to facilitation where the activity of afferent input (conditioning input) enhances the activity of other nociceptor and non-nociceptor fibres (test input) (Thompson et al., 1993).

Central sensitisation constitutes an augmented responsiveness of the nociceptive system that is triggered by the release of excitatory neurotransmitters (such as glutamate and substance P) in the dorsal horn to enhance synaptic efficacy (Woolf and King, 1990). Moreover synaptic strength is enhanced by increasing post-synaptic membrane excitability and reducing inhibition (Sivilotti and Woolf, 1994). The functional properties, activation thresholds and kinetics of post-synaptic membrane ion channels and receptors are altered. Moreover, normally subthreshold synaptic inputs, including low-threshold Aβ fibres are now recruited see references in (Woolf and Salter, 2000).These changes all act to enhance pain transmission.

Key glutamatergic receptors involved in central sensitisation are the *N*-methyl-$_{D}$-aspartate (NMDA) and ionotropic amino-3- hydroxy-5-methyl-4-isoxazole propionate (AMPA) receptors. SP also plays a key role in the development of hyperalgesia (Moochhala and Sawynok, 1984) and generating central sensitisation (Khasabov et al., 2002)

Central sensitisation is also characterised by expansion of peripheral receptive fields. Receptive fields refer to the area over which a stimulus leads to a nociceptive response. Expansion of receptive fields occurs in chronic pain when a hyper-excitable dorsal horn neuron is depolarised by areas adjacent to the normal receptive field (Neziri et al., 2010).

Central sensitisation plays an important role in symptomatic OA. Pain is observed at areas remote from the site of injury, which is referred to as secondary hyperalgesia or referred pain (Hunter et al., 2008, Neziri et al., 2010). Moreover, pain pressure thresholds in OA patients are reduced both at the arthritic joint and at remote sites compared to healthy controls, as measured by quantitative sensory testing (QST) (Suokas et al., 2012). Furthermore OA patients have enhanced duration of pain intensity compared to non-arthritic age matched controls following intramuscular infusion of saline (Bajaj et al., 2001), implying a strong role of central sensitisation in OA patients. There is a poor correlation between structural pathology and pain (Bedson and Croft, 2008) which may be partly explained by the presence of central sensitisation in OA patients.

1.5 Peripherally mediated pain in osteoarthritis

Pain is the most distressing concern of patients with knee OA and is the main reason sufferers seek medical assistance. OA is the biggest cause of joint pain in the elderly (Dieppe and Lohmander, 2005). Pain is initially managed through pharmacological treatment strategies. However despite many years of pain research, some patients are refractory to current medical interventions and long term use of analgesic and anti-inflammatory therapies are limited by safety concerns and tolerability. Patients whose constant and severe pain impairs their quality of life may benefit from TKR. The direct cause of pain in OA remains unclear.

The knee joint is innervated by sensory and sympathetic branches of the nervous system (Gardner, 1948). The synovial lining, joint capsule, subchondral bone, periosteum, outer region of the meniscus, peri-articular ligaments and muscle are richly innervated therefore any of these structures may be involved in pain genesis (Hunter et al., 2008, Felson, 2009, Hunter et al., 2013). Difficulty arises in determining the earliest events leading to the onset of OA and the time course where pain develops, as the disease is often diagnosed at a later stage.

1.5.1 Structural associations of pain

The relationship between OA knee pain and structural pathology is not entirely clear, due to the discordance between radiographic features and clinical symptoms (Dieppe et al., 1997, Bedson and Croft, 2008). Radiographs are less sensitive than MRI and are unable to detect all associations of symptomatic OA. MRI studies have provided evidence for a possible association of BMLs and synovitis with pain (Felson et al., 2001, Hill et al., 2007); these features are not easily detected on radiographs which may partly explain the discordance. Additionally, disparities within the literature may result from differences in defining knee pain. A recent systematic review showed the association between pain and radiographic OA was dependent upon the definition of pain in each study (Bedson and Croft, 2008). Nevertheless Duncan et al reported an association between radiographic OA with pain, both in terms of duration and severity, stiffness and disability (Duncan et al., 2007). However, the study

sample only included patients over 50 years old with knee pain, had the group also looked at asymptomatic individuals it is likely they too would have radiographic evidence of OA.

TKR is an effective intervention in alleviating pain and disability in sufferers with end-stage OA where non-surgical methods have proved unsuccessful. Over 69,000 procedures were performed by the NHS in 2014 (Njr, 2015). The degree and extent at which knee pain impacts on the patients' quality of life is a clear determinant in the decision to undergo surgery.

Cartilage loss has shown to be indicative of future TKR. In one study a 1% loss as measured using MRI, increased surgery risk by 20% in patients with OA (Cicuttini et al., 2004). In support, a recent longitudinal study of patients with knee OA found annual cartilage loss to be strongly associated with increasing BMLs, which in turn was shown to be a strong predictor (57%) of TKR after four years (Tanamas et al., 2010b). Furthermore, subchondral bone cysts have been shown to be associated with annual medial cartilage loss which may increase the risk of TKR (Tanamas et al., 2010a).

The next sub-sections will describe evidence for the association of pain with various structural features including synovitis and subchondral bone alterations (Torres et al., 2006) identified by imaging studies. However it should be considered that it is difficult to determine independent associations between structural pathology and pain as findings may be confounded as structural change is co-linear as OA progresses.

1.5.2 Synovitis and pain

The role of synovitis is increasingly being recognised as an important feature of early and late OA (Smith et al., 1997, Haywood et al., 2003, Bondeson et al., 2006). The synovium is richly innervated with nociceptive fibres (Mapp, 1995). The overproduction of pro-inflammatory mediators such as cytokines and prostaglandins (De Lange-Brokaar et al., 2012) during inflammation or tissue injury is believed to play a key role in OA pathogenesis (Bondeson et al., 2006). These mediators may cause pain by sensitising or activating sensory nerves (Kidd et al., 2004). The pro-inflammatory cytokines that are regarded to

play a major role in OA pathogenesis include IL-1α, IL-1β and TNF-α (Fernandes et al., 2002). The association between pain, and synovial fluid levels of TNF-α and IL-6 have been investigated recently; TNF-α was strongly correlated with pain as assessed by the Western Ontario and McMaster Universities Osteoarthritis index (WOMAC) questionnaire. IL-6 was correlated with joint stiffness and negatively correlated with Kellgren-Lawrence radiographic grading, suggesting a role for the cytokine in the initial progression of OA (Orita et al., 2011).

Fluctuations in pain are common in OA patients (Hawker et al., 2008). A recent study demonstrated that fluctuations in synovitis are associated with fluctuations in knee pain (Zhang et al., 2011b). In support, other imaging studies have demonstrated a strong association of synovitis with knee pain (Hill et al., 2001, Torres et al., 2006, Hill et al., 2007, Baker et al., 2010). Moreover, the therapeutic benefit of intra-articular glucocorticosteroids (Raynauld et al., 2003) and NSAIDs (Pincus et al., 2001, Boureau et al., 2004) reflect the importance of synovial inflammation in OA pathophysiology. Conversely a recent study failed to show an association between synovitis and pain, but did show an association with functional impairment and disability (Liu et al., 2010). The reasons for the dissociation between pain and synovitis are unclear; they may be due to differences in patient populations studied.

In advanced OA, it is believed that matrix fragments of eroded articular cartilage in addition to segments of osteophytes may become detached and form loose bodies (Swales and Athanasou, 2010). Loose bodies may be incorporated into the synovial membrane through synoviocyte phagocytosis (Sellam and Berenbaum, 2010). This may then induce an inflammatory synovial response; proteolytic enzymes and pro-inflammatory mediators diffuse into the cartilage to stimulate chondrocytic protease synthesis, amplifying cartilage degradation (Sellam and Berenbaum, 2010).

1.5.3 Subchondral pathology and pain

Bone marrow lesions may be associated with symptomatic OA. Felson and colleagues (Felson et al., 2001) undertook a cross-sectional observational study and showed that BMLs were present in 77.5% of individuals with symptomatic

knee OA. Furthermore, BMLs have been found to be associated with not only the presence of pain but also pain severity (Torres et al., 2006). A recent study demonstrated that fluctuations in BMLs are correlated with fluctuations in knee pain, providing further evidence for a role of BMLs in OA (Zhang et al., 2011b). Moreover, BMLs larger than 1cm were more frequent in patients with painful knee OA than in those with asymptomatic OA (Sowers et al., 2003). Nevertheless, there are a small number of studies which challenge the relationship between BMLs and pain. For example, Kornaat and colleagues (Kornaat et al., 2006) examined the association between MRI features of OA and pain, and reported that bone marrow oedema (BME) was observed in 45% of patients who were pain free. The disparities may be explained by differences between experimental criteria; Kornaat's group included patients with various types of OA (hand, spine and hip) but did not necessarily show evidence of radiographic knee OA, whereas Felson included patients with more severe knee OA.

Bone attrition (flattening of the subchondral bone) in OA may be associated with knee pain. In the Framingham osteoarthritis study of patients with OA, knee pain was present in 74% of cases with attrition, and in 58% without. However attrition was often observed alongside BMLs and effusion, which suggests attrition may not be independently associated with pain (Hernandez-Molina et al., 2008b).

Subchondral bone sclerosis has been shown to be strongly associated with pain; more so when the pathology occurs in both patella-femoral and tibial plateau compartments, as opposed to in just one compartment (Szebenyi et al., 2006). Furthermore, a recent study showed that specific alterations of the bone including BMLs in the lateral patella were predictive of knee pain developing after 15 months in individuals with OA but without knee pain at baseline (Javaid et al., 2010).

1.5.4 Meniscal pathology and pain

MRI has been pivotal in characterising meniscal changes throughout the course of OA. Meniscal damage and abnormal positioning have been found to be detrimental in heightening the risk of cartilage loss (Hunter et al., 2006c), thus

are strongly related to the progression of OA (Berthiaume et al., 2005). OA induced morphological changes in the joint can be monitored through measurement of JSN in weight-bearing radiographs. JSN is indicative of both cartilage and meniscus degeneration (Hunter et al., 2006b) . The relationship between meniscal damage and knee pain has been studied by Englund et al (Englund et al., 2007). The group concluded that after 15 months from baseline measurements, meniscal damage was slightly higher in patients with knee pain than control knees (38% compared to 29%). Although these differences could be attributed to the slightly higher percentage of females in the case group (72% compared with 60%) as OA is more common in females (Grotle et al., 2008).

A study examining the correlation between pathological lesions and pain severity showed that meniscal tears, in addition to BMLs, synovitis/effusion, and bone attrition were significantly associated with knee pain (Torres et al., 2006). However, meniscal pain may not be associated with pain independent of synovitis or bone marrow lesions. Structural change is co-linear; people with severe OA are more likely to have worse structural change in many different tissues.

Another study (Bhattacharyya et al., 2003) demonstrated that meniscal tears were more common in symptomatic OA cases compared with asymptomatic controls (91% vs. 76%), respectively. Nevertheless OA knees with meniscal tears were no more painful than those without tears (Bhattacharyya et al., 2003) and meniscal tears are commonly observed in the general population (Englund et al., 2008). However, angiogenesis (the growth of new blood vessels) and accompanied sensory nerve growth in the meniscus, may mediate an association between meniscal pathology and pain (Ashraf et al., 2011).

1.6 Inflammatory mediators in osteoarthritis

OA pathogenesis is underpinned by a complex interplay of noxious biochemical signals released within the knee joint following trauma. Cytokines, chemokines, growth factors and MMPs play a crucial role in perpetuating inflammation through activating downstream signalling pathways. Furthermore inflammatory mediators induce or facilitate pain and hyperalgesia.

1.6.1 Nerve growth factor

NGF was first discovered more than 60 years ago as the founding member of the neurotrophin family (Levi-Montalcini and Hamburger, 1951). NGF is essential for promoting sympathetic and parasympathetic neuronal growth and survival in the developing nervous system (Levi-Montalcini, 1987). NGF is secreted as a pro-neutrophin and cleaved to its mature form by endoproteinases such as plasmin and MMP7 (Lee et al., 2001, Le and Friedman, 2012).

The biological effects of NGF are mediated through two cell surface receptors; transmembrane tyrosine kinase (Trk) A, and p75 neurotrophin receptor ($p75^{NTR}$) (Chao and Hempstead, 1995) located on sensory nociceptive terminals. The β-subunit of NGF binds selectively and with high affinity to TrkA, whereas $p75^{NTR}$ is a pan-neurotrophin receptor, binding all members of the neurotrophin family (brain derived neurotrophic factor (BDNF), and neurotrophin (NT) -3 and 4) with similar low affinity (Pezet and Mcmahon, 2006).

Clinical and experimental evidence has suggested an important role for NGF in the genesis and maintenance of hyperalgesia (Woolf, 1996). NGF levels are elevated in inflammation and in a variety of rheumatic diseases (Seidel et al., 2010), particularly in the synovial fluid of patients with inflammatory arthritis (Halliday et al., 1998, Barthel et al., 2009, Raychaudhuri et al., 2011). NGF may play a key role in mediating inflammatory pain through increasing nociceptor excitability in OA (Ashraf et al., 2014).

Genetic mutations in the genes that encode TrkA or NGF are clinically classified as type IV and V hereditary sensory autonomic neuropathies (HSANs), respectively. Individuals with the mutations are characterised by congenital insensitivity or decreased ability to perceive pain (Mckelvey et al., 2013). Antagonism of NGF therefore has potential analgesic properties in the treatment of chronic pain.

Clinical trials using various humanised monoclonal antibodies directed against NGF have shown great success in reducing pain and improvement of function in patients with moderate to severe knee OA; inferring a causal link between

NGF and symptomatic OA. Tanezumab was the first agent placed into clinical trials (Lane et al., 2010, Brown et al., 2012). Other agents including Fulranumab (Sanga et al., 2013) and Fasinumab (Tiseo et al., 2014) have also shown analgesic benefits in alleviating symptoms in OA. However the concerns regarding long term safety and efficacy of these agents has been highlighted following reports of rapidly progressive OA leading to joint replacement surgery. Subsequently the US Drug and Food Administration (FDA) halted clinical trials in 2010. Trials were resumed in 2012 but were subsequently put on hold further due to sympathetic problems (Tiseo et al., 2014). Trials may resume, but have not done yet.

NGF facilitates pain transmission by various mechanisms, which ultimately induce peripheral sensitisation of nociceptors, manifesting clinically as hyperalgesia. Inflammatory states and tissue damage mediate local production of inflammatory mediators such as IL-1 and TNF-α (Sellam and Berenbaum, 2010). Subsequently, IL-1 and TNF-α promote the production of NGF (Manni et al., 2003), along with other inflammatory mediators from local structural and inflammatory cell types such as macrophages, fibroblasts and lymphocytes. Binding of NGF to TrkA receptors on mast cells induces further release of inflammatory mediators such as serotonin, histamine, and NGF (Bruno and Cuello, 2006).

The binding of NGF to its cognate receptor TrkA on sensory nerve terminals initiates various pathological processes:

1. The ligand-receptor complex is retrogradely transported to the neuronal cell body to regulate gene transcription (Ginty and Segal, 2002). During pathology there is enhanced expression of proteins such as SP, BDNF and sodium channel,$Na_v1.8$ that act to increase nociceptor excitability (Bruno and Cuello, 2006).

2. NGF binding to TrkA receptor on sensory terminals mediates rapid post-translational changes to Transient Receptor Potential Vanilloid 1 (TRPV1) heat-gated ion channel, including up regulation and phosphorylation of channel expression (Zhang et al., 2005b).

The aforementioned post-translation changes reduce the channel activation threshold of various ion channels (including TRPV1 and acid sensing ion channel 3 [ASIC3]) (Mantyh et al., 2011), which act to increase channel excitability and facilitate chronic pain states. The sequence of NGF induced modulation of gene expression and TRPV1 channels is illustrated in figure 1.8.

NGF induced hyperalgesia is believed to be mediated by the three mitogen activated protein kinase (MAPK) downstream signalling pathways; ERK, p38 MAPK and c-JUN N-terminal kinase (Ji et al., 2002, Zhuang et al., 2004, Doya et al., 2005).

In addition to NGF, TRPV1 is also sensitised by a variety of stimuli including capsacin, noxious heat (>43°C), low pH, lipids such as anandamide (Cavanaugh et al., 2011). TRPV1 is involved in peripheral sensitisation and primary hyperalgesia (Delozier et al., 2007). Other pathways are up-regulated in hyperalgesia include ASIC channels (Abramova et al., 2013).

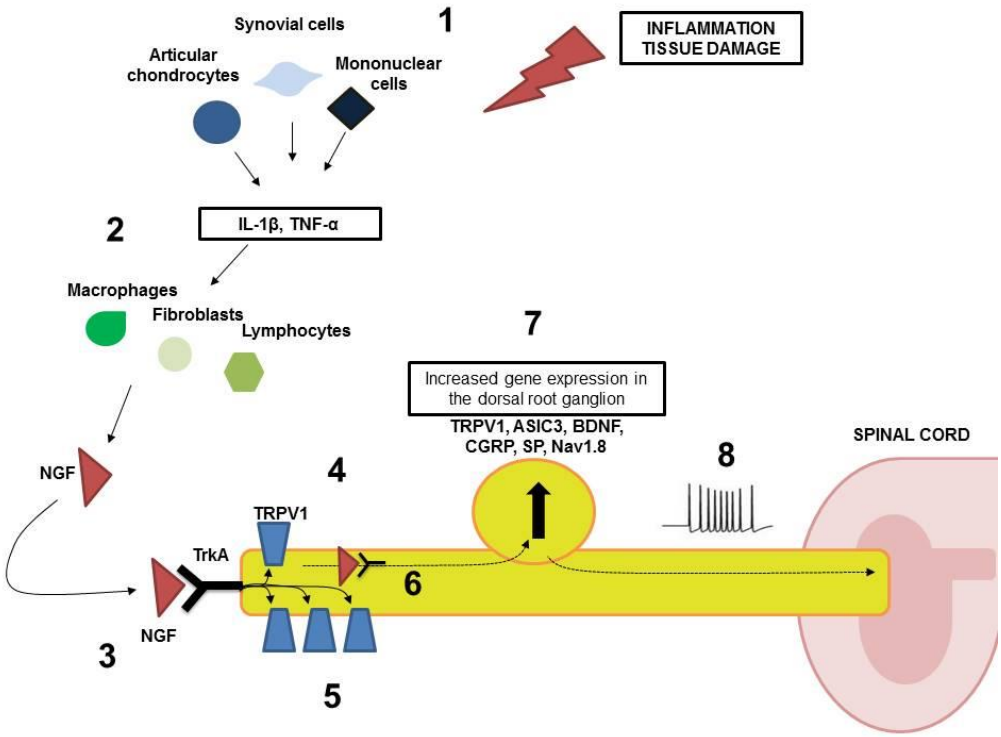


Figure 1.8: Schematic diagram showing the modulation and up-regulation of pro-inflammatory mediators in the dorsal root ganglion by NGF following inflammation or tissue damage.

1. During inflammation or tissue damage pro-inflammatory cytokines IL-1β and TNF-α are released from synovial cells, mononuclear cells and articular chondrocytes. **2.** Subsequently the cytokines stimulate the release of proNGF and other mediators from immune cells. **3.** proNGF is cleaved to its biologically active form NGF by MMP7 and plasmin. **4.** NGF binds to its cognate receptor TrkA on sensory nerve terminals. **5.** NGF binding to TrkA receptor on sensory terminals mediates rapid post-translational changes to TRPV1, including up regulation of channel expression. **6.** The ligand-receptor complex is reterogradely transported to the neuronal cell body in the dorsal root ganglion to regulate gene transcription **(7)**. **8.** The aforementioned post-translation changes reduce channel activation threshold which increases the excitability of the channel, thus facilitating chronic pain states.

1.6.2 Cytokines

Cytokines are small glycoprotein molecules secreted from inflammatory cells (Zhang and An, 2007) that have a critical role in relaying information within the immune system. Cytokines have pro-inflammatory or anti-inflammatory modes of action (Fernandes et al., 2002). Inflammatory cytokines may be associated with disease progression.

Two major pro-inflammatory cytokines implicated in OA pathogenesis are TNF-α and IL-1β. These cytokines are produced by synovial cells, mononuclear cells and articular chondrocytes (Sellam and Berenbaum, 2010). Pro-IL-1β is cleaved to its active form IL-1β by caspase-1 (previously known as interleukin 1β converting enzyme) (Denes et al., 2012). The cytokines can induce peripheral sensitisation through the up-regulation of MMP gene expression (Fernandes et al., 2002). Furthermore IL-1β and TNF-α can perpetuate the disease process by stimulating their own production in an autocrine manner (Bondeson et al., 2006), in addition to triggering the release of other cytokines such IL-6, IL-8 and leukocyte inhibitory factor (Fernandes et al., 2002). IL-1β and TNF-α can also upregulate COX-2 (Fehrenbacher et al., 2005, Goldring and Otero, 2011). COX-2 mediates the synthesis and secretion of prostaglandin PGE_2 (Martel-Pelletier et al., 2003). PGE_2 may be involved in neuropathic pain (Ma and Quirion, 2008).

Downstream signalling pathways such as the nuclear factor kappa-B (NF-κB) and c-Jun n-terminal kinase (JNK) and p38 mitogen-activated protein kinase pathways are activated by IL-1β and TNF-α during inflammation and cellular stress (Baldwin, 1996, Kapoor et al., 2011). The NF-κB pathway plays a crucial role in inflammation (Tak and Firestein, 2001), through inducing the transcription of various pro-inflammatory cytokines. Examples include IL-1β, IL-2, IL-6, IL-8, IL-12, interferon gamma (IFN-γ) (Baldwin, 1996), in addition to genes that encode chemokines (Baldwin, 1996, Roman-Blas and Jimenez, 2006).

The association between pro-inflammatory cytokines and pain has been explored. The association between OA knee pain and expression of the pro-inflammatory cytokine TNF-α in the human synovium has been well

documented (Smith et al., 1997, Orita et al., 2011, Stannus et al., 2012). Recent studies using TNF-α antagonists demonstrated reduction in pain, stiffness, function and joint swelling in patients with inflammatory knee OA (Le and Friedman, 2012). Nevertheless only a small sample size of patients were studied (n=20). The lack of a healthy control group in this study impedes a definitive conclusion of the effectiveness of the drug, which may partly be attributed to the placebo effect.

IL-6 is another important cytokine involved in OA pathogenesis (Wojdasiewicz et al., 2014b). IL-6 has been shown to be correlated with heighted pain sensitivity in OA patients (Lee et al., 2011). Furthermore elevated serum levels of IL-6 may be a predictor of radiographic OA severity in OA (Livshits et al., 2009) and are associated with cartilage loss in knee OA (Stannus et al., 2010). Pain intensity has been shown to be correlated with an increase in concentration of IL-6 in addition to IL-1β, IL-2, IFN-γ and TNF-α in the plasma (Koch et al., 1995), implying a crucial role of inflammatory cytokines in mediating OA pain.

Other cytokines have been implicated in OA pathophysiology. IL-17 stimulates the production of chemokines such as IL-8 from chondrocytes and synovial fibroblasts (Honorati et al., 2002), which may have a catabolic role in OA pathogenesis. Elevated levels of IL-15 are found in the synovial fluid of early knee OA compared with end-stage OA patients, and are positively correlated with MMP1, MMP3, IL-6 expression in synovial fluid (Scanzello et al., 2009). IL-15 may therefore be a future therapeutic target.

1.6.3 Chemokines

Cytokines with chemotactic properties are termed chemokines (Zhang and An, 2007). Chemokines can induce chemotaxis (movement) of a variety of immune cells such as fibroblasts, monocytes, neutrophils, lymphocytes and eosinophils (Wojdasiewicz et al., 2014a). The chemokine family consists of four groups illustrated in table 1.3 In OA chemokines play an important role in the recruitment of inflammatory cells (Haringman et al., 2006) and migration of subchondral progenitor cells (Endres et al., 2010).

Elevated levels of some chemokines in the joint have been associated with pain. Patient-reported pain scores in patients with acute knee pain are associated with intra-articular concentrations of monocyte chemoattractant protein-1/chemokine ligand 2 (MCP-1/CCL2), macrophage inflammatory protein-1 beta/chemokine ligand 4 (MIP-1β), interleukin (IL)-6 and interferon (IFN)- γ (Cuellar et al., 2009). In arthritic disease MCP-1/CCL2 and MIP-1β/CCL4 are significantly associated with acute knee pain (Cuellar et al., 2009). Furthermore MCP-1 has shown to be associated with pain behaviour in the destabilisation of the medial meniscus (DMM) model of OA (Miller et al., 2012).

Fractalkine (CX3CL1) is the only member of the CX3C subfamily (Wojdasiewicz et al., 2014a). Elevated CX3CL1 is detected in the serum and synovial fluid of OA patients compared with healthy controls and is correlated with radiographic severity of OA (Zou et al., 2013).

Table 1.3: The four chemokine groups, and examples of family members.

Chemokine group	Examples of members
C-C	Regulated on activation normal T cell expressed and secreted (RANTES), monocyte chemotactic protein (MCP)-1, macrophage inflammatory protein (MIP)-1α, MIP-1β.
C-X-C	Chemokine ligand 1 (CXCL1), 2 (CXCL2), 5 (CXCL5), 10 (CXCL10).
C	Lymphotactin
CXXXC	Fractalkine

References: (Zhang and An, 2007).

1.6.4 Matrix metalloproteases

MMPs are a large enzymatic family of zinc dependent endopeptidases (Ji et al., 2009), which function as secreted molecules or are cell surface bound (Parks et al., 2004). MMPs can be classified into 5 main groups (Murphy et al., 2002) as illustrated in table 1.4. Normally the enzymatic activity of MMPs is balanced by tissue inhibitors of metalloproteases (TIMPs) (Ji et al., 2009). In OA MMPs have been implicated in joint destruction through proteolytic matrix degradation (Parks et al., 2004) and may play a role in inflammation (Manicone and Mcguire, 2008) through the modulation of inflammatory mediators such as cytokines and chemokines (Mcquibban et al., 2001, Mcquibban et al., 2002) . For example, MMP2 (gelatinase A), MMP3 (stromelysin 1) and MMP9 (gelatinase B) can cleave proIL-1β into biologically active IL-1β (Schönbeck et al., 1998, Kawasaki et al., 2008).

Pro-inflammatory cytokines (Il-1 and TNF) can induce MMP release from articular chondrocytes (Goldring, 2000, Reboul et al., 1996).

Table 1.4: Classification of matrix metalloproteases

Group	Family members
Collagenases	MMP1, MMP8, MMP13
Gelatinases	MMP2, MMP9
Stomelysins	MMP3, MMP10, MMP11
Membrane type	MMP14 to MMP17, MMP24
Other	MMP7, MMP11, MMP12, MMP20, MMP23, MMP28

MMPs are also involved in nociception and hyperalgesia. The gelatinases MMP9 (gelantinases B) and MMP2 (gelatinase A) are associated with central sensitisation (Burston et al., 2013). MMP9 may contribute to the early stage of

neuropathic pain, whereas MMP2 may contribute to the later stages, through the induction of microglia and astrocyte production in the dorsal root ganglion (Kawasaki et al., 2008). Furthermore significant elevations of MMP2 and MMP9 in the spinal cord are observed in the monosodium iodoacetate (MIA) model of OA compared to saline controls (Burston et al., 2013).

1.6.5 Protease-activated receptors

Protease-activated receptors (PARs) are G protein receptors (Macfarlane et al., 2001), four members have been identified (Dai et al., 2004). Of these PAR-2 and PAR-4 have been strongly implicated in joint inflammation and pain (Ferrell et al., 2003). During inflammation the release of serine proteases such as trypsin, mast cell tryptase and thrombin activate PARs through proteolytic cleavage (Russell and Mcdougall, 2009). PAR-2 is activated by trypsin and mast cell tryptase (Steinhoff et al., 2000), whereas PAR-4 is activated by thrombin, trypsin and cathepsin G (Asfaha et al., 2007). Cleavage of the PAR extracellular N terminus site subsequently releases a tethered ligand domain which binds and actives the receptor (Russell and Mcdougall, 2009).

PAR-2 is expressed in epithelial, endothelial and inflammatory cells such as macrophages, neutrophils and mast cells (Helyes et al., 2010, Russell and Mcdougall, 2009). PAR-2 expression can be elevated following stimulation of immune cells by pro-inflammatory cytokines (Nystedt et al., 1996) supporting an inflammatory role for PAR-2. Moreover, PAR-2 has been localised to spinal sensory neurons and is co-expressed with TRPV1 (Dai et al., 2004). Activation of PAR-2 induces the release of SP and CGRP which contribute to inflammation (Steinhoff et al., 2000), and CGRP induces peripheral sensitisation (Bullock et al., 2014).

PAR-4 is co-expressed with CGRP and SP in sensory nerves in the dorsal root ganglion (Asfaha et al., 2007). Intra-articular injection of a PAR-4 activating peptide into the knee joint of mice has been shown to enhance hyperalgesia. The nociceptive response was inhibited by both a PAR-4 and bradykinin antagonist, suggesting a role for kallikrein–kinin (bradykinin) system in mediating PAR-4 inflammatory responses (Mcdougall et al., 2009).

1.6.6 Cyclo-oxygenases

Cyclo-oxygenase (COX)-1 and 2, are key enzymes involved in prostaglandin synthesis from arachidonic acid. Prostaglandins contribute to the generation of the inflammatory response. The inflammatory response can be alleviated with pharmacologic agents, such as NSAIDs that block COX-1 and COX-2 enzymes, thus inhibiting the biosynthesis of prostaglandins. COX-1 is constitutively expressed in most tissues, whereas pro-inflammatory cytokines induce COX-2 during inflammation (Seibert and Masferrer, 1994).

1.6.7 Damage associated molecular patterns

Recent evidence has suggested a role of damage associated molecular patterns (DAMPS), which are also known as alarmins, in cartilage and synovial pathology in OA (Van Lent et al., 2012). Of particular interest are calcium binding proteins S100A8 (myeloid-related protein (MRP)-8 and S100A9 (MRP-14), which demonstrate cytokine and chemokine-like functions (Vogl et al., 2012). Elevation of S100A8 and S100A9 messenger RNA (mRNA) and protein in the synovial fluid of patients OA patients are correlated with joint destruction (more severe radiographic severity using the Kellgren Lawrence scoring system) over 2 years (Van Lent et al., 2012) and are associated with synovial inflammation (Van Lent et al., 2012, Lambert et al., 2014).

Recently S100A8 has been shown to rapidly activate naïve mouse dorsal root ganglion (DRG) neurons, in addition to upregulating MCP-1 protein following overnight stimulation. The ability of sensory nerves to respond to alarmins may contribute to OA pain (Miller et al., 2014).

1.6.8 Nitric oxide

Nitric oxide (NO) is produced by nitric oxide synthases; endothelial, neuronal and inducible (eNOS, nNOS, iNOS, respectively) (Fischer et al., 2010). The role of NO in hyperalgesia is demonstrated by the reduction of hyperalgesia following local NO inhibition (Lawand et al., 1997). NO is increased in the plasma of chronic pain patients compared to controls (Koch et al., 1995).

1.6.9 Bradykinin

Bradykinin is an inflammatory peptide generated in the synovium that is involved in the induction and maintenance of pain in OA (Meini and Maggi, 2008). Bradykinin is formed by cleavage of kininogen by the enzyme kallikrein (Campbell, 2001).

1.6.10 Resolvins

In contrast to the pro-inflammatory and nociceptive agents described so far, a novel class of lipid mediators, termed resolvins, have recently gained considerable interest for their ability to resolve inflammation and reduce arthritic pain. Resolvins are potent anti-inflammatory local mediators derived from omega-3 polyunsaturated fatty acids (PUFAs) which play a key role in the resolution of inflammation (Arita et al., 2007, Norling and Perretti, 2013). The effects of resolvin E1 (RvE1) appear to be mediated through a selective interaction with the leukotriene B4 receptor (BLT1) and Chemerin receptor 23 (ChemR23) (Arita et al., 2007).

1.7 Signalling pathways

1.7.1 Nuclear factor-kappa B

Various downstream signalling pathways such as the nuclear factor kappa-B (NF-κB) play a key role in the inflammatory response (Tak and Firestein, 2001). The five transcription factors of the NF-κB family are ubiquitously expressed. The family is comprised of RelA (p65), RelB, c-Rel, NF-κB1 (p50 and its precursor p105) and NF-κB2 (p52 and its precursor p100) (Roman-Blas and Jimenez, 2006). An inactive form of NF-κB resides within the cell cytoplasm, bound to inhibitory κB proteins (IκB) (figure 1.9). During inflammation in the synovium, cell surface receptors are activated by a host of pro-inflammatory mediators, which subsequently activate NF-κB dimers within the cytoplasm. Upon activation associated IκB proteins are phosphorylated and then degraded allowing NF-κB dimers to translocate to the nucleus to mediate gene expression (Rigoglou and Papavassiliou, 2013). Various pro-inflammatory and angiogenic factors are consequently upregulated, including

IL-8, chemokine ligand 5 (CCL5), receptor activator of nuclear factor-kappaB ligand (RANKL), IL-1β, IL-6, tumour necrosis factor (TNF)-α and vascular endothelial growth factor (VEGF) (Rigoglou and Papavassiliou, 2013). These mediators act to further potentiate inflammation and joint destruction.

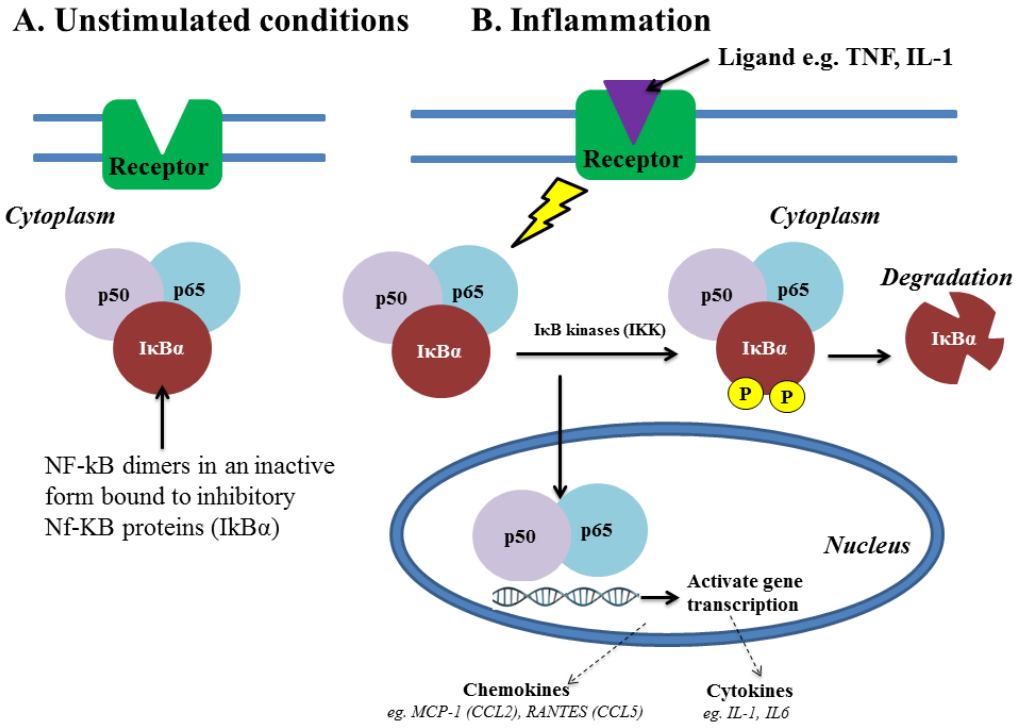


Figure 1.9: Classical NF-κB signalling pathway.

During unstimulated conditions an inactive form of NF-κB (p50 and p65) is bound to inhibitory proteins (IκB) within the cytoplasm. During inflammation, pro-inflammatory mediators including cytokines activate cell surface receptors to subsequently induce phosphorylation of IκB proteins. The IκB proteins are subsequently degraded, which then facilitates translocation of NF-κB dimers to the nucleus to activate gene transcription.

1.7.2 Janus activated kinase/signal transducers and activators of transcription (JAK/STAT)

Another important signalling pathway involved in cytokine signalling is the Janus activated kinase/signal transducers and activators of transcription (JAK/STAT) pathway. A variety of ligands activate the JAK/STAT pathway including interleukins, interferons (IFN) and growth hormones (Tamiya et al., 2011). Ligands binding to their cell surface receptors activate associated JAKs, which subsequently self-phosphorylate tyrosine residues. STAT proteins bind to the phosphotyrosine complex of the JAKs, subsequently dimerise and translocate to the nucleus where they promote translation of gene transcription. JAK/STAT signalling is inhibited by suppressors of cytokine signalling (SOCS) and protein inhibitors of activated STATs (PIAS). SOCS-1 inhibits the catalytic activity of JAK, whereas SOCS-3 blocks the cytokine receptor to block signal transduction (Kishimoto, 2006).

1.7.3 Mitogen activated protein kinase (MAPK)

The MAPK family of enzymes also play an important role during inflammation to regulate the production of pro-inflammatory cytokines such as IL-1β and TNF-α. Three principle pathways define MAPK signalling; extra-cellular signal-related kinase (ERK), c -jun NH2-terminal kinase (JNK) and p38. P38 consists of four isoforms: p38-α/β/δ/γ. P38-α is the major isoform to regulate cytokine expression(Hammaker and Firestein, 2010).

P38 MAPK is expressed in the synovial lining in patients with rheumatoid arthritis (RA) but was absent from the synovial tissue of the 5 OA patients in one study (Schett et al., 2000). The transduction pathway components involved in p38 MAPK signalling are illustrated in figure 1.10. Inflammatory mediators and extracellular stresses activate a MAPK kinase kinase (MAP3K), which in turn phosphorylate and activate a MAPK kinase (MKK3 and MKK6). MKK3 then phosphorylates three of the p38 (MAPK) isoforms, namely -α, -γ,-δ, whereas MKK6 phosphorylates all four isoforms (Enslen et al., 1998). P38 can then activate downstream MAPK-activated protein kinases (MAPKAP2/MK2) to initiate increased expression of pro-inflammatory mediators (Moens et al., 2013).

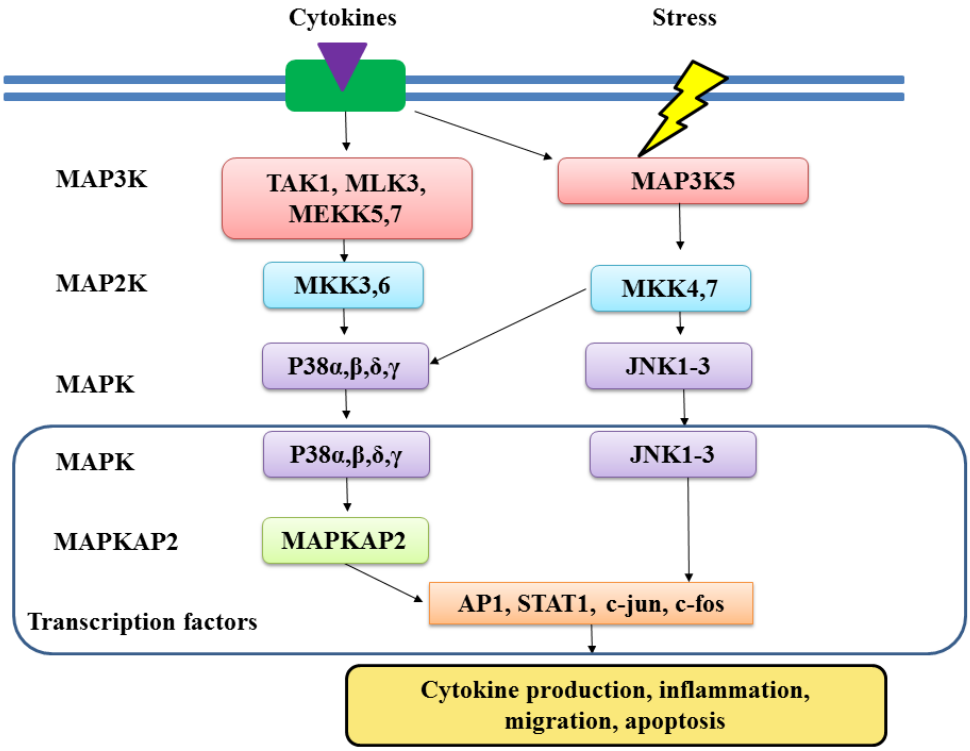


Figure 1.10: Simplified mitogen activated protein kinase (MAPK) pathway.

An overview of the mitogen activated protein kinase (MAPK) pathway. Activation of the MAPK pathway by inflammatory mediators and extracellular stress activates several intracellular signalling cascade where ultimately activated MAPKs enter the nucleus to mediate gene transcription. The MAPK kinase kinase (MAP3K) are at the beginning of the signalling cascade activation subsequently activates a MAP2K kinase (MKK3 and MKK6), which subsequently activate a MAPK such as P38. In the nucleus P38 can then activate downstream MAPK-activated protein kinases (MAPKAP2/MK2). The MAPKAP2 phosphorylate effector proteins such as gene transcription factors including AP1, STAT1, c-jun and c-fos, to inc to initiate increased expression of pro-inflammatory mediators.

1.8 Conclusions

OA is a major cause of pain and disability. The prevalence is set to increase due to the ageing population and obesity epidemic. Pathologically OA is characterised by focal cartilage loss, accompanied by subchondral bone remodelling. Synovial inflammation is increasingly being recognised as an important contributor to OA pathophysiology (Smith et al., 1997).

Despite extensive research into OA, many questions remain unanswered. The exact cause of OA and identification of the earliest pathological events is extremely difficult to determine. Furthermore, there is no clear correlation between structural and symptomatic features of the disease (Dieppe et al., 1997, Bedson and Croft, 2008). Radiographic features of OA are often weakly associated with pain. Imaging studies have indicated possible associations between pain and synovitis (Hill et al., 2001, Torres et al., 2006, Hill et al., 2007, Baker et al., 2010) or subchondral changes (Felson et al., 2001, Szebenyi et al., 2006, Torres et al., 2006, Hernandez-Molina et al., 2008b). Additionally, it is currently unclear whether early OA comprises a single disease entity, or discrete subgroups representing distinct pathological processes.

Current treatment for OA has limited efficacy and adverse effects. TKR surgery is successful for the majority of patients; however it is associated with a financial burden. In one study just under half of patients (44%) experienced post-surgical pain 3-4 years after arthroplasty (Wylde et al., 2011).

Better understanding of the structural and molecular modifications in the knee joint that are associated with symptomatic OA will help refine strategies for developing disease modifying OA drugs (DMOADs). Furthermore identifying the earliest pathological changes in OA pathogenesis is crucial for the development of targeted treatments to slow down, or even reverse the disease process. The identification of homogenous subgroups of patients based on OA histopathological phenotypes may ultimately result in important changes in the classification of patients with OA. Furthermore, subgrouping patients will allow for stratification of treatments, by focusing on those which are most likely to modify disease progression and improve outcomes.

1.9 Aims, Objectives and Hypotheses

The major aim of this thesis was to better understand the role of histopathological and molecular pathological modifications in symptomatic human knee OA.

The main objectives were:

1. To determine which histopathological features in the medial tibial plateaux and synovium are associated with OA, and which of those are specifically associated with symptomatic OA.

2. To determine synovial gene expression patterns and their association with symptomatic OA.

3. To develop a histopathological scoring system that better reflects OA as a multi-tissue disease.

4. To identify the earliest histopathological features of knee OA.

5. To classify subgroups of post-mortem and total knee replacement cases based on histological characteristics.

It was hypothesised that:

- Symptomatic OA is mediated by specific structural, biochemical and molecular changes within the knee joint, whereas other changes may be coincidental or even protective.

- Discrete patient subgroups can be defined based on validated measures of knee OA histopathological features, and different pathological subgroups reflect different stages of OA progression.

- OA is a multi-tissue disease, and affects several joint tissues in parallel throughout OA progression.

CHAPTER 2: MATERIALS AND METHODS

INTRODUCTION

This chapter describes general methodology used within this thesis. Human tissue was obtained with informed consent from patients at the time of total knee replacement (TKR) for symptomatic OA, or the next of kin of post-mortem (PM) cases (Walsh and Wilson, 2003). All procedures involving human tissue were approved by the United Kingdom National Research Ethics Service (Nottingham Research Ethics Committee 1 (05/Q2403/24) and Derby Research Ethics Committee 1 (11/H0405/2)). Patient consent forms, reagents and buffer recipes are found in the appendix (chapter 8).

2.1 Patient Selection

The Arthritis Research UK Pain Centre's joint tissue repository, containing samples from > 1800 cases was screened to select cases according to each study criterion. All TKR tissue samples were collected from patients fulfilling ACR classification criteria for OA (Altman et al., 1986) at the time of TKR, with their consent. PM tissue samples were collected from recently deceased patients, informed consent was obtained from next of kin. In the studies detailed below PM patients were carefully selected that had not reported knee pain in the last year of life. Clinical data acquisition in PM cases relies on case notes, where knee pain may not have been reported, and from interviews with bereaved relatives, who may not have been aware of symptoms. Limited clinical data were available for the PM cases, including knee pain status, presence of osteophytes previous surgery and previous diagnosis of OA. Information was not available for PM cases regarding joint stiffness.

For the majority of PM cases tissue samples were available for the left and right knee, for all studies tissue from the right knee was selected in PM cases.

For TKR cases the laterality of tissue samples was selected based on availability of biopsied tissue.

2.1.1 Histological features of osteoarthritis

In order to identify histopathological features associated with knee OA, medial tibial plateaux and synovia obtained from 26 non-arthritic PM control cases were compared with 26 aged-matched TKR cases. The joint tissue repository was screened to select non-arthritic control samples collected from PM cases without OA, to each of which one TKR (OA) case was selected and age matched within 1 year at the time of tissue collection. Where no matching case was available, a TKR case aged within 2 years of the index non-arthritic case was selected, and again, where no matching case was available, a TKR case aged within 3 years, until all cases had a matching pair (figure 2.1).

Non-arthritic control samples were collected from recently deceased patients with no history of rheumatoid arthritis or pseudogout, who had not previously sought help for knee pain in their last year of life, as determined by interviews with relatives and case note review. Additional exclusion criteria included; history of OA, Heberden's nodes on clinical examination, macroscopic chondropathy lesions grade 3 or 4 in the medial tibiofemoral compartment (Walsh et al., 2009) and osteophytes on direct visualisation of the dissected knee. Results from this study are found in chapter 3, section 3.4. Due to availability of suitable tissue and cases, these cases were age-matched but were not simultaneously matched for gender. However gender differences were adjusted for in the analysis (see section 2.13.1).

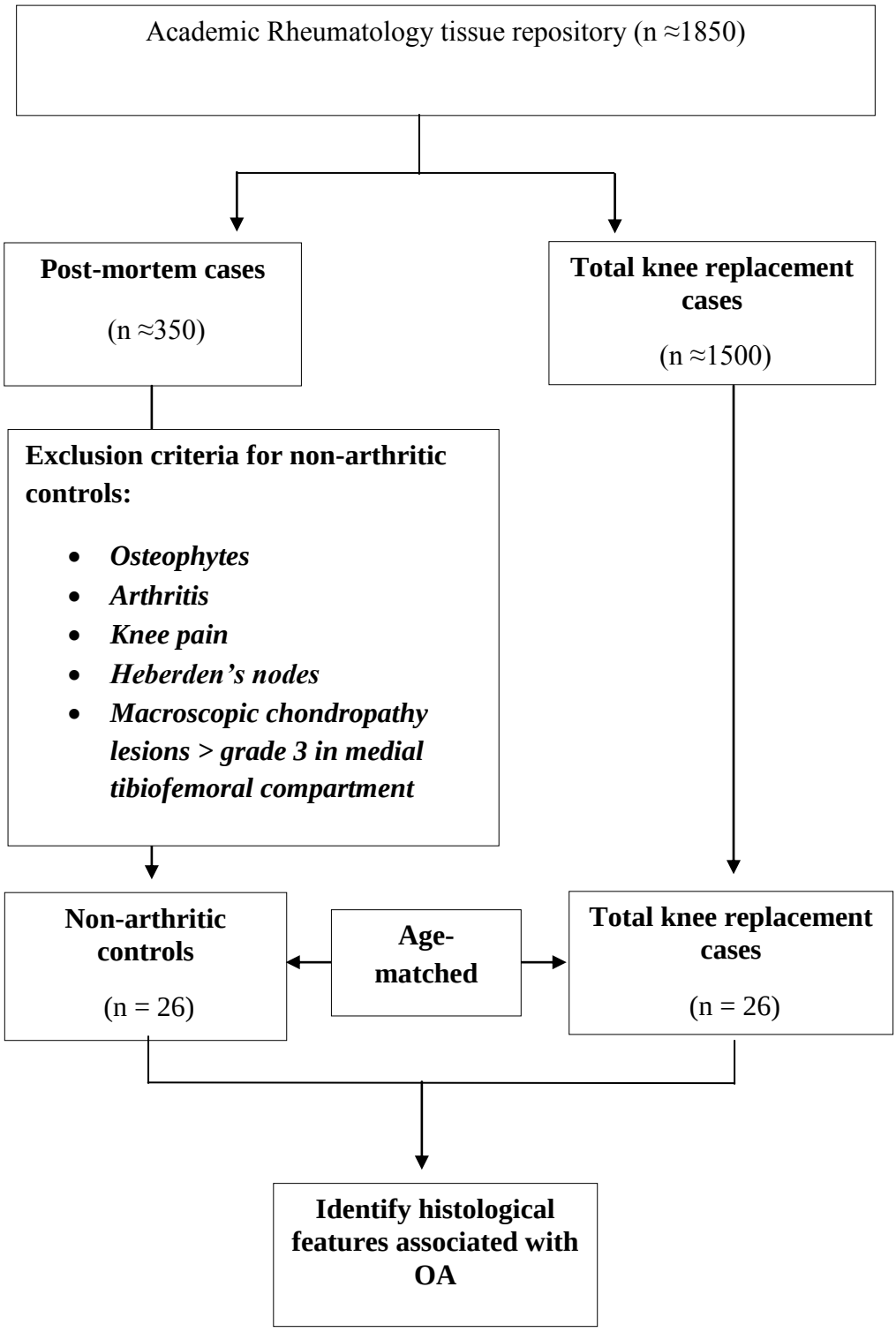


Figure 2.1: Overview of the strategy undertaken to select non-arthritic control post-mortem cases and age-matched total knee replacement cases.

2.1.2 Histological associations with symptomatic osteoarthritis

In order to identify histopathological features associated with symptoms, cases with similar macroscopic chondropathy scores who had not presented with knee pain in the last year of their life (asymptomatic chondropathy) or had undergone TKR for symptomatic OA (symptomatic chondropathy) were selected (n = 29/group). The selection process is detailed in figure 2.2. Results from this study are found in chapter 3, section 3.4.

Structural change in the OA knee joint can be evaluated using a variety of methods. The severity and extent of articular cartilage loss (chondropathy) in the knee joint in PM and TKR cases can be measured macroscopically using a photographic chondropathy score (PCS) (Walsh et al., 2009). Macroscopic chondropathy scores are useful and complementary measures of structural severity changes in OA. Moreover, the PCS was developed to compare structural change in cadaver with clinical specimens. Macroscopic chondropathy scores were calculated for each of the four articular surfaces; medial and lateral tibial plateau and femoral condyles. Whole knee macroscopic chondropathy scores ranged from 0 (no cartilage defects) to 400 (complete tibiofemoral subchondral bone exposure). Further details are described in section 2.7).

Whole knee macroscopic chondropathy scores were calculated for each PM case in the joint tissue repository at the time of tissue collection, and for TKR cases where all four articular surfaces were available. Macroscopic chondropathy scores for PM cases ranged from 9 to 361. PM cases that displayed the most severe macroscopic chondropathy score were selected, and each PM case was then matched to one TKR case with a similar macroscopic chondropathy score (n = 29/group). PM samples were collected from recently deceased patients with no history of rheumatoid arthritis or pseudogout, who had not previously sought help for knee pain in their last year of life, as determined by interviews with relatives and case note reviews.

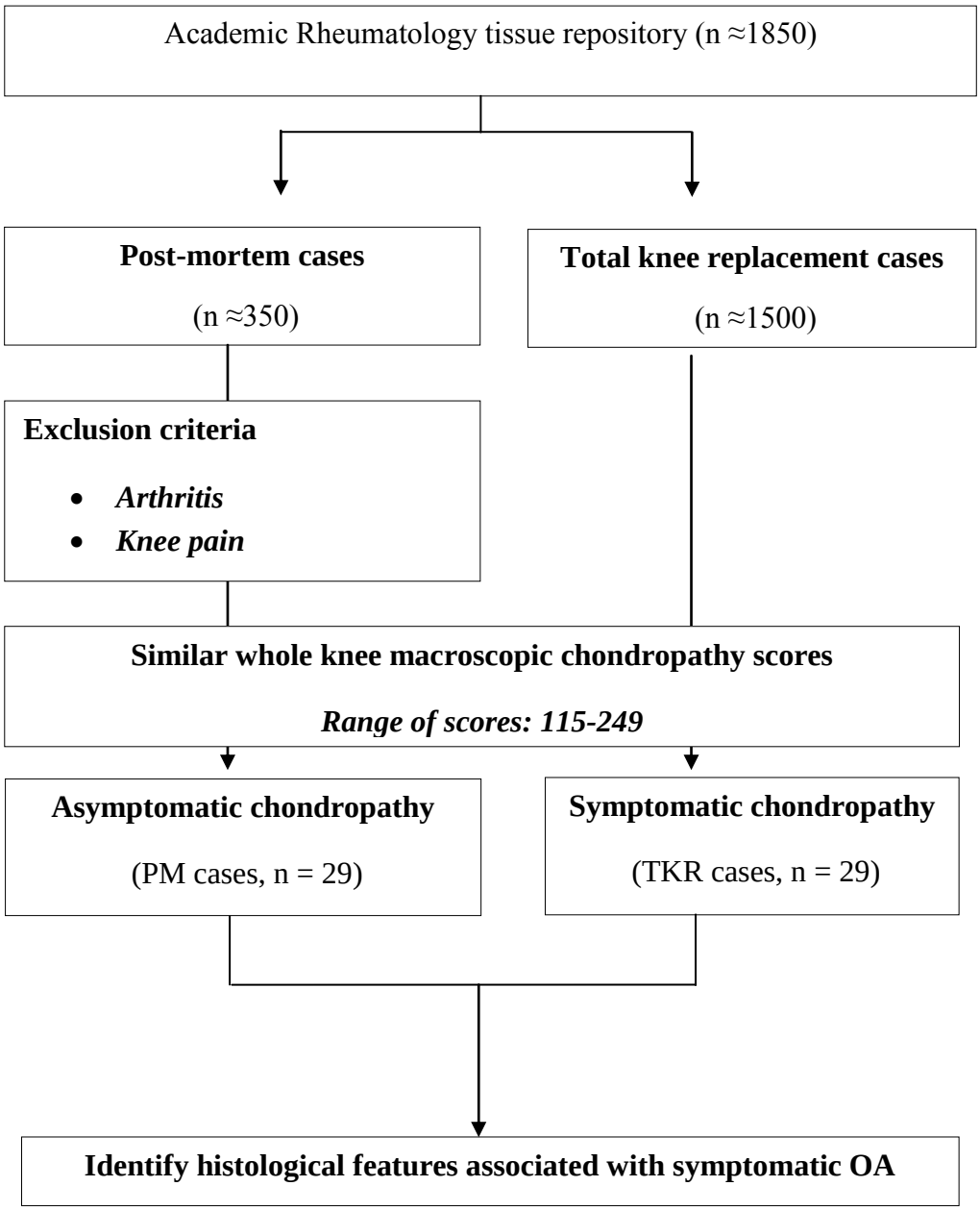


Figure 2.2: Overview of the strategy undertaken to select post-mortem and total knee replacement cases with similar macroscopic chondropathy scores cases and age-matched total knee replacement cases.

2.1.3 Gene patterns in the synovium and their association with symptomatic osteoarthritis

In order to examine gene expression patterns in the synovium which may mediate an association between synovitis and symptomatic OA, a subgroup of

symptomatic and asymptomatic chondropathy cases with similar tibiofemoral macroscopic chondropathy scores were selected based on availability of suitable tissue (n=12/group). Total RNA was extracted from the snap frozen synovia of these cases (described in further detail in section 2.12.1). Results from this study are found in chapter 4, section 4.6.2.

2.1.4 Cellular source of synovial NGF

The cellular source of synovial nerve growth factor was determined qualitatively using a small subgroup of TKR and PM cases. Cases were selected as convenience samples from the studies described in 2.1.1 and 2.1.2. The subgroup consisted of 3 TKR cases, 3 asymptomatic chondropathy cases (PM cases selected previously for high chondropathy scores) and 2 non-arthritic PM controls. Results from this study are reported in chapter 3, section 3.7.

2.1.5 Early and mild osteoarthritis and histopathological subgroups

In order to identify the earliest histological features of knee OA and to determine the presence of patient subgroups based on histology, consecutive PM samples collected from Sherwood Forest Hospitals NHS Foundation Trust over 10 years (2004-2014) were selected from the joint tissue repository. Cases with both medial tibial plateaux and synovium available were selected for histological analysis (n = 343).

PM samples were collected from recently deceased patients with no history of rheumatoid arthritis or pseudogout. Of these, 48/343 (14%) were classified as non-arthritic control cases based on criteria defined in section 2.1.1. The remaining PM cases that did not fit the selection criteria for non-arthritic controls were classified as ‘early OA’ (n=295, figure 2.3).

For these studies, TKR cases previously used to identify histological features associated with OA (n = 26) and symptomatic OA (n = 29) were supplemented with 88 consecutive TKR cases from the joint tissue repository. TKR cases with both medial tibial plateaux and synovium were selected for the histological comparison analysis. An overview of selection methods are

illustrated in figure 2.3. Results for this study are reported in chapter 5, section 5.17.

For identification of histopathological subgroups histological scoring from all PM and TKR cases were investigated together as a single group, in order to provide a spread of different severities of OA change. Results from these studies are reported in chapter 5, section 5.18.

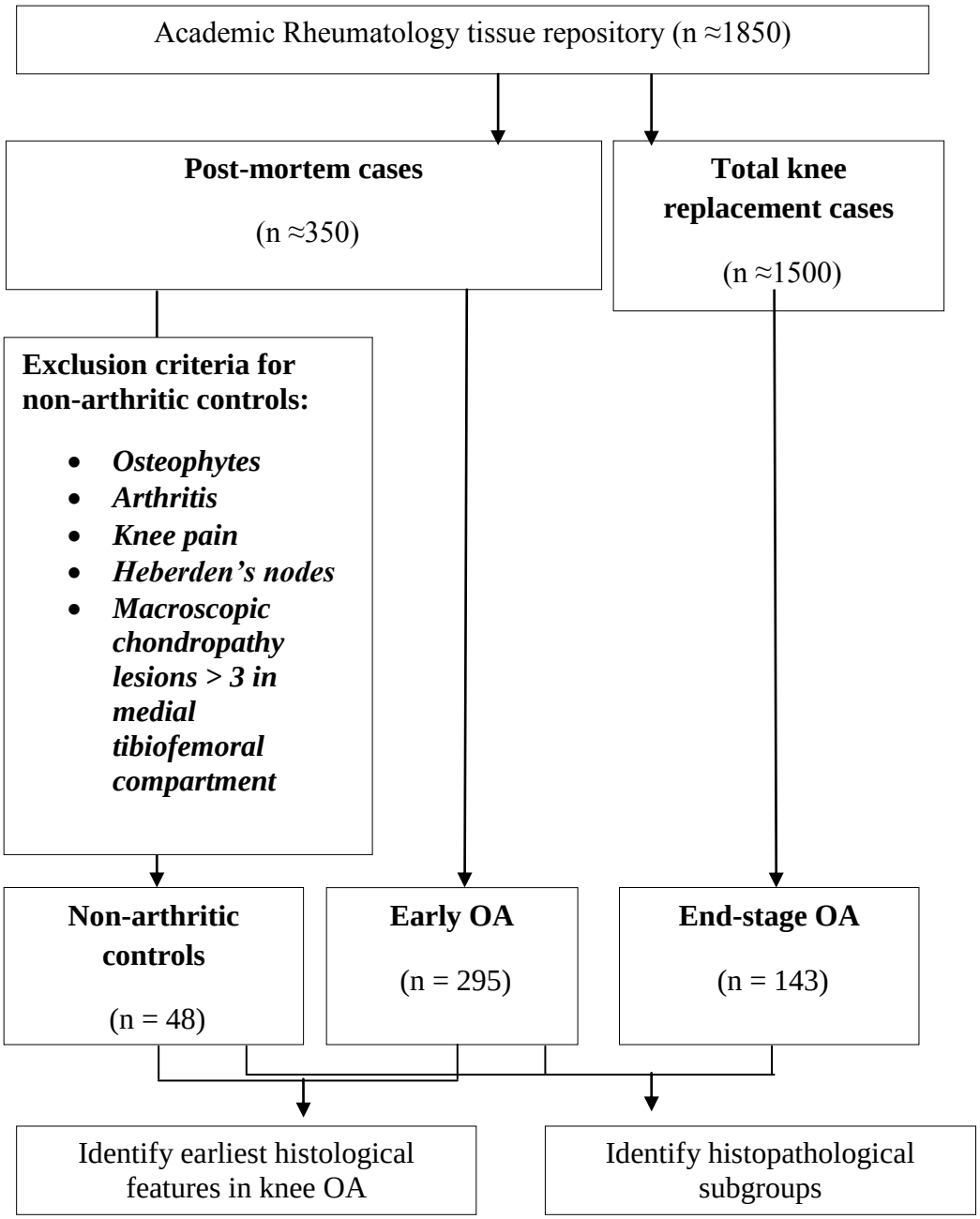


Figure 2.3: Overview of the strategy undertaken to select characterise post-mortem cases as non-arthritic controls or early OA cases.

Non-arthritic controls and early OA cases were histologically compared to identify early histopathological features in knee OA. Histological scores for all PM and TKR cases were used to identify histopathological subgroups.

2.1.6 Rasch analysis and development of a weighted histopathological OA score

Rasch analysis was conducted to assess the validity of the Mankin histopathological scoring system. Two analyses were performed using histological scores from the medial tibial plateaux and synovium of 343 PM and 143 TKR cases, see section 2.13.3.

1. Test group which included histology scores from 181 PM and 55 TKR cases.

2. Validation group which included histology scores from 162 PM and 88 TKR cases. The validation group consisted of a different set of cases to the test group.

The Mankin score was analysed in two stages. First, in order to examine the measurement properties of the score for use in early OA histological scores from only PM cases were analysed. Following this Rasch analysis was performed on all PM and TKR cases representing the full range of OA pathological change from normal to end stage.

2.1.7 Effects of post mortem delay in surgical tissue

In order to mimic the effects of PM delay in surgical tissue, synovial tissue was collected from 6 consecutive TKR cases. A full overview of the protocol is described in section 2.11.

2.2 Tissue collection and processing

All tissue biopsy samples were processed on site at King's Mill Hospital by an experienced research technician (Roger Hill). A variety of processing methods were employed dependent upon tissue type and experimental objective.

2.2.1 Medial tibial plateaux

Mid-coronal sections (1.5mm thick) of the middle one-third of medial tibial plateaux were fixed in neutral-buffered formalin for 3-5 days. Tissue fixation is crucial to permanently preserve architecture of cellular components in a life-like state prior to histological staining techniques and examination by microscopy. Furthermore, fixation prevents autolysis and bacterial degradation of the tissue. During fixation cross-linking methylene bridges are formed between protein molecules, forming a stabilising meshwork.

Following fixation the tissue was decalcified in 10% ethylenediaminetetraacetic acid (EDTA), with 7.5% polyvinylpyrrolidone (PVP) in 10 mM Tris buffer (pH 6.95, 4°C). Decalcification is essential to remove calcium and other minerals from the subchondral bone in order to soften the tissue and permit histological sectioning and staining. Decalcifying agents typically include chelating agents, such as EDTA to sequester calcium ions, and acids (e.g. formic) that form soluble calcium salts. EDTA decalcification is a very gentle but relatively slow process; the full decalcification process lasts between 5-7 weeks. Decalcification fluid was changed every other day. After 5 weeks, radiography was used to confirm decalcification of the medial tibial plateaux. Radiographs were compared to baseline images. If calcium deposits remained in the subchondral bone the decalcification process was continued. Samples were then radiographed on a weekly basis to prevent over decalcification.

Once fully decalcified the samples were prepared for wax embedding. First the samples were placed in labelled plastic cassettes, and then underwent a series of dehydration and clearing steps in the Shandon Pathcentre enclosed tissue processor (Shandon ThermoScientific, Leicestershire, UK). For embedding, metal moulds were placed onto a hot plate; a small amount of molten paraffin wax was dispensed from a Tissue Tek® embedding centre (model TEC5

EME2; Sakura Finetek Europe, The Netherlands) into the mould. The tissue samples were placed into the mould and orientated parallel to the block surface before the mould was transferred to a cold plate to allow the wax to set. The tissue was pressed down using forceps. Labelled cassettes were then placed on top of the mould and more wax was dispensed to fill the cassette. Moulds were placed back on top the cold plate, once the wax had completely solidified the cassette was removed from the metal mould and excess wax trimmed off.

Thin paraffin tissue sections (5µm) were cut using a Reichert-Jung rotary microtome. Individual tissue sections were carefully placed onto the surface of a 40ºC water bath for 2 minutes to allow the section to completely flatten. Sections were then transferred to electrostatically charged poly-l-lysine glass slides. In order to promote adherence of sections to the slides, the slides were placed in a 50ºC incubator for 2 hours and then stored in a sealed slide box at room temperature prior to histology or immunohistochemistry staining procedures.

2.2.2 Synovium

Surgeons and the technician (RH) were instructed to collect synovium from the medial joint line from PM and TKR cases. Synovia were fixed in formalin for 3-5 days and embedded in paraffin wax blocks without decalcification. A Reichert-Jung rotary microtome was used to cut thin sections (5µm) of tissue, which were subsequently processed as described above.

Additionally, fresh synovial tissue was processed for frozen sectioning. Cryopreservation allows optimal protection of cellular antigens and tissue morphology. For identification of gene expression patterns in the synovium, fresh synovium tissue biopsies were snap frozen in liquid nitrogen, without fixation. A small amount of optimal cutting temperature (OCT) mounting medium (Raymond Lamb, Eastbourne, UK) was placed onto a cork mould. Synovial tissue was embedded in the OCT until the entire specimen was covered. Forceps were used to slowly immerse the OCT tissue block into a beaker containing melting isopentane, which was suspended over liquid nitrogen. After 10-20 seconds the frozen OCT tissue block was removed and

stored at -80C prior to cryostat sectioning. OCT embedded synovium were used to identify the cellular localisation of synovial nerve growth factor.

2.3 Histological staining

2.3.1 Haematoxylin and eosin

Haematoxylin and eosin (H&E) is one of the most commonly used staining techniques in histology. The two contrasting dyes enable identification of specific morphological features within the tissue architecture. Haematoxylin is chemically oxidised to produce haematin (King and King, 1986), which is then combined with a mordant, such as aluminium ions, to produce haemalum. Haemalum acts as the active staining agent within the haematoxylin solution (Bancroft and Stevens, 1996). Haematoxylin is a basic dye that stains basophilic (or acidic) structures, specifically the chromatin within the cell nuclei a blue/black colour. Eosin is an acidic dye, and is used as a counterstain to identify basic (or acidophilic) structures. Cytoplasmic material and connective tissue fibres are stained varying degrees of pink, red and orange by the eosin stain (Bancroft and Stevens, 1996).

Paraffin wax embedded tissue sections (5µm) were first immersed in xylene (a paraffin solvent) to remove the wax for 5 minutes. Sections were then rehydrated in decreasing concentrations (100%, 70%) of ethanol followed by distilled water. Tissue sections were immersed in each solution twice, for 5 minutes. The sections were then stained with Mayer's haematoxylin for 15 minutes, then rinsed in running tap water, and differentiated in acid alcohol (1% concentrated hydrochloric acid [HCl] in 70% ethanol) for 20 seconds. Sections were then rinsed with running tap water for 3 minutes, briefly placed in 1% eosin for 1 minute, which was differentiated with running tap water for 1 minute. Sections were dehydrated in increasing concentrations (70%, 100%) of ethanol and xylene, mounted using DePeX and coverslipped.

Frozen unfixed synovial tissue sections (7µm) were stained with H&E in order to determine the presence of synovial lining before immunofluorescence staining. Following cryostat sectioning, synovial sections were placed on the bench for 15 minutes to reach room temperature. The sections were placed in

x1 phosphate buffered saline (PBS), then water for 5 minutes in each, followed by staining in Harris haematoxylin for 5 minutes. The sections were placed under running tap-water for 2 minutes, and then dipped in 1% Eosin for 5 seconds, then running tap water for 5 minutes to differentiate the staining. The sections were then dehydrated in 70% ethanol, 100% ethanol then xylene for 5 minutes each. Finally the sections were mounted using DePeX and coverslipped.

2.3.2 Safranin-O and Fast green

Articular cartilage is mainly comprised of proteoglycans and type II collagen, which provide compressive and tensile strength, respectively. Altered proteoglycan expression is a feature of knee OA (Carney et al., 1984). Safranin-O is employed to visualise proteoglycan loss. Safranin-O is a basic dye that binds to acidic glycosaminoglycan (GAG) chains (part of the proteoglycan complex), to produce a red/orange stain (Kiviranta et al., 1985). Fast green is an acidic substrate which stains the subchondral bone a blue/green colour (Bulstra et al., 1993).

Paraffin wax embedded sections (5µm) were deparaffinised with xylene followed by hydration in decreasing concentrations of ethanol (100%, 70%), then distilled water. Sections were placed in Weigert's haematoxylin for 2 minutes, rinsed with running tap water for 1 minute, differentiated in acid alcohol for 20 seconds and immersed in fast green solution for 5 minutes. Subsequently sections were dipped in 1% acetic acid solution for approximately 1 second, followed by submersion in Safranin-O for 5 minutes. Running tap water was then used to differentiate the staining for 5 minutes; sections were then dehydrated in increasing grades of ethanol (70%, 100%) and xylene, and mounted with DePeX and coverslipped.

2.4 Immunohistochemistry

2.4.1 Introduction

Immunohistochemistry (IHC) is a commonly used technique combining immunological, histological and biochemical methods. Labelled antibodies are used to determine the presence, localisation and abundance of specific cellular

components (antigens) in tissue samples or cell preparations. Antigenic molecules may be protein, lipid or carbohydrate. The epitope of an antigen refers to the highly specialised antibody binding site. The antigen-antibody binding reaction is pivotal to the technique. Visualisation of the reaction is achieved by enzyme or fluorophore conjugation to the antibodies. The first pioneering IHC experiment was reported in 1950 (Coons and Kaplan, 1950). Currently IHC is widely used within research and plays a central role in clinical disease diagnosis.

Antibodies are immunoglobulins formed in the humoral immune system by plasma cells following the recognition of foreign antigens. There are five different types of antibodies; IgA, IgD, IgE IgG and IgM. IgG is the most common type of antibody used. IgG antibodies are Y-shaped structures formed of two light and two heavy polypeptide chains (figure 2.4) linked by disulphide bonds (Odell and Cook, 2013). The antibody structure is divided into three regions comprising of two F(ab), and one Fc section. The Fc region binds to Fc receptors on the surface of immune cell types. Specificity of antigen-antibody binding is achieved by the variation in amino acid sequences of the variable or terminal region of the antibody. These variable regions are specific to a particular antigenic epitope.

Antibodies used in immunohistochemistry are either classified as monoclonal or polyclonal. Monoclonal antibodies are formed by a hybridoma technique (Kohler and Milstein, 1975). B lymphocytes (B cells) constitute an important part of the immune defence system. B cells are removed from the spleen of an animal immunised with the antigen of interest. The fusion of a B cell with a myeloid (tumour) cell creates a hybridoma, which rapidly multiplies to generate a cloned population of identical antibodies which are highly specific to one epitope (Pandey, 2010). Polyclonal antibodies are formed following immunisation of an animal with a specific antigen to elicit an immune response.

Monoclonal antibodies are more specific than polyclonal as they recognise a single antigenic epitope, whereas polyclonal antibodies can recognise more than one epitope on any one antigen. Furthermore hybridomas are reliable and

consistent supply of monoclonal antibodies. Polyclonal antibodies on the other hand are cheaper and quicker to produce.

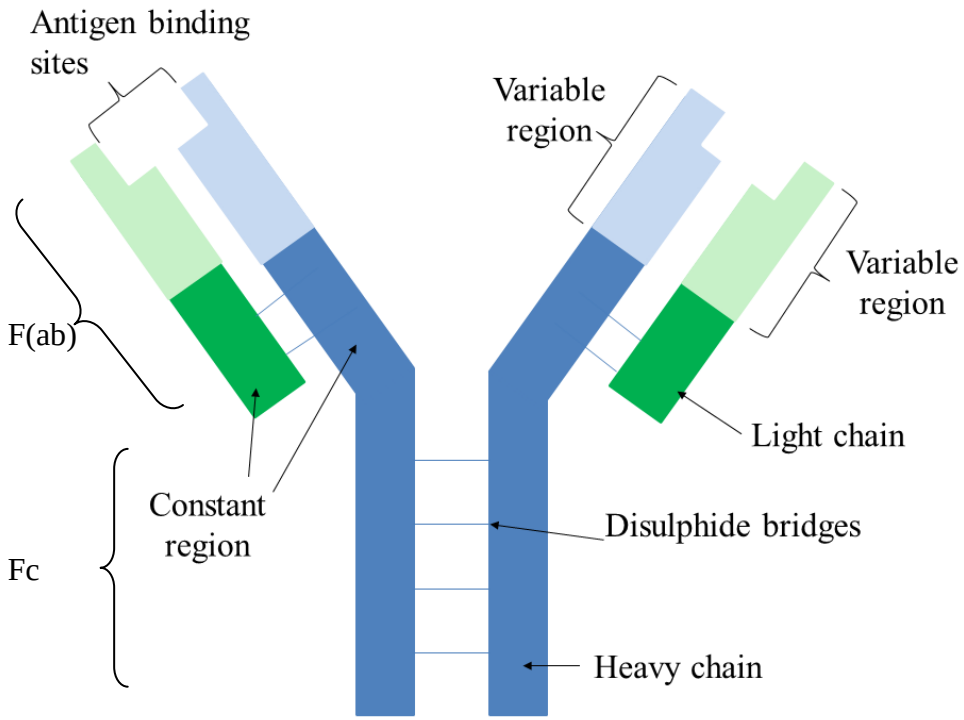


Figure 2.4: A schematic illustration of the "Y-shaped" structure of an IgG antibody molecule.

Two heavy and two light chains are joined together by disulphide bonds. Specificity of antigen-antibody binding is achieved by the variation in amino acid sequences of the variable region of the antibody. These variable regions are specific to a particular antigenic epitope. The antibody is comprised of two regions; the Fc and F(ab) regions.

2.4.2 Indirect immunohistochemistry

Immunohistochemical methods may detect the antigen of interest directly, where the primary antibody is directly coupled a label, or, indirectly. Indirect immunohistochemistry uses a two-step process. The first step includes the unlabelled primary antibody binding to the antigen of interest. The second step involves incubation with a labelled secondary antibody directed against the primary antibody. Direct IHC is a faster method than indirect; however indirect

IHC is more sensitive as more than one secondary antibody can bind to one primary antibody which amplifies the signal. The avidin-biotin complex (ABC) method is an example of indirect IHC.

The ABC method was first developed in 1981 (Hsu et al., 1981). Avidin, a large glycoprotein reacts with a strong affinity to the vitamin biotin. Avidin has 4 binding sites available for biotin, which amplifies the antigen-antibody signal. Biotin can be conjugated to enzymes or antibodies (figure 2.5). In indirect immunohistochemistry, 'biotinylayed' secondary antibodies bind to primary antibodies. Incubation of the tissue section with avidin biotin peroxide forms macromolecular complexes which can then be visualised by a variety of chromagens including diaminobenzidine (DAB), or nickel enhanced DAB to produce a brown or purple stain, respectively.

There are several advantages of the using the indirect ABC method compared to direct IHC. The ABC method is highly sensitive due to the macromolecular complex which amplifies the antigen-antibody signal therefore less primary antibody is needed. The ABC method is useful for detecting more than one antigen of interest in an individual tissue section, using two or more primary antibodies. Different enzyme markers and chromagens can be used to visualise the different antigens. A stable and rapidly formed complex is formed due to the high affinity for avidin to biotin.

Non-specific staining is thought to occur due to antibody binding to antigens other than the desired target, in addition to physicochemical interactions. Consequently, high background staining impairs identification of the antigen of interest. A blocking step can therefore be applied before incubation with the primary antibody. Blocking serum prevents binding to cell surface Fc receptors, by occupying all Fc receptors on the tissue. Serum derived from any species can be used, except for the species used to produce the primary antibody, as the secondary antibody would bind to the serum antibodies too. Usually, serum from the host species that the secondary antibody is generated in used to reduce non-specific staining.

Antigen retrieval is often required for IHC on formalin-fixed paraffin-embedded tissues. During fixation antigenic sites are masked by protein cross-

links, limiting the antigen-antibody interaction. Antigen retrieval is achieved using a variety of techniques. Proteolytic-induced epitope retrieval (PIER) uses enzymes such as pepsin, trypsin and protease to enzymatically degrade protein cross links. Alternatively, concealed antigens can be retrieved using heat-induced epitope retrieval (HIER) Samples are placed in a buffer solution inside a water bath (Shi et al., 1991), microwave or pressure cooker at high temperatures to encourage degradation of the cross-links.

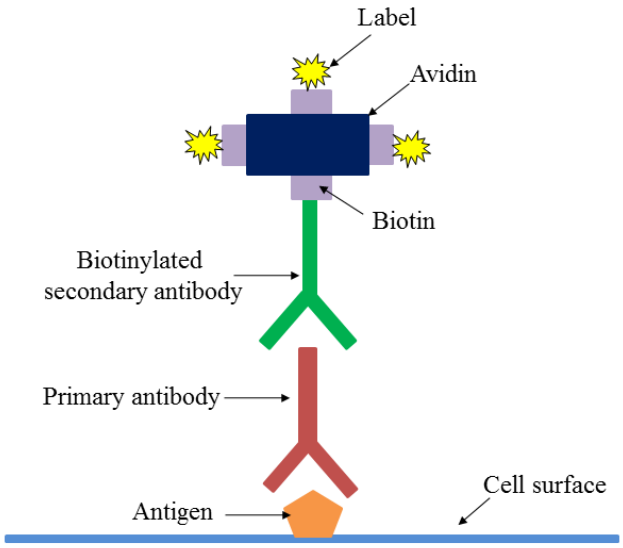


Figure 2.5: Illustrative representation of the ABC method in indirect immunohistochemistry.

An unlabelled primary antibody binds specifically to an antigen of interest on the cell surface. A biotinylated secondary antibody binds to the primary antibody. Incubation of the tissue section with avidin biotin peroxide forms macromolecular complexes which can then be visualised by a variety of chromagens labels including diaminobenzidine (DAB), or nickel enhanced DAB.

Indirect IHC was used to visualise macrophages and NGF-immunoreactivity in the human synovium. Sections of wax-embedded formalin-fixed synovia were processed as described in section 2.2.2. Sections were dewaxed in xylene, and dehydrated using decreasing concentrations of ethanol (100% and 70%). Macrophage (CD68) immunoreactivity was visualised following PIER

(1mg/ml pepsin in 0.5M acetic acid, 37˚C, 2hrs) using monoclonal mouse anti-human CD68 (clone PG-M1, Dako, Cambridge, UK), followed with biotinylated horse anti-mouse IgG secondary antibody (Vector, Peterborough, UK). NGF immunoreactivity was visualised using citrate buffer HIER (90°C, 20 mins), sections were blocked with 5% bovine serum albumin (BSA) containing goat serum followed by incubation with rabbit monoclonal antibody to NGF (clone EP1320Y,Abcam, Cambridge, UK), and bioinylated goat anti-rabbit IgG secondary antibody (Vector). Visualisation of both immunoreactivites used avidin-biotin complex (ABC) peroxidise (Vector) with DAB development (Shu et al., 1988).

2.4.3 Optimising conditions for immunohistochemistry

The aim of IHC is to achieve specific staining whilst minimalizing non-specific background staining. There are many different conditions that impact the outcome and quality of IHC. These include:

- Antibody concentration, incubation time, temperature, diluent.
- The presence or absence of a blocking agent.
- Antigen retrieval method (type, incubation time, temperature etc.) if necessary.
- Tissue fixation time and method if applicable.

Optimisation of conditions for IHC was achieved by conducting a series of initial experiments in parallel whilst changing a single parameter between runs. For example, as previously mentioned antigen retrieval was required to visualise NGF staining in formalin-fixed sections of the human synovium. As the optimal concentration of primary antibody was unknown a series of dilution titrations was tested. The primary antibody was first diluted (1:20, 1:100, 1:200, 1:400), in order to give an indication of a suitable concentration. Concurrently different antigen retrieval methods were explored, including incubating in pepsin (2hr, 37C), citrate buffer or Tris buffer (both 20 mins at 90°C).

The inclusion of appropriate controls is essential for interpretation of IHC results and to confirm the specificity of the antibodies used (Burry, 2011). Negative controls should always be run in parallel with each experiment. In order to confirm the specificity of the secondary antibody, the primary antibody should be omitted from the staining run and replaced with normal serum from the same species, containing bovine album serum (BSA). If the secondary antibody is specific to the primary antibody then no staining should be visualised. Occasionally in fixed tissues the secondary antibody can bind non-specifically to charged groups in cells. This occurrence is prevented by the addition of BSA to the normal serum. BSA will block the charged groups to prevent nonspecific binding (Burry, 2011).

If negative controls display positive staining this would indicate a lack of specificity of the antibody, or high levels of unspecific background staining. A positive control should always be included in each experiment if available. A tissue sample or section which has previously displayed positive staining when using the same experimental protocol as present should be included as a positive control. The positive control serves as an indication whether the experiment has been carried out correctly. If the positive controls do not stain as expected, the validity of the experiment should be questioned.

2.4.4 Principles of fluorescence microscopy

Immunofluorescence is a commonly used histological technique to detect the location and abundance of an antigen using fluorescence. Furthermore the relationship between two molecules can be explored by using double immunofluorescence staining which will be described further in section 2.4.5. Primary or secondary antibodies directed against the antigen of interest are conjugated to a fluorophore label (direct and indirect immunofluorescence, respectively (Odell and Cook, 2013)).

Fluorescence occurs when molecules with fluorescent properties (fluorophores) emit light extremely rapidly following the absorption of excitation light. This phenomenon is due to a rapid, but temporary conformational change in the atomic structure of the fluorophore. Typically electrons are arranged in discrete orbitals around the nucleus. When electrons in their ground state become

‘excited’ following absorption of photons (light energy) they very rapidly move to a less stable orbital further away from the nucleus. The excited state of the electrons is short lived, and the light emitted is of lower energy as the electron moves back to its ground state (Lichtman and Conchello, 2005).

There are a large spectral range of fluorophores commercially available. Each fluorophore is excited by a specific range of light wavelengths. The difference between the peak of the excitation and emission wavelengths for each fluorophore is called the Stokes shift (Lichtman and Conchello, 2005) and is depicted in figure 2.6.

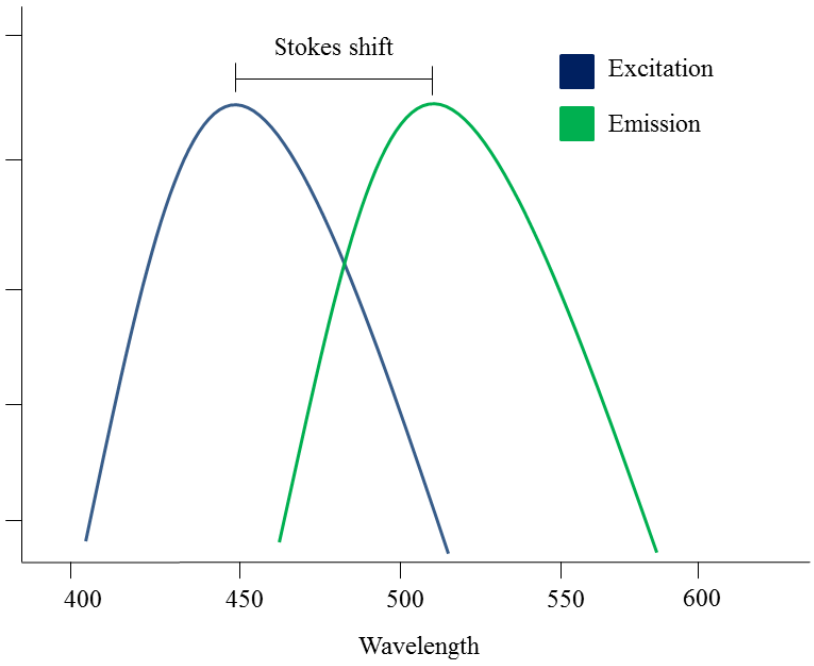


Figure 2.6: Graphical representation of the Stokes shift.

In fluorescence microscopy the Stokes shift is defined as the difference between the peak of the excitation (left curve, blue) and the emission (right curve, green) wavelength.

In immunofluorescence staining specimens are examined using a fluorescence microscope. The process is depicted in figure 2.7. In brief, illumination of the specimen requires a light source usually from a mercury bulb. As mentioned

previously, each fluorophore absorbs a specific wavelength of light therefore the excitation filters on the fluorescent microscope are specially tailored to a particular fluorophore. The excitation filter allows only the desired wavelength of light to pass towards the specimen, whilst blocking all other wavelengths. Typically fluorescence microscopes are equipped which three excitation filters; DAPI (4',6-diamidino-2-phenylindole), FITC (fluorescein isothiocyanate) and TRITC (tetramethylrhodamine isothiocyanate). Specimens examined using the three filters appear blue, green and red, respectively.

The dichroic mirror is a thin piece of glass angled at 45-degrees to the light source. It is specialised to reflect excitation light towards the specimen and pass emission wavelengths towards the eye piece. The emission filter blocks excitation light and permits only emitted wavelengths to pass through to the eye piece or to a camera.

2.4.5 Double immunofluorescence

The distribution and association of two or more co-localised antigens of interest in the same tissue sample can be evaluated using double immunofluorescence. As mentioned previously a direct or indirect approach is undertaken where the fluorophore is conjugated to the primary or secondary antibody, respectively. In the indirect method, two different secondary antibodies are each directly labelled with a different fluorophore. There should be no overlap in the excitation-emission spectra of the two fluorophores; otherwise discrimination between the two targets using different excitation filters would not be possible.

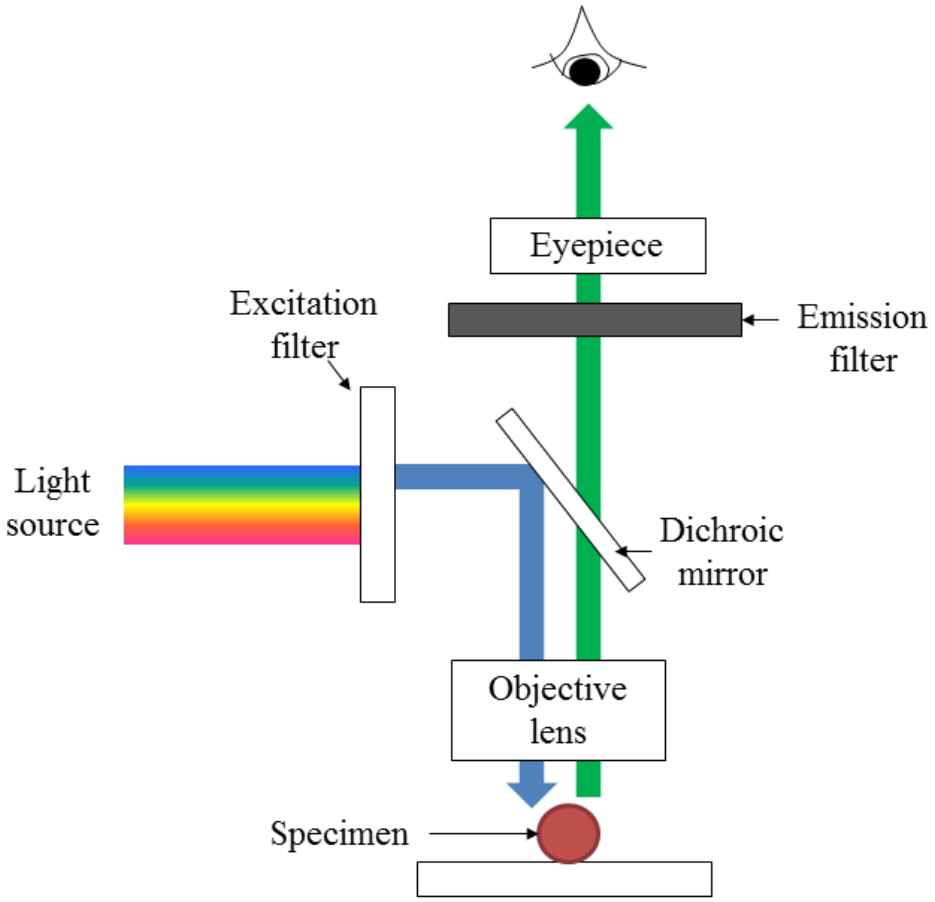


Figure 2.7: Schematic representation of a fluorescent microscope.

The excitation filter permits only the desired wavelength of light to pass through. The light is reflected off the dichroic mirror to illuminate the fluorophore bound to the molecule of interest in the specimen. Emitted light from the fluorophore passes through the dichroic mirror and emission filter to the eyepiece.

Careful planning prior to staining should be untaken to ensure cross-reactivity between reagents is avoided. Each primary antibody should be from different species. For co-localisation the two primary antibodies are mixed together and applied simultaneously to the tissue specimen, followed by simultaneous application of the two fluorophore labelled secondary antibodies.

Synovial fibroblasts can be visualised using IHC with antibodies directed against heat shock protein (Hsp) 47, a collagen-specific molecular chaperone,

(Izquierdo et al., 2011), not expressed by macrophages or endothelial cells (Kuroda and Tajima, 2004). Macrophages can be identified by the transmembrane glycoprotein CD68 (Holness Cl and Simmons, 1993).

Simultaneous double immunofluorescence was undertaken to determine the cellular co-localisation of synovial NGF, using an indirect IHC method. Secondary antibodies for detection of macrophage (CD68+) and fibroblast (Hsp47) immunoreactivity were labelled with Texas Red, and for NGF detection were labelled with Fluorescein. DAPI counterstain was used to detect cell nuclei. The full protocol is detailed in section 2.4.7. The excitation and emission spectra for each fluorophore; along with the excitation filter acquisition channel is illustrated in table 2.1.

Table 2.1: Spectral properties of fluorophores used to determine localisation of synovial NGF.

Fluorophore	Acquisition channel	Marking	Excitation	Emission	Image colour
DAPI	DAPI	Nuclei	340 nm	488 nm	Blue
Fluorescein	FITC	NGF	490-500 nm	510-520 nm	Green
Texas Red	TRITC	Hsp47	595-604 nm	606-615 nm	Red
Texas Red	TRITC	Cd68	595-604 nm	606-615 nm	Red

Abbreviations DAPI = 4',6-diamidino-2-phenylindole, FITC = fluorescein isothiocyanate, TRITC = tetramethylrhodamine isothiocyanate.

2.4.6 Auto fluorescence

Frozen tissue sections were cut (7µm thickness) using a Bright cryostat. Prior to staining sections were examined under the fluorescence microscope and were found to display autofluorescence.

Autofluorescence is a naturally occurring process in which endogenous fluorophores (for example, elastin, lipofusin, haemoglobin etc.) emit light over

a broad range of wavelengths (Burry, 2011). The presence of autofluorescence may mask or hinder immunofluorescence analysis, making it difficult to visualise protein targets of interest. Different techniques can be undertaken to quench autofluorescence in fluorescence microscopy. Sudan black B (0.1%-1%) has previously been shown to effectively block autofluorescence in various tissues (Schnell et al., 1999, Sun et al., 2011).

Unfixed fresh cryostat synovia sections (7µm) were treated with concentrated solutions of Sudan Black B (0.3%, 0.7%, 1%) and then examined microscopically. Sudan black B at a concentration of 1% was found to be most effective in quenching the autofluorescence.

2.4.7 Immunofluorescence protocol

Prior to simultaneous double-staining optimisation of staining methods was achieved by initial single staining runs for NGF, macrophage and fibroblast immunoreactivity. Different combinations of primary and secondary antibody concentrations were explored. Optimal concentrations for each antibody are listed in the appendix (chapter 8).

Double immunofluorescence determined the cellular co-localisation of synovial NGF. Synovia from TKR (n=3), PM cases with high chondropathy (n=3) and non-arthritic controls (n=2) were simultaneously double-stained for NGF and either macrophage or fibroblast markers. Frozen synovial tissue sections (7µm) were fixed in 4% paraformaldehyde followed by acetone, then blocked with 5% BSA containing goat and horse serum. Sections were incubated with a mixture of antibodies directed to NGF (clone EP1320Y,Abcam, Cambridge, UK) and either CD68 (clone PG-M1, Dako, Cambridge, UK), or Hsp47 (M16.10A1, Enzo Life Sciences, Exeter, UK) overnight, followed by incubation with a mixture of secondary antibodies; Texas Red horse anti-mouse IgG, and Fluorescein goat anti-rabbit IgG (Vector). Sections were counterstained with 4',6-diamidino-2-phenylindole (DAPI) to visualise cell nuclei. Autofluorescence was blocked with 1% Sudan black (Sigma-Aldrich, Poole, UK) in 70% ethanol. Sections were mounted in PBS/glycerol.

Controls were run in parallel with the experiment to determine the validity of staining.

The run consisted of three negative controls where;

i. Both of the primary and secondary antibodies were omitted.

ii. The primary antibody was omitted but the secondary antibody Texas Red horse anti-mouse was applied.

iii. The primary antibody omitted but the secondary antibody Fluorescein goat anti-rabbit was applied.

Three positive control sections were included in the experiment. Synovial tissue samples that had previously showed specific staining for NGF, Hsp47 and CD68 when stained in a single immunofluorescence protocol run were included.

i. Section stained for NGF only, using Fluorescein goat anti-rabbit secondary antibody.

ii. Section stained for CD68 only, using antibody Texas Red horse anti-mouse secondary antibody.

iii. Section stained for Hsp47 only, using antibody Texas Red horse anti-mouse secondary antibody.

The experiment was considered invalid if positive staining was detected in any of the negative controls or if the positive controls did not stain as expected.

2.5 Histological scoring

2.5.1 Medial tibial plateau

The histological-histochemical grading system developed by Mankin is a widely used histopathological tool for evaluating the severity of osteoarthritic changes in articular cartilage**.** The grading system was initially developed in 1971, by assessing femoral heads obtained at OA hip replacement surgery

(Mankin et al., 1971). The grading system evaluates the severity of OA based on the histological and histochemical changes of the articular cartilage. Cartilage surface integrity (figure 2.8), chondrocyte morphology (figure 2.9), proteoglycan loss (Safranin-O loss) (figure 2.10) and tidemark integrity (figure 2.11) are each assessed and graded (see table 2.2). The score for each feature is then summed to provide a total score (0-14), where 0 indicates normal articular cartilage and 14 indicates severe OA.

Despite being the most widely used histopathological system; there are several limitations of the Mankin score. For example, the score was developed using specimens with advanced OA therefore the validity of the score in distinguishing early or mild features of OA is questionable (Ostergaard et al., 1999). More recently the Osteoarthritis Research Society International (OARSI) aimed to develop a more useful tool for histological grading of cartilage pathology (Pritzker et al., 2006). The OARSI score assesses grade of pathology, which refers to the severity of disease (0 [normal cartilage architecture] to 6 [subchondral bone remodelling]) and the stage which refers to surface extent of lesion (0 [no OA activity] to 4 [>50% involvement]). Several comparative studies have found a strong positive correlation between Mankin and OARSI histopathological scores (Custers et al., 2007, Pearson et al., 2011, Pauli et al., 2012).

Despite being a more comprehensive assessment of OA there are several limitations of the OARSI score. For example, each grade boundary addresses multiple features, and contradictory observations can occur (Pearson et al., 2011). Moreover, determining the precise stage (or surface extent) of OA progression can be subjective leading to variation in the degree of involvement of the cartilage surface. Furthermore grades 1 to 4 of the OARSI score only consider articular cartilage changes. Subchondral bone pathology is a feature of grades 5 to 6. This sequence implies cartilage alterations precede subchondral bone pathology which may not always be the case.

Table 2.2: The histological-histochemical grading system for osteoarthritic articular cartilage developed by Mankin et al

Grade	Cartilage surface integrity	Proteoglycan loss†	Chondrocyte morphology	Tidemark integrity
0	Normal	No loss	Normal	Normal
1	Mild surface irregularities	Mild loss	Hypercellularity	Breached
2	Pannus and surface irregularities	Moderate loss	Cloning	-
3	Clefts to transitional zone	Severe loss	Hypocellularity	-
4	Clefts to radial zone	Complete loss	-	-
5	Cleft to calcified zone	-	-	-
6	Complete disorganisation	-	-	-

†Proteoglycan loss measured by loss of intensity of Safranin-O stain.

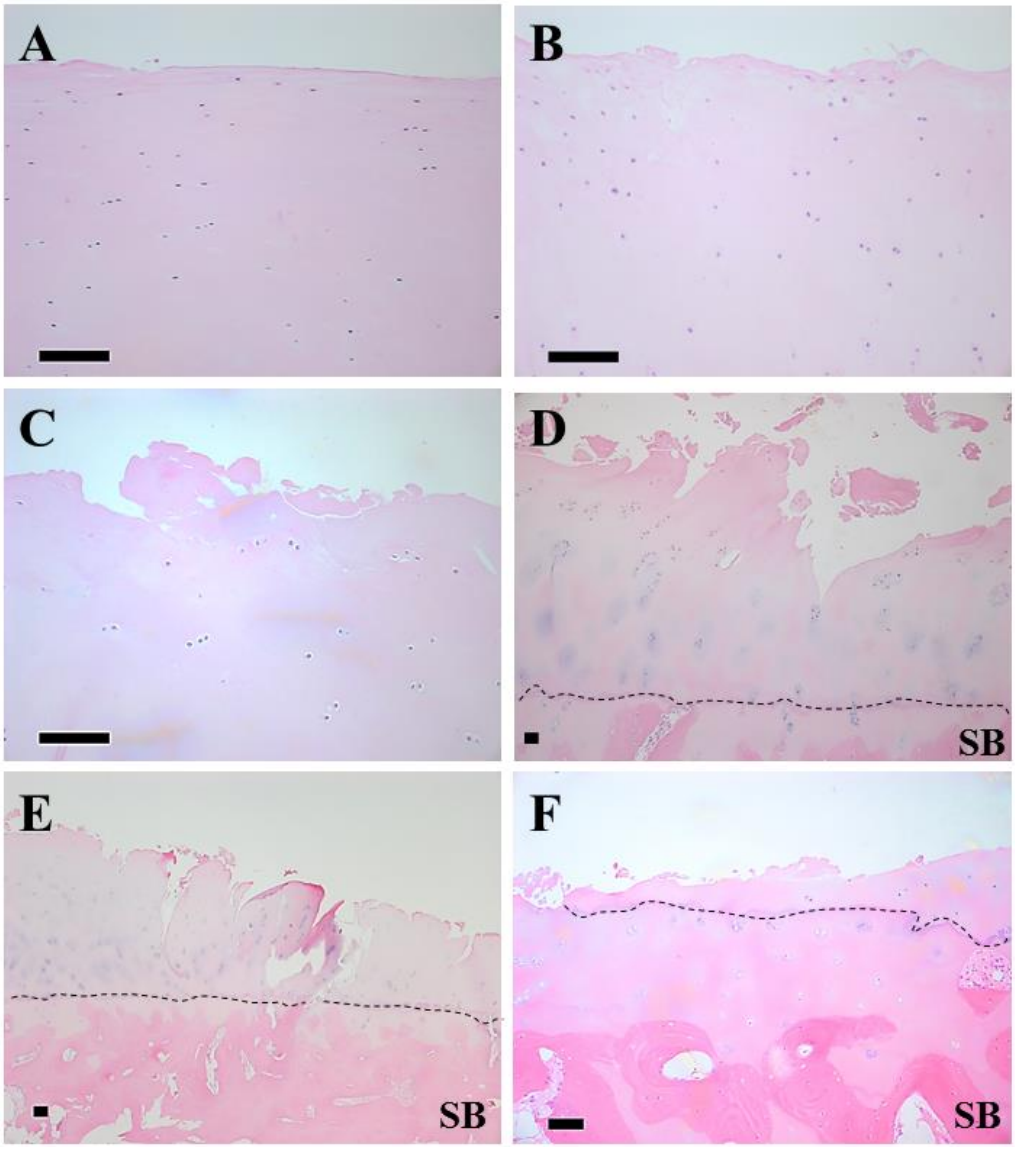


Figure 2.8: Histological assessment of cartilage surface integrity

Mild clefts to the superficial cartilage surface, grade 1 **(A)**. Slightly more severe clefts to surface, grade 2 **(B)**, 2 or more clefts to transitional (middle) zone, grade 3 **(C)**, 2 or more clefts to the radial (deep zone), grade 4 **(D)**. Cleft breaching tidemark and entering calcified cartilage, grade 5 **(E)**. Complete disorganisation, cartilage almost completely eroded from specimen, grade 6 **(F)**. Arrows indicate synovial lining surface Dotted line indicate tidemark. Abbreviations: SB Subchondral bone. Images captured at x4 magnification. Scale bar = 100µm.Visualised with haematoxylin and eosin stain.

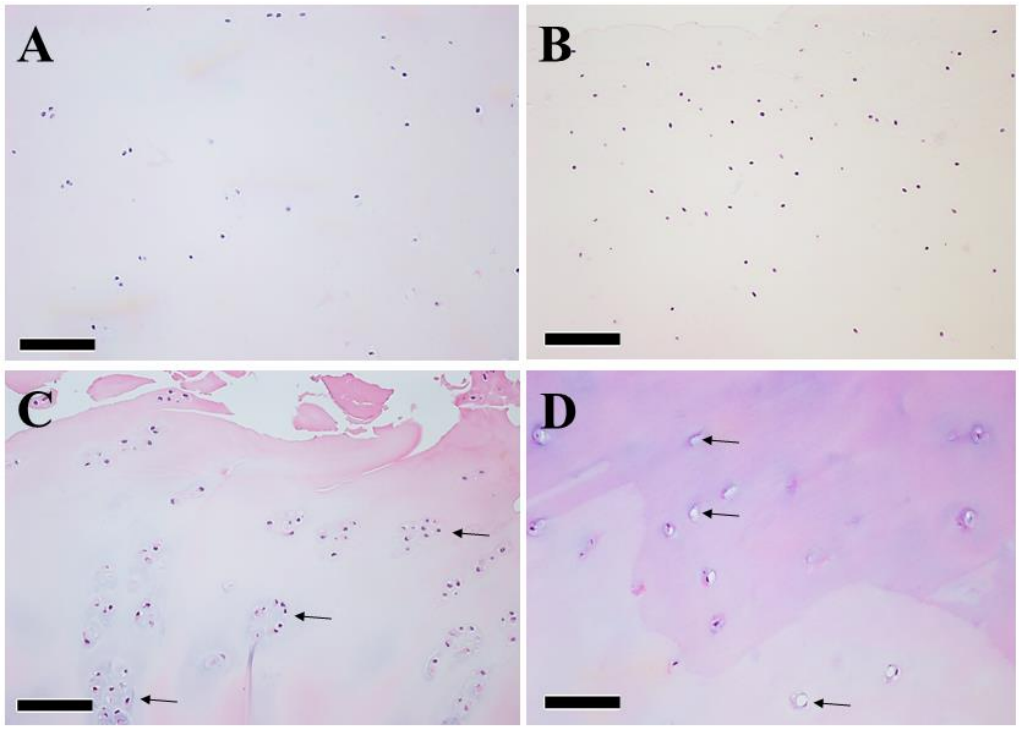


Figure 2.9: Chondrocyte morphology in the medial tibial plateau.

Normal chondrocyte morphology, grade 0 **(A)**, Chondrocyte hypercellularity, grade 1 **(B)**, Chondrocyte cloning (arrows), grade 2 **(C)**, Chondrocyte hypocellularity, grade 3, arrow indicates empty lacunae **(D)**. Images captured at x20 magnification. Scale bar = 100µm. Visualised with haematoxylin and eosin stain.

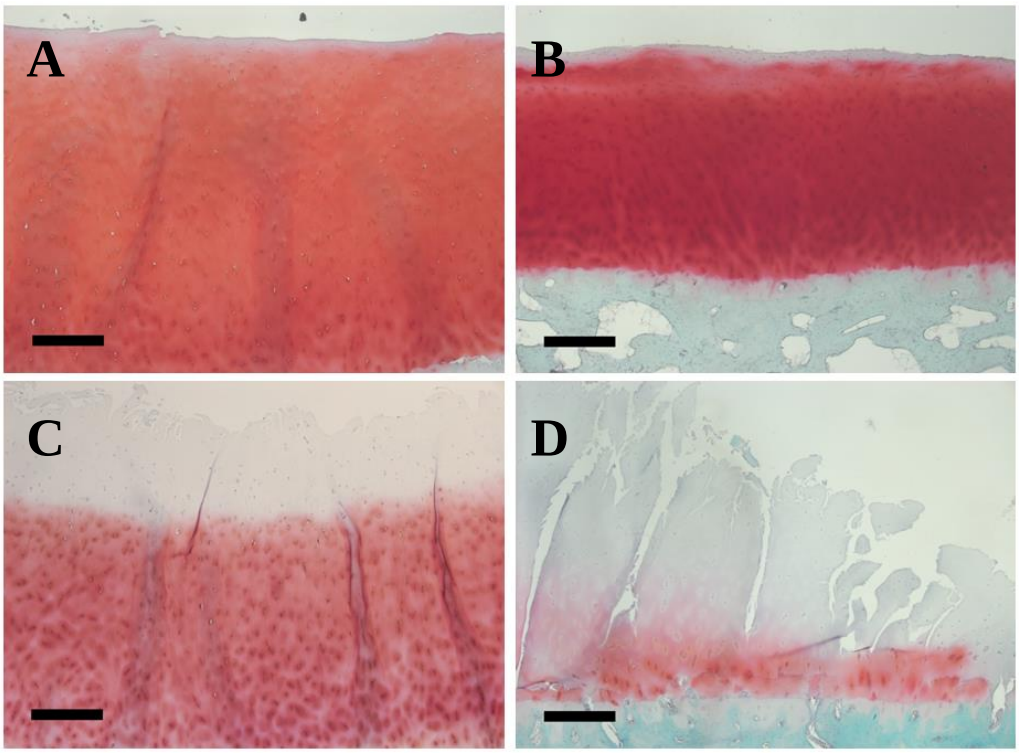


Figure 2.10: Histological assessment of proteoglycan scoring in the medial tibial plateaux of PM (A-B) and TKR (C-D) cases.

Normal proteoglycan content in the articular cartilage, grade 0 **(A)**. Mild proteoglycan loss in the superficial cartilage layer, grade 1 **(B)**. Moderate proteoglycan loss, grade 2 **(C)**. Severe proteoglycan loss, grade 3 **(D)**. Abbreviations SB = subchondral bone. Images captured at x4 magnification, scale bar = 500µm. Visualised with Safranin-O with Fast green stain.

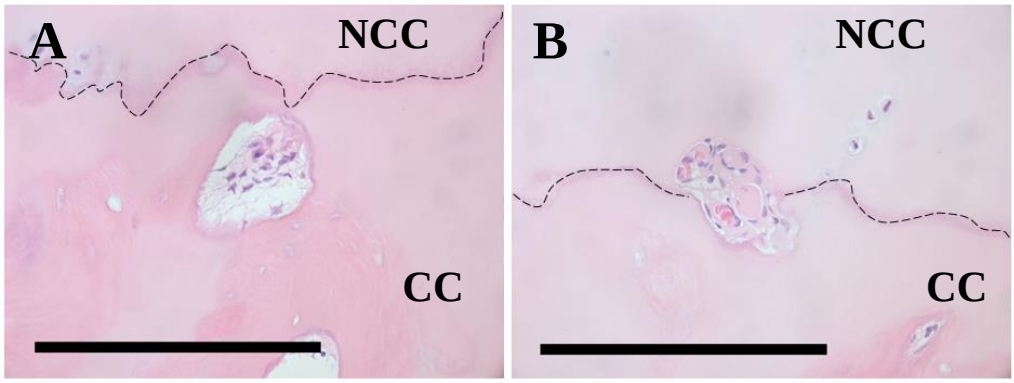


Figure 2.11: Histological assessment of tidemark integrity.

Channels were observed in calcified cartilage (CC) beneath an intact tidemark (indicated by dotted line), Mankin score of 0 **(A).** Whereas **(B)** shows a channel breaching the tidemark and entering non-calcified cartilage (NCC). Images captured at x20 magnification, scale bar = 500µm. Visualised with haematoxylin and eosin stain.

Typically subchondral bone marrow spaces contain fatty marrow tissue (figure 2.12A). During OA, focal areas of fatty marrow may be replaced with fibrovascular tissue (figure 2.13B) (Milgram, 1983, Walsh et al., 2010). Fibrovascular tissue has been characterised as manifestations of subchondral bone marrow necrosis, fibrosis and oedema (Zanetti et al., 2000). The presence of subchondral bone marrow replacement by fibrovascular tissue was assessed in each case as either present (pathological) or absent (normal).

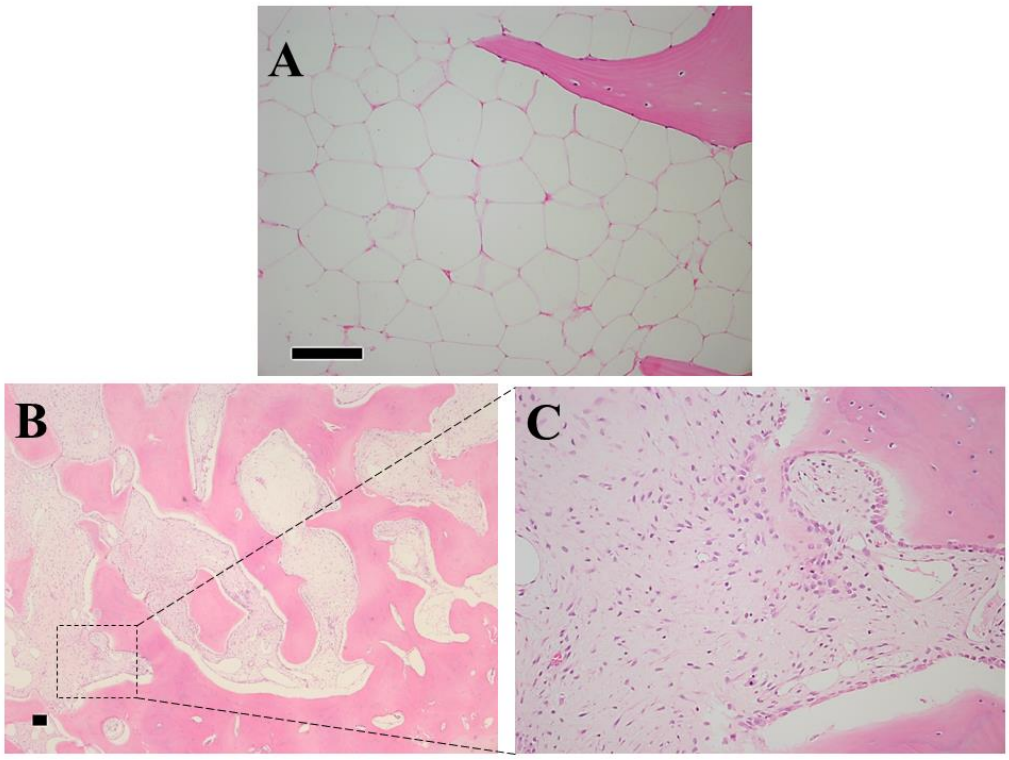


Figure 2.12: Histological assessment of the subchondral bone marrow in human tibial plateau.

Normal subchondral bone marrow spaces were filled with fatty tissue in a non-arthritic knee **(A),** whereas **(B)** subchondral bone marrow was replaced by fibrovascular tissue in an OA knee. High power image **(C)** of the area indicated by the dotted box in **B**. Images captured at x10 **(A&B)** and x20 **(C)** magnification, scale bar = 100µm. Visualised with haematoxylin and eosin stain.

2.5.2 Synovitis histological score

Synovial inflammation is increasingly being recognised as an important contributor to knee OA. During inflammation, synovitis is typified histologically by a marked increase in synovial cell lining layer thickness in addition to infiltration of inflammatory cells and increased cellularity. Several scoring systems have been established to measure the degree of synovitis in histological specimens. Krenn et al have developed a 9-point based histopathological score which examines three specific criteria independently (Krenn et al., 2002, Krenn et al., 2006). Hyperplasia, cellularity and

inflammatory infiltrate are each graded from 0 (feature is absent) to 3 (severe). The summation of each feature provides a total synovitis score. A score of 0-1 indicates no synovitis, 2-4 low grade synovitis and 5-9 high grade synovitis.

In contrast the score developed by Haywood et al classifies synovitis based on a simpler 3-point scoring system (Haywood et al., 2003). A score of 0 indicates no synovitis, 1 mild synovitis, 2 moderate synovitis and 3 severe synovitis (figure 2.13). Whereas the Krenn score examines the three criteria independently, the Haywood score examines all three criteria together as illustrated in table 2.3.

Table 2.3: Classification system for histologically assessing synovial tissue inflammation in haematoxylin and eosin tissue sections, developed by Haywood et al. 2003.

Grade	Synovial lining thickness	Cellularity	Inflammatory cells
0: Normal	< 4 cells	Sparse	None or few
1: Mild inflammation	4 – 5 cells	Increased	Some
2: Moderate inflammation	6- 7 cells	Dense	Many, but no lymphoid aggregates
3. Severe inflammation	> 7 cells	Dense	Many including lymphoid aggregates

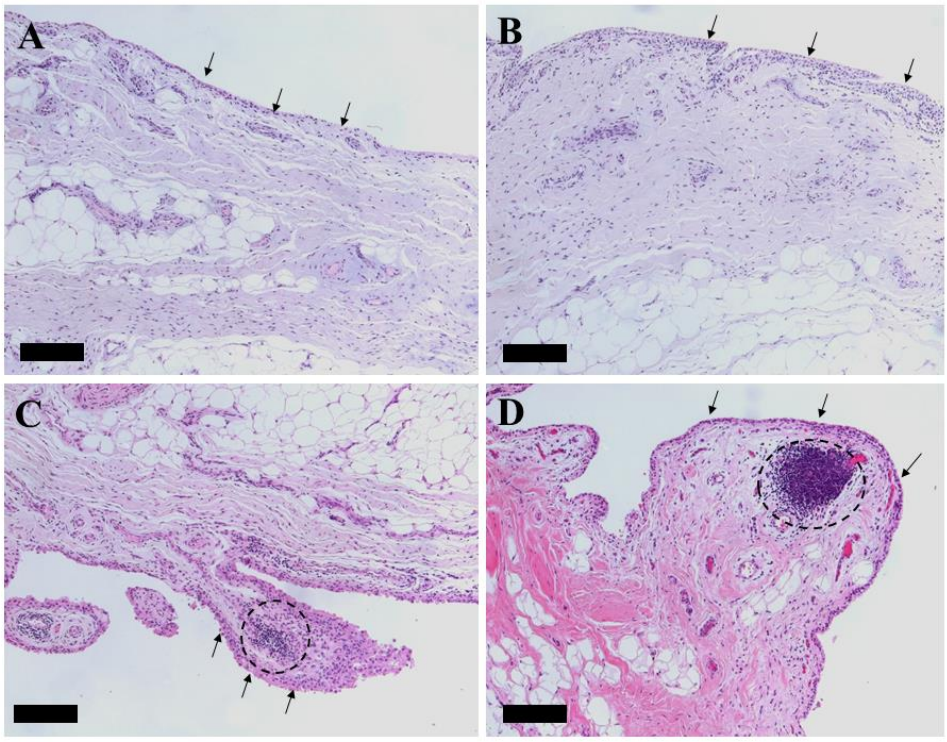


Figure 2.13: Histological scoring of synovial inflammation according to Haywood et al criteria.

Normal synovium, grade 0 **(A)**, Mild inflammation, grade 1 **(B),** Moderate inflammation, grade 2, dotted circles indicate small cluster of inflammatory cells **(C).** Severe inflammation, dotted circle indicates perivascular lymphoid aggregate grade 3 **(D).** Arrows indicate synovial lining surface. Images captured at x4 magnification, scale bar = 100µm. Visualised with haematoxylin and eosin stain. The synovium tissue was not decalcified during tissue processing.

2.5.3 Meniscus histological classification

Meniscal degeneration was graded according to the modified Copenhaver classification system (Copenhaver W, 1978, Ishihara et al., 2009), detailed in table 2.4. Photomicrographs of meniscal scoring are illustrated in figure 2.14.

Table 2.4: Modified Copenhaver classification system for histologically assessing meniscal degeneration in haematoxylin and eosin tissue sections.

Grade	Appearance of collagen bundles	Chondrocytes
0: Normal	Homogenous staining, collagen bundles closely set	Normal distribution
1: Mild degeneration	Mild cleft formation of collagen bundles, irregular staining	Reduction of chondrocytes
2: Severe degeneration	Severe cleft and cysts formation of collagen bundles	Areas of complete chondrocyte loss (hypocellularity)

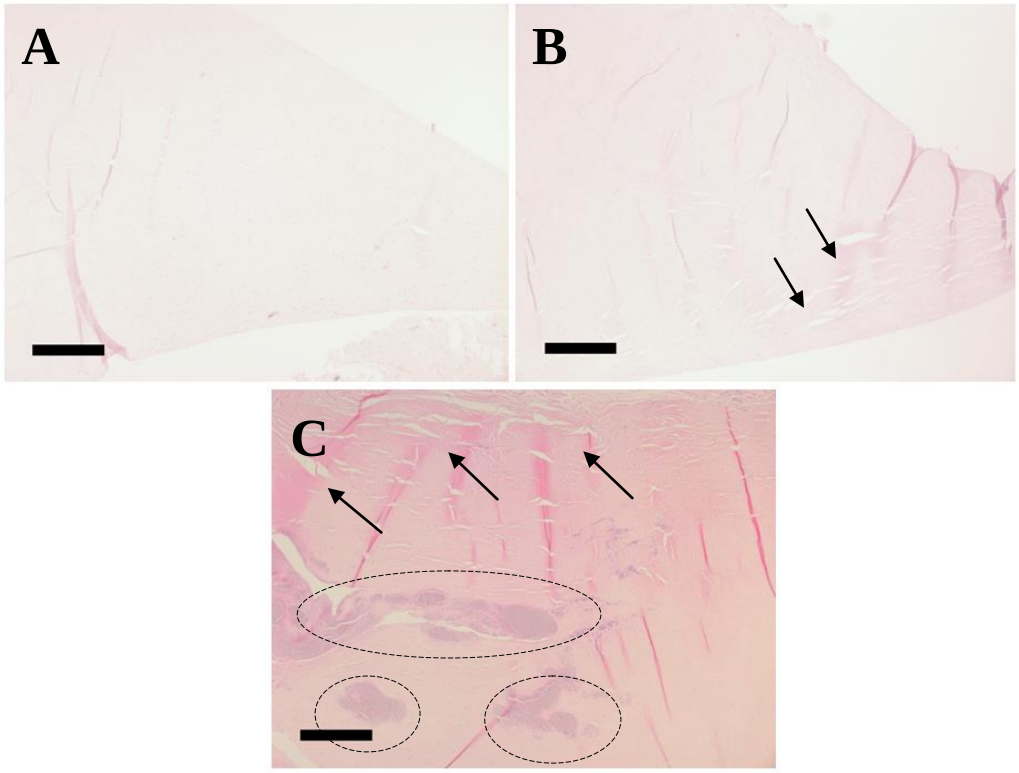


Figure 2.14: Histological appearance of human menisci.

Normal meniscus, collagen bundles closely set, grade 0 **(A),** Mild degeneration, mild clefs of the collagen bundles can be observed (arrow) **(B),** Severe degeneration, severe cleft formation (arrows) and cyst formation (dotted circles) **(C)**. Images captured at x4 magnification, scale bar = 500µm. Visualised with haematoxylin and eosin stain.

2.6 Image analysis and quantification

All histological and immunohistological scoring was carried out by a single observer blinded to diagnostic classification and clinical details, using a Zeiss Axioscop-50 microscope (Carl Zeiss, Welwyn Garden City, UK).

Mid-coronal sections of the middle third of medial tibial plateaux were stained by H&E, or to visualise proteoglycan content, with Safranin-O and examined for osteoarthritic alterations, according to the histological histochemical grading system proposed by Mankin (Mankin et al., 1971).

Cartilage surface integrity and the presence of subchondral bone marrow replacement by fibrovascular tissue were first evaluated using a x4 objective lens under transmitted light, and were more closely inspected using a x10 then x20 objective lens. Chondrocyte morphology and tidemark integrity was evaluated using a x20 and x40 objective lens. Tidemark breaching was accepted if channels in the calcified cartilage penetrated the tidemark and were touching the non-calcified layer, but was not if they were just touching the tidemark. Occasionally tidemark breaching could not be assessed due to loss of integrity of the osteochondral junction.

Histological synovial inflammation grade was determined by examining a H&E preparation using x20 and x40 lens. Meniscal degeneration was examined on a H&E preparation using x4, x10 and x20 objective lens.

Macrophage and NGF fractional area were quantified using a 3-CCD video camera and KS300 image analysis software. Areas of the synovium with the highest density of CD68 or NGF positive staining were identified. Briefly, an image was captured and area of interest which included synovial lining and sublining was delineated. Positive staining was differentiated from background by thresholding the image according to hue to create a mask. The area of positive staining and total area were measured. Fractional area was determined as the percentage of synovial area positive for CD68 or NGF immunoreactivity within the total area. Data were collected using a x20 objective lens in four different fields of view. Only samples with synovial lining were included in analyses.

2.7 Macroscopic chondropathy scoring

Structural pathology in OA can be measured by a variety of methods. Athroscopic studies examine the macroscopic appearance of the affected joint to evaluate degree of global structural change. The Systeme Francaise D'Athroscoprie (SFA) system was established in 1994 by Dougados et al to detect macroscopic changes in chondropathy severity (Dougados et al., 1994). The system has since been further developed (Ayral et al., 1994, Walsh et al., 2009). Macroscopic chondropathy scoring is a useful measure of global disease severity, but does require access to intact joint specimens.

Following tissue harvesting, articular surfaces of the medial and lateral tibial plateaux and femoral condyles were evaluated on the extent and severity of loss of surface integrity by a single assessor, according to the method described by Walsh et al (Walsh et al., 2009), after Ayral et al (Ayral et al., 1994). Femoral condyles and tibial plateaux were photographed from a fixed distance of 23 cm using a Kaiser RS 2 XA camera stand, under standard illumination with a Sony DSC-s85 CyberShot digital camera fitted with a Carl Zeiss lens at ×4 zoom (Carl Zeiss Ltd., Welwyn Garden City, UK).

The extent and severity of articular cartilage loss of medial and lateral femoral condyles and tibial plateaux were graded as follows:

- Grade 0 = normal: smooth, unbroken surface, homogeneous white to off-white colour.
- Grade 1 = swelling and softening: a light brown homogenous colouration.
- Grade 2 = superficial fibrillation: lightly broken surface, white to off-white/light brown in colour.
- Grade 3 = deep fibrillation: coarsely broken cartilage surface, dark brown, grey or red in colour.
- Grade 4 = subchondral bone exposure: stippled white and dark brown/red in colour.

The proportion of each articular surface area corresponding to each grade was used to calculate a chondropathy score (0-100):

Chondropathy score = (Grade 1 x 0.14) + (Grade 2 x 0.34) + (Grade 3 x 0.65) + Grade 4

Scores for each of the 4 compartments were summated to give a tibiofemoral chondropathy score (0-400). Surgical damage precluded the calculation of macroscopic chondropathy scores for some TKR cases.

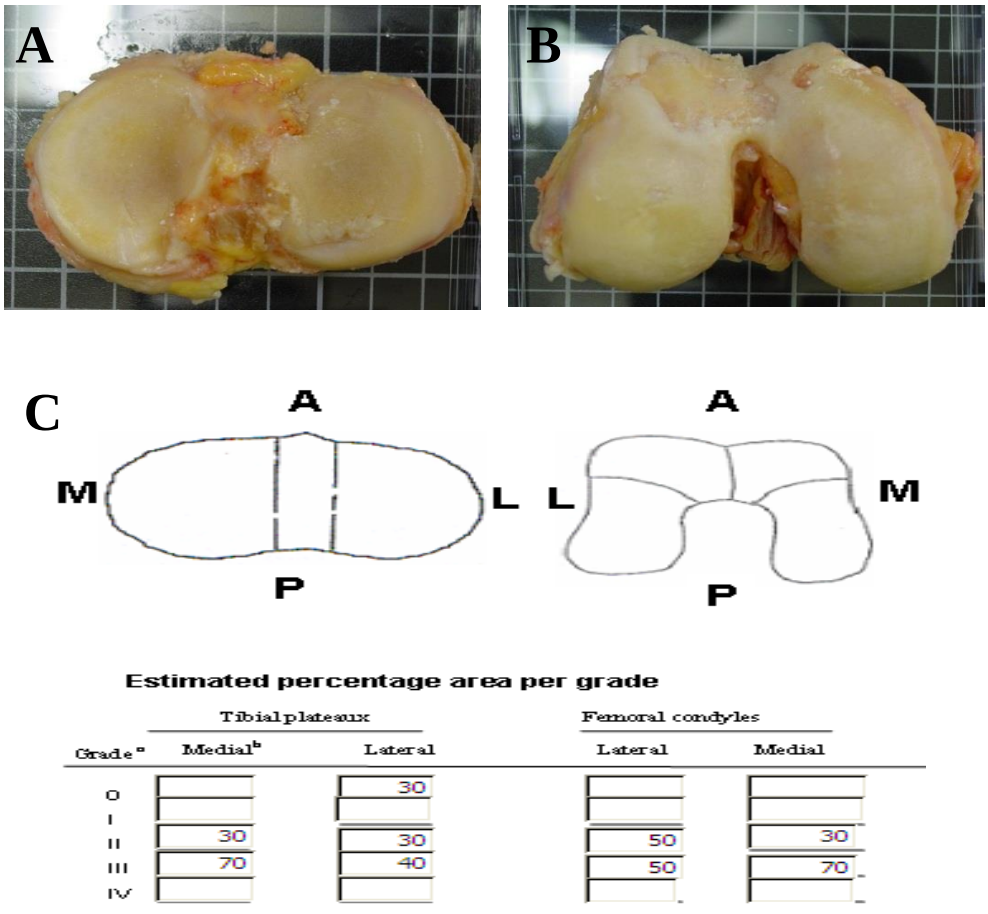


Figure 2.15: Severity of macroscopic chondropathy at the articular surface of tibiofemoral joints obtained at post-mortem.

Macroscopic appearance of tibial plateaux **(A)** and femoral condyle **(B)** obtained post-mortem**.** Scoring sheet **(C)** displaying the percentage of each articular surface estimated at each grade i.e., medial tibial plateaux articular surface was scored as 30% grade 2, 70% grade 3. Total knee chondropathy score for this case was 197.1. A = anterior, P = posterior, M = medial, L = lateral.

2.8 Radiographic osteoarthritis score

Radiographic assessment of OA is often considered as the gold standard in defining knee OA and assessing structural alterations. The Kellgren and Lawrence grading system developed in 1957 is the most widely used scoring system in arthritis (Kellgren and Lawrence, 1957). The score assesses osteophyte formation and JSN. Although the grading system is widely used in

clinical practice and research there are several criticisms (Spector and Cooper, 1993). For example prominence is given to the presence of osteophytes rather than JSN. Furthermore, the sequence of pathological events in OA remains unclear; the scoring system assumes the formation of osteophytes precedes joint space narrowing which may not necessarily always be the case.

More recently a line drawn atlas has been developed to assess and grade joint space narrowing and osteophytes on knee radiographs (Nagaosa et al., 2000, Wilkinson et al., 2005). The atlas is advantageous as it provides separate line drawn images for joint space and osteophyte narrowing for males and females and in three compartments of the knee.

Radiographic severity scores were derived using preoperative postero-anterior knee radiographs as previously described (Walsh et al., 2009). A line drawn atlas was used to grade medial and lateral joint space narrowing (JSN) and osteophytes (OST) (Nagaosa et al., 2000). JSN (0-6) and OST (0-12) scores were summated to provide a total radiographic OA severity score (0-18). (Walsh et al., 2009). Radiographs were not available for PM cases.

2.9 Clinical characteristics of total knee replacement cases

Prior to TKR surgery, clinical data was collected from OA patients in pre-operative assessment clinic and from medical notes. Data were recorded for the duration of symptom onset, morning stiffness and inactivity stiffness in the biopsied joint. The presence or absence of effusion, increased warmth and synovial thickening in the biopsied joint were assessed by physical examination (Deborah Wilson) during pre-operative assessement. Data regarding laterality of the biopsied joint, in addition to previous fractures or surgery were also recorded.

2.10 Body mass index

Body mass index (BMI; kg/m^2) was calculated from height (meters; m) and weight (kg) measurements documented in the cases notes of the TKR cases included in the histological associations of OA and symptomatic OA study groups. BMI data were not available for PM cases. Classification of BMI is detailed in table 2.5.

Table 2.5: BMI Classification

BMI (kg/m^2)	Classification
< 18.5	Underweight
18.5 – 24.9	Normal
25-29.9	Overweight
>30	Obese

2.11 Simulating the effects of post-mortem decay in surgical tissue

Knee tissue obtained from total knee replacement patients was formalin fixed soon after surgery. In comparison, PM tissue biopsies were not collected generally until 24- 48 hours after death. Tissue might undergo natural decay in the body before fixation.

In chapter 3 immunohistochemical differences in macrophage and nerve growth factor (NGF) expression in the synovium of PM and TKR cases are explored. Several approaches were undertaken to establish whether differences in macrophage and NGF expression between the two groups are due to differences between the groups.

First, PM delay was calculated as the time (hours) between death and opening of the knee for tissue collection, as documented in the case notes of PM cases. Following death cadavers were stored at 4°C before tissue collection. PM delay intervals were available for all non-arthritic control (n=26) and asymptomatic chondropathy PM cases (n=29).

Second, the effects of PM delay were mimicked using tissue obtained at TKR. Following TKR surgery for symptomatic OA, synovial biopsies were collected and placed in Dulbecco's Modified Eagle's medium (DMEM) at 4°C until collected for processing (see section 2.2.2).

One quarter of the synovial tissue was immediately fixed in formalin at room temperature; the remaining synovium was placed back in to DMEM at 4°C. Twenty-four hours after collection a second section of the synovium stored in DMEM was dissected and immersed in formalin, the remaining synovium was placed back into DMEM at 4°C. Forty-eight hours after collection, the third section of synovium was dissected from tissue stored in DMEM, and immersed in formalin. The remains of the synovium were placed back in same DMEM at 4°C. Seventy two hours after collection the final piece of synovium was dissected and immersed in formalin. Tissues at all 4 time points were fixed for 3 days before wax-embedding.

The tissue was then stained for nerve growth factor expression using IHC Expression was quantified and compared at each time point using repeated measures analysis.

2.12 Gene expression patterns in the synovium

The following section will describe methods undertaken to extract and isolate total RNA from snap frozen synovial samples obtained post-mortem or following total knee replacement surgery for OA. Following extraction, the RNA was then reverse transcribed to produce complementary DNA (cDNA), and the expression of 96 (including 4 reference) genes was quantified. Selection criteria for cases within this study are described in section 2.1.3. Brief overviews of methods employed are illustrated in figure 2.16.

2.12.1 Extraction of total RNA from synovia

Synovial biopsies obtained PM and at the time of TKR surgery for symptomatic OA were immediately snap frozen in liquid nitrogen without fixation, as described in section 2.2.2.

For RNA extraction, snap frozen synovia were placed on top of a metal block that had been precooled in dry ice for 20 minutes. The tissue was stabilised using forceps and the synovial lining identified as a light white band in the tissue. A scalpel was used to dissect a piece of tissue (approximately 50 mg)

containing the synovial lining. Care was taken to avoid collecting fatty tissue, which was identified as a pale yellow colour. The tissue was transferred into a 5ml polypropylene snap-cap tube containing 1ml of ice cold TRI reagent (Sigma Aldrich, UK). The tissue was immediately homogenised using an Ultra-Turrax T25 homogeniser (Janke and Kunkel) for approximately 30 seconds or until complete homogenisation of the tissue. The homogenate was placed on ice until all isolations were complete, and then incubated at room temperature for 5 minutes to permit complete dissociation of nucleoprotein complexes.

RNA was isolated by adding 0.2ml of 1-bromo-3-chloro-propane (BCP) to the homogenate. The mixture was centrifuged at 10,000g for 15 minutes at 4°C. The aqueous upper phase was carefully transferred into a fresh tube. RNA was precipitated by adding 0.5ml isopropanol and 20mg/ml glycogen solution. After thorough mixing the solution was incubated at room temperature for 20 minutes.

The precipitated RNA was collected by centrifugation at maximum speed (21,000g) for 10 minutes at 4°C. The precipitated RNA formed a small pellet on the bottom of the tube. The supernatant was removed and pellet was gently agitated with a pipette and washed twice with 80% ethanol, followed by centrifugation for 10 minutes at 4°C (maximum speed). Following removal of the supernatant the pellet was allowed to air dry for 5 minutes until all ethanol had evaporated from inside the tube. DEPC-treated water was added to dilute pellet, dissolution was facilitated by heating the extraction to 65°C for 5 minutes. RNA concentration was assessed using a nanodrop spectrophotometer (as described in the following section 2.12.2). The diluted RNA solution was stored at -80°C until further processing.

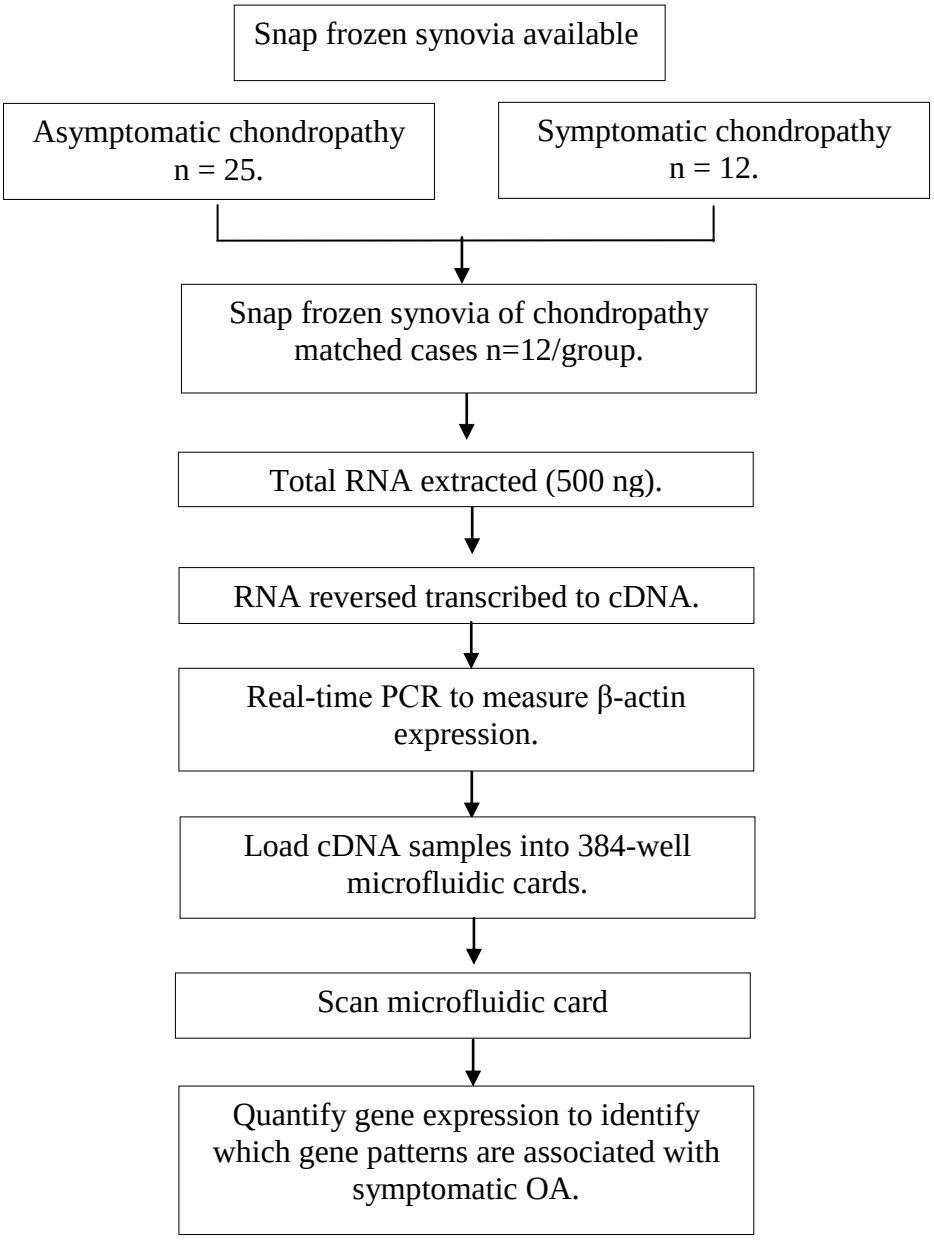


Figure 2.16: Flowchart illustrating steps undertaken to isolate total RNA and quantify gene expression in human synovial samples.

Snap frozen synovia were obtained from 12 asymptomatic OA (PM) cases and 12 symptomatic OA cases (TKR).

2.12.2 Spectrophotometric analysis of RNA

RNA purity and concentration were determined using a NanoDrop™ spectrophotometer 2000/2000c. The spectrophotometer measures the wave length absorbance of all molecules within the samples to define nucleic content. All nucleotides (including RNA) absorb at 260 nm. Purity of RNA is assessed by evaluating ultraviolet absorbance at 260 nm and 280 nm and was estimated by the 260:280 nm ratios. Pure RNA has a ratio of 2. Ratios less than 2 may indicate co-extraction of other molecules such as proteins. Such contaminants may affect gene expression analysis; therefore the addition of RNase inhibitors during reverse transcription is necessary.

2.12.3 Reverse transcription

Reverse transcription is the process by which complementary DNA (cDNA) is synthesised from an RNA template. The reaction is catalysed by the enzyme reverse transcriptase (RTr). The cDNA then acts as a template in the real-time polymerase chain reaction (RT-PCR).

Occasionally, gDNA (genomic DNA) is co-extracted with RNA. Genomic DNA is constructed of interrupting coding and non-coding regions (exons and introns, respectively), whereas during splicing introns are removed from the sequence, to produce messenger RNA (mRNA). Co-extraction of gDNA may interfere with gene expression analysis by serving as an amplification template during PCR. The presence of gDNA contamination can be assessed by running a negative control sample during reverse transcription. The negative control contains all of the reaction components needed to reverse transcribe RNA into cDNA with the exception of the essential enzyme, reverse transcriptase. Amplification in a negative control sample therefore is most likely derived from contaminating gDNA. Absence of amplification indicates the absence of gDNA in the sample.

Aliquots of total RNA were removed from storage at -80°C. RNA concentration was determined using a nanodrop spectrophotometer. The samples were diluted to 100 ng/µl in preparation for cDNA synthesis.

Total RNA (100ng) from each sample was reverse transcribed to cDNA using Affinity Script Reverse Transcriptase (Agilent Technologies) and random primers, according to the manufacturer's protocol. Briefly, 5µl of total RNA was mixed with 15.7µl RNase free water and 3µl random primers, the reagents were heated to 65ºC for 5 minutes and then cooled to 4ºC for 10 minutes. Next, 2µl AffinityScript RT buffer, 0.8µl dNTP mix, 0.5µl of RNase block ribonuclease inhibitor and 1µl AffinityScript multiple temperature reverse transcriptase (RTr) enzyme was added to each sample and pulse spun for 5 seconds. The reaction was incubated at 25°C for 10 minutes to extend the random primers, followed by incubation at 50°C for 60 minutes; the reaction was terminated by incubating at 70°C for 15 minutes. The cDNA was in a total reaction volume of 28µl. In negative control samples RTr enzyme was omitted.

2.12.4 Real-time polymerase chain reaction

Polymerase chain reaction (PCR) was developed to exponentially amplify specific nucleic acid sequences in vitro (Mullis and Faloona, 1987). In traditional PCR results are collected at the end of the reaction. More recently the technique has been advanced to allow for the detection and quantification of gene expression as it occurs in real time. Real-time polymerase chain reaction (RT-PCR) is an extremely sensitive technique used to amplify and quantify gene expression.

Fluorescent probes are used to detect amplification product as the reaction occurs in real time. Two specific DNA sequences called primers are essential to the reaction. Primers are single stranded DNA which were designed to attach (by complementary base pairing) to the beginning and end of the DNA sequence to be amplified (forward and backwards primers, respectively). As an additional step to further eliminate amplification of gDNA in the RT-PCR step, primers should be designed to flank long gDNA containing introns (figure 2.17A), or to span exon-exon junction (figure 2.17B). Genomic DNA is therefore not amplified as the primer cannot anneal to the template.

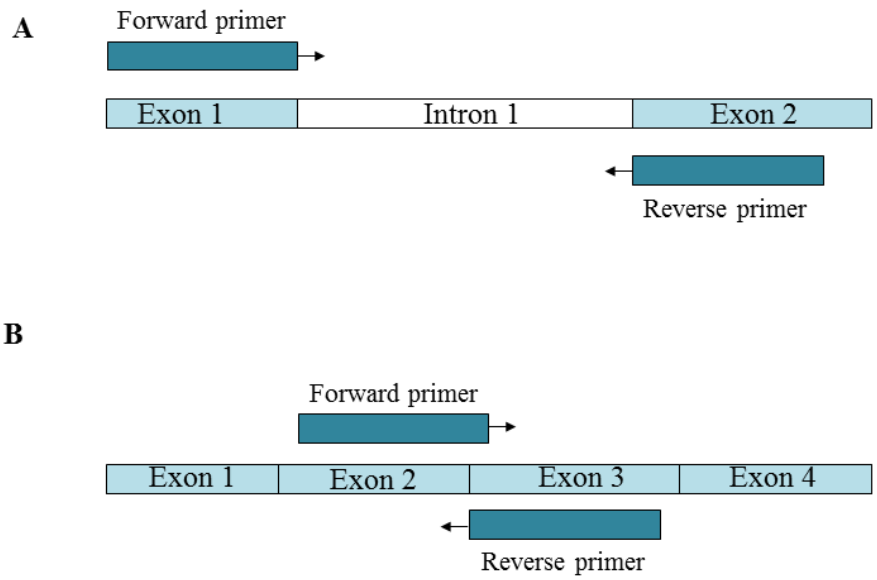


Figure 2.17: Primer design for quantitative polymerase chain reaction.

In order to eliminate genomic DNA, primers are designed to flank a long intron **(A**), or to span exon-intron boundaries **(B).**

2.12.5 TaqMan®

In 1991 Holland and colleagues designed an oligonucleotide probe to hybridise with the DNA target sequence for use in PCR (Holland et al., 2003). TaqMan® PCR chemistry exploits the 5' to 3' exonuclease activity of Taq DNA polymerase. The enzyme adds new nucleotides to the 3' end of the growing strand. The process is illustrated in figure 2.18.

The TaqMan® probe is designed to anneal to the specific DNA target sequence. The probe is covalently labelled at each end by two dyes. A fluorophore reporter dye labels the 5' end of the probe, and a quencher dye at the 3' end. When the probe in intact the fluorescent signal of the reporter dye is supressed due to close proximity to the quencher dye. This is known as fluorescence resonance energy transfer (FRET) (Didenko, 2001).

The RT-PCR reaction takes place in a thermal cycler. The reaction mix is first heated to denature the double stranded DNA to make two separate strands. The temperature is lowered to allow binding of the primer and probes to the DNA strand. If the cDNA target sequence is present the probe will anneal

downstream from the primer. As Taq polymerase extends the primer, the 5' exonuclease activity of the enzyme cleaves the annealed probe. Consequently the probe dissociates from the strand separating the reporter and quencher dye, which results in an increase in fluorescence from the reporter dye. As the reaction proceeds the amount of fluorescence increases throughout each cycle. Measuring the increase in fluorescence is a reflection of the amount (or amplification) of PCR amplicon product detected in the sample.

Gene expression was quantified by examining the cycle threshold (C_t) value. The C_t value was defined as the PCR cycle number in which the fluorescent signal of the reporter dye reaches an arbitrarily placed threshold (Schmittgen and Livak, 2008). The C_t value is inversely proportional to the amount of target in the reaction (i.e., the more target present in the sample the sooner a significant increase in fluorescence is detected, therefore the lower the C_t value).

During the initial PCR cycles the fluorescence signal is weak and is not easily detected. As the cycles increase the amount of PCR amplicon product increases exponentially (Kubista et al., 2006) which is illustrated on an amplification plot in figure 2.19. Eventually the fluorescent signal is saturated and levels off. Usually the thermal cycler is used to run 30 to 40 PCR cycles.

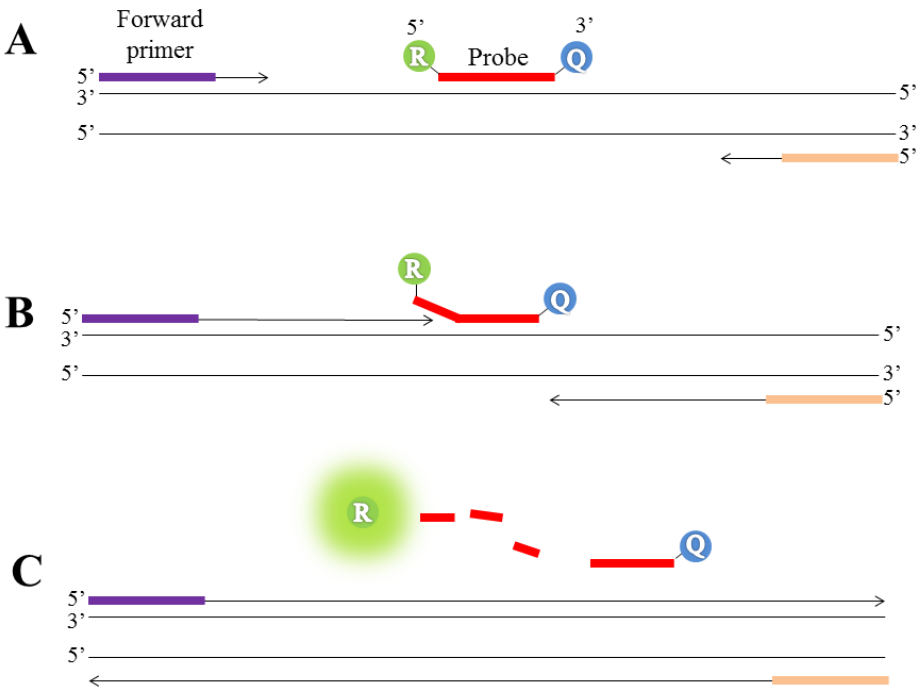


Figure 2.18: TaqMan® chemistry.

Forward and reverse primers bound to cDNA are extended by Taq polymerase **(A)**. An oligonucleotide TaqMan probe labelled with a reporter dye (labelled as 'R') and a quencher dye ('Q') are bound to the specific DNA sequence. As Taq polymerase extends the primer it encounters and displaces the probe, cleaving the reporter dye in the process **(B)**. A fluorescent signal is generated from the reporter dye following release from the probe **(C)**.

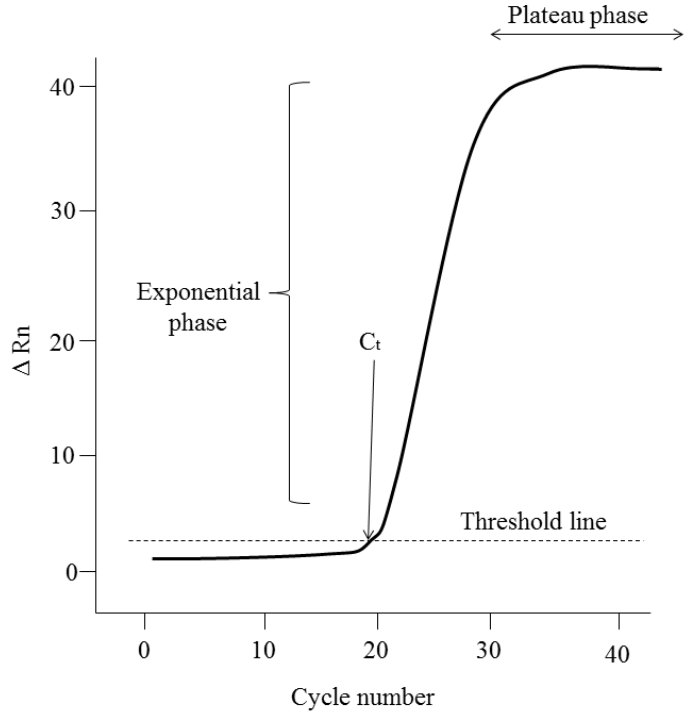


Figure 2.19: Graphical representation of TaqMan® real-time PCR data.

The C_t value indicates the cycle number at which fluorescence emitted from PCR product formation crosses the threshold line. The fluorescence increases exponentially with increasing cycles until a plateau is reached. ΔRn corresponds to the normalised fluorescence of the reporter fluorophore.

2.12.5.1 Gene expression analysis: standard curve method

Following reverse transcription, RT-PCR was undertaken to ensure cDNA synthesis was successful prior to running the samples on the microfluidic cards. The expression of the reference gene beta actin (ACTB) was quantified in the samples using the standard curve method. A 5-point standard curve was generated from pooled cDNA from each experimental sample. The pooled cDNA was diluted (1:8) with high performance liquid chromatography (HPLC) water to make a 'neat' solution. The neat solution was diluted four fold (1:4, 1:16, 1:64, 1:256) to create a 5-point standard curve. Each experimental cDNA

sample was diluted 1:8 using HPLC water. Primer and probes needed for the reaction were diluted according to the manufacturer's instructions. These were then further diluted to 1:10. A master mix solution consisting of Blue Taqman fast (enzyme and buffer solution), forward and reverse primers, probe and HPLC water was prepared. A 96-well plate was used for the reaction; 7µl of master mix was pipetted into each well. The first 15 wells consisted of the standard curve dilutions (3µl of standard curve solution added to each well). Each standard curve dilution was run in triplicate. Three wells were used for the non-template control (NTC). The NTC is an internal negative control where 3µl HPLC water was pipetted into each well instead of experimental sample; therefore gene expression should not be detected in these three wells. The remaining wells were each filled with the experimental samples (in duplicate), positive control (rat liver sample) and negative controls (where no RTr enzyme was added to the RNA in the reverse transcription reaction). The thermo cycler was set to run 40 cycles.

Quantification of gene expression can be either absolute or relative. Absolute expression uses an internal standard curve with known quantities to determine the amount of RNA in an unknown sample. Relative quantification is based on normalising the target gene expression to that of a stable internal control (reference gene) in a single sample, or to the standard curve. The normalised gene expression values can then be compared between groups. Results presented in this thesis are presented using relative quantification.

The C_t values obtained from RT-PCR were exported into Microsoft Excel and log (to base 10) values calculated. The standard curve was plotted as cycle threshold (C_t) values (y-axis) against log concentration values (x-axis). The efficiency of the PCR reaction was calculated by examining the slope of the standard curve. The slope of the standard curve is used to determine PCR efficiency, a slope of -3.32 indicates a 100% efficient reaction. The correlation coefficient between the logarithms and C_t values of the standard curve is expressed as an R^2 value, which is expected to be ≥ 0.99.

The slope and intercept of the line generated by the 5-point standard curve were calculated, using the following equation of a line:

$Y = MX+B$

Where Y = C_t values of the standards.

M = slope.

X= log quantity of the standards (i.e., 1, 0.25, 0625, 0. 015625, 0.0039062).

B = intercept.

Beta actin gene expression for each sample was calculated using the Ct value and the intercept and slope of the standard curve:

$$Gene\ expression = \frac{Ct\ value - intercept\ of\ standard\ curve}{slope\ of\ standard\ curve}$$

The gene expression levels of the samples should fall within the limits of the standard curve.

2.12.6 384-well microfluidic cards

In order to elucidate differences in gene expression patterns in the synovium of asymptomatic and symptomatic chondropathy cases, custom made 384-well microfluidic cards (TaqMan® Array Card, Applied biosystems) were designed. The microfluidic card allows for 384 simultaneous quantitative RT-PCR reactions to occur in parallel to determine relative mRNA expression changes.

Each 384-well microfluidic card contained specific primers for 96 genes, 4 of these were reference (or housekeeping) genes for gene normalisation.

2.12.6.1 Assay selection criteria

Several criteria were considered to select the assay for each gene. Each assay consisted of one of three ID suffixes; m, g and s. The suffix letter was indicative of the probe location. The probe placement of assays labelled with

an “m” suffix spanned an exon-exon junction; these assays were preferentially selected in order to avoid amplification of gDNA. Contamination with gDNA can affect the measurement of gene expression levels. If an “m” assay was not available for the gene of interest, then “g” assays were selected. The probe of these assays may be placed within a single exon therefore may detected genomic DNA. Finally, in the case that there were no “m” or “g” assays, the “s” assay was selected. In this assay the probe is located within a single exon; therefore it is likely to detect genomic DNA.

The amplicon (PCR product produced by amplification) length of the assay was examined, and assays with smaller amplicon lengths were preferentially selected as shorter lengths are more robust against RNA fragmentation and are have more stable delta C_t values compared to longer lengths (Antonov et al., 2005).

The reference genes included beta-actin (ACTB, assay Hs01060665_g1), glyceraldehyde 3-phosphate dehydrogenase (GAPDH Hs99999905_m1), hydroxymethylbilane synthase (HMBS Hs00609297_m1) and ubiquitin C (UBC Hs00824723_m1). Full assay IDs and amplicon lengths for all 96 genes are listed in the appendix (chapter 8, section 8.4).

2.12.6.2 Protocol

Upon arrival the microfluidic cards were stored at 4°C. Prior to use the cards were removed from the fridge and allowed to stand at room temperature for 30 minutes. The card layout was imported into SDS2.3 programme and set to run for 40 cycles and used the delta delta (ΔΔ) CT relative quantification assay.

Total RNA (500 ng) was extracted and prepared from the snap frozen synovia of symptomatic and asymptomatic chondropathy cases using TRI reagent (section 2.12.1) and was reverse transcribed to cDNA (section 2.12.3). A reaction mix was made using 100µl of diluted cDNA (1:4) and 100µl of TaqMan Universal PCR Master Mix into a microcentrifuge tube. The tubes were gently vortexed then pulse spun to thoroughly mix the components and to eliminate air bubbles. For each sample, 100ml of reaction mix was added to two adjacent ports in the microfluidic card, which allowed for duplicate runs.

Each microfluidic card had 8 ports, therefore could run 4 samples. The microfluidic cards were centrifuged at 1200 rpm for 2 minutes which ensured delivery of the samples into each of the 384 wells. Reactions wells were isolated by sealing the cards using TaqMan Array Microfluidic card sealer and the loading ports cut off. The microfluidic card was then run on the 7900HT Fast Real-Time PCR system (Applied Biosystems). Data were analysed using relative quantification.

2.12.7 Selecting the most stable reference genes for normalisation

Suitable normalisation of gene expression data against internal reference genes is essential for reliable and accurate interpretation of results. Normalisation is required to control for differences in inter-sample preparation, run-to-run variations and pipetting errors.

The expression levels of reference genes should be adequately expressed, relatively invariant across samples, and should not be affected by experimental conditions. To further increase accuracy of results multiple reference genes should be used and the geometric mean of most stable reference genes calculated. The geometric mean better controls for outliers and abundance differences than the arthritic mean (Vandesompele et al., 2002).

NormFinder (Andersen et al., 2004), a Microsoft Excel based application was used to determine the most stable individual reference gene C_t values, or the most stable geometric mean of different combinations of reference genes. NormFinder considers inter-group and intra-group variation in C_t values and ranks the reference genes according to stability. The most stable geometric mean of the reference genes C_t values was used to normalise gene expression, and C_t value outliers were identified using the Grubb's test (Grubbs, 1969) (http://graphpad.com). Samples where the reference gene C_t values were an outlier (obtained from the most stable geometric mean) were excluded from analyses to avoid misinterpretation of results.

2.12.8 Determining fold change in gene expression between the groups

Fold change in target gene expression levels were calculated for each sample, and using the comparative Ct method (Livak and Schmittgen, 2001, Schmittgen and Livak, 2008), also known as $2^{-\Delta Ct}$

$2\text{-}\Delta C_t = 2\text{-}[(C_t \text{ target gene} - C_t \text{ reference gene})]$

The mean and standard deviation was calculated for both the asymptomatic chondropathy and symptomatic chondropathy group. Statistical differences in gene expression between groups were assessed using Mann Whitney U-test. Fold difference between gene expressions in the two groups was calculated as:

$$\text{Fold change} = \frac{\text{Mean gene expression of symptomatic chondropathy group}}{\text{Mean gene expression of asymptomatic chondropathy group}}$$

For genes which were down regulated in the symptomatic chondropathy group, fold change was calculated as 1 divided by the fold change (as calculated above).

2.13 Statistical analysis

2.13.1 Univariate and regression analyses

Data were analysed using SPSS (statistical package for social sciences) v.21. Normality of the data was assessed using a Shapiro Wilk test which determined whether parametric (e.g. t-tests, ANOVA and linear regression) or non-parametric equivalent tests (e.g. Mann Whitney U-test, Kruskall Wallis, logistic regression, Spearman's correlation) were used in analyses. Normality was accepted when $P>0.05$. For all of the statistical tests, significance was accepted when $P<0.05$. All graphical figures reported in this thesis were constructed using GraphPad Prism 6.

Mann-Whitney U test was used to compare histological and genetic differences between TKR and PM groups. T-tests were used to compare ages between TKR and PM groups. In histological comparisons, Chi squared test was used to compare the presence of subchondral bone marrow replacement between

groups. Logistic regression was used to adjust for gender differences in non-arthritic control and age-matched OA comparisons and for age differences in asymptomatic chondropathy and symptomatic chondropathy group histological comparisons.

Spearman correlations were used to determine associations between BMI and outcome measures, combining data from both groups. Linear regression was used in additional analysis to determine the association between BMI and immunohistochemical fractional areas, adjusting for age and experimental group.

To determine the effect of PM delay on immunohistological analyses, Spearman's rank correlations were used to determine the association between PM delay and NGF and CD68 fractional areas in PM cases. In additional analyses logistic regression was used combining both non-arthritic control and asymptomatic chondropathy PM cases. The median of fractional areas for CD68 and NGF were quantified and cases below or above the median value were used as the dependent variable.

Repeated measures ANOVA was used to test NGF expression in synovial TKR tissue left to decay at 24hour interval time points (0h, 24h, 48h, 72h).

Multinomial logistic regression analysis was used to determine differences in histological characteristics between non-arthritic controls, early OA and end-stage OA cases, adjusting for age and gender.

The Kruskall-Wallis test with post-hoc pairwise comparisons was used to examine differences in histological and clinical characteristics of the histopathological subgroups identified in latent class analyses (section 2.13.6).

2.13.2 Intra and inter-observer reliability

Intra–observer and inter-observer reliability for histology scores were assessed by rescoring 20-25, randomly selected cases, on 2 separate occasions 6 months apart. For reproducibility analyses the kappa and weighted kappa statistics (Viera and Garrett, 2005) was used for cartilage, subchondral bone and synovia scores using StatsDirect software. The Kappa statistic examines the degree of

agreement between two or more observers. Weighted kappa assigns less weight to agreement as the categories chosen are further apart. For example a disagreement of normal proteoglycan content (grade 0) and mild proteoglycan content (grade 1) between observers would be recognised as partial agreement, whereas a disagreement of normal proteoglycan (grade 0) and severe proteoglycan loss (grade 3) would be interpreted as no agreement. The intra-class correlation coefficient was used for fractional area values using SPSS.

Intra- and inter- observer reliability for histology scoring is depicted in table 2.6. Intra- and inter-observer variability was at least moderate to almost perfect agreement (0.41- 0.86) using the kappa and weighted kappa statistics. For fractional area measurements, intra-class correlation coefficient was 0.85, indicating good reproducibility.

Table 2.6: Intra- and inter-observer reliability kappa and weighted kappa statistics for histological scores.

Variable	Intra-observer reliability		Inter-observer reliability	
	Kappa	Weighted kappa	Kappa	Weighted kappa
Cartilage surface	0.76	0.80	0.59	0.78
Chondrocyte morphology	0.53	0.41	0.74	0.78
Proteoglycan loss	0.69	0.76	0.44	0.57
Tidemark integrity	0.64	0.64	0.74	0.85
Synovitis	0.72	0.86	0.68	0.75
Subchondral bone marrow replacement	0.53	0.41	0.44	0.44

Interpretation of Kappa statistics; < 0 less than chance agreement, 0.01- 0.20 slight agreement, 0.21- 0.40 fair agreement, 0.41 -0.60 moderate agreement, 0.61-0.80 substantial agreement, 0.81 – 0.99 almost perfect agreement.

2.13.3 Ingenuity Pathway analysis

Ingenuity Pathway analysis (IPA, QIAGEN Redwood City, www.qiagen.com/ingenuity) was used to identify canonical pathways and networks previously attributed to differentially expressed genes identified from the microfluidic card analysis. The fold change and direction of expression of genes that were differentially expressed ($P<0.05$) between asymptomatic and symptomatic chondropathy cases were uploaded into IPA for analysis. The probability that the genes were connected to an established canonical pathway or network by a non-random association was determined using significant *P* values from the right-tailed Fisher's exact test. The top three major networks identified by IPA are presented in section 4.6.8.

2.13.4 Rasch analysis

The ability of a well-functioning scale where individual component or item scores are summed to produce a total score can be explored using Rasch analysis. Rasch analysis is a psychometric tool used to validate newly developed outcome scales or reform existing ones.

The basic principles of Rasch analysis can be applied to validate the histological-histochemical scoring system developed by Mankin et al. The scoring system is essentially a scale whereby 4 individual 'item' scores (cartilage surface integrity, chondrocyte morphology, proteoglycan loss and tidemark breaching) are summed to an overall measure of histological OA severity (0, normal to 14, severe OA) in the articular cartilage.

Rasch analysis examines the extent of which observed data conform to the Rasch model expectations, through the assessment of various key attributes. Rasch analysis was conducted to assess the fit of the 4-item Mankin histopathological scoring system to the Rasch model. Analysis was performed using RUMM2020 software (Andrich D et al., 2003). The partial credit model was used to examine the scoring system, as the distance between thresholds of individual items are not expected to be equal (Tennant and Conaghan, 2007).

Fit of data to the model expectations is examined using three key summary fit statistics. Two of the statistics are 'item' and 'person' fit statistics. As

mentioned previously ‘item’ refers to each of the 4 histological features assessed (cartilage surface integrity, chondrocyte morphology, proteoglycan loss and tidemark breaching). Person scores refer to each individual PM or TKR case histologically scored. Individual item and person fit statistics are expressed as transformed z scores which represent standardised normal distribution, mean and standard deviation values should approximate 0 and 1, respectively which would indicate perfect fit. Item and person residuals were produced and were expected to be between -2.5 and +2.5, in order to fit the model (Pallant and Tennant, 2007, Shea et al., 2009). Hierarchical ordering of item-trait interaction should be invariant across class intervals (groups) and was explored using a chi-squared test. A significant *P* value after a Bonferroni adjustment for multiple testing indicates variation of item ordering (Tennant and Conaghan, 2007, Pallant and Tennant, 2007) i.e., demonstrates misfit to the model.

Ideally, a well-fitting model should demonstrate ordered thresholds for item responses (or in this case, histological categories) (Tennant and Conaghan, 2007). Disordering of thresholds could indicate redundancy of response options; this was resolved by merging adjacent response options to improve fit to the model.

Differential item functioning (DIF) is a bias which can influence model fit. DIF occurs when subgroups (e.g., males and females) respond differently to an item despite displaying the same levels of the measured trait (knee OA) (Tennant and Conaghan, 2007). Histopathological scoring systems should be universal in measuring severity of knee OA and gender should not bias the response to individual items.

In order for adequate fit to the model there should be absence of local item dependency, i.e., one item should not have a bearing upon another. The residual correlation matrix was assessed for response dependency, which was signified by a positive correlation exceeding 0.3 (Moreton et al., 2012).

Unidimensionality is essential for scoring systems where individual items are summated to give an overall score, i.e. all items on the scale should be measuring the same internal construct. Dimensionality of the scoring systems

was assessed using principal component analysis. Person estimates are derived from divergent subsets (positively and negatively correlated items). Independent t-tests are used to compare person estimates. The number of t-tests displaying significance at the 0.05 level should not exceed 5%, as this would portray scale multidimensionality. Targeting of the scale is assessed by examining the mean location of person-item threshold distribution. A mean of 0 demonstrates ideal targeting. The person separation index (PSI) which indicates internal consistency and ability to differentiate between different groups of participants was reported for the scoring system.

Two analyses were performed using:

1. Test group of 181 PM and 55 TKR cases.

2. Validation group of 162 PM and 88 TKR cases. The validation group consisted of a different set of cases to the test group.

Within the analysis, the Mankin score was analysed in two stages:

1. Validity of the Mankin score in early OA. In order to examine the measurement qualities of the score for use in early OA histological scores, only knee joints collected from PM donors were analysed.

2. Validity of the Mankin score as a general measure of OA histological changes. Rasch analysis was performed on the PM donors as above in addition to a supplementary sample of knee joints collected at the time of TKR for symptomatic OA.

Cases with missing data were included in the Rasch analysis as the programme can accommodate missing data.

2.13.5 Principle components analysis

The underlying structure and interactions of a dataset can be explored using principle components analysis (PCA). The relationship between the principle component and each variable can be assessed by examining the loading matrix. The loading matrix displays correlations between the variables and principle

component. A larger loading value is indicative of a larger contribution of the factor to the variables (Abdi and Williams, 2010).

Rasch rescaled items were used to refine histopathological assessment of knee OA through introducing a weighting scheme based on factor loadings from principle components analysis. Principle components analysis (PCA) was conducted using histological data obtained from 343 PM and 143 end-stage OA cases using SPSS v.21, using a forced one-factor extraction. Correlations between histological variables and the principle component were displayed in the form of a component matrix. The absolute scores for each variable were used as coefficients in the weighted score. For ease, the score was converted to a 0-10 scale. Histologic scores for synovial inflammation and subchondral bone marrow replacement were included in the weighted score.

2.13.6 Receiver operator characteristic (ROC) curves

Receiver operating characteristic (ROC) curve analysis is a useful measure to examine the overall performance of a diagnostic test or classification system. The basic performance of a diagnostic test is measured in terms of its sensitivity and specificity. Sensitivity refers to the ability of the test to correctly identify cases *with* the disease (true positives). Specificity refers to the ability of the test to correctly identify cases *without* the disease (false positives) (Park et al., 2004). In ROC curve analysis sensitivity is plotted (y-axis) against 1-specificity (x-axis) (Zhang et al., 2011a). Sensitivity values increase as specificity values decrease.

The overall ability of the test to discriminate between two measures (for example, cases with OA and cases without OA) is reported by the area under the curve (AUC). Larger values indicate greater discrimination abilities (Altman and Bland, 1994). An AUC of 0.5 is indicated by diagonal or chance line (figure. 2.20) this indicates no apparent discrimination ability whereas a score of 1 indicates perfect discrimination ability of the test (Hanley and Mcneil, 1982).

In ROC analysis each data point is associated with a cut-off, sensitivity and specificity value. The cut-off point where optimal sensitivity and specificity

measures of a test are achieved is determined by two commonly used methods (Akobeng, 2007) and are graphically illustrated in figure 2.20. The Youden index (*J*) refers to the maximum vertical distance between the diagonal line and the ROC curve is detailed in the equation below.

J = maximum value of (sensitivity (decimal) + specificity (decimal)) -1

The (0,1) method uses the equation below to determine the data point on the ROC cruve closest to the coordinates (0,1). As a data point of (0,1) would indicate perfect fit.

Optimal cut off = minimal value for $(1\text{-sensivity})^2 + (1\text{-specificity})^2$

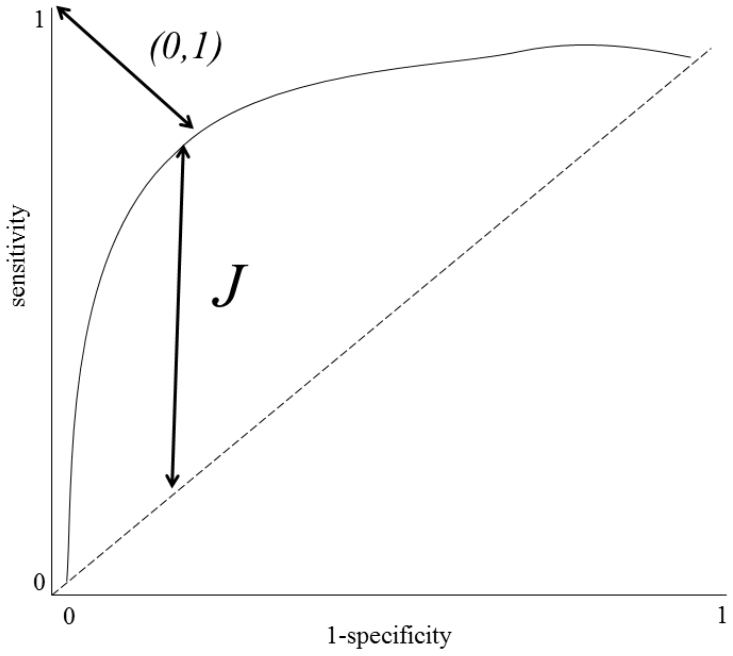


Figure 2.20: ROC curve illustrating the Youden Index (J) and (0,1) method for determining optimal cut-offs on ROC curves.

The Youden index is determined as the maximum vertical distance between the chance (dotted) line and the curve. The (0,1) method refers to the point of the ROC curve closest to the (0,1) coordinates.

The original Mankin and weighted score were compared for their ability to discriminate between OA and non-OA specimens. Specimens were considered as non-OA or OA based on two different factors. Firstly, if the knees had evidence of osteophytes (hallmark feature of OA) and secondly, if they had undergone TKR for painful OA (end-stage OA group).

For each PM and TKR case, the total Mankin score (0-14) and total weighted score (0-10) were calculated. Only cases with a full set of histological scores for cartilage pathology, synovitis and subchondral bone marrow replacement were used in the analysis. The total Mankin score and weighted score were compared, and areas under the curves (AUC) for distinguishing between non-OA and OA specimens were calculated using receiver operating characteristic (ROC) curves. This analysis was first conducted using all PM and TKR cases with a full set of histological data (total n = 333; 240 PM and 93 TKR cases).

Multiple partitioning of the data was used to test reliability of the results. The whole dataset of 333 cases was randomly split into two subgroups. This process was repeated a further four times, to produce ten random subgroup datasets in which to validate the scoring systems on.

Further analyses were conducted to assess the discriminative ability of the weighted score to distinguish between symptomatic and asymptomatic cases. Additionally, the use of the weighted score in cases with early OA was assessed.

2.13.7 Latent class analysis

Latent class analysis (LCA) is a mixture modelling data analysis technique used to identify unobserved meaningful subgroups or classes with similar characteristics. The aim of latent class analysis is to determine the number of classes or unobserved groups within the study population. The number of classes in a mixture analysis is based on various fit indices including the Vuong-Lo-Mendell-Rubin (LMR) test and the bootstrapped likelihood ratio test (BLRT) (Nylund et al., 2007).

The LMR (Vuong, 1989, Lo et al., 2001) and BLRT tests are used to compare the number of latent class models in mixture models. The tests compare the fit

between adjacent models (comparing *k* class model with *k*-1 model)(Jung and Wickrama, 2008). The data is initially examined to determine the presence of two classes (in this case '*k'* is two). The LMR produces a *P* value statistic to indicate whether fit is improved when compared to the *k*-1 model (i.e., one class model). Significant *P* values (< 0.05) reject the *k*-1 class model (i.e., one class) in favour of the *k* class (i.e. two class) model. Subsequent analyses examine the fit of a three class model compared to a two class model, if $P < 0.05$ then the two class model is rejected in favour of the three class model. This process continues by comparing the four class model to the three class model, and so forth. When $P > 0.05$ then *k*-1 class model is sufficient.

Additional fit indices include the Akaike Information Criteria (AIC)(Akaike, 1974) and sample size-adjusted Bayesian Information Criteria (SS.Adj BIC)(Sclove, 1987) values. These indices examine the log likelihood function for individual models, rather than compare values between models. The best fitting model is determined by the model with the lowest AIC and SS.Adj BIC values. Entropy is a further fit statistic used to determine the accuracy of class allocations. LCA assigns cases to latent classes based on the highest probability of membership, rather than assign cases to distinct categories. For example, one individual may have probability of membership to class 1 (0.84), class 2 (0.11) and class 3 (0.05), therefore the individual would be assigned to class 1 as the probability is greatest in this class. Models with entropy values over 0.8 are considered most trustworthy. It is important to consider the percentage of cases per latent class; this value should not be less than 1%. Furthermore the average latent class probabilities for each class should all be reasonably high (around 1). (Jung and Wickrama, 2008). All fit indices should be considered to inform judgement of the number of classes within the sample.

The latent class model was specified using Mplus version 7.2 software, following guidance from (Asparouhov and Muthen, 2012). A mixture model with continuous (cartilage surface integrity, chondrocyte morphology, proteoglycan loss and synovitis scores) and categorical (tidemark breaching and subchondral bone marrow replacement) variables was specified. Latent class models assume independence amongst items (i.e. no correlation) therefore the correlation between variables was specified in the set-up, using

the ‘WITH’ function of Mplus. The syntax code for the model is listed in the appendix (chapter 8, section 8.5.1).

The number of random starts was increased until the best loglikelihood value was replicated. The optimal number of optimal classes of classes was explored by starting with 2 classes, then increasing until the optimal number was found by examining the fit of data, using the LMR and BLRT.

2.14 Reagents

Monoclonal antibody to CD68 (clone PG-M1) was obtained from Dako UK Ltd. (Cambridge, UK). The following secondary antibodies were obtained from Vector Laboratories Ltd. (Peterborough,UK); biotinylated horse anti-mouse IgG, biotinylated goat anti-rabbit IgG, Texas Red horse anti-mouse IgG, and Fluorescein goat anti-rabbit IgG. Avidin-biotin complexes (ABC kit, PK6100) were obtained from Vector Laboratories Ltd. Monoclonal antibody to NGF (clone EP1320Y) was obtained from Abcam (Cambridge, UK). Monoclonal antibody to Hsp47 (clone M16.10A1) was from Enzo Life Sciences, Exeter, UK). OCT mounting medium, Mayers haematoxyin, Harris haematoxylin and eosin were from Raymond Lamb (Eastbourne, UK). The microfluidic cards were from Applied biosystems. PBS and DePeX mounting medium were from VWR Ltd (Lutterworth, UK). Sudan black B, BSA, DAPI and all other reagents were purchased from Sigma-Aldrich (Poole, UK).

CHAPTER 3: HISTOLOGICAL FEATURES ASSOCIATED WITH SYMPTOMATIC OSTEOARTHRITIS

INTRODUCTION

Osteoarthritis (OA) is the most common joint disease in the middle age to elderly population. OA is a disease that encompasses all tissues within the affected joint. Pathological features in knee OA include articular cartilage degradation, synovial inflammation, osteophyte formation, meniscal pathology and subchondral bone marrow lesions.

A variety of histological scoring methods have been developed to measure OA changes in the knee joint. However it is not known whether these histological features are specific to OA, or are a feature of normal ageing. The grading system developed by Mankin and colleagues examines osteoarthritic alterations in the articular cartilage (Mankin et al., 1971). Cartilage surface integrity is assessed by examining the degree of cartilage fibrillation. During OA, articular chondrocytes undergo phenotypic modification. Typical characteristics include chondrocyte hypercellularity (increase in number), cloning (clustering) or chondrocyte hypocellularity (chondrocyte death). Invasion of vascular channels from the subchondral bone, through the tidemark and into the avascular and aneural articular cartilage is visualised microscopically by assessing the tidemark integrity. The intensity of Safranin-O staining in the articular cartilage is used to visualise proteoglycan loss. The range of scoring extends from normal (no loss of stain) to complete loss of proteoglycan content.

Synovial inflammation can be assessed histologically by examining the synovial lining thickness, cellularity and presence of inflammatory cell infiltrate (Haywood et al., 2003). Furthermore subchondral bone marrow can be examined to determine whether the spaces are filled with normal fatty tissue, or fibrovascular tissue containing matrix, vascular and mononuclear cells (Walsh et al., 2010).

In OA, pain is the main reason sufferers first seek clinical assistance. Pain is initially managed through a combination of non-pharmacological and pharmacological modalities. Patients with end-stage OA who are no longer responsive to treatment may eventually benefit from partial or total knee replacement (TKR) surgery.

Although joint pathology makes an important contribution to OA pain, the precise relationship between pain and structural pathology is not entirely clear (Dieppe et al., 1997, Bedson and Croft, 2008). Radiographic features of OA are often weakly associated with pain, suggesting that structural, cellular or biochemical changes in the OA joint that directly mediate pain may not be easily detected on radiographs. Imaging studies have indicated possible associations between pain and synovitis (Hill et al., 2001, Torres et al., 2006, Hill et al., 2007, Baker et al., 2010) and with subchondral changes (Felson et al., 2001, Torres et al., 2006, Szebenyi et al., 2006, Hernandez-Molina et al., 2008b) but associations with histopathology have not been explored in detail. Such studies have previously been limited by age differences between OA cases and normal controls, and by limited access to joint tissue from people with OA whose pain is less than that which would lead them to undergo joint replacement surgery.

The role of synovial inflammation (synovitis) in the pathogenesis of OA is increasingly being recognised as an important contributor to OA knee pain. The cause of synovitis in OA is incompletely understood, but has been observed in both early (Benito et al., 2005) and late disease (Haywood et al., 2003). Synovitis may mediate pain through the production of factors which sensitise or activate sensory nerves.

Recent evidence has suggested an important role for nerve growth factor (NGF) in mediating inflammatory pain through increasing nociceptor sensitivity or by facilitating sensory nerve growth (Walsh et al., 2010). NGF blockade improved pain from knee OA (Lane et al., 2010, Brown et al., 2012, Sanga et al., 2013), inferring a causal link between NGF and OA pain.

NGF is elevated in a variety of rheumatic diseases, particularly in the synovial fluid of patients with inflammatory arthritis such as rheumatoid arthritis and

spondyloarthritis (Halliday et al., 1998, Barthel et al., 2009). NGF is expressed by synovial macrophages in rheumatoid arthritis, spondyloarthritis and to a lesser extent in OA (Barthel et al., 2009), and by OA synovial fibroblast cell cultures (Manni et al., 2003). However the expression and cellular profile of NGF in synovial biopsies from people with knee OA has not been explored in detail. Synovial fibroblasts can be visualised using IHC with antibodies directed against heat shock protein (Hsp) 47, a collagen-specific molecular chaperone (Izquierdo et al., 2011). Macrophages can be identified by the transmembrane glycoprotein CD68 (Holness Cl and Simmons, 1993).

3.1 Objectives

1. To validate the measurement of histopathological characteristics of knee OA by comparing samples obtained at TKR surgery for OA (advanced OA), with age-matched non-arthritic control cases collected post-mortem (PM).

2. To identify histopathological features associated with symptomatic knee OA, by comparing cases with similar macroscopic chondropathy, half of whom had sought help for knee pain and undergone TKR (symptomatic chondropathy), the other half of whom had not sought help for knee pain but had died from unrelated illness (asymptomatic chondropathy).

3. To identify the cellular localisation of synovial nerve growth factor (NGF) using double immunofluorescence staining.

4. To determine whether the intensity of synovial NGF and macrophage (CD68) immunohistochemical staining decrease with increasing delay between death and tissue processing, in tissues obtained at PM.

3.2 Hypothesis

Symptomatic OA is mediated by specific structural and biochemical changes within the knee joint, whereas other changes may be coincidental or even protective.

METHODS

General methodology is given in chapter 2. Patient selection details are given in section 2.1.1 and 2.1.2. Tissue collection and sample processing are described in section 2.2. Details for histological grading are given in section 2.5. Calculation of macroscopic tibiofemoral chondropathy and radiographic OA severity scores are explained in sections 2.7 and 2.8, respectively. Immunohistochemical and immunofluorescence techniques are described in section 2.4. Image analysis and quantification and statistical analysis are described in section 2.6 and 2.13 respectively. Reliability analysis is described in detail in section 2.13.2.

3.3 Study subgroups

To identify histopathological features associated with OA, two groups were compared:

- **Non-arthritic controls;** 26 samples were collected from recently deceased patients and were classified as non-arthritic controls, based on history and articular cartilage surface appearances (see section 2.1.1).
- **Advanced OA cases;** 26 samples were collected at the time of total knee replacement surgery for symptomatic OA. Advanced OA cases were aged matched to non-arthritic controls (see section 2.1.1).

To identify histopathological features associated with **symptomatic** OA, two additional groups of cases with similar macroscopic chondropathy scores (i.e., similar degree of macroscopic cartilage loss) were compared:

- **Asymptomatic chondropathy**; 29 samples were collected from recently deceased patients who had not sought help for knee pain in the last year of life, but had died from an unrelated illness (see section 2.1.2).
- **Symptomatic chondropathy**; 29 samples were collected at the time of total knee replacement surgery for symptomatic OA. Symptomatic chondropathy cases were selected to have similar macroscopic

chondropathy scores to asymptomatic chondropathy cases (see section 2.1.2).

RESULTS

3.4 Histopathological features of knee osteoarthritis

Patient demographics are reported in table 3.1 and histopathological features are illustrated in figure 3.1. Samples displayed a range of cartilage appearances, including mild clefts to the articular surface with normal proteoglycan content (figure 3.1A) compared to deep clefts and loss of proteoglycan in some advanced OA cases (figure. 3.1B). Channels from the subchondral bone were found in close proximity to the tidemark (figure 3.1C) and also breached the tidemark to invade non-calcified cartilage (figure.3.1D). Subchondral bone spaces mostly contained normal fatty tissue (figure. 3.1E); however in some cases this was replaced by fibrovascular tissue (figure 3.1F). Synovial inflammation was sometimes marked, with lining hyperplasia and lymphoid aggregates (figure 3.1H). CD68 (figure 3.1I) and NGF-positive cells (figure 3.1J) were evident in the synovial lining and sublining regions and surrounded blood vessels.

Advanced OA cases displayed more severe cartilage surface changes, proteoglycan loss, tidemark breaching, changes in chondrocyte phenotype and synovitis than did non-arthritic controls (each $P < 0.05$, figure. 3.2). Tidemark breaching was observed in 17/25 (68%) of advanced OA and 9/26 (35%) of non-arthritic control cases, ($P = 0.012$). Subchondral fibrovascular replacement was present in 5/26 (19%) of advanced OA cases and absent from non-arthritic controls; however significance was lost after adjusting for gender differences. Synovial fractional area positive for CD68 and NGF-immunoreactivities were greater in advanced OA cases compared with non-arthritic controls ($P = 0.031$ and 0.035, respectively, figures. 3.2E-F).

Table 3.1: Clinical details and pathological characteristics of study groups*****.

Clinical or pathological characteristics	Features of OA		Features of symptomatic OA	
	Non-arthritic control	**Advanced OA**	**Asymptomatic chondropathy**	**Symptomatic chondropathy**
	(n = 26)	**(n = 26)**	**(n = 29)**	**(n = 29)**
Age, years	61 (48-67)	61 (50 -67)	**71 (66-79)**	**68 (61-74)**†
Male (%)	**62**	**31**†	55	55
BMI	NA	32 (29-40)	NA	31 (28-37)
Macroscopic chondropathy score (0-400)	51 (40-69)	NA	199 (177 – 215)‡	223 (185-234)‡
Total radiographic score (0-18)§	NA	12 (10-13)	NA	12 (10-13)
JSN score (0-6)	NA	5 (4-5)	NA	5 (4-5)
OST score (0-12)	NA	7.5 (5-8)	NA	8 (5.7-8)
Histology				
Total Mankin score (0-14) ¶	**5 (3-7)**	**8 (7-9)#**	7 (7-8)	8 (7.5 – 9)
Cartilage surface integrity (0-6)	**2 (2-3)**	**4(4-4)‡**	**4 (3-4)**	**4 (4-4)**†
Tidemark breached	**35%**	**68%**†	66%	67%
Proteoglycan loss (0-4)	**1(1-1)**	**1(1-2)**†	1 (1-2)	1 (1-2)
Chondrocyte morphology (0-4)	**1 (0-3)**	**2.5 (2-3)**†	**3 (1.5-3)**	**3 (2-3)**†
Subchondral bone marrow replacement	0	19%	18%	32%
Synovitis (0-3)	**0 (0-0)**	**0 (0-3)**†	**0 (0-0.25)**	**2 (0 – 3)#**
Macrophage fractional area **	**3.4 (1.8-4.6)**	**4.8 (3.1-8.7)**†	7.4 (4.2-13.2)	13.1(6.6-15.3)
NGF fractional area **	**1.4 (0.4 – 1.8)**	**4.0 (1.5 – 8.3)** †	**8.7 (5.9 – 12.4)**	**12.9 (9.4 – 18.6)**†

* Tissues were obtained at the time of total knee replacement for OA or were obtained PM from cadaver donors. Data for the body mass index (BMI) were available for 23 patients with advanced OA and 20 patients in the symptomatic chondropathy group.

(one TKR patient was included in both the symptomatic chondropathy and advanced OA groups and was therefore counted twice). Statistical comparisons for the immunohistochemical and histomorphometric data were not made between the features of OA and the features of symptomatic OA subgroups because staining was carried out in separate experiments. Except where indicated otherwise, values are the median (interquartile range). NA = not available.

†$P<0.05$ versus the corresponding subgroup (i.e., non-arthritic control or asymptomatic chondropathy group).

#$P<0.01$ versus the corresponding subgroup (i.e., non-arthritic control or asymptomatic chondropathy group).

‡$P\leq0.001$ versus the non-arthritic control group. There was no significant difference between the macroscopic chondropathy scores of asymptomatic and symptomatic chondropathy groups.

§ The total radiographic score is the sum of the scores for tibiofemoral joint space narrowing (JSN) and osteophytes (OST).

¶ The total Mankin score is the sum of the scores for cartilage surface integrity, tidemark breaching, proteoglycan loss and chondrocyte morphology. #Tidemark breaching is expressed as the percentage of subjects in whom cartilage integrity permitted assessment (25 in the advanced OA group and 24 in the symptomatic chondropathy group).

**Fractional areas are the percentage of synovial area occupied by CD68-immunoreactive macrophages or nerve growth factor-immunoreactive cells. Fractional areas are reported only for the samples that displayed synovial lining (n = 15-26 group).

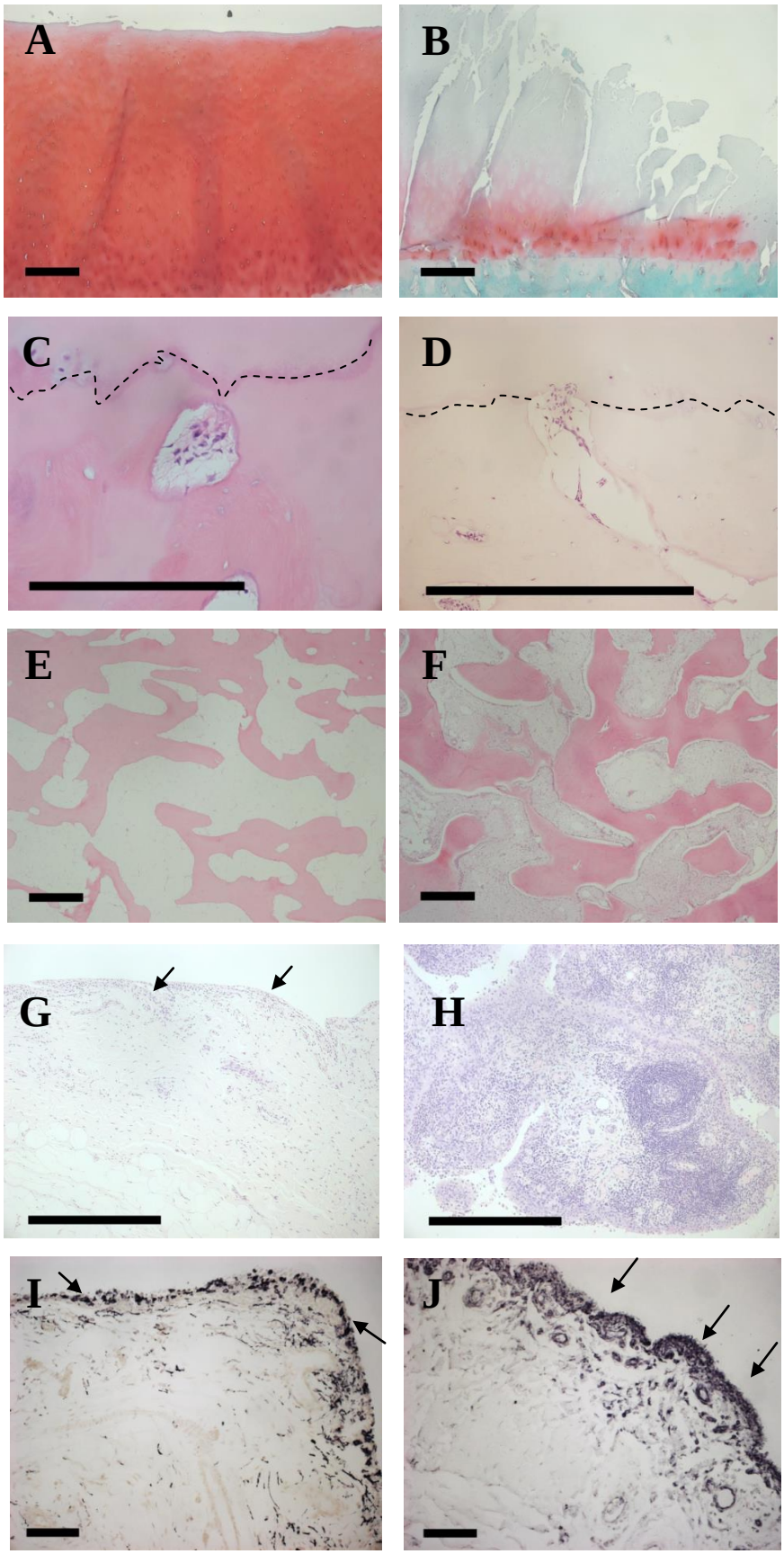


Figure 3.1: Histopathological features of non-arthritic (A,C,E,G) and OA ((B,D,F,H,I,J) knees.

Non-arthritic knees displayed mild cartilage surface irregularities to the superficial zone, with normal proteoglycan staining **(A),** whereas deep clefts in the articular cartilage surface and severe proteoglycan loss are shown from an OA knee **(B).** Channels were observed in calcified cartilage beneath an intact tidemark (indicated by dotted line) **(C),** whereas **(D)** shows a channel breaching the tidemark and entering non-calcified cartilage. Normal subchondral bone marrow spaces were filled with fatty tissue in a non-arthritic knee **(E)**, whereas **(F)** subchondral bone marrow was replaced by fibrovascular tissue in an OA knee. Mild synovial lining hyperplasia is shown in a sample from a non-arthritic knee **(G)**, whereas **(H)** severe synovitis, characterised by hyperplasia and hypertrophy of synovial lining and sublining hypercellularity, is shown from an OA knee. CD68-immunoreactive macrophages **(I)** and NGF-immunoreactivity **(J)** (each stained blue/black) were localised to the synovial lining and sublining regions. A, B; Safranin-O with Fast green stain, **C-D, E-H**; haematoxylin and eosin stain, **I, J**; immunohistochemistry developed with nickel-enhanced DAB (blue/black). Arrows; synovial surface. Scale bars = 500 μm.

Figure 3.2: Histopathological features of OA.

Figure 3.2: Histopathological features of OA.

Scatterplots illustrating differences between non-arthritic control and advanced OA cases for cartilage surface integrity score **(A)**, proteoglycan loss score **(B)**, chondrocyte morphology score **(C)**, synovitis score **(D)**, synovial fractional area positive for CD68-immunoreactive macrophages **(E)**, or nerve growth factor **(F)**. Lines represent medians and IQR. **P*<0.05, ****P*<0.001, advanced OA versus non-arthritic controls.

3.5 Histological features associated with symptomatic osteoarthritis

Both asymptomatic and symptomatic chondropathy groups displayed evidence of structural OA. Symptomatic chondropathy cases displayed similar macroscopic chondropathy to asymptomatic chondropathy cases, indicating appropriate matching (table 3.1). Severe macroscopic chondropathy lesions graded as III or IV (deep cartilage fibrillation or subchondral bone exposure, respectively) were present in the medial tibiofemoral compartment of 28/29 (97%) asymptomatic chondropathy and 29/29 (100%) symptomatic chondropathy cases.

Loss of cartilage surface integrity and alteration in chondrocyte morphology were greater in the symptomatic chondropathy than in the asymptomatic chondropathy group (table 3.1, figures 3.3A and B), whereas proteoglycan loss, tidemark integrity and subchondral bone marrow replacement by fibrovascular tissue did not differ significantly between groups.

Synovitis scores were greater in symptomatic chondropathy compared with asymptomatic chondropathy cases (table 3.1 and figure 3.3D). Severe inflammation with perivascular lymphoid aggregates was observed in 8/29 (28%) of symptomatic chondropathy cases compared to 1/29 (3%) asymptomatic chondropathy case ($P = 0.021$). The synovial area positive for NGF was greater in symptomatic chondropathy than in asymptomatic chondropathy cases (table 3.1, figure 3.3E). Differences in macrophage infiltration between groups did not reach statistical significance (table 3.1, figure 3.3F).

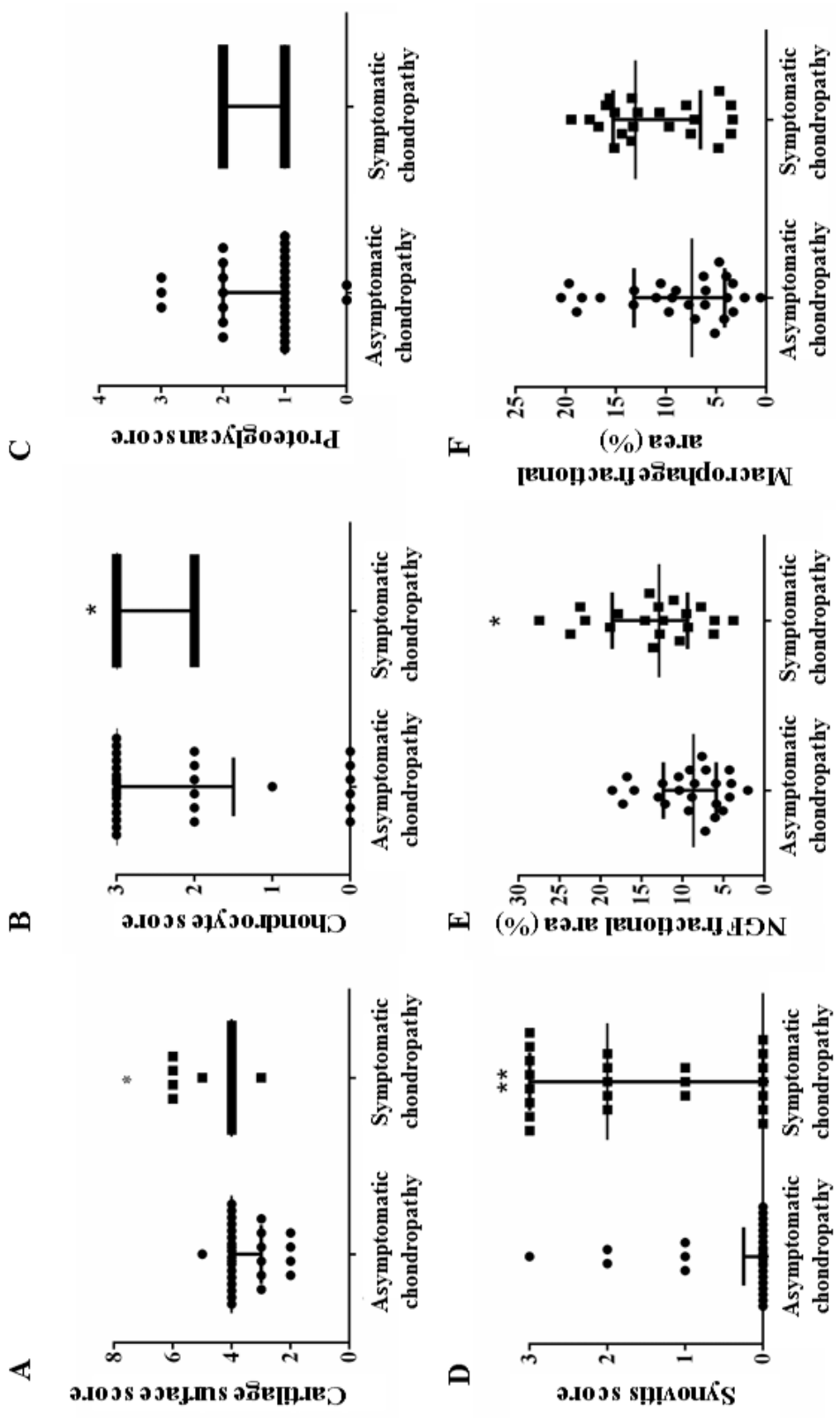


Figure 3.3: Histopathological associations of symptomatic of OA.

Figure 3.3: Histological associations of symptomatic OA.

Scatterplots illustrating differences between patients with similar macroscopic chondropathy scores who did not (asymptomatic chondropathy) or did (symptomatic chondropathy) undergo total knee replacement surgery. Cartilage surface integrity score **(A)**, chondrocyte morphology score **(B)**, proteoglycan loss score **(C)**, synovitis score **(D)** and NGF fractional area in the synovium **(E**) were greater in the symptomatic chondropathy group, whereas differences in CD68-immunoreactive macrophage fractional areas **(F)** did not reach statistical significance. Lines represent medians and IQR. **P*<0.05 ***P*<0.01, symptomatic chondropathy vs. asymptomatic chondropathy cases.

Logistic regressions were used to examine whether the association between symptomatic OA and synovitis was explained by increased synovial NGF immunoreactivity and/or macrophage fractional area. Associations between synovitis and symptomatic chondropathy remained significant in each regression model (P = 0.004 for each independent NGF and macrophage fractional area model, and P = 0.008 when combining both parameters).

3.6 Association of BMI with histological outcomes

BMI (kg/m^2) was calculated for both TKR groups (advanced OA and symptomatic chondropathy). Data were available for 42 of 54 cases (78%). Of these, 29/54 (69%) were classified as obese (BMI ≥ 30), 11/54 (26%) were overweight (25-29.9) and 2/54 (5%) were a healthy weight (18.5-24.9).

Spearman correlations were used to determine associations between BMI and outcome measures, combining data from both TKR groups. BMI was not significantly associated with any histopathological parameter (figure 3.4). In additional analyses, linear regression was used to determine associations between BMI and immunohistochemical fractional areas combining data from both groups. BMI, age and experimental group (advanced OA or symptomatic chondropathy) were used as independent covariates. NGF or CD68 fractional areas were used as the dependent variable. There were no significant associations between BMI and CD68 or NGF fractional area (P = 0.95 and 0.086 respectively).

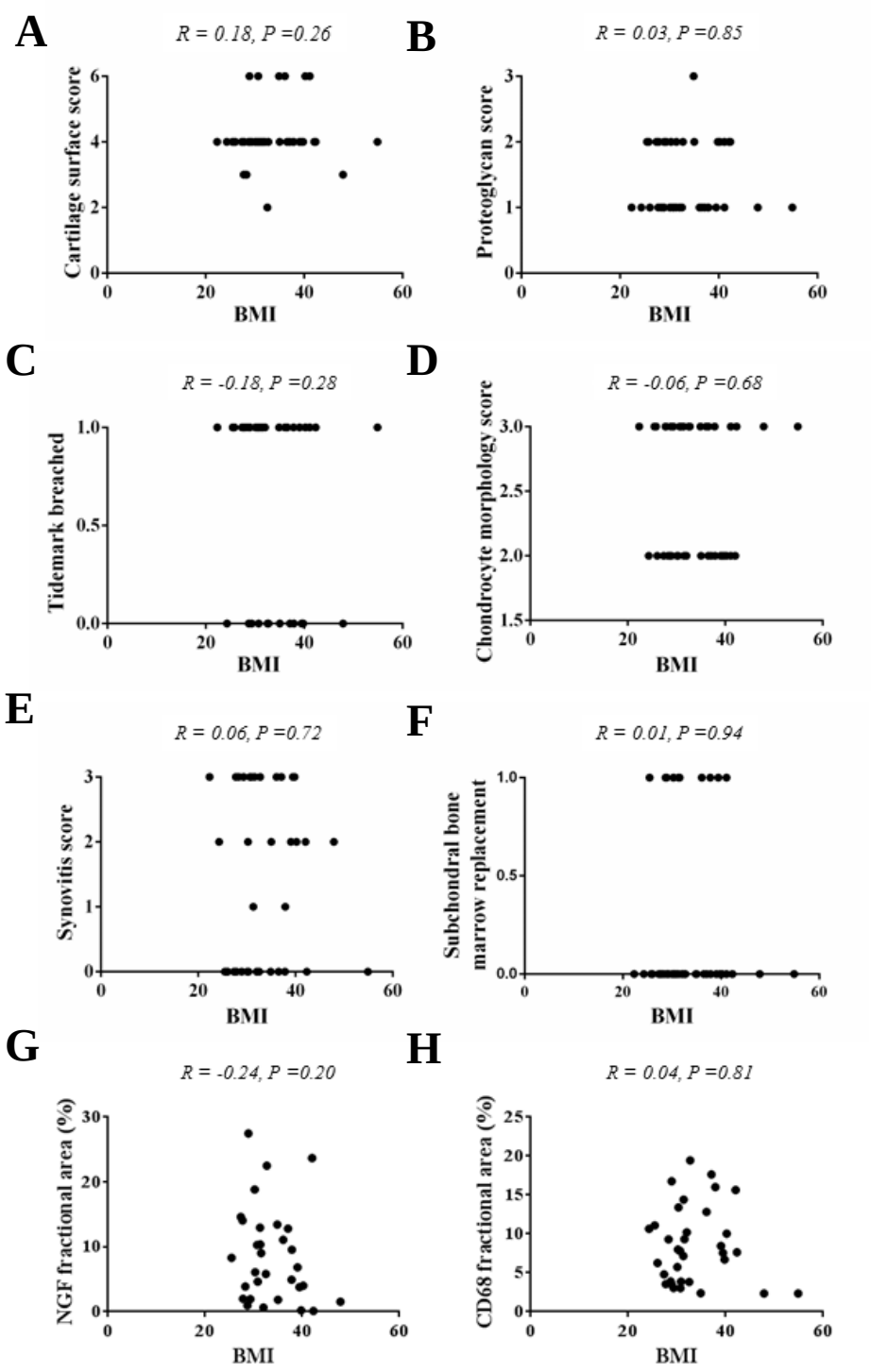


Figure 3.4: Scatterplots illustrating the relationship between histological scores and body mass index (BMI) from TKR cases.

In correlation analyses, BMI was not significantly associated with cartilage surface integrity **(A)**, proteoglycan loss **(B)**, tidemark breaching **(C)**, chondrocyte morphology score **(D)**, synovitis score **(E)**, subchondral bone marrow replacement **(F)** or synovial

NGF **(G)** and CD68 fractional areas **(H)**. Data from both TKR groups (advanced OA and symptomatic chondropathy) was combined. Statistical significance was accepted when $P < 0.05$.

3.7 Determining the cellular localisation of synovial nerve growth factor

NGF immunoreactivity in the synovium was predominantly localised to Hsp47 positive spindle shaped and mononuclear cells consistent with fibroblast morphology (figure 3.5). However, some $NGF^{+}/Hsp47^{-}$ and $NGF^{-}/Hsp47^{+}$ cells were also observed. Some CD68 positive macrophages in the lining and sublining regions also displayed NGF immunoreactivity (figure 3.6). Similar distributions were found in OA and non-arthritic control cases (figures 3.7 and 3.8). The work presented in this thesis shows co-localisation of NGF with macrophages and fibroblasts, further work would be required to determine the proportion of macrophages or fibroblasts that were NGF positive.

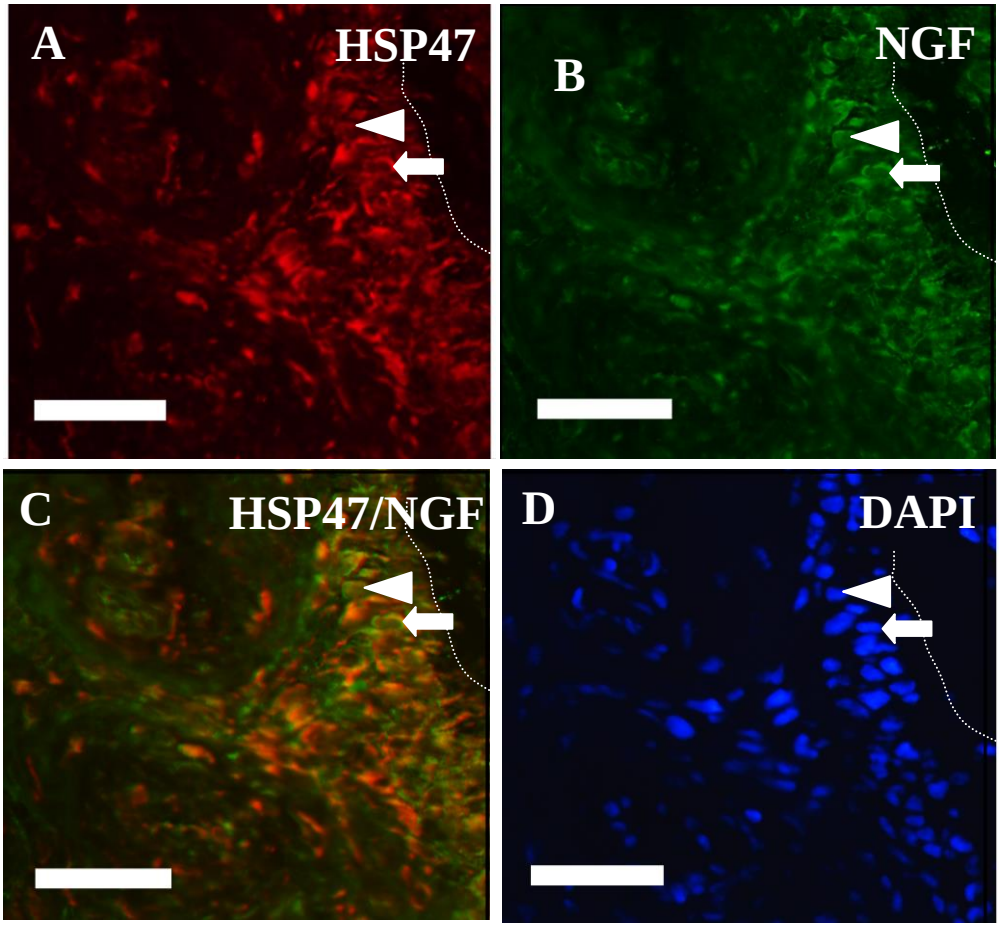


Figure 3.5: Cellular localisation of nerve growth factor (NGF) with Hsp47 immunoreactivity in osteoarthritic human synovium.

Hsp47-immunoreactivity localised to cells with fibroblast morphology in lining and sublining regions of synovium from a patient with OA **(A),** NGF-immunoreactivity in the section shown in panel A showing colocalisation with Hsp47 (arrow), or in a cell that is not immunolabeled for Hsp47 (arrowhead) **(B). (C)** shows a merge of panel A and B, arrow indicates a fibroblast colocalised to NGF (same cell as indicated in A and B); arrowhead indicates NGF-immunoreactivity in a cell that is not colocalised to Hsp47. **(D)** 4',6-diamidino-2-phenylindole (DAPI) nuclear counterstain of sections shown in panels **A-C**. Double immunohistochemistry visualised by Texas-red (Hsp47 [red]) and fluorescein (NGF [green]) staining. Scale bar = 50 µm. Synovial lining indicated by white dotted line.

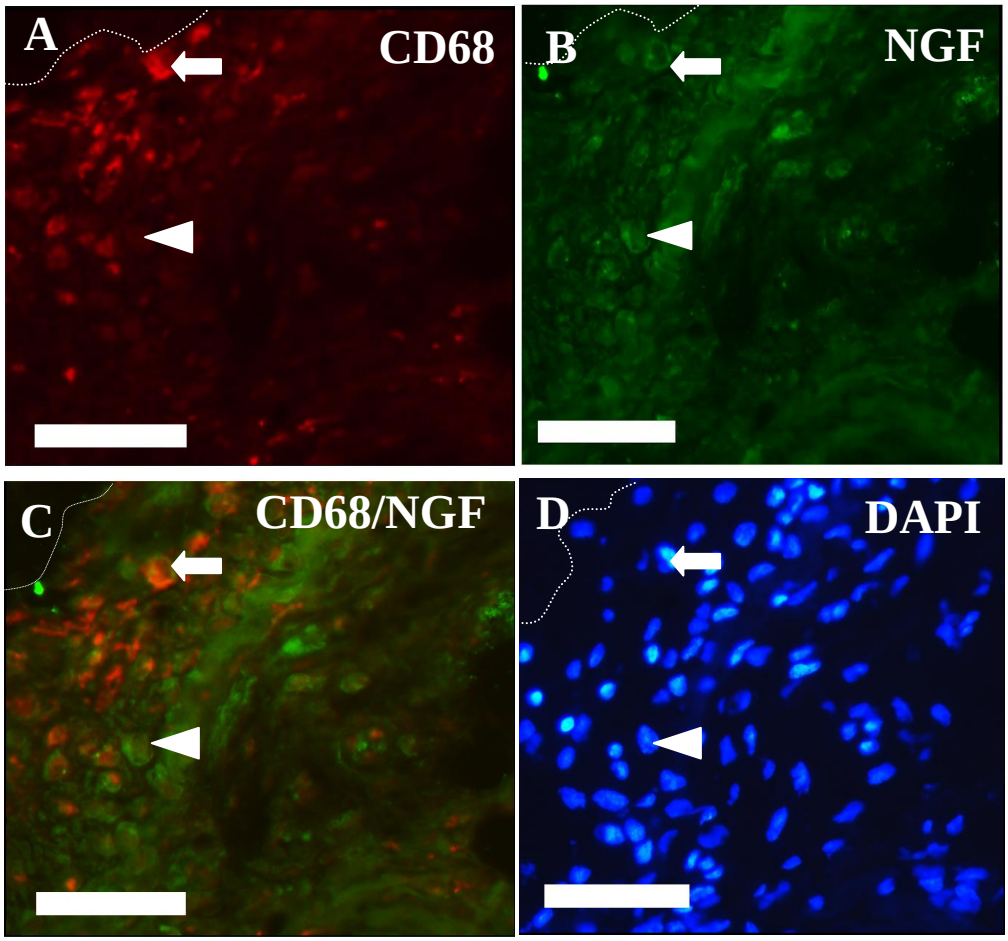


Figure 3.6: Cellular localisation of nerve growth factor (NGF) with CD68 immunoreactivity in osteoarthritic human synovium.

CD68-immunoreactive macrophages in synovium from a patient with OA **(A).** NGF-immunoreactivity in the section shown in panel A showing colocalisation with CD68 (arrow), or in a cell that is not immunolabeled for CD68 (arrowhead) **(B). (C)** Merge of panel A and B. **(D)** 4',6-diamidino-2-phenylindole (DAPI) nuclear counterstain of sections shown in panels A-C. Double immunohistochemistry visualised by Texas-red (CD68 [red]) and fluorescein (NGF [green]) staining. Scale bar = 50 µm. Synovial lining indicated by white dotted line.

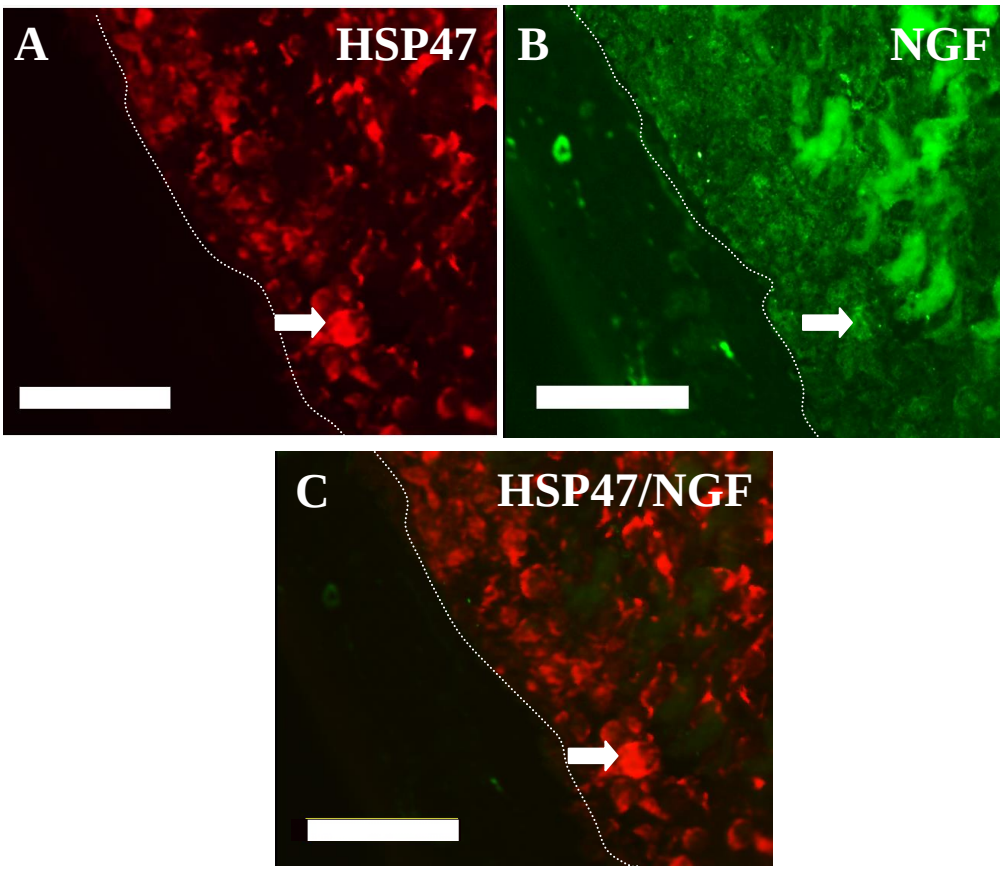


Figure 3.7: Cellular localisation of nerve growth factor (NGF) with Hsp47 immunoreactivity in non-arthritic control synovium.

Hsp47 immunoreactivity localised to cells with fibroblast morphology in lining and sublining regions of synovium from a non-arthritic PM control case **(A),** NGF-immunoreactivity in the section shown in panel A showing colocalisation with Hsp47 (arrow) **(B)**. **(C)** Shows a merge of panel A and B, arrow indicates a fibroblast colocalised to NGF (same cell as indicated in A and B)**.** Double immunohistochemistry visualised by Texas-red (Hsp47 [red]) and fluorescein (NGF [green]) staining. Scale bar = 50 µm. Synovial lining indicated by white dotted line.

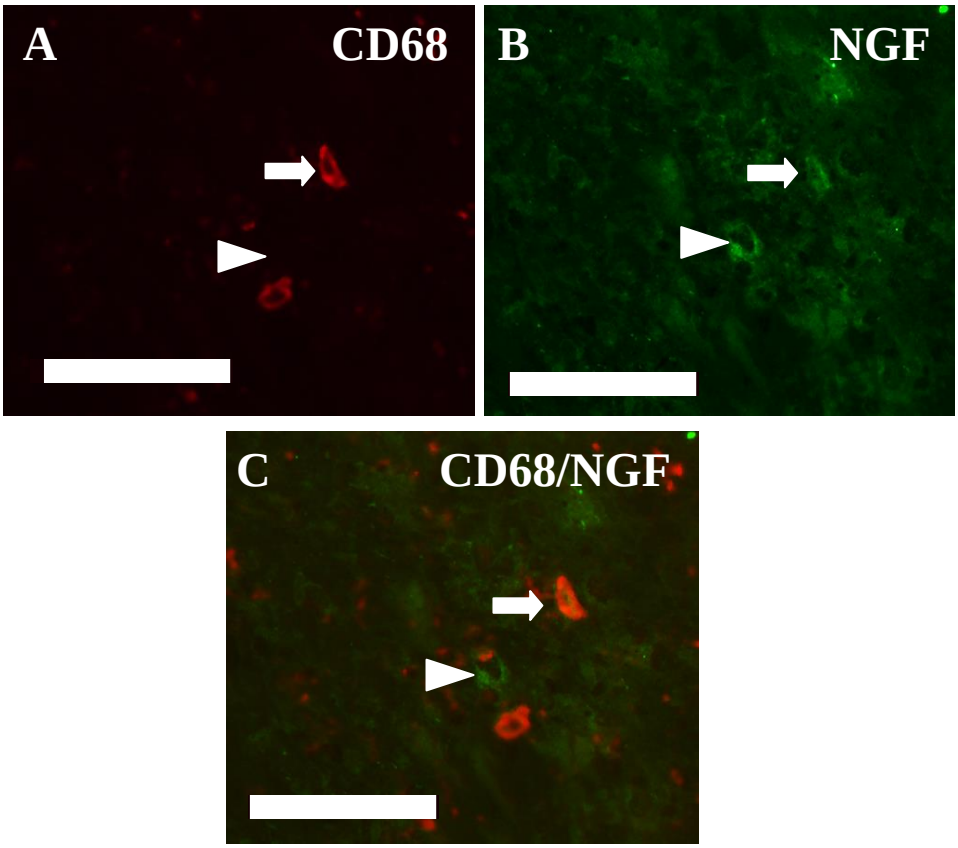


Figure 3.8: Cellular localisation of nerve growth factor (NGF) with CD68 immunoreactivity in non-arthritic control synovium sublining.

CD68-immunoreactive macrophages in the synovium **(A).** NGF-immunoreactivity in the section shown in panel A showing colocalisation with CD68 (arrow), or in a cell that is not immunolabeled for CD68 (arrowhead) **(B). (C)** Merge of panel A and B. Double immunohistochemistry visualised by Texas-red (CD68 [red]) and fluorescein (NGF [green]) staining. Scale bar = 50 µm.

3.8 Effect of post-mortem delay on nerve growth factor and macrophage immunoreactivity in the human synovium.

Two approaches were undertaken to examine whether decreased expression of NGF in asymptomatic chondropathy cases reflected different in vivo abundance of NGF between patient groups, or, may have resulted from loss of NGF immunoreactivity with increasing time between death and tissue processing in the PM group. First, the possible association between the length of PM delay, NGF and CD68-immunoreactivity was assessed. Second, the effects of PM decay were mimicked using synovial tissue collected at the time of TKR. See chapter 2, section 2.11 for detailed methods.

3.8.1 Associations between post-mortem delay and immunohistochemical outcomes

The median time of PM delay was 54 hours (IQR: 34-73hours). Separate correlation analyses were run for the non-arthritic control cases and asymptomatic chondropathy cases. Spearman's correlation coefficients (R value) and *P* values for each immunohistochemical outcome measure are reported in figure 3.9. In correlation analyses, PM delay was not significantly associated with CD68 fractional area in either group (figures 3.9 A&C), but was positively correlated with NGF fractional area in asymptomatic chondropathy cases ($P = 0.042$, figure 3.9D). Normality of the data was assessed using the Shapiro-Wilk test, fractional area measurements were not normally distributed ($P = 0.018$ and ≤ 0.001 for NGF and CD68 fractional areas, respectively). Therefore logistic regression was used in additional analyses, combining both non-arthritic control and asymptomatic chondropathy PM cases and adjusting for disease group. Median fractional areas for CD68 and NGF immunoreactivities were 4.57 and 5.94, respectively and cases below or above the median value were used as the dependent variable. After adjusting for age and experimental group, there were no significant associations between PM delay and CD68 or NGF fractional area ($P = 0.51$ and 0.92, respectively).

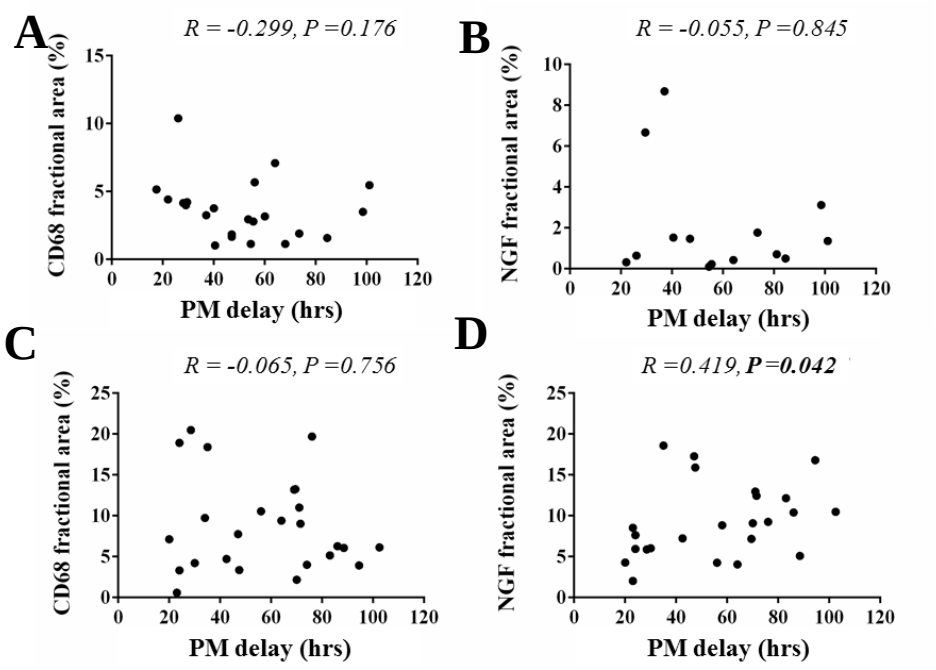


Figure 3.9: Associations between PM delay and CD68 and NGF immunoreactivity.

In non-arthritic control cases PM delay was not significantly associated with CD68 **(A)** or NGF **(B)** fractional areas. There was no significant association between PM delay and CD68 fractional area in asymptomatic chondropathy cases **(C)**, but delay was positively correlated with NGF fractional area **(D).** Data reported as Spearman's correlations coefficients. Fractional areas are reported only for the samples that displayed synovial lining (n = 15-26 group). Statistical significance was accepted when $P \leq 0.05$.

3.8.2 Mimicking the effects of post-mortem delay in synovial tissue obtained at TKR

NGF-immunoreactivity did not significantly differ between synovial tissues that had been exposed to 4°C temperatures for differing lengths of time (24, 48 or 72 hours) before fixation (figure. 3.10). In qualitative analysis there was no difference in the expression of NGF-immunoreactive cells in the synovial lining of TKR cases between the four time points (figures 3.10 A-D). In a one way ANOVA there was no significant difference in NGF expression between

any of the 4 time points (figure 3.10E, P = 0.97 for 24h vs. 48h comparison, and P = 1.00 for all other comparisons).

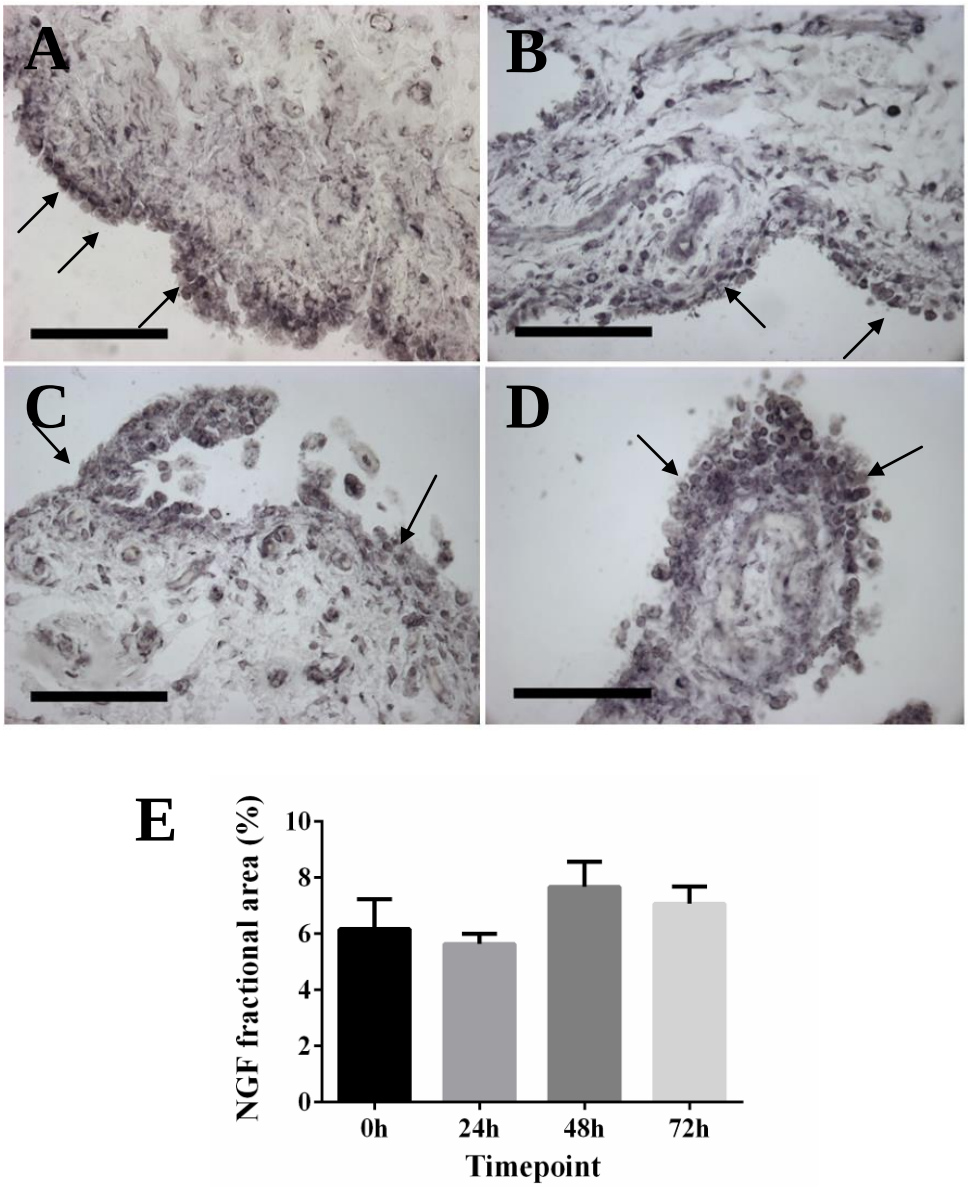


Figure 3.10: Comparison of NGF-immunoreactivity in osteoarthritic synovial tissue left to 'decay' for 24h, 48hr and 72 hours following tissue collection.

Synovium tissue was processed immediately following tissue collection **(A),** or left to decay for 24h **(B)**, 48h **(C)** and 72h **(D)** in DMEM at 4°C before fixation. NGF immunoreactivity in the synovium from one representative TKR case is shown. NGF fractional area was not significantly different at any of the 4 time points **(E)**. Data expressed as mean (S.E.M). Fractional areas are reported only for the samples that displayed synovial lining (n = 2-4 group). Arrows indicate synovial lining. Immunohistochemistry developed with nickel-enhanced DAB. Scale bar = 100μm.

3.9 Summary of results

- Loss of cartilage surface integrity, proteoglycan loss, tidemark breaching, alterations in chondrocyte morphology and synovitis are all features of OA.

- Symptomatic OA is associated with increased synovitis, increased synovial NGF-immunoreactivity, alteration of chondrocyte phenotype and loss of cartilage surface integrity, and compared to cases with similar macroscopic chondropathy who did not seek TKR.

- Synovial NGF is predominantly expressed by synovial fibroblasts and to a lesser extent by synovial macrophages.

- BMI was not significantly associated with any histopathological or immunohistological parameter.

- These results provide evidence that NGF- immunoreactivity appears stable with a range of post mortem delay or ex vivo incubation of tissues.

DISCUSSION

A range of histopathological features in the synovium and tibial plateaux were associated with symptomatic OA; synovitis, increased synovial NGF immunoreactivity, chondrocyte changes and loss of cartilage surface integrity, compared to cases with similar macroscopic joint surface appearances who did not seek TKR. Increased synovitis and synovial NGF expression by fibroblasts and some macrophages may be key features associated with pain in OA.

OA prevalence and severity are strongly associated with increasing age, raising doubts in earlier studies as to whether histopathological features are specifically associated with OA, rather than characteristics of healthy ageing. This was addressed by carefully age matching advanced OA and non-arthritic control cases, a process that required a large source repository from which to select cases.

Synovitis, the densities of CD68-immunoreactive macrophages or NGF-immunoreactive cells within the synovium, proteoglycan loss, chondrocyte changes, loss of tidemark integrity and tidemark breaching, were all greater in advanced OA cases compared with age-matched non-arthritic controls. This indicates that in this study these pathological features of OA are not explained by ageing alone. However, each of these features were also observed to a lesser extent in the age-matched control group, indicating either 'preclinical' early OA in this group, or normal structural features that are exaggerated by OA disease. A key question, therefore, is which pathological features are associated with clinical OA?

The relevance of structural changes to OA symptoms has been difficult to determine. Magnetic resonance imaging (MRI) evidence of synovitis has been associated with pain in people with OA or who are at high risk of OA (Baker et al., 2010). Furthermore a recent study demonstrated that fluctuation in synovitis corresponds to a fluctuation in knee pain, providing further evidence of the contribution of synovitis to symptomatic OA (Zhang et al., 2011b). Patients with greater synovitis display more severe chondropathy and synovitis may predict progressive structural damage in knee OA (Ayral et al., 2005,

Walsh et al., 2009). Therefore it can be difficult to be certain as to whether synovitis itself is a cause of pain, or acts as a surrogate for other aspects of OA pathology. This work extends these findings by indicating that synovitis is associated with symptomatic OA, independent of chondropathy severity.

The characteristics of synovitis that were associated with symptomatic OA were explored. This work confirms previous findings of increased macrophage infiltration in OA (Benito et al., 2005), but the presence of macrophages may not be sufficient to explain OA pain. NGF is elevated in the synovial fluid of patients with rheumatoid arthritis (Halliday et al., 1998, Raychaudhuri et al., 2011), and present to a lesser extent in OA cases (Barthel et al., 2009), but a previous study did not localise NGF to the synovium of the single reported OA case (Aloe et al., 1992). Nevertheless, monoclonal antibodies directed against NGF reduce pain and improve function in people with OA (Lane et al., 2010, Brown et al., 2012, Sanga et al., 2013).

The current study demonstrated that in OA, NGF-immunoreactivity is present in synovium predominantly in Hsp47-positive fibroblasts, and in some macrophages. NGF immunoreactivity was greater in the synovial tissue of symptomatic chondropathy compared to asymptomatic chondropathy cases. The abundance of NGF in asymptomatic chondropathy cases did not appear to be associated with PM delay. These findings suggest an important contribution from fibroblast-derived NGF in the generation of OA pain.

Pro-inflammatory cytokines, interleukin (IL)-1β and tumour necrosis factor (TNF)-α can stimulate NGF release from synovial fibroblasts; additionally NGF can modulate TNF-α release (Manni et al., 2003). NGF may act on sensory nerves to increase pain in OA. After adjusting synovitis for NGF and/or CD68 immunoreactivity the significant association of synovitis with symptomatic OA remained, suggesting increased NGF or macrophage infiltration alone or together do not completely explain pain. The production of pain mediators, for example by fibroblasts may yet be driven by macrophages or other aspects of inflammation.

Previous OA histopathological studies have often relied on samples obtained at joint replacement surgery, which display a range of OA structural severity

(Walsh et al., 2009). Chondropathy severity overlaps to a small extent between PM and surgical cases (Walsh et al., 2009) and therefore this study of pathological associations of symptomatic OA required selection of cases with matched macroscopic chondropathy from a large tissue repository. Radiographic scores for the symptomatic chondropathy group were similar to those for the advanced OA cases used to compare with non-arthritic controls, and macroscopic chondropathy scores for symptomatic chondropathy and asymptomatic chondropathy groups were significantly higher than non-arthritic controls, indicating that both symptomatic and asymptomatic chondropathy groups had pathological features of knee OA.

Limitations of the study are detailed in chapter 6, section 6.2.1. In brief, cadaver tissues were collected 54 (34-73) hours (median, IQR) after death therefore the tissue is likely to have been subjected to natural decay in the body before fixation. However, synovial NGF and CD68 immunohistochemical staining did not decrease with increasing delay between death and tissue processing. These results provide evidence that NGF- immunoreactivity appears stable with a range of post mortem delay or ex vivo incubation of tissues. NGF and CD68-immunoreactivity was assessed using quantification of fractional areas, using previously published methods (Haywood et al., 2003, Walsh et al., 2007. The density of immunopositive cells (stained with nickel enhanced DAB) particularly in the synovial lining disallowed evaluation using individual cell counting techniques. However further work could be undertaken to quantify the number of macrophages or fibroblasts that were NGF positive. These studies could involve using a nuclear counterstaining and counting the nuclei, for example by using unenhanced DAB with haematoxylin.

Although the symptomatic and asymptomatic chondropathy group were matched for similar macroscopic chondropathy scores, microscopic loss of cartilage surface integrity was greater in symptomatic chondropathy patients. Cases were selected on the basis of similar total tibiofemoral macroscopic chondropathy scores where appearance of the four articular surfaces was evaluated; medial and lateral femoral condyles and tibial plateaux. Histological grading was examined in one mid-coronal section from the middle third of the medial tibial plateaux because this is an important weight-bearing area

characteristically affected by OA. Macroscopic and microscopic analyses therefore reflect distinct but related aspects of OA pathology (Walsh et al., 2009).

Not all histopathological features associated with OA were associated with symptomatic chondropathy. Tidemark breaching was found in twice as many asymptomatic chondropathy cases than in non-arthritic controls, suggesting it may be an early feature of OA, but it was no more common in the symptomatic chondropathy than the asymptomatic chondropathy group. By contrast, osteochondral vascularity was previously associated with pain behaviour in rats with OA, after medial meniscal transection (Mapp et al., 2010). The current data suggest that tidemark breaching alone is insufficient to cause OA symptoms and additional factors such as sensory innervation or local expression of NGF may be necessary mediators of pain from osteochondral channels (Walsh et al., 2010). The current study provides novel insights into the incidence of tidemark breaching in a subgroup of asymptomatic PM cases with macroscopic chondropathy similar to cases that underwent TKR. Further work would be required to determine the time course and mechanisms by which channels breaching the tidemark may predispose to pain.

Fibrovascular replacement of subchondral bone marrow was twice as common in symptomatic chondropathy than in the asymptomatic chondropathy group, but this did not reach statistical significance after adjusting for age differences between groups. Bone marrow replacement has been associated with bone marrow lesions on MRI (Zanetti et al., 2000), which, in turn, has been associated with pain in knee OA (Felson et al., 2001, Felson et al., 2007). This study may have had insufficient power to detect differences between groups, and further work would be required to define the structural and biochemical features of bone marrow lesions that may explain their association with pain.

Obesity is a major risk factor for OA (Felson et al., 1988, Ackerman and Osborne, 2012, Jiang et al., 2012), and has been associated with pain (Goulston et al., 2011) and cartilage changes (Roemer et al., 2009a, Antony et al., 2011). The majority of advanced OA cases in the cohort were classified as overweight

or obese, but histopathological factors associated with symptoms were not significantly associated with BMI in this study.

PM cases were classified as having OA based on the presence of cartilage changes comparable to those seen in patients undergoing TKR for OA, and small, homogeneous patient groups were selected in order to undertake detailed histopathological experiments. This work extends imaging and arthroscopic studies that indicate the relative importance of synovitis (Hill et al., 2007, Baker et al., 2010) and macroscopic cartilage changes (Hunter et al., 2003, Sowers et al., 2003) to symptoms in the broader OA population.

3.10 Conclusions

Histopathological features that are associated with OA were identified, however not all of these features may cause pain. Symptomatic OA was associated with synovitis, synovial NGF immunoreactivity, changes in chondrocyte morphology and loss of cartilage surface integrity compared to asymptomatic chondropathy cases with similar macroscopic joint surface appearances who did not seek TKR. Different pathological features of OA typically coincide, and better understanding of the structural features that are associated with symptomatic OA would help refine strategies for developing structure-modifying treatments (disease-modifying OA drugs) by focussing on those which are most likely to improve symptoms. Synovitis and synovial NGF expressed by fibroblasts and some macrophages may be key mediators associated with OA knee pain.

CHAPTER 4: IDENTIFICATION OF GENE EXPRESSION PATTERNS IN THE SYNOVIUM AND THEIR RELATIONSHIP WITH SYMPTOMATIC OSTEOARTHRITIS

INTRODUCTION

OA is a complex disease involving all tissues within the knee joint. The causes of OA are not fully understood, but both biochemical and inflammatory factors contribute to the pathogenesis. In the previous chapter histological synovitis was shown to be associated with symptomatic OA. Indeed, previous imaging studies support an association between synovial inflammation and pain (Hill et al., 2007, Baker et al., 2010). The contribution of synovial inflammation to symptomatic OA may be mediated by the release of noxious inflammatory signals which act to facilitate pain and hyperalgesia through the activation of downstream signalling pathways. Understanding gene expression patterns that may contribute to symptomatic OA is crucial to developing new analgesic treatment strategies.

Numerous inflammatory mediators such as cytokines, chemokines, growth factors, and matrix metalloproteinase (MMPs) have been implicated in joint destruction in OA. These noxious molecules are released from chondrocytes and synoviocytes during inflammation and tissue damage and may also contribute to OA pain through the activation or sensitisation of peripheral nerves in the joint. Sensitisation of nerve terminals enables stimuli that would not usually elicit pain to be perceived as painful.

There are multiple molecular identities of nociceptor sensitisers, including cytokines and chemokines. Much of the literature to date describes a key role in the involvement of the pro-inflammatory cytokines interleukin (IL)-1β and

tumour necrosis factor (TNF)-α in mediating pain through the release of other downstream inflammatory mediators such as matrix metalloproteases (MMPs) and cytokines (Fernandes et al., 2002). TNF-α can activate the mitogen activated protein kinase (MAPK) signalling pathway, which regulates the production of other pro-inflammatory mediators. In the synovial fluid of patients with knee OA, increased expression of TNF-α protein has been correlated with pain, as assessed by the WOMAC score (Orita et al., 2011). Elevated levels of some chemokines such as monocyte chemoattractant protein-1/chemokine ligand 2 (MCP-1/CCL2), macrophage inflammatory protein-1 beta/chemokine ligand 4 (MIP-1β), interleukin (IL)-6 and interferon (IFN)- γ have been associated with pain (Cuellar et al., 2009).

Nerve growth factor (NGF) may play a key role in mediating inflammatory pain through increasing nociceptor excitability in OA. Strategies to block NGF have shown success in alleviating knee pain and improving function in patients with symptomatic knee OA (Lane et al., 2010, Tiseo et al., 2014) implying an association with NGF expression and pain.

Prostaglandin synthesis by the cyclo-oxygenase (COX) enzymes, COX-1 and COX-2 contribute to the generation of the inflammatory response. In particular, COX-2 is upregulated during inflammation (Seibert and Masferrer, 1994) and may contribute to pain (Lee et al., 2005).

Various downstream signalling pathways play a role in the inflammatory response. The nuclear factor kappa-B (NF-κB) pathway contributes to the up-regulation of various pro-inflammatory and angiogenic factors (Tak and Firestein, 2001). The Janus activated kinase/signal transducers and activators of transcription (JAK/STAT) pathway is the major signalling cascade for a range of cytokines and growth factors (Rawlings et al., 2004). The MAPK pathway regulates the production of pro-inflammatory cytokines such as IL-1β and TNF-α.

In order to identify molecular determinants of symptomatic OA, gene expression patterns in the synovium were compared between OA patients who had sought TKR for symptoms (symptomatic chondropathy) and asymptomatic PM donors (asymptomatic chondropathy). Symptomatic and asymptomatic

chondropathy cases were matched for severity of macroscopic articular surface appearances. Custom made 384-well microfluidic cards (TaqMan® Array Card, Applied biosystems) were designed to determine changes in relative mRNA expression of 96 genes (92 target and 4 reference) between groups.

4.1 Objectives

1. To identify synovial gene expression patterns that may mediate an association with symptomatic OA.

2. To examine whether molecular associations of pain are associated with synovial inflammation.

METHODS

General methodology for this chapter is given in chapter 2. Patient selection and sample processing are stated in sections 2.1.3 and 2.2.2, respectively. Histologic and macroscopic grading is detailed in sections 2.5 and 2.7, respectively. Extraction of total RNA from synovia is described in section 2.12.1. Spectrophotometric analysis of RNA concentration is detailed in section 2.12.2. Reverse transcription of RNA to complementary DNA (cDNA) is described in section 2.12.3. Loading of microfluidic cards is described in section 2.12.6. Analysis of gene expression data is described in section 2.12.8.

4.2 Patient subgroups

4.2.1 Preliminary study; assessing RNA integrity.

Initially, a pilot study was conducted to ensure suitability of methods for extracting RNA, ability to transcribe to cDNA and ultimately to select the most appropriate microarray technique. RNA was extracted from 4 synovium samples; 2 from PM donors, and 2 from TKR cases. These four samples were selected from the tissue repository, and were different cases to those used in the main study. The integrity of RNA of these 4 samples was assessed in order to decide the most appropriate microarray technique. The RNA integrity number (RIN) for each of the 4 samples was determined using an Agilent RNA 6000 Nano Kit (Agilent Technologies).

The RIN score (1-10) is an indication of RNA quality, with 1 being the most degraded RNA and 10 being the most intact (Schroeder et al., 2006). The RIN of each sample was determined by examining ribosomal bands using gel electrophoresis and through visual inspection of ribosomal peaks at 18s and 28s on an electropherogram recording. The 18s and 28s peaks should be high in an intact specimen. In addition, the 28s:18s ratio should be between 1.8-2 in an intact specimen (Fleige and Pfaffl, 2006), whereas the ratio is decreased in degraded samples (Mueller et al., 2004).

For all 4 test samples in the pilot study the RNA was degraded on visualisation of the electropherograms (figures 4.1 A-D). The analyser was unable to calculate a RIN score for all 4 samples (RIN score = N/A). The rRNA 28s:18s ratio were available for one TKR case (figure 4.1B) and one PM case only (figure. 4.1C), ratios were 0.7 and 0.4, respectively. For the remaining TKR and PM case (figures 4.1A&D, respectively), the ratio could not be calculated (rRNA 28s:18s = 0).

The RIN score of the positive control sample (human brain, figure. 4.1E) was 7, which indicated that the RNA was of good quality. The rRNA 28s:18s ratio was 1.0. Based on these pilot data, microarray analysis using real-time polymerase chain reaction (RT-PCR) was employed to analyse gene expression analysis in the main study, as RT-PCR is a robust method for partially degraded samples (Paik et al., 2005) .

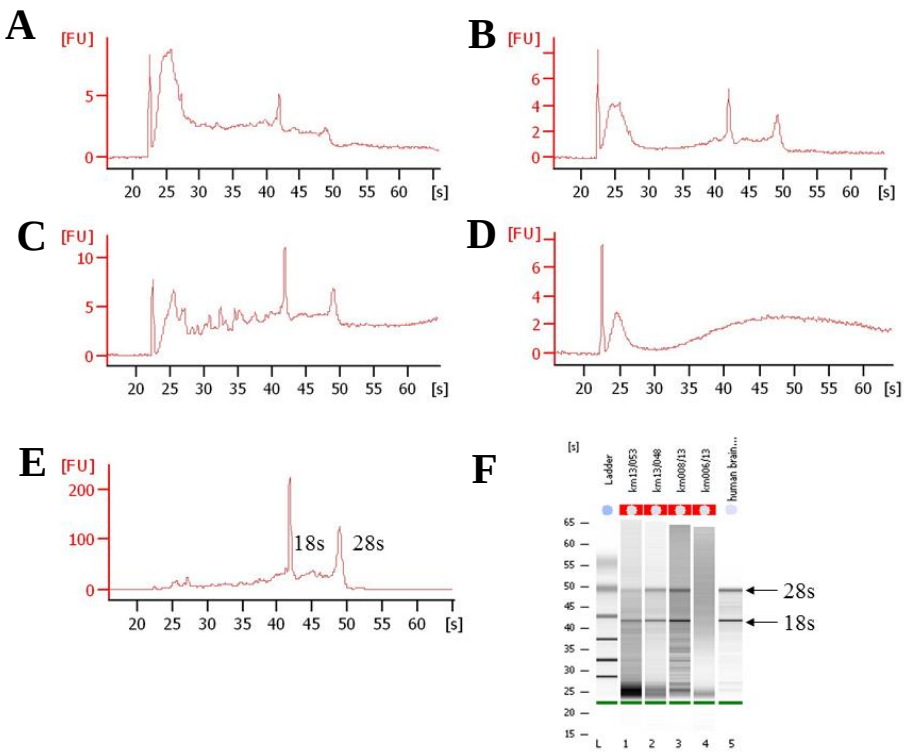


Figure 4.1: RNA integrity assessments using micro-chip based electrophoresis (Agilent RNA 6000 Nano kit).

Electropherograms of two samples obtained at the time of TKR for symptomatic OA **(A &B)** and two synovial samples obtained at post-mortem TKR **(C&D).** A positive control sample (human brain) is shown in **(E)**, where clear 18s and 28s peaks can be identified. Gel electrophoresis of RNA integrity **(F)**. Columns from left to right: ladder, 2 TKR cases, 2 PM cases and positive control. Prominent 18s and 28s bands are evident for the positive control sample. (final column on the right).

4.2.2 Main study

A subgroup of 12 PM and 12 TKR cases (asymptomatic and symptomatic chondropathy, respectively) were selected from the larger study group of cases used in the previous chapter. Asymptomatic and symptomatic chondropathy cases were matched for macroscopic chondropathy scores, and were selected based on availability of snap frozen synovium biopsies. RNA was extracted and reversed transcribed to cDNA, as described in section 2.12.1 and 2.12.3.

4.3 Microfluidic cards

4.3.1 Gene selection criteria

Custom-made 384 well microfluidic (Low density TaqMan array) cards were designed to examine differences in synovial gene expression patterns between asymptomatic and symptomatic chondropathy cases. Each card allowed for up to four samples to be run in parallel, 96 different genes were included in the microfluidic card, 4 of these were reference genes (internal controls).

An extensive review of the literature was conducted to select the 96 genes to include in the microfluidic card. Various criteria were applied for selection. First, the literature was reviewed to identify genes which may be mediating pain through sensitising nerve terminals. Second, genes selected were those that had previously been shown to be differentially expressed at the RNA level. Third, signalling pathways were identified and pathway components were selected. For selection of the reference genes, the literature was reviewed to select the most stable reference gene expression in synovial tissue (table 4.1).

The full list of target genes included in the microfluidic card is detailed in table 4.2. The genes selected were pro-inflammatory mediators (interleukins, chemokines and MMPs), NGF signalling pathway components, protease activator receptor (PAR) signalling components, involved in prostaglandin and nitric oxide synthesis, NF-kB or MAPK signalling pathway components. Other molecular targets included angiogenic mediators.

Table 4.1: Selection of references genes included in the microfluidic card.

GENE NAME (SYMBOL)	FUNCTION
REFERENCE GENES	
Beta actin (ACTB)	• Cytoskeletal structural protein widely used as a reference gene in different experimental conditions.(Li et al., 2011).
Glyceraldehyde-3-phosphate dehydrogenase (GAPDH)	• Encodes a catalysing enzyme involved in glycolysis.
Hydroxymethylbilane synthase (HMBS)	• Encodes an enzyme involved in the production of heme.
Ubiquitin C (UBC)	• Gene involved in protein degradation.

Table 4.2: Selection of target genes included in the microfluidic card.

GENE (SYMBOL)	FUCTION
INFLAMMATORY MEDIATORS	
Tumour necrosis factor alpha (TNF-α)	• Major pro-inflammatory multifunctional cytokine associated with OA pathophysiology (Bondeson et al., 2006, Stannus et al., 2010). • Produced by synoviocytes in addition to chondrocytes, mononuclear cells and osteoblasts (Kou and Wu, 2014). • Regulator of inflammatory processes, activates p38/MAPK and protein kinase c (PKC) (Vandenabeele et al., 1995).
Tumour necrosis factor converting enzyme (ADAM17)	• Member of the 'A Disintegrin And Metalloprotease' family converts precursor molecules to soluble forms of TNF (Black, 2002).
Interleukin-1β (IL1B)	• Major pro-inflammatory cytokine involved in OA pathogenesis. • Induces COX-2 up-regulation by NF-κB pathway (Lee et al., 2004). • Directly and rapidly sensitises nociceptors to induce hyperalgesia (Binshtok et al., 2008).
Interleukin-1 receptor type I (IL-1R1)	• Interleukin-1 receptor.
Interleukin-1β-converting enzyme (CASP1)	• Coverts cytokine precursor pro-IL-1B into its active form (Saha et al., 1999).
Interleukin-4 (IL4)	• Anti-inflammatory cytokine which activates the JAK/STAT pathway(Busch-Dienstfertig and González-Rodríguez, 2013).
Interleukin-4 receptor (IL4R)	• Cognate receptor for IL-4. • Elevated levels of IL4R in the serum of patients with OA compared to a healthy control group (Silvestri et al., 2006).
Interleukin-6 (IL6)	• Pro-inflammatory cytokine. • Production up-regulated by CCL5 in human OA synovial fibroblasts (Tang et al., 2010). • Elevated circulating levels of IL-6 are a strong predictor of radiographic knee OA (Kellgren Lawrence grade ≥2) (Livshits et al., 2009).

	• IL-6 activates JAK/STAT pathway (Kishimoto, 2006).
Interleukin-8 (IL8)	• Pro-inflammatory cytokine. • Elevated in the synovial fluid of OA patients relative to controls (Kaneko et al., 2000).
Interleukin-10 (IL10)	• Anti-Inflammatory cytokine. • Signalling is initiated by the JAK/STAT pathway, through activation of JAK1 and tyrosine kinase 2 (TYK2 (Finbloom and Winestock, 1995).
Interleukin-15 (IL15)	• Pro-inflammatory cytokine • Elevated in the synovial fluid of patients with early knee OA (patients with meniscal tears and early cartilage thinning) compared to end-stage OA cases (Scanzello et al., 2009). • Serum levels are associated with pain severity in patients with knee OA (Sun et al., 2013).
Interleukin-17 (IL17)	• Pro-inflammatory cytokine. • Serum and synovial fluid levels of IL-17 are significantly higher in OA patients compared to healthy controls. Furthermore, levels of IL-17 in the synovial fluid are correlated with pain and physical disability as assessed by the Lequesne index (Chen et al., 2014a). • In the articular cartilage IL-17 upregulates nitric oxide production via NF- κB activation (Attur et al., 1997).
Protein S100A8 (S100A8)	• Pro-inflammatory mediator also known as an alarmin. • May aggravate osteophyte formation in experimental OA (Schelbergen et al., 2014).
Protein S100A9 (S100A9)	• Pro-inflammatory mediator also known as an alarmin. • May aggravate osteophyte formation in experimental OA (Schelbergen et al., 2014). • Shown to be strongly upregulated in inflamed synovium (Lambert et al., 2014).
Interferon gamma (IFNG)	• Type II interferon with pro-inflammatory actions • Activates the JAK/STAT signalling pathway (Horvath, 2004).
Connective tissue growth factor (CTGF)	• Pro-inflammatory mediator. • CTGF interacts with IL-1β to initiate the expression of the inflammatory cascade in fibroblast-like synoviocytes from patients with knee OA (Wang et al., 2013).
Triggering receptor expressed on myeloid cells (TREM1)	• Receptor expressed on neutrophils, monocytes and macrophages (Collins et al., 2009) • Plays an important role in the amplification of inflammation.

	• Strongly up-regulated in inflamed areas of synovium from OA patients compared to non-inflamed areas (Lambert et al., 2014).
Annexin 1 (ANXA1)	• Endogenous anti-inflammatory mediator (Chen et al., 2013). • Mediates the anti- inflammatory effects of glucocorticoids • Endogenous ANXA1 in the dorsal root ganglion produces anti-nociceptive effect through formyl peptide receptor-2 (FRR2/ALX) (Pei et al., 2011).
Annexin 6 (ANXA6)	• Cytoplasmic protein that stimulates NF-kB signalling in pathology (Minashima et al., 2013).

GENE NAME (SYMBOL)	FUNCTION
CHEMOKINES	
Monocyte chemotactic protein-1/chemokine ligand 2 (MCP-1/CCL2)	• Pro-inflammatory • Recruits inflammatory cells including monocytes and memory T cells to sites of inflammation (Voscopoulos and Lema, 2010). • Synovial fluid levels of CCL2 are correlated with pain and physical disability in patients with knee OA (Li and Jiang, 2015). • Levels increased in primary sensory neurons following nerve injury (White et al., 2009). • STAT3 target gene (Dauer et al., 2005)
Macrophage inflammatory protein/chemokine ligand 3 (MIP-1α/CCL3)	• Pro-inflammatory. • Can sensitise TRPV1 channels (Zhang et al., 2005a).
Macrophage inflammatory protein/ chemokine ligand 4 (MIP-1β/CCL4)	• Pro-inflammatory. • Levels of MIP-1 β greater in OA synovial fluid compared to RA (Koch et al., 1995).

RANTES (regulated on activation normal T cell expressed and secreted)/chemokine ligand 5 (CCL5)	• Pro-inflammatory. • Induces IL-6 production by PKCδ/c-Src/c-Jun and AP-1 signalling pathways in synovial fibroblasts. • Expression is increased in OA synovial fibroblasts compared to normal fibroblasts (Tang et al., 2010).
Monocyte chemotactic protein-2/chemokine ligand 8 (MCP-2/CCL8)	• Pro-inflammatory. • May induce IL-6 in synovial fibroblasts from patients with OA, thus may be a biomarker for IL-6 activation (Kuziora et al., 2013).
Chemokine ligand 1 (CXCL1)	• Pro-inflammatory. • During inflammation CXCL1 secretion from spinal astrocytes enhances pain by mediating downstream ERK activation and COX-2 expression (Zhang et al., 2013).
Chemokine ligand 2 (CXCL2)	• Pro-inflammatory • Can be induced by receptor activator of nuclear factor-κB ligand (RANKL) to enhance osteoclastogenesis (Ha et al., 2010) • STAT3 target gene(Dauer et al., 2005)
Chemokine ligand 5 (CXCL5)	• Pro-inflammatory. • Involved in NF-κB mediated angiogenesis (Pickens et al., 2011).
Chemokine ligand 6 (CXCL6)	• Attracts neutrophils during inflammation (Scaife et al., 2004)
Chemokine ligand 10 (CXCL10)	• Pro inflammatory • Activates and recruits immune cells such as monocytes, T cells and eosinophils (Lee et al., 2013) • Regulates immune responses by activating and recruiting leukocytes such as T cells, eosinophils, monocytes, and natural killer cells
Fractalkine (CX3CL1)	• Induces the migration of OA fibroblasts. • Elevated fractalkine in the serum and synovial fluid is correlated with radiographic severity (Zou et al., 2013) and with symptomatic severity (Huo et al., 2015). • Expressed in monocytes (in the synovial fluid) during inflammation, and in macrophages, fibroblasts, endothelial and dendritic cells in RA synovial tissue (Ruth et al., 2001)

GENE NAME (SYMBOL)	FUNCTION
MATRIX METALLOPROTEASES	
Matrix metalloproteinase 1 (MMP1)	• Secreted enzyme which catalyses interstitial collagenases in OA. • Serum levels of MMP-1 are elevated in patients with OA compared to healthy controls (Mahmoud et al., 2005).
Matrix metalloproteinase 2 (gelatinase-A/MMP2)	• Expressed in fibroblasts, endothelial and epithelial cells (Galasso et al., 2012). • May be involved in the maintenance of neuropathic pain (Kawasaki et al., 2008)
Matrix metalloproteinase 3 (stromelysin/ MMP3)	• Secreted from chondrocytes and synovial cells. • Degrades non-collagen matrix proteins. • Expression is increased in OA synovium fluid (Lohmander et al., 1993) and tissue (Chen et al., 2014b) compared to normal controls. • Pro-NGF processing enzyme.
Matrix metalloproteinase 7 (MMP7)	• Pro-NGF processing enzyme (Lee et al., 2001).
Matrix metalloproteinase 9 (gelatinase-B/MMP9)	• May be involved in the early phase of neuropathic pain (Ji et al., 2009)
Matrix metalloproteinase 12 (macrophage elastase/MMP12)	• The predominant MMP secreted by inflammatory macrophages (Banda and Werb, 1981).

GENE NAME (SYMBOL)	FUNCTION
NERVE GROWTH FACTOR SIGNALLING	
Nerve growth factor (NGF)	• Essential for promoting sympathetic and parasympathetic neuronal growth and survival (Levi-Montalcini, 1987)). • Plays an important role in the genesis and maintenance of pain during inflammatory states (Raychaudhuri et al., 2011).
Neurotrophic tyrosine kinase, receptor, type 1	• High affinity nerve growth factor receptor transmembrane tyrosine kinase (Trk) A.

(NTRK1)	• The β-subunit of NGF binds selectively and with high affinity to TrkA (Pezet and Mcmahon, 2006).
p75 neurotrophin receptor (NGFR)	• A low affinity pan-neurotrophin receptor, binds all members of the neurotrophin family (Pezet and Mcmahon, 2006).
Phosphatidylinositol-4,5-bisphosphate 3-kinase, catalytic subunit alpha (PIK3CA)	• Class 1A isoform. Often activated by growth factor and cytokines (Rommel et al., 2007).
Phosphatidylinositol-4,5-bisphosphate 3-kinase, catalytic subunit beta (PIK3CB)	• Class 1A isoform. Often activated by growth factor and cytokines (Rommel et al., 2007).
Phosphatidylinositol-4,5-bisphosphate 3-kinase, catalytic subunit delta (PIK3CD)	• Class 1A isoform Often activated by growth factor and cytokines (Rommel et al., 2007).
Phospholipase C beta 1 (PLCB1)	• Increases the concentration of diacylglycerol (DAG) (Garcia Del Cano et al., 2014) which activates protein kinase C epsilon.
Protein kinase C epsilon (PRKCE)	• Phosphorylates TRPV1, the pro-nociceptive channel involved in hyperalgesia (Srinivasan et al., 2008).
Transient receptor potential cation channel, subfamily V, member 1 (TRPV1)	• Pro-nociceptive thermosensitive channel in subpopulation of primary afferent and sensory neurons. • Plays important roles in inflammatory hyperalgesia. • Variants of TRPV1 are associated with symptomatic OA (Valdes et al., 2011).

GENE NAME (SYMBOL)	FUNCTION
NEUROTROPHINS	
Brain Derived Neurotrophic factor (BDNF)	• Plasma BDNF concentrations are higher in OA patients compared to healthy controls, and levels correlated with self-reported pain as assessed by the WOMAC index (Simao et al., 2014).
Tissue plasminogen activator (PLAT)	• Catalyses the conversion of the zymogen plasminogen to plasmin, which can also cleave proNGF (Le and Friedman, 2012).
Plasminogen activator inhibitor 1 (SERPINE1)	• Inhibits conversion of plasminogen to plasmin, which cleaves proNGF into NGF (Ghosh and Vaughan, 2012).

GENE NAME (SYMBOL)	FUNCTION
JANUS ACTIVATED KINASE- SIGNAL TRANSDUCER AND ACTIVATOR OF TRANSCRIPTION (JAK/STAT) SIGNALLING	
Tyrosine kinase-2 (TYK2)	• A member of the Janus Activate Kinase (JAK) family (Rawlings et al., 2004).
Signal transducer and activator of transcription-1 (STAT1)	• Member of the Signal transducer and activator of transcription (STAT) family. • Expression increased in the synovial tissue in inflammatory arthritis (Walker et al., 2006).
Signal transducer and activator of transcription-3 (STAT3)	• Member of the Signal transducer and activator of transcription family.
Suppressors of cytokine signalling -1 (SOCS1)	• Negative regulator of cytokine signalling, inhibit the JAK/STAT pathway (Isomaki et al., 2007).
Suppressors of cytokine signalling -3 (SOCS3)	• Negative regulator of cytokine signalling, inhibit the JAK/STAT pathway (Isomaki et al., 2007).
Protein inhibitors of activated STATs 3 (PIAS3)	• Inhibit STAT3 signal transduction (Chung et al., 1997).

GENE NAME (SYMBOL)	FUNCTION
NUCLEAR FACTOR-KAPPA B (NF-KB) SIGNALLING	
Nuclear factor of kappa light polypeptide gene enhancer in B-cells 1 (p50/NFKB1)	• Transcription factor that plays important role in inflammatory response (Rigoglou and Papavassiliou, 2013).
v-rel avian reticuloendotheliosis viral oncogene homolog A (p65/RelA)	• Subunit of Nuclear factor -kB receptor (Rigoglou and Papavassiliou, 2013).
Jun (C-JUN)	• Transcriptional factor.
Fos (C-FOS)	• Transcription factor, encode zipper proteins that can dimerise with proteins of the JUN family, forming transcription factor complex AP-1.
Nuclear factor of kappa light polypeptide gene enhancer in B-cells inhibitor, alpha (NFKBIA)	• Inhibitor of NF-κB (Rigoglou and Papavassiliou, 2013).
B-Cell CLL/Lymphoma 3 (BCL3)	• Transcriptional repressor, belonging to the IκB family of proteins (Nolan et al., 1993). • Also plays a role as a STAT3 target gene (Dauer et al., 2005).
Receptor activator of nuclear factor kappa B ligand (TNFRSF11B/ (RANKL)	• Required for osteoclastogenesis • Member of the tumour necrosis superfamily • Ligand for receptor activator of nuclear factor-κB (RANK)
Osteoprotegerin (TNFSF11)	• Member of the tumour necrosis superfamily • Decoy receptor of RANKL

GENE NAME (SYMBOL)	FUNCTION
MITOGEN-ACTVATED PROTEIN KINASE (MAPK) SIGNALLING	
Mitogen-activated protein kinase kinase 3 (MKK3/MAP2K3)	• Activates p38-α/MAPK14 (Raingeaud et al., 1996).
Mitogen-activated protein kinase kinase 6 (MKK6/MAP2K6)	• Activates p38-α/MAPK14 (Raingeaud et al., 1996).
Mitogen-activated protein kinase 14 (p38-α/MAPK14)	• Members of protein kinases involved in the transduction of extracellular signals to the nucleus. • Activated by inflammatory mediators such as IL-1β and TNF-α and environmental stress (Korb et al., 2006).
Mitogen-activated protein kinase-activated protein kinase 2 (MAPKAPK2)	• Downstream target of p38-α (Hammaker and Firestein, 2010).

GENE NAME (SYMBOL)	FUNCTION
PROTEASE-ACTIVATED RECEPTOR (PAR) SIGNALLING	
Protease-activated receptor-2 (F2RL1/PAR2)	• G protein-coupled receptor for inflammatory proteases, mediator of neurogenic inflammation and pain (Ferrell et al., 2003) • Activated by trypsin and tryptase (Macfarlane et al., 2001)
Tyrosine receptor potential vanilliod 4 (TRPV4)	• Mediates neurogenic inflammation and pain. Downstream target of PAR2 (Poole et al., 2013).
Protease-activated receptor-4 (F2LR3/PAR4)	• G protein-coupled receptor involved in joint inflammation (Mcdougall et al., 2009) • Activated by thrombin and trypsin

Transient receptor potential ankyrin 1 (TRPA1)	• Downstream target of PAR2 • Excitatory ion channel on primary sensory nerves(Dai et al., 2007)
Protein kinase D1 (PRKD1)	• Involved in thePAR2 signalling pathway (Amadesi et al., 2009).
Protein kinase D2 (PRKD2)	• Involved in the PAR2 signalling pathway (Amadesi et al., 2009).
Protein kinase D3 (PRKD3)	• Involved in the PAR2 signalling pathway (Amadesi et al., 2009).

GENE NAME (SYMBOL)	FUNCTION
PROSTAGLANDIN & NITRIC OXIDE SYNTHESIS	
Cyclooyxgenase-1 (PTGS1)	• Enzyme, catalyses the conversion of arachidonic acid to prostaglandin (PG) H2, the precursor of PGs and thromboxane. Constituently expressed in many cells and tissues, including resident inflammatory cells (Ricciotti and Fitzgerald, 2011).
Cyclooxygenase-2 (PTGS2)	• Enzyme, primarily present at sites of inflammation. • Catalyse the conversion of arachidonic acid to prostaglandin (PG) H2, the precursor of PGs and thromboxane. • Key role in sensitization to sensory stimuli during acute inflammation in spinal cord.
Peroxisome proliferator-activated receptor alpha (PPARA)	• Anti-inflammatory receptor. • Decreases inflammatory responses in articular cartilage (Clockaerts et al., 2011).
Inducible nitric oxide synthase (NOS2)	• Inducible form of NOS. • Catalyses formation of nitric oxide from L-arganine.
Endothelial nitric oxide synthase (NOS3)	• Endothelial form of NOS. • Catalyses formation of nitric oxide from L-arganine.

GENE NAME (SYMBOL)	FUNCTION
LIPID METABOLISM	
Formyl peptide receptor 2 (FPR2/ALX)	• G protein coupled receptor. • Mediates the anti-nociceptive effects of annexin I (Chen et al., 2013).
Chemerin (RARRERS2)	• Adipokine that stimulates chemotaxis of cells involved in the innate immune system. • Chemoattractant for monocytes and macrophages (Herova et al., 2015)
Chemerin receptor 23 (CMKLR1)	• Resolvin E series receptor (G protein coupled). • Receptor is triggered by Chemerin and resolvin E1. Resolvin E1 is anti-inflammatory (Herova et al., 2015). • Reduces NF-κB signalling stimulated by TNF (Serhan et al., 2008).
Leukotrine B4 receptor 1 (LTB4R/BLT1)	• Resolvin E series receptor (G protein coupled) • High affinity receptor for leukotriene B4, expressed in several immune cells such as leukocytes, monocytes/macrophages, mast cells (Shao et al., 2006).
Cytochrome P450, family 2, subfamily J, polypeptide 2 (CYP2J2)	• Cytochrome p450 enzyme. • Metabolises Arachidonic acid to epoxyeicosatrienoic acids (EETS)
Epoxide Hydrolase 2 (EPHX2)	• Rapidly metabolises EETS to corresponding dihydroxyeicosatreinoic acids (DHETs)

GENE NAME (SYMBOL)	FUNCTION
ANGIOGENESIS	
Angiotensin converting enzyme (ACE)	• Coverts angiotensin I to angiotensin II, which is a stimulator of angiogenesis.
Vascular endothelial growth factor-A (VEGFA)	• Potent stimulator of angiogenesis, also plays a role in the nervous system. • May be involved in neuropathic pain (Lin et al., 2010).
Vascular endothelial growth factor-A receptor (KDR)	• Receptor for VEGF-A. • May be involved in neuropathic pain (Lin et al., 2010).

GENE NAME (SYMBOL)	FUNCTION
OTHER	
Cannabinoid receptor 2 (CNR2)	• Inhibitory receptor. • Cannabinoid system produces analgesic effects. • Activation of CB2 receptors may inhibit central sensitisation in a model of OA pain (Burston et al., 2013).
Acid ion sensing channel 3 (ASIC3)	• Sodium selective ion channels activated by low pH (acidosis) (Deval et al., 2008). • Senses acidic and inflammatory pain.
Thyroglobulin (TG)	• Made in the thyroid gland, used to make thyroxine and triiodothyronine.
Kallikrein (KLK1)	• Enzyme, cleaves kinonogen to release bradykinins (Dai et al., 2012).
Cathepsin (CTSK)	• Marker of bone turnover. • Subchondral bone turnover associated with pain in OA (Sagar et al., 2013).

4.3.2 Gene expression analysis

Differential gene expression analysis is described in chapter 2 section 2.12.8. In brief, fold changes in gene expression levels were calculated for each sample using the comparative C_t method also known as $2^{-\Delta Ct}$, where ΔC_t refers to C_t value of each individual target gene value minus C_t value of the reference gene. The mean and 95% confidence intervals (95% C.I) were calculated for both groups and statistical differences between the ΔC_t of each group compared using Mann-Whitney U test. Fold change in gene expression were calculated by dividing the mean of the symptomatic chondropathy group by the mean of the asymptomatic chondropathy group. In the instance that the fold change was decreased in the symptomatic chondropathy group the fold change was calculated as 1 divided by the fold change.

RESULTS

4.4 Patient demographics

Patient demographics for the study groups are reported in table 4.3. Results for the full dataset of cases included in the study (n = 12/group) are reported. Two samples were excluded from the analysis. One asymptomatic chondropathy case was excluded due to inability to transcribe RNA to cDNA (low RNA concentration) and one symptomatic chondropathy case due an outlier reference gene C_t value. Clinical and pathological characteristics are therefore also reported in table 4.3 for the dataset after removing both cases (n = 11/group). Symptomatic chondropathy cases were significantly younger than asymptomatic chondropathy cases, and macroscopic chondropathy scores were similar between groups. Loss of cartilage surface integrity and synovial inflammation were greater in the symptomatic chondropathy group compared with the asymptomatic chondropathy group, although significance was lost following removal of one case from each group. Synovial NGF immunoreactivity was increased in symptomatic chondropathy cases compared with asymptomatic cases. Out of the symptomatic chondropathy patients, 5 patients were taking opiates (co-codamol, Tramadol and MST) and 1 was taking NSAIDs (diclofenac).

Table 4.3: Clinical and pathological characteristics of the study groups*

	Full dataset (n = 12/group)			Dataset after removing 2 cases (n = 11/group)¶		
	Asymptomatic chondropathy	**Symptomatic chondropathy**	**P value**	**Asymptomatic chondropathy**	**Symptomatic chondropathy**	**P value**
Age, years	79 (67-88)	65 (54-73)	**0.005**	79 (65-88)	**61 (54-73)**	**0.005**
% male	33	50	0.514	36	46	0.748
BMI, kg/m^2	NA	36 (30-40)	NA	NA	36 (30-40)	NA
Post-mortem delay (hrs)‡	57 (30-85)	NA	NA	58 (29-89)	NA	NA
Macroscopic chondropathy	213 (204-228)	227 (214-238)	0.178	214 (204-229)	223 (213-239)	0.300
Cartilage surface integrity	4 (3-4)	4(4-6)	0.020	4 (3-4)	4 (4-5)	0.065
Chondrocyte morphology	3 (2-3)	3 (2-3)	1.000	3 (2-3)	2 (2-3)	1.00
% with breached tidemark	75	60	0.582	73	56	0.552
Proteoglycan loss	1 (1-2)	1 (1-2)	0.242	1 (1-2)	2 (1-2)	0.217
Synovitis	0 (0-0.25)	1 (0-3)	**0.024**	0 (0-0.5)	1 (0-3)	0.053
Bone marrow replacement	18	36	0.478	20	30	0.481

	Full dataset (n = 12/group)			Dataset after removing 2 cases (n = 11/group)¶		
	Asymptomatic chondropathy	Symptomatic chondropathy	P value	Asymptomatic chondropathy	Symptomatic chondropathy	P value
CD68 fractional area (%)†	8.8 (57-18.7)	13.5 (7.6-16.0)	0.387	10.5 (6.1-19.0)	14.3 (7.5-16.2)	0.604
NGF fractional area (%)†	7.2 (4.5-10.2)	13.6 (9.57-22.5)	**0.016**	7.2 (4.3-10.5)	14.1 (9.1-22.8)	**0.029**

*Tissues were obtained at the time of total knee replacement for OA (symptomatic chondropathy) or were obtained PM from cadaver donors (asymptomatic chondropathy). Data reported as median (IQR) unless otherwise stated.

Data for body mass index (BMI) were available for 9/12 (full dataset) and 9/11 (dataset after removing 2 cases) symptomatic chondropathy cases.

¶Results reported for all cases not excluded from analysis.

†Fractional areas are the percentage of synovial area occupied by CD68-immunoreactive macrophages or nerve growth factor immunoreactive cells. Fractional areas are only reported for samples that displayed synovial lining (n = 9 – 11/group).

‡Post-mortem delay was calculated as the time (hrs) between death and tissue collection for asymptomatic chondropathy cases.

4.5 RNA purity and concentration

RNA concentrations and purity for all samples are listed in the appendix (chapter 8, section 8.3). As previously described, RNA concentration for one asymptomatic chondropathy sample was too low for reverse transcription (16 ng/µl) therefore this sample was excluded from subsequent analyses. The median value of the 260:280 ratio was 2.02 (IQR:1.99-2.04).

4.5.1 Taqman: Beta actin expression

First gene expression of beta actin was assessed using the standard curve method. The standard curve was constructed from 5 concentrations of cDNA template (figure 4.5A). The slope of the standard curve was -3.3 indicating acceptable PCR amplification efficiency. The Ct values of each standard are inversely correlated with the log quantity of each standard, with a correlation coefficient of -0.99.

Beta actin was expressed in all experimental samples (median concentration was 0.45ng/µl, IQR 0.24-0.69, figure 4.2 B), and the positive control (sample 24), but expression was absent from the negative control (sample 25).

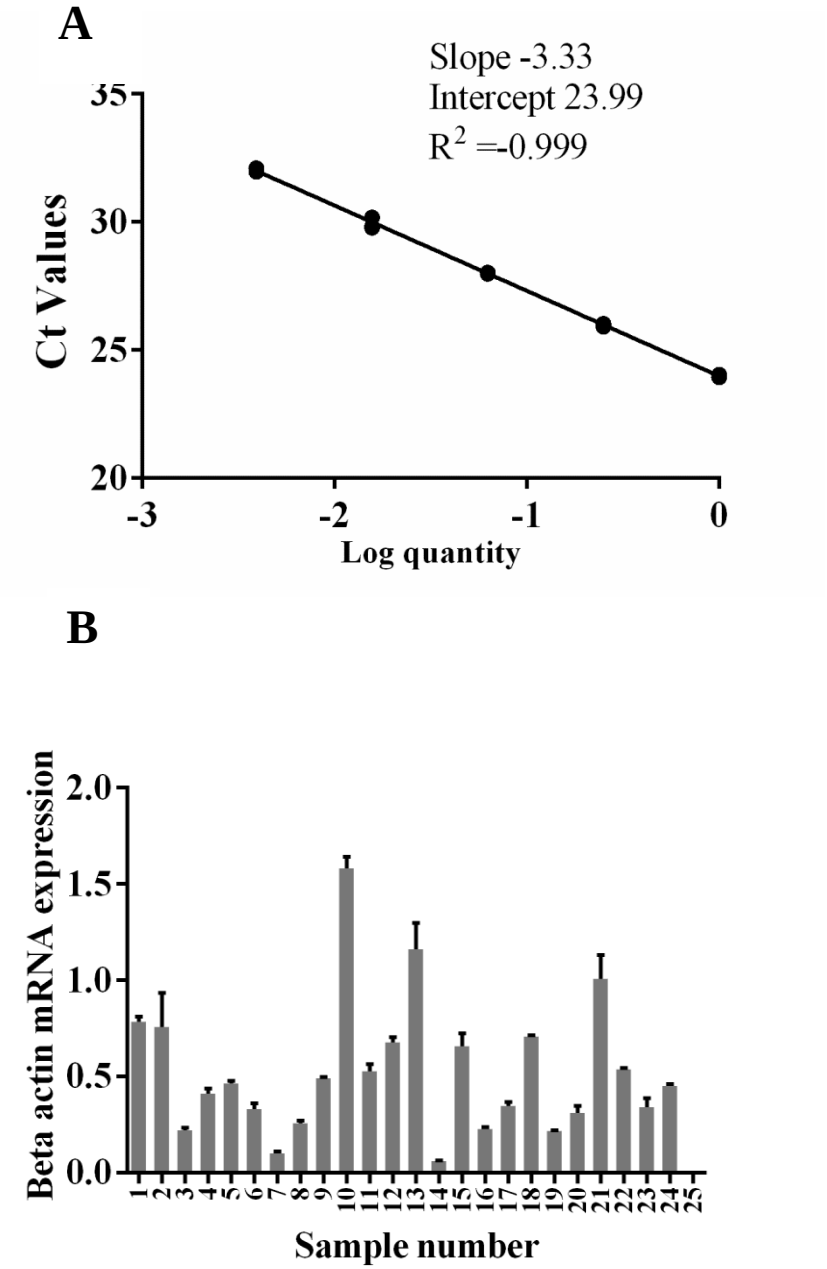


Figure 4.2: Taqman quantitative real time polymerase chain reactions for beta actin expression.

Standard curve for beta actin expression **(A).** Expression of beta actin in the synovium of 23 cases in a positive and negative control (samples 24 & 25, respectively) **(B).**

4.6 Microfluidic cards

4.6.1 Reference gene stability

The variability of reference gene expression between asymptomatic and symptomatic chondropathy cases was compared by examining differences in C_t values (table 4.4). A Mann Whitney U-test was used to compare differences between groups. Gene expression of the 4 reference genes was not significantly different between asymptomatic and symptomatic chondropathy groups.

Table 4.4: Comparison of reference gene Ct values in asymptomatic and symptomatic chondropathy cases.

Reference gene	Asymptomatic chondropathy (n=11)± C_t values	Symptomatic chondropathy (n=12) C_t values	P value
ACTB	23 (23-23)	22 (22-23)	0.242
GAPDH	26 (25-26)	25 (25-27)	0.932
HMBS	33 (33-34)	33 (32-33)	0.514
UBC	26 (25-26)	25 (25-27)	0.799

Data expressed as median (IQR) unless otherwise stated. Mann Whitney test used to compare C_t values between groups. ± One asymptomatic chondropathy case was excluded from analysis due to low RNA concentration.

Reference gene stability was determined using NormFinder (Microsoft Excel Add-in). The stability of the geometric means of a combination of different references genes were also assessed using NormFinder. The geometric mean of all 4 reference genes ('ALL', figure 4.3 A) was found to be the most stable factor for normalisation (stability value = 0.001).

The C_t values calculated from the geometric mean of all 4 reference genes ('ALL') were assessed for the presence of outlier values using the Grubb's test (GraphPad software). Gene expression of the target genes was calculated by normalising each sample to its reference gene C_t value; therefore inclusion of outliers may distort the analysis. One symptomatic chondropathy sample (no.14) had a C_t value of 29.7, and a Z score of 3.05, therefore was detected as an outlier and removed from subsequent analysis (figure 4.3 B).

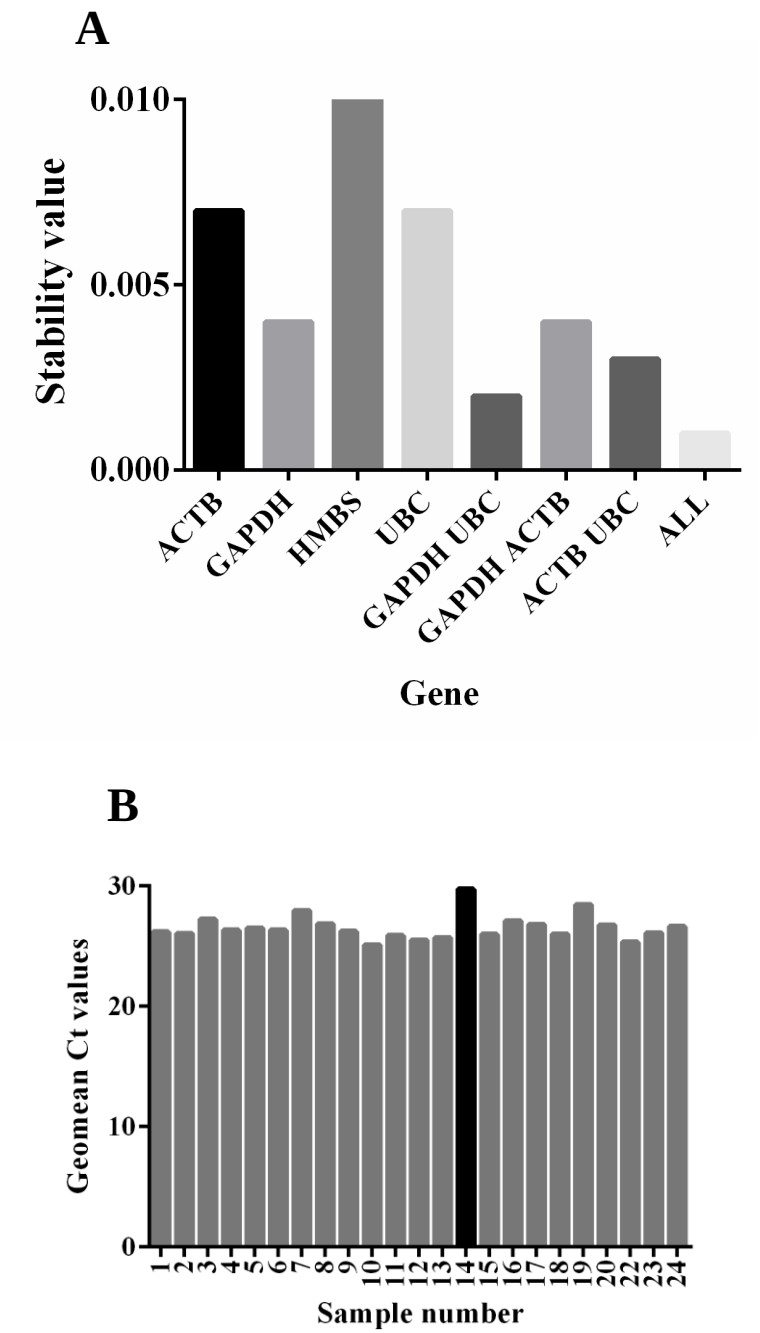


Figure 4.3: Reference gene stability.

NormFinder analysis of reference gene stability. NormFinder calculated stability values based on Ct values for each sample **(A).** Genes with lower values indicate greatest stability. The geometric mean of all 4 reference genes "ALL" was the most stable. The geometric mean of all 4 references genes for each sample is illustrated in **(B).** The Grubb's outlier test was used to detect outlying values. One sample, number 14 (black bar) was detected as an outlier due to a high C_t value, therefore was excluded from subsequent analysis.

4.6.2 Gene expression patterns in the synovium associated with symptomatic OA

Out of 92 target genes examined, 44 were up-regulated and 41 were down-regulated in the synovium of symptomatic chondropathy cases. Of the 44 up-regulated genes, 17 (39%) were significantly differentially expressed between groups (table 4.4). Of the 41 down-regulated genes 17 (41%) were significantly different between groups. A summary table of the 34 genes that were significantly differentially expressed between groups is illustrated in table 4.5. A more detailed analysis of differences in gene expression analysis for all 92 target genes is listed in table 4.6. Five genes (BDNF, CYP2J2, KLK1, PLAT, TRPA) were not expressed in any asymptomatic or symptomatic chondropathy cases. Whereas IL17A and IL4 were expressed in only one symptomatic chondropathy case (this one case was different for both genes).

Table 4.5: Summary table of differentially expressed genes*

Components	Up-regulated¶	Down-regulated†
Inflammation		
Cytokines	**TNF (3.86)****	**CX3CL1 (2.76)****, CXCL2 (2.71)
Chemokines	CCL2 (1.65), CCL4 (1.90) CCL5 (1.40), CCL8 (3.87), CXCL6 (3.38)	-
Other	**CTGF (2.22)****	**SERPINE1 (4.25)****, **VEGFA (8.15)****
Receptors	NTRK1 (2.24)	**IL1R1 (2.07)****, KDR (2.32)
Enzymes	ACE (2.05), **CASP1 (2.90)****, **PTGS1 (3.68)****, EPHX2 (1.68), **MMP1 (13.93)****	PTGS2 (2.60) ,MMP-2 (2.07), MMP-7 (4.91), NOS3 (2.20), **PRKD2 (1.90)****
Anti-inflammatory	ANXA1 (1.41), IL-10 (2.31)	-
Lipid metabolism	CMKLR1 (1.99)	LTB4R (2.29)
MAPK pathway	-	**MAPKAPK2 (1.52)****
JAK/STAT pathway		**SOCS1 (2.69)****
NF-kB pathway	**TNFSF11 (2.67)****	**REL-A (1.85)****, NFKB1 (27.54), **NFKBIA (2.37)****

*Values in brackets indicate fold change; all genes listed above were significantly different between groups. Significance was accepted when P <0.05. Genes where P< 0.005 are highlighted in bold and double asterisks. ¶Genes which are upregulated, or

†down-regulated in the symptomatic chondropathy group compared to asymptomatic chondropathy cases. Abbreviations: ACE; angiotensin I converting enzyme, ANXA1; annexin A1, CASP1; interleukin converting enzyme, CCL2; chemokine ligand 2/monocyte chemoattractant protein-1, CCL4; chemokine ligand 4/macrophage inflammatory protein-1β, CCL5; chemokine ligand 5, CCL8; chemokine ligand 8/monocyte chemoattractant protein-2,, CMKLR1; chemokine-like receptor 1, CTGF, connective tissue growth factor, EPHX2; epoxide hydrolase 2, IL-10; interleukin-10, IL1R1; interleukin-1 receptor, KDR; vascular endothelial growth factor receptor-2, LTB4R; leukotriene B4 receptor, MAPKAPK2; mitogen-activated protein kinase-activated protein kinase 2, MMP; matrix metalloprotease-1/2/7, NFKB1; nuclear factor kappa B, NFKBIA; nuclear factor kappa B inhibitor, NOS3; Nitric oxidase synthase-3 (endothelial), NTRK1; tyrosine kinase, receptor, type 1, PRKD2; protein kinase D2, PTGS1/2; cyclooxygenase 1/2, REL-A; v-rel avian reticuloendotheliosis viral oncogene homolog A, SERPINE-1; plasminogen activator inhibitor, SOCS1; suppressor of cytokine signalling-1, TNF; Tumour necrosis factor, TNFSF11, VEGFA; vascular endothelial growth factor-A.

Table 4.6: Synovial gene expression analysis (mean, 95% C.I) for asymptomatic and symptomatic chondropathy cases.

	Asymptomatic chondropathy (n=11)			Symptomatic chondropathy (n=11)			Fold difference	Direction¶	P value
	Mean	95% CI		Mean	95% CI				
		Lower	Upper		Lower	Upper			
Matrix metalloproteases									
MMP1	0.005	0.0006	0.009	0.070	0.024	0.117	**13.928**	**UP**	**<0.001**
MMP12	0.0001	9.58E-06	0.0003	0.0006	4.72E-05	0.001	3.965	UP	0.270
MMP2	2.787	1.657	3.917	1.346	0.935	1.757	**2.071**	**DOWN**	**0.016**
MMP3	0.111	0.031	0.190	0.460	0.051	0.868	4.155	UP	0.116
MMP7	0.001	7.49E-05	0.002	0.0002	4.25E-05	0.0003	**4.908**	**DOWN**	**0.034**
MMP9	0.032	-0.002	0.067	0.021	0.009	0.032	1.563	DOWN	0.699
Inflammatory mediators									
TNF	0.004	0.001	0.008	0.017	0.013	0.021	**3.856**	**UP**	**<0.001**
ADAM17	0.062	0.049	0.074	0.059	0.044	0.075	1.036	DOWN	0.847
IL1B	0.0019	7.54E-05	0.004	0.0024	0.001	0.004	1.290	UP	0.519
IL1R1	0.335	0.231	0.440	0.162	0.131	0.192	**2.070**	**DOWN**	**0.001**

CASP1	0.011	0.007	0.014	0.031	0.023	0.038	**2.898**	**UP**	**0.000**
IL4R	0.110	0.082	0.138	0.086	0.073	0.099	1.277	DOWN	0.193
IL6	0.0056	0.001	0.010	0.0057	-0.001	0.013	1.005	UP	0.401
IL8	0.043	0.014	0.072	0.015	0.004	0.026	2.858	DOWN	0.056
IL10	0.012	0.003	0.022	0.028	0.0123	0.0446	**2.314**	**UP**	**0.023**
IL15	0.0004	6.22E-05	0.001	0.0008	-0.0002	0.002	2.197	UP	1.000
S100A8	0.253	0.094	0.412	0.363	0.081	0.644	1.432	UP	0.243
S100A9	0.365	0.134	0.595	0.172	0.091	0.268	2.119	DOWN	0.606
IFNG	0.0001	-9.12E-07	0.0003	0.0004	0.0001	0.0008	2.577	UP	0.332
CTGF	1.446	0.862	2.029	3.209	2.275	4.144	**2.220**	**UP**	**0.003**
TREM1	0.138	0.073	0.203	0.170	0.079	0.261	1.228	UP	0.652
ANXA1	1.182	0.804	1.560	1.668	1.239	2.097	**1.411**	**UP**	**0.040**
ANAX6	0.211	0.148	0.274	0.187	0.155	0.218	1.132	DOWN	0.847
Chemokines									
CCL2	0.071	0.027	0.115	0.117	0.076	0.157	**1.650**	**UP**	**0.013**
CCL3	0.007	0.003	0.012	0.015	0.008	0.023	2.015	UP	0.056

CCL4	0.011	0.001	0.020	0.020	0.012	0.029	**1.909**	**UP**	**0.023**
CCL5	0.110	0.009	0.211	0.154	0.082	0.225	**1.400**	**UP**	**0.034**
CCL8	0.004	0.002	0.005	0.014	0.005	0.022	**3.874**	**UP**	**0.016**
CXCL1	0.023	0.001	0.004	0.046	0.002	0.025	1.985	UP	0.171
CXCL2	0.019	0.008	0.030	0.007	0.003	0.011	2.714	DOWN	0.013
CXCL5	0.0008	2.3E-05	0.002	0.0002	3.23E-05	0.0004	3.355	DOWN	0.056
CXCL6	0.0004	4.1E-05	0.001	0.002	0.001	0.003	**3.377**	**UP**	**0.028**
CXCL10	0.002	0.011	0.036	0.013	0.020	0.072	5.814	UP	0.133
CX3CL1	0.080	0.046	0.113	0.029	0.021	0.038	**2.725**	**DOWN**	**<0.001**
NGF signalling									
NGF	0.007	0.004	0.010	0.012	-0.0004	0.025	1.773	UP	0.898
NTRK1	0.006	-0.003	0.016	0.014	9.12E-05	0.027	**2.236**	**UP**	**0.016**
NGFR	0.022	0.012	0.033	0.027	0.019	0.035	1.201	UP	0.3
PIK3CA	0.033	0.021	0.044	0.024	0.016	0.033	1.335	DOWN	0.27
PIK3CB	0.026	0.020	0.032	0.030	0.018	0.042	1.137	UP	0.847
PIK3CD	0.011	0.008	0.014	0.009	0.007	0.011	1.232	DOWN	0.217

PRKCE	0.028	0.019	0.037	0.022	0.016	0.028	1.284	DOWN	0.101
TRPV1	0.022	0.015	0.028	0.015	0.010	0.020	1.433	DOWN	0.133
Neurotrophins									
SERPINE1	0.259	0.087	0.432	0.061	0.043	0.079	**4.265**	**DOWN**	**<0.001**
Janus activated kinase- signal transducer and activator of transcription (JAK/STAT) signalling									
TYK2	0.072	0.053	0.090	0.070	0.043	0.095	1.037	DOWN	0.898
STAT1	0.163	0.124	0.202	0.203	0.147	0.258	1.244	UP	0.151
STAT3	0.471	0.338	0.605	0.423	0.343	0.503	1.115	DOWN	0.652
SOCS1	0.010	0.006	0.013	0.004	0.002	0.005	**2.697**	**DOWN**	**0.002**
SOCS3	0.093	0.054	0.133	0.042	0.024	0.060	2.234	DOWN	0.056
PIAS3	0.051	0.038	0.064	0.036	0.028	0.045	1.409	DOWN	0.088

Nuclear Factor-Kappa B Signalling									
NFKB1	2.027	-2.267	6.321	0.074	0.062	0.085	**27.541**	**DOWN**	**0.040**
NFKBIA	1.227	0.859	1.595	0.517	0.345	0.689	**2.372**	**DOWN**	**0.003**
RELA	0.501	0.386	0.616	0.271	0.201	0.342	**1.846**	**DOWN**	**0.002**
JUN	0.579	0.398	0.759	0.711	-0.071	1.493	1.229	UP	0.171
FOS	0.860	0.364	1.356	1.749	0.978	2.521	2.033	UP	0.056
BCL3	0.253	0.103	0.404	0.133	0.098	0.168	1.910	DOWN	0.116
TNFRSF11B	0.113	0.029	0.197	0.089	0.061	0.116	1.275	DOWN	0.562
TNFSF11	0.001	-0.0008	0.003	0.003	0.002	0.004	**2.668**	**UP**	**0.001**
Mitogen activated protein kinase signalling									
MAP2K3	0.076	0.066	0.086	0.075	0.069	0.080	1.014	DOWN	0.478
MAP2K6	0.007	0.004	0.011	0.010	0.008	0.013	1.384	UP	0.056
MAPK14	0.099	0.071	0.128	0.082	0.065	0.099	1.204	DOWN	0.478
MAPKAPK2	0.093	0.077	0.109	0.061	0.050	0.072	**1.524**	**DOWN**	**0.004**

Protease-Activated Receptor Signalling									
F2RL1‡	9.1E-05	7.0E-05	0.0001	0.0007	0.0002	0.001	8.045	UP	0.101
TRPV4	0.008	0.004	0.012	0.012	0.008	0.015	1.450	UP	0.088
F2RL3	0.050	-0.019	0.120	0.007	-0.003	0.017	7.451	DOWN	0.101
PRKD1	0.015	0.008	0.022	0.009	0.006	0.011	1.748	DOWN	0.193
PRKD2	0.060	0.046	0.073	0.031	0.023	0.040	**1.903**	**DOWN**	**0.003**
PRKD3	0.070	0.050	0.090	0.081	0.061	0.100	1.158	**UP**	0.478
Prostaglandin & Nitric Oxide Synthesis									
PTGS1	0.023	0.013	0.034	0.085	0.061	0.110	**3.677**	**UP**	**<0.001**
PTGS2	0.010	0.005	0.015	0.004	0.002	0.005	**2.607**	**DOWN**	**0.010**
PPARA	0.046	0.028	0.064	0.068	0.018	0.117	1.478	UP	0.322
NOS2	0.004	-0.001	0.009	0.002	0.001	0.003	1.732	DOWN	0.478
NOS3	0.027	0.013	0.041	0.012	0.006	0.018	**2.198**	**DOWN**	**0.019**
Lipid Metabolism									
FPR2	0.0005	0.0001	0.001	0.0003	8.69E-05	0.001	1.661	DOWN	0.438

RARRES2	0.079	0.029	0.131	0.076	0.041	0.110	1.058	DOWN	0.949
CMKLR1	0.075	0.037	0.114	0.150	0.122	0.178	**1.989**	**UP**	**0.008**
LTB4R	0.012	0.008	0.016	0.005	0.003	0.008	**2.294**	**DOWN**	**0.007**
EPHX2	0.015	0.008	0.022	0.026	0.018	0.033	**1.682**	**UP**	**0.034**
Angiogenesis									
ACE	0.017	0.011	0.022	0.034	0.023	0.045	**2.050**	**UP**	**0.010**
VEGFA	0.072	0.025	0.119	0.009	0.006	0.012	**8.152**	**DOWN**	**<0.001**
KDR	0.124	0.070	0.179	0.054	0.032	0.075	**2.326**	**DOWN**	**0.010**
Other									
CNR2	0.0002	2.2E-06	0.001	0.001	0.0003	0.001	2.848	UP	0.088
ASIC3	0.004	0.003	0.006	0.005	0.003	0.006	1.045	UP	0.949
TG	0.002	0.0005	0.003	0.002	0.001	0.003	1.083	UP	0.606
CTSK	0.143	0.099	0.187	0.170	0.130	0.210	1.189	UP	0.562
PLCB1	0.023	0.017	0.029	0.037	0.020	0.055	1.625	UP	0.193

Fold change calculated by mean of symptomatic chondropathy group divided by mean of asymptomatic chondropathy group. Significance was accepted when $P < 0.05$.

‡F2RL1 (gene that codes for protease activated receptor-2) was not expressed in any asymptomatic chondropathy samples, but was expressed in low levels in 5/11 symptomatic chondropathy cases. A simplistic chi squared analysis comparing the groups for the presence/absence of the gene, showed a significant difference in the presence of gene expression between the groups (chi squared = 6.47, $P = 0.04$).

4.6.3 Nerve growth factor signalling pathway in symptomatic OA.

NGF gene expression in the synovium of symptomatic chondropathy cases compared with asymptomatic chondropathy cases was not significantly different (mean [95% C.I] expression 0.012 [-0.0004 – 0.025] vs 0.007 [0.004-0.009]) $P = 0.90$ (figure 4.4B).

TrkA (NTRK1), the high affinity receptor for NGF, expression was significantly upregulated by 2.67 fold in the synovium of symptomatic chondropathy cases compared to asymptomatic cases (0.014 [0.00009-0.027] vs 0.006 [-0.003-0.016], $P<0.001$) (figure 4.4A). Additionally, expression of the low affinity receptor, p75, was increased by 1.2 fold in the symptomatic group (0.027 [0.019-0.034] vs 0.022 [0.012-0.032]), but this did not reach statistical significance $P=0.30$, (figure 4.4C).

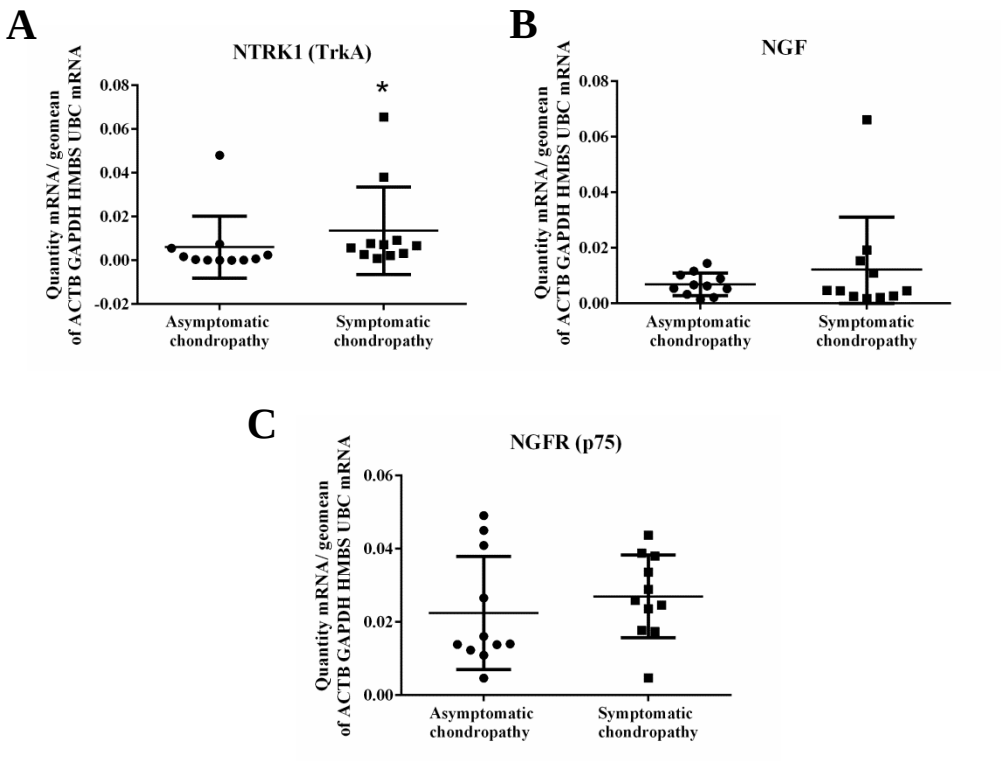


Figure 4.4: Molecular associations with symptomatic OA.

Scatterplots illustrate the molecular differences in the synovium of subjects with similar macroscopic chondropathy scores who did not (asymptomatic chondropathy) or did (symptomatic chondropathy) undergo total knee replacement for symptomatic OA. The high affinity receptor for NGF, TrkA, was significantly upregulated in the synovium of symptomatic chondropathy cases **(A),** whereas NGF **(B)** and the low affinity receptor for NGF, p75 **(C)** were upregulated in the synovium of symptomatic chondropathy cases but did not reach statistical significance. Data displayed as mean (95% C.I). *P<0.05 versus the asymptomatic chondropathy group. Abbreviations: NGF; nerve growth factor, NTRK1(TrkA); tyrosine kinase receptor, type 1, NGFR (p75); nerve growth factor receptor.

NGF immunoreactivity as measured by immunohistochemistry was greater in symptomatic chondropathy cases compared to asymptomatic chondropathy cases, as previously reported in chapter 3, section 3.5. Correlation analyses determined associations between NGF gene expression and NGF immunoreactivity (figure 4.5). There was no significant association between the two parameters. NGF immunoreactivity data were reported previously in chapter 3, section 3.5.

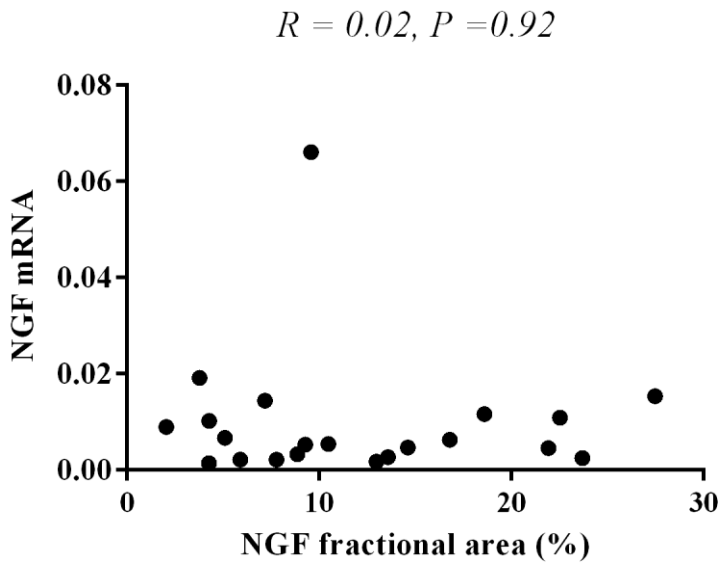


Figure 4.5: Scatterplot illustrating the relationship between NGF immunoreactivity and NGF gene expression.

There was no significant relationship between NGF immunoreactivity and NGF gene expression Data reported as Spearman's correlations coefficients.

4.6.4 Associations of gene expression patterns with post-mortem delay

Correlation analyses determined associations between PM delay (the time between death and tissue processing) and synovial gene expression in the asymptomatic chondropathy cases. Two out of 92 target genes were negatively associated with PM delay, CCL4 and IL-8 (table 4.7). The average R value of all 92 genes was 0.026, which was not significantly different to 0 using a one sampled t test (P = 0.366).

Table 4.7: Correlations between gene expression and PM delay.

Gene	*R* (P value)	Gene	*R* (P value)	Gene	*R (P value)*	Gene	*R (P value)*
ACE	0.391 (0.235)	CNR2	0.191 (0.574)	FPR2	-0.009 (0.979)	MAP2K6	0.4 (0.223)
ADAM17	-0.009 (0.979)	CTGF	0.200 (0.555)	IFNG	0.364 (0.272)	MAPK14	0.282 (0.401)
ANXA1	0.436 (0.180)	CTSK	0.136 (0.689)	IL10	-0.045 (0.894)	MAPKAPK2	0.218 (0.519)
ANXA6	0.145 (0.670)	CX3CL1	0.345 (0.298)	IL15	0.300 (0.370)	MMP1	-0.145 (0.670)
ASIC3	-0.100 (0.770)	CXCL1	-0.600 (0.051)	IL1B	-0.018 (0.958)	MMP12	0.355 (0.285)
BCL3	-0.109 (0.750)	CXCL10	-0.300 (0.370)	IL1R1	-0.018 (0.958)	MMP2	-0.264 (0.433)
CASP1	0.327 (0.326)	CXCL2	-0.191 (0.574)	IL4R	0.309 (0.355)	MMP3	-0.255 (0.450)
CCL2	0.091 (0.790)	CXCL5	-0.345 (0.298)	IL6	0.155 (0.650)	MMP7	-0.309 (0.355)
CCL3	-0.473 (0.142)	CXCL6	0.382 (0.247)	**IL8**	**-.618 (0.043)**	MMP9	0.082 (0.811)
CCL4	**-.764 (0.006)**	EPHX2	0.336 (0.312)	JUN	0.209 (0.537)	NFKB1	0.191 (0.574)
CCL5	-0.318 (0.340)	F2RL1	0.191 (0.574)	KDR	0.182 (0.593)	NFKBIA	0.027 (0.937)
CCL8	-0.264 (0.433)	F2RL3	0.073 (0.832)	LTB4R	-0.464 (0.151)	NGF	-0.136 (0.689)
CMKLR1	-0.182 (0.593)	FOS	-0.427 (0.190)	MAP2K3	0.582 (0.060)	NGFR	0.191 (0.574)

Gene	*R* (P value)	Gene	*R* (P value)	Gene	*R (P value)*
NOS2	-0.309 (0.355)	PTGS2	-0.327 (0.326)	TREM1	-0.109 (0.750)
NOS3	-0.045 (0.894)	RARRES2	0.282 (0.401)	TRPV1	0.091 (0.790)
NTRK1	-0.336 (0.312)	RELA	-0.036 (0.915)	TRPV4	-0.418 (0.201)
PIAS3	0.391 (0.235)	S100A8	-0.064 (0.853)	TYK2	0.182 (0.593)
PIK3CA	0.155 (0.650)	S100A9	-0.045 (0.894)	VEGFA	-0.127 (0.709)
PIK3CB	-0.509 (0.110)	SERPINE1	0.118 (0.729)		
PIK3CD	-0.073 (0.832)	SOCS1	-0.109 (0.750)		
PLCB1	0.191 (0.574)	SOCS3	-0.245 (0.467)		
PPARA	0.127 (0.709)	STAT1	-0.373 (0.259)		
PRKCE	0.318 (0.340)	STAT3	0.255 (0.450)		
PRKD1	0.464 (0.151)	TG	0.145 (0.670)		
PRKD2	-0.191 (0.574)	TNF	0.191 (0.574)		
PRKD3	-0.055 (0.873)	TNFRSF11B	0.145 (0.670)		
PTGS1	0.218 (0.519)	TNFSF11	0.073 (0.832)		

Significant genes are highlighted in bold.

4.6.5 Associations with age

Asymptomatic chondropathy cases were significantly older than symptomatic chondropathy cases; therefore associations of target gene expression with age were explored. Expression of 5 out of the 92 target genes decreased as the age of patients increased; CASP1, IL-1R1, PPAR, TNF and TNFSF11 (figure 4.6 A-E, respectively), whereas the expression of LTB4R increased with age (figure 4.6F). The full list of associations between gene expression and age are reported in table 4.8.

Expression of CASP1, TNF and TNFSF11 were significantly decreased in the older asymptomatic chondropathy cases compared with the younger symptomatic chondropathy cases. Therefore associations with age may decrease possible associations with symptom status.

4.6.6 Associations with synovitis

Correlation analyses were used to determine associations between gene expression and synovitis. Out of the 92 target genes 4 were positively associated with synovitis; CNR2, NTRK1 (TrkA), PTGS1 (COX-1) and TNFSF11 (RANKL) (table 4.9) Whereas, IL1R1 expression was negatively associated with synovitis (table 4.9).

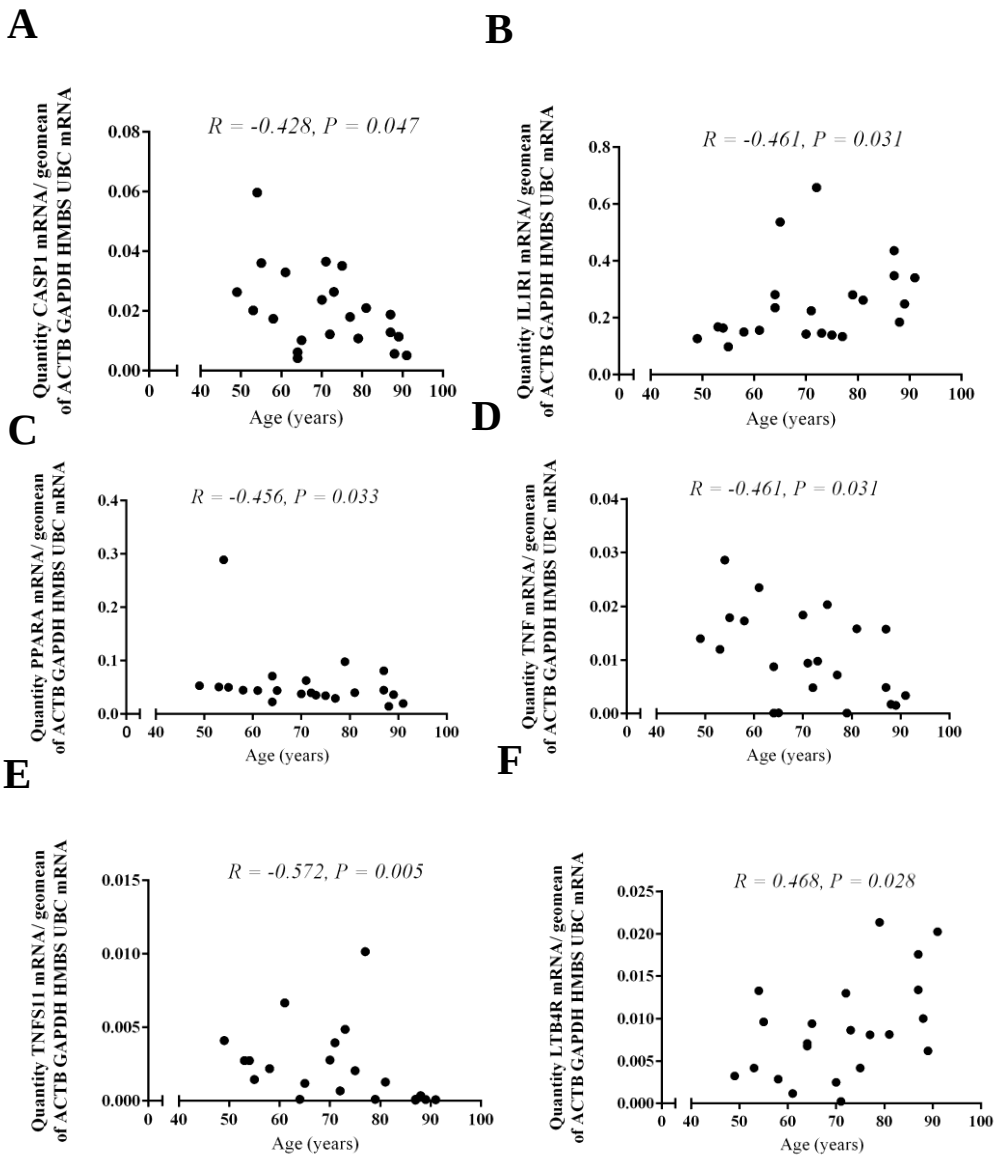


Figure 4.6: Scatterplots illustrating the relationship between gene expression and age.

Gene expression of CASP1 **(A)**, IL1R1 **(B)**, PPARA **(C)**, TNF **(D)** and TNFSF11 **(E)** were inversely correlated with age, whereas LTB4R **(F)** was positively correlated with age. Statistical significance was accepted when $P \leq 0.05$.

Table 4.8: Associations between gene expression and age.

Gene	*R* (P value)	Gene	*R* (P value)	Gene	*R (P value)*	Gene	*R (P value)*
ACE	-0.32 (0.147)	CNR2	-0.177 (0.430)	FPR2	0.112 (0.618)	MAP2K6	-0.068 (0.762)
ADAM17	-0.024 (0.915)	CTGF	-0.369 (0.091)	IFNG	-0.331 (0.132)	MAPK14	0.078 (0.730)
ANXA1	-0.218 (0.331)	CTSK	-0.273 (0.219)	IL10	-0.084 (0.710)	MAPKAPK2	0.353 (0.107)
ANXA6	0.057 (0.801)	CX3CL1	0.305 (0.167)	IL15	0.099 (0.660)	MMP1	-0.177 (0.430)
ASIC3	0.189 (0.399)	CXCL1	-0.035 (0.167)	IL1B	-0.042 (0.853)	MMP12	-0.103 (0.647)
BCL3	0.205 (0.360)	CXCL10	-0.073 (0.745)	**IL1R1**	**.461 (0.031)**	MMP2	0.239 (0.284)
CASP1	**-.428 (0.047)**	CXCL2	0.173 (0.442)	IL4R	0.092 (0.685)	MMP3	-0.096 (0.671)
CCL2	-0.208 (0.352)	CXCL5	0.260 (0.243)	IL6	0.351 (0.109)	MMP7	0.142 (0.529)
CCL3	-0.258 (0.247)	CXCL6	-0.283 (0.202)	IL8	0.136 (0.547)	MMP9	-0.138 (0.541)
CCL4	-0.241 (0.279)	EPHX2	-0.233 (0.297)	JUN	-0.02 (0.930)	NFKB1	0.276 (0.213)
CCL5	-0.129 (0.568)	F2RL1	-0.124 (0.582)	KDR	0.283 (0.202)	NFKBIA	0.325 (0.139)
CCL8	-0.24 (0.283)	F2RL3	-0.066 (0.770)	**LTB4R**	**.468 (0.028)**	NGF	-0.093 (0.682)
CMKLR1	-0.347 (0.113)	FOS	-0.293 (0.186)	MAP2K3	0.156 (0.488)	NGFR	-0.078 (0.730)

Gene	*R* (P value)	Gene	*R* (P value)	Gene	*R (P value)*
NOS2	-0.19 (0.396)	PTGS2	0.056 (0.803)	TREM1	0.120 (0.594)
NOS3	0.260 (0.242)	RARRES2	0.028 (0.901)	TRPV1	-0.039 (0.863)
NTRK1	-0.381 (0.08)	RELA	0.416 (0.054)	TRPV4	-0.206 (0.357)
PIAS3	0.241 (0.279)	S100A8	-0.088 (0.698)	TYK2	0.132 (0.559)
PIK3CA	0.026 (0.909)	S100A9	0.204 (0.363)	VEGFA	0.123 (0.585)
PIK3CB	-0.089 (0.693)	SERPINE1	0.262 (0.239)		
PIK3CD	0.006 (0.980)	SOCS1	0.237 (0.288)		
PLCB1	-0.31 (0.160)	SOCS3	0.223 (0.318)		
PPARA	**-.456 (0.033)**	STAT1	-0.053 (0.814)		
PRKCE	0.014 (0.952)	STAT3	0.198 (0.378)		
PRKD1	0.033 (0.885)	TG	-0.063 (0.780)		
PRKD2	0.133 (0.556)	**TNF**	**-.461 (0.031)**		
PRKD3	-0.095 (0.674)	TNFRSF11B	-0.29 (0.190)		
PTGS1	-0.396 (0.068)	**TNFSF11**	**-.572 (0.005)**		

Significant associations are highlighted in bold.

Table 4.9: Associations between gene expression and synovitis.

Gene	*R* (P value)	Gene	*R* (P value)	Gene	*R (P value)*	Gene	*R (P value)*
ACE	0.238 (0.326)	**CNR2**	**.570 (0.011)**	FPR2	-0.038 (0.876)	MAP2K6	0.015 (0.950)
ADAM17	0.02 (0.935)	CTGF	0.141 (0.566)	IFNG	-0.138 (0.574)	MAPK14	-0.316 (0.187)
ANXA1	0.278 (0.249)	CTSK	0.281 (0.244)	IL10	0.006 (0.981)	MAPKAPK2	-0.235 (0.332)
ANXA6	-0.224 (0.357)	CX3CL1	-0.388 (0.101)	IL15	-0.312 (0.194)	MMP1	0.181 (0.459)
ASIC3	0.225 (0.355)	CXCL1	0.158 (0.101)	IL1B	-0.06 (0.807)	MMP12	0.375 (0.114)
BCL3	-0.166 (0.496)	CXCL10	-0.018 (0.941)	**IL1R1**	**-.630 (0.004)**	MMP2	-0.347 (0.146)
CASP1	0.444 (0.057)	CXCL2	-0.156 (0.524)	IL4R	-0.293 (0.223)	MMP3	-0.119 (0.629)
CCL2	0.33 (0.168)	CXCL5	0.139 (0.571)	IL6	-0.379 (0.110)	MMP7	-0.235 (0.332)
CCL3	0.092 (0.709)	CXCL6	0.152 (0.535)	IL8	-0.111 (0.651)	MMP9	0.17 (0.486)
CCL4	0.201 (0.410)	EPHX2	0.212 (0.383)	JUN	-0.226 (0.353)	NFKB1	-0.098 (0.688)
CCL5	0.089 (0.717)	F2RL1	0.303 (0.207)	KDR	-0.411 (0.080)	NFKBIA	-0.368 (0.121)
CCL8	0.006 (0.981)	F2RL3	-0.227 (0.351)	LTB4R	-0.309 (0.198)	NGF	0.033 (0.892)
CMKLR1	0.358 (0.133)	FOS	-0.196 (0.421)	MAP2K3	-0.288 (0.232)	NGFR	-0.116 (0.637)

Gene	*R* (P value)	Gene	*R* (P value)	Gene	*R (P value)*
NOS2	0.066 (0.788)	PTGS2	-0.333 (0.164)	TREM1	-0.149 (0.542)
NOS3	-0.044 (0.858)	RARRES2	-0.103 (0.674)	TRPV1	-0.025 (0.920)
NTRK1	**.636 (0.003)**	RELA	-0.373 (0.116)	TRPV4	0.023 (0.926)
PIAS3	-0.181 (0.459)	S100A8	0.102 (0.677)	TYK2	-0.034 (0.889)
PIK3CA	-0.308 (0.200)	S100A9	-0.216 (0.374)	VEGFA	-0.178 (0.466)
PIK3CB	-0.245 (0.313)	SERPINE1	-0.247 (0.309)		
PIK3CD	-0.019 (0.938)	SOCS1	-0.396 (0.094)		
PLCB1	-0.105 (0.668)	SOCS3	-0.282 (0.242)		
PPARA	0.205 (0.401)	STAT1	0.025 (0.920)		
PRKCE	0.054 (0.828)	STAT3	-0.247 (0.309)		
PRKD1	0.003 (0.991)	TG	0.257 (0.288)		
PRKD2	-0.088 (0.720)	TNF	0.392 (0.097)		
PRKD3	-0.191 (0.433)	TNFRSF11B	0.117 (0.634)		
PTGS1	**.533 (0.019)**	**TNFSF11**	**.504 (0.028)**		

Significant genes are highlighted in bold.

4.6.7 Correlations between genes

Expression of suppressor of cytokine signalling (SOCS)-1 was inversely correlated with the majority of pro-inflammatory mediators listed in table 4.10 Negative associations were significant for CCL2, CCL8, CXCL6, PTGS-1 (COX-1) and TNF-α expression. SOCS-3 expression was significantly correlated with MMP7 and PTGS-2 (COX-2) expression.

Expression of RANKL/TNFSF11 (receptor activator of NF- κB [RANK] ligand) was increased in the synovium of symptomatic chondropathy cases compared to asymptomatic cases. Correlation analyses were performed to determine whether RANKL expression was inversely correlated to OPG/TNFSF11B expression (endogenous inhibitor of RANK). In this study, there was no significant association between the two regulators of the RANK osteoclast system ($R = 0.352$, $P = 0.108$).

Table 4.10: Correlations between suppressors of cytokine signalling (SOCS)-1 and 3, with chemokines and cytokines.

	SOCS1	**SOCS3**
CCL2	-0.572**	0.011
CCL3	-0.344	0.083
CCL4	-0.359	-0.012
CCL5	0.002	-0.039
CCL8	-0.430*	-0.103
CTGF	-0.481	0.042
CX3CL1	0.846**	0.307
CXCL10	-0.058	0.023
CXCL2	0.514*	0.274
CXCL5	0.430*	0.277
CXCL6	-0.494*	-0.294
IFNG	0.276	-0.056
IL1B	-0.151	0.082
IL6	-0.097	0.366
IL8	0.24	0.351
MMP1	-0.423	-0.135
MMP2	0.697**	0.268
MMP3	-0.094	0.112
MMP7	0.393	0.476*
MMP9	0.075	0.345
MMP12	0.019	-0.387
PTGS1	-0.578**	-0.398
PTGS2	0.253	0.486*
TNF-α	-0.529*	0.381

Data reported as Spearman's correlations coefficients. Statistical significance was accepted when *$P \leq 0.05$ **$P \leq 0.01$.

4.6.8 Pathway analysis

Ingenuity Pathway Analysis (IPA) revealed three major networks were formed from the analysis (table 4.11). The top canonical pathways revealed by IPA included "role of macrophages, fibroblasts and endothelial cells in rheumatoid arthritis" (*P* = 2.33E-14) and "role of IL-17A in arthritis" (*P* = 2.87E-14). NGF signalling pathways did not appear in any of the pathways revealed.

Table 4.11: Top three networks revealed by Ingenuity Pathway Analysis.

Molecules in Network	**Top Diseases and Functions**
↑ACE, ↑ CCL2, ↑CCL4, ↑CCL5, ↑CCL8, ↑CTGF, ↓CX3CL1, ↑CXCL6, ↑MMP1, ↓MMP2, ↓MMP7, ↓NFKBIA, ↓PRKD2, ↓PTGS2 ↑TNF, ↓VEGFA	Cellular Movement, Hematological System Development and Function, **Immune Cell Trafficking**
↑ANXA1, ↑CASP1, ↑CCL2, ↑IL10, ↑IL1R1,↓KDR, ↓MAPKAPK2, ↓NOS3, ↑NTRK1, ↓RELA, ↓SOCS1, ↑TNFSF11	Cellular Movement, Hematological System Development and Function, **Immune Cell Trafficking**
↑ACE, ↑EPHX2, ↑MMP1, ↑PTGS1, ↓SERPINE1	Hematological System Development and Function, Cellular Growth and Proliferation, Organismal Injury and Abnormalities

4.7 SUMMARY OF RESULTS

- Monocyte/macrophage derived chemokines were associated with symptomatic OA.
- Signalling components in the NF-κB signalling pathway were differentially expressed between groups. Gene expression was lower in symptomatic chondropathy cases compared to asymptomatic chondropathy cases.
- Expression of suppressor of cytokine signalling-1 was lower in the symptomatic chondropathy cases compared to asymptomatic chondropathy cases.

DISCUSSION

This chapter describes synovial gene expression patterns that are associated with OA symptoms in TKR cases (symptomatic chondropathy) compared with PM cases with similar macroscopic joint surfaces who had not sought help for knee pain (asymptomatic chondropathy). The up-regulation of pro-inflammatory mediators (such as chemokines associated with the immune response) in concert with the down-regulation of genes involved in inhibition of the pro-inflammatory pathways may mediate an association with symptomatic OA.

In this study, expression of several chemokines (CCL2/MCP-1, CCL4/MIP-1β, CCL5/RANTES, CCL8/MCP-2 and CXCL6) were significantly up-regulated in the synovium of symptomatic chondropathy cases, suggesting a potential role in mediating OA pain. The association between chemokines and pain has been well documented (White et al., 2007).

Chemokine ligand-2 also known as monocyte chemoattractant protein-1 (CCL2/MCP-1) is a chemoattractant for monocytes. During inflammation, CCL2 is released from synovial fibroblasts (Eisinger et al., 2012) and acts to recruit and activate inflammatory cells including monocytes and memory T cells to sites of inflammation (Voscopoulos and Lema, 2010). Immune cells

may therefore contribute to the early stages of inflammation (Benito et al., 2005).

The results from this study suggest that elevated expression of CCL2 in the synovial tissue may be associated with pain in OA. In support, levels of CCL2 in the synovial fluid have previously been shown to be associated with severity of OA knee pain, in addition to physical disability (Li and Jiang, 2015). Unavailability of pain severity and disability scores for symptomatic chondropathy cases in this study precludes such analyses; nevertheless, elevation of CCL2 was associated with OA knee pain. The association of CCL2 and OA pain has also been demonstrated in experimental models of OA. Indeed, CCL2 mRNA and protein is upregulated in peripheral tissues from the tibiofemoral joint (Dawes et al., 2013). Furthermore, in a surgical model mouse model of OA, mice that lack the CCL2 receptor (CCR2) do not develop movement-provoked pain, in contrast to wild type mice that did develop pain behaviour. Moreover, macrophage infiltration of innervating dorsal root ganglia (DRG) was a feature of wild type mice, but was not apparent in the CCR2 deficient mice (Miller et al., 2012). Taken together these studies support a role for CCL2 in mediating pain through recruiting immune cells to areas of inflammation.

In this study monocyte chemotactic protein-2/chemokine ligand 8 (MCP-2/CCL8) expression was significantly increased in symptomatic chondropathy cases. MCP-2/CCL8 is a pro-inflammatory cytokine that may induce IL-6 in synovial fibroblasts from patients with OA, thus may be a biomarker for IL-6 activation (Kuziora et al., 2013). CCL8 expression has previously been detected in fibroblasts and macrophages in the synovial lining of arthritic patients (Haringman et al., 2006). In addition to CCL2, CCL8 also serves as a ligand for chemokine receptor 2 (CCR2) (Haringman et al., 2006), suggesting an important role of the CCL2/CCR2 and CCL8/CCR2 axis in mediating OA pain.

The chemokine fractalkine (CX3CL1) was down-regulated in the synovial tissue of symptomatic chondropathy cases, suggesting a lack of association with pain. This finding is in contrast to previous studies which have reported an

association of fractalkine in the serum and synovial fluid with symptomatic severity (Zou et al., 2013, Huo et al., 2015). CX3CL1 is elevated in the synovial fluid and serum of OA patients compared to healthy controls (Zou et al., 2013, Huo et al., 2015). In this study, levels of fractalkine were not examined in non-arthritic controls; therefore it is possible that both asymptomatic and symptomatic chondropathy groups may be increased compared to normal levels. CX3CL1 is a chemotactic agent for a variety of immune cells including monocytes (Isozaki et al., 2008) and mast cells (Papadopoulos et al., 2000). CX3CL1 expression is stimulated by NF-κB and STAT-1 signalling pathways (Isozaki et al., 2008), in this study NF-κB signalling was significantly down-regulated in symptomatic chondropathy cases, which may partly explain the suppressed levels of fractalkine. Furthermore, previous studies have sought to determine immunoreactivity the serum or synovial fluid, rather than in the synovial tissue. It is possible that synovial tissue may not be an important source of CX3CL1in the later stages of OA.

IL -1β is one of the major pro-inflammatory mediators associated with OA pathogenesis (Wojdasiewicz et al., 2014b), formed within the cytoplasm as a precursor protein (pro- IL-1β). Cleavage by caspase 1 (CASP1), converts the precursor to its active form, IL-1β (Saha et al., 1999). IL-1β expression was increased in the synovium of symptomatic chondropathy cases, but did not reach statistical significance, whereas CASP1 was significantly increased in the symptomatic chondropathy group. Previously CASP1 has shown to be upregulated in synovial membrane and cartilage of OA patients compared to control tissue (Saha et al., 1999), suggesting an active involvement of the enzyme in the later stages of OA.

The pro-inflammatory actions of IL-1β are exerted through binding its membrane receptor, interleukin-1 receptor (IL-1R1). In the current study expression of IL-1R1 was significantly down-regulated in symptomatic chondropathy cases. Previously, expression of IL-1R1 has been shown to be increased in OA synovial fibroblasts, compared to normal controls (Sadouk et al., 1995). In this study absence of a control group precludes such analyses.

Nevertheless this study demonstrates that in asymptomatic PM donors expression of synovial IL-1R1 is increased compared to OA cases with similar macroscopic appearances. These data suggest a role of elevated expression of IL-1R1 in the earlier stages of OA before symptoms occur. Although evidence in animal models of OA reports favourable benefits of IL-1 receptor antagonist therapy (Fernandes et al., 1999, Pelletier et al., 1997), clinical trials in human subjects have been less promising (Chevalier et al., 2009, Cohen et al., 2011). It is possible that a compensatory homeostatic mechanism acts to attenuate receptor expression in the later stages of OA in order to dampen the inflammatory response. Certainly this finding is interesting but further work would be necessary to validate these findings and to elucidate the underlying mechanism.

The NF-κB signalling pathway plays an essential role in the inflammatory response (Tak and Firestein, 2001) through up-regulating the transcription of pro-inflammatory mediators. Since inflammation was a feature of symptomatic chondropathy cases, these pathway components might be expected to be increased in this group. In contrast three components of the NF-κB pathway; NF-κB (p50), its inhibitor NF-KBIA and Rel-A (p65) were significantly down-regulated in the symptomatic chondropathy group compared to elevated levels in the asymptomatic chondropathy group. In support, expression of NF-κB and Rel-A is increased in patients with early OA compared to patients undergoing joint replacement for severe OA (Benito et al., 2005). It is therefore plausible that increased expression of NF-κB components before symptoms (i.e., in asymptomatic chondropathy cases) reflects increased activation of inflammatory signalling pathways in early OA. These pathways may contribute to severe inflammation and the consequent up-regulation of pro-inflammatory mediators in the later stages of OA. Moreover, the decreased expression of the inhibitor of NF-κB may play an important role in OA pathogenesis.

The suppressors of cytokine signalling (SOCS) family of proteins constitute a negative feedback loop in the JAK/STAT pathway to supress cytokine signalling. SOCS1 and SOCS3 are the best characterised members of the SOCS family, they both inhibit the tyrosine kinase activity of JAKs through a

direct interaction (Yasukawa et al., 1999) and through receptor binding (Alexander, 2002), respectively. Pro-inflammatory cytokines including IL-1 (Boisclair et al., 2000) and IL-6 (Starr et al., 1997) and anti-inflammatory cytokines such as IL-4 and IL-10 (Shen et al., 2000) can induce expression of SOCS1 and SOCS3.

In the present study, expression of SOCS-1 and SOC-3 were differentially expressed in the synovium of symptomatic chondropathy cases, although the differential expression of SOCS-3 did not reach statistical significance. Previously SOCS-2 mRNA, but not SOCS-1 or SOCS-3 was reduced in OA chondrocytes compared to healthy controls (De Andres et al., 2011), suggesting the down-regulation of SOCS activity in the cartilage is not mediated through inhibition of tyrosine kinase activity. In the synovium, the down-regulation of SOCS-1, in particular, may play an important role in OA pathogenesis. Moreover, decreased expression of SOCS-1 was correlated with an increase with pro-inflammatory mediators including CCL-2 and TNF-α. The reduction of SOCS proteins in the osteoarthritic synovium offers a plausible hypothesis, where lack of suppression of the JAK/STAT signalling pathways may potentiate inflammatory processes and mediate pain.

The NGF signalling pathway was examined for differential expression between the two groups. Previous results reported in this thesis found an elevated abundance of synovial NGF in the symptomatic chondropathy group compared to asymptomatic chondropathy cases using IHC.

In the current study, NGF mRNA was increased in the synovium of the symptomatic chondropathy group, but did not reach statistical significance. TrkA, the high affinity receptor for NGF was significantly upregulated in the synovium of symptomatic chondropathy cases, suggesting a key role for TrkA in mediating pain. Indeed, treatment strategies to antagonise TrkA have shown analgesic effects in models of OA pain (Nwosu et al., 2015).

The correlation between protein levels of NGF (as measured by IHC) and mRNA was low. A discordance between protein abundance and mRNA expression has previously been described (Haider and Pal, 2013) and may be attributed to post-translational and transcriptional modifications of proteins

occurring after mRNA is synthesised. NGF quantification using IHC replies on the primary antibody to specifically detect cells expressing the protein of interest. In contrast, RNA is extracted from many different cell types all of which may express differing levels of NGF which may confound analysis. Furthermore IHC measures an increase in NGF-expressing cells, whereas the RNA assay measures NGF expression relative to total gene expression. In the latter, total mRNA was adjusted for, whereas IHC results may be due to increased numbers of cells which would have increased total mRNA. In other words, increased NGF in the synovium of symptomatic chondropathy cases compared to asymptomatic chondropathy cases might be due to an increase in NGF expressing cells, rather than necessarily an increase in NGF expression by each of those cells. Further work to validate the results using techniques such as Western blotting or in situ hybridisation would be necessary to clarify differences in protein expression between the two groups.

During inflammation, the release of anti-inflammatory mediators in the joint is an essential homeostatic mechanism to suppress inflammation. Various anti-inflammatory mediators have been implicated in OA including IL-4 and IL-10 (Moore et al., 2001, Wojdasiewicz et al., 2014b). In this study, two anti-inflammatory mediators IL-10 and annexin A1 (ANXA1) expression were increased in the synovia of symptomatic chondropathy patients compared to asymptomatic chondropathy cases.

ANXA1 previously known as lipocortin-1 is a key endogenous mediator involved in the anti-inflammatory actions of glucocorticoids (Flower, 1988, Buckingham and Flower, 1997). One of the protective actions of ANXA1 involves regulating the production of the prostaglandin precursor, arachidonic acid (Sampey et al., 2000). In OA patients, abundant ANXA1 has previously been detected in the synovial lining in monocyte and macrophage cells (Goulding et al., 1995) which is in support of the current study's findings.

In addition to possessing anti-inflammatory properties ANXA1 may be involved in pain modulation. The anti-nociceptive properties of ANXA1 have been demonstrated in vivo where hyperalgesic responses to inflammatory mediators including TNF-α and IL-1β were inhibited by ANXA1 (Ferreira et

al., 1997). Furthermore, ANXA1 knock out mice show exacerbated pain responses compared to wild type mice, in addition to elevated levels of spinal prostaglandin E_2 (Ayoub et al., 2008). The effects of ANXA1 are mediated through the formyl-peptide-receptor-like 1 (FPR2/ALX) (Perretti and D'acquisto, 2009, Pei et al., 2011). Elevated levels of ANXA1 in the synovium of patients with symptomatic OA suggest a compensatory reaction of the body to attempt to supress inflammatory and nociceptive processes possibly through the inhibition of prostaglandin synthesis.

Limitations of this study are discussed in detail in chapter 6. In brief, this study examines gene expression patterns in the synovium using microfluidic cards. The *P* value threshold for significance was ≤ 0.05.Since multiple statistical comparisons were undertaken (multiple Mann Whitney tests) there is a risk that some of the significant results reported may have occurred by chance. One approach to correct the significance value for multiple testing is to apply a correction for the false discovery rate (Benjamini and Hochberg, 1995). The false discovery rate is used to control the Type I error rate (rejecting the null hypothesis when it is true, ie. finding a statistically significant difference by chance).

This work requires further validation to examine whether the gene expression patterns that are associated with OA can be replicated using bespoke Taqman, and differences at the protein level could be examined using individual Western blotting. Furthermore, this study should serve as a pilot study and replication using different asymptomatic and symptomatic cases with similar chondropathy should be conducted to validate molecular associations with symptomatic OA.RNA is highly unstable and susceptible to degradation by RNAases and post-mortem processes (Holland et al., 2003). Therefore, the presence of RNA decay in PM tissues was a potential concern when comparing gene expression from PM samples with tissue obtained at TKR. In order to address these issues, correlation analyses were used to examine whether gene expression in asymptomatic chondropathy cases was reduced with increasing delay between death and tissue processing (PM delay). In this study only 2 out of the 92 target genes (CCL4 and IL8) were associated with PM delay, i.e.,

gene expression decreased as PM delay increased. As CCL4 was significantly increased in the symptomatic chondropathy group, it is possible that the association may be partly due to PM delay. Although, overall, synovial gene expression patterns in this study appear to be stable with increased post mortem delay, since the average correlation coefficient (R value) was not significantly different to zero.

There were no significant differences in the expression of the 4 reference genes between groups. The reference genes act as an internal control, and should remain constant between different experimental conditions. A global decrease in RNA expression would also be detected at the level of the reference genes if all of the RNA from the asymptomatic group was degraded. Furthermore, normalisation of target gene expression to reference gene expression compensates for any error between samples, or confounding results due to RNA degradation.

Matching for chondropathy severity and availability of snap frozen synovium biopsies precluded age matching between symptomatic and asymptomatic chondropathy groups, even when using a source repository containing samples from > 1700 cases. The expression of a small number of genes was associated with age, therefore possible associations with symptom status may be decreased which is one limitation of the study. The small ‘n’ number of cases in each group precludes adjusting for age.

The synovial lining was absent in a small number of cases on microscopic inspection of a haematoxylin and eosin stained preparation. However, during RNA extraction (using larger snap frozen synovium biopsies) the synovial lining could be identified macroscopically on all cases as a white band. Therefore these cases, even if the synovial lining was absent in the H&E preparation, were included in the study.

4.8 Conclusions

In conclusion, symptomatic OA might be associated with a variety of analgesic mediators including chemokines compared to asymptomatic chondropathy cases with similar macroscopic joint surface appearances who did not seek

TKR. Synovial inflammation is a feature of symptomatic OA, and better understanding of the gene expression patterns would lead to refinement of existing therapies and development of new treatments to reduce pain. This work has potentially identified novel molecular targets that may be promising treatment strategies to alleviate symptoms in patients with OA. However further work is necessary to validate these findings.

CHAPTER 5: OSTEOARTHRITIS AS A MULTI-TISSUE DISEASE AND FEATURES OF EARLY KNEE OSTEOARTHRITIS

INTRODUCTION

5.1 What is early knee osteoarthritis?

OA is regarded as the end result of a variety of pathological processes including structural change and inflammation. There remains uncertainty regarding the key features of early knee OA. Defining the earliest changes specific to disease onset is challenging as the disease is usually diagnosed when pain first develops. Pain may precede or follow development of structural modifications in the joint. Radiographs and magnetic resonance imaging (MRI) lack sensitivity for the detection of cellular or molecular pathological changes in people with newly diagnosed knee OA. Furthermore, there is limited access to joint tissue from people with early knee OA which has restricted investigation of these earliest changes associated with preclinical knee OA. OA is strongly associated with age (Felson et al., 1987); therefore access to a large joint tissue repository obtained at the time of post-mortem examination from generally older donors is of benefit.

Diagnostic features such as osteophytes may occur late in the progression of OA, while putatively early features such as cartilage fibrillation may lack OA specificity. Histopathological changes have been defined in joint tissues from people with end-stage OA obtained at joint replacement surgery, and scoring systems developed to assess OA structural severity. OA is a multi-tissue disease (Loeser et al., 2012) whereas histopathological scoring systems often focus on pathology in a single tissue type only, most commonly the articular cartilage.

It is important to define the difference between early and mild OA, which may be different depending on stages of disease progression. Early OA refers to the initial pathologic alterations that occur at the beginning of the disease onset; it is possible that in some people where OA is progressing quickly that these changes may not necessarily be mild. Indeed patients with slow progressing OA may have mild pathological changes within their joints even at later stages of the disease process. At present it is challenging to differentiate between early and mild pathological alterations in the osteoarthritic joint.

5.2 Models of OA progression

OA is a multi-tissue disease that may progress over many years. Various models have been proposed to describe the sequence of progression in OA from early to end-stage disease (figure 5.1). The traditional model perceives OA as a disease primarily affecting the articular cartilage (Soren et al., 1988, Bobinac et al., 2003, Heijink et al., 2012), progressing to multi-tissue disease with accompanying secondary changes in the synovium and subchondral bone in later phases of the disease (figure 5.1A). Alternatively, primary pathology in the subchondral bone may initiate secondary pathology in the surrounding articular and periarticular tissues (figure 5.1B) (Radin and Rose, 1986). More recent models suggest that OA affects several joint tissues in parallel throughout the progression of OA, with histopathological severity progressing over time (figure 5.1C). Alternatively, OA may begin in any tissue type and progress to multi-tissue disease in end stage OA (figure 5.1D).

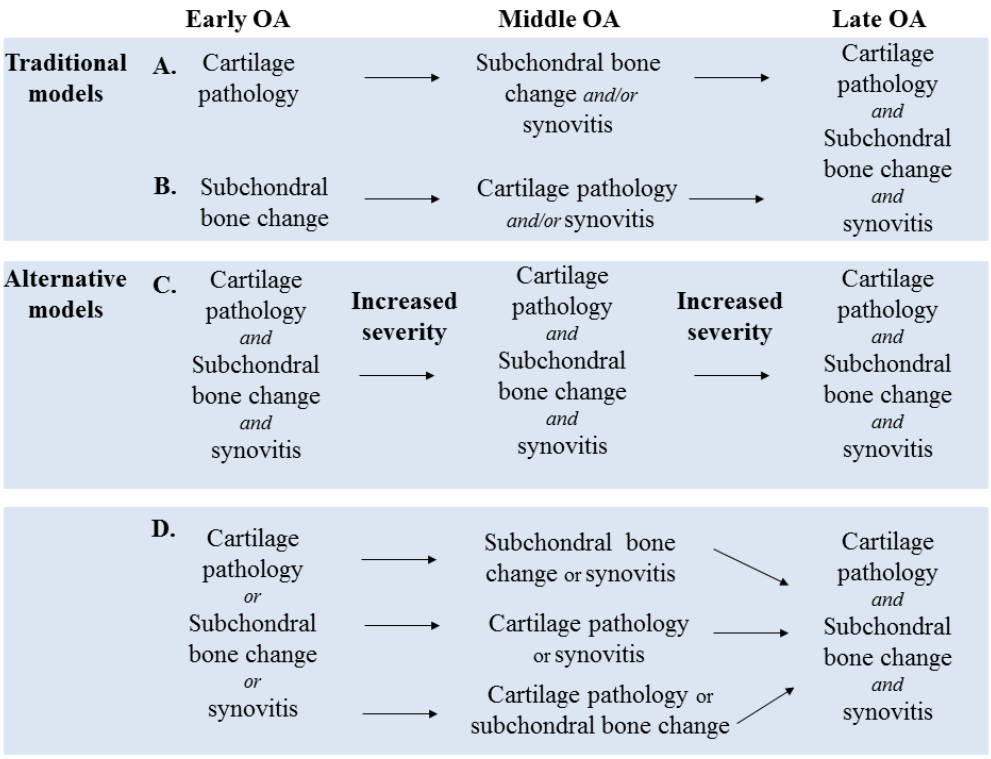


Figure 5.1: Models of OA progression.

Traditional models propose progression from primary pathology in the articular cartilage **(A)**, or subchondral bone **(B)**, progressing to secondary structures resulting in multi-tissue disease. Alterative models suggest OA affects all tissues in parallel and pathology severity progresses over time **(C)**, or pathology may affect any tissue type in early OA, progressing to multi-tissue disease in the later stages of OA.

5.3 Osteoarthritic changes in the articular cartilage

The earliest morphological changes in the osteoarthritic cartilage have been well documented; these include fibrillation, chondromalacia, necrosis and alteration of macromolecule composition. Early OA is believed to be associated with chondrocytic failure to retain homeostatic catabolic and anabolic processes. Whereby chondrocyte mediated overexpression of collagen type II and aggrecan synthesis is followed by degradation driven by the release of proteolytic enzymes such as metalloproteases (MMPs). Aberrant chondrocyte morphology is typified by proliferation (hyperplasia and clustering) (Sandell and Aigner, 2001) and hypocellularity. Moreover, proteoglycan loss and tidemark breaching by channels from the subchondral

bone into the non-calcified cartilage (Suri et al., 2007, Franses et al., 2010, Walsh et al., 2010) are features of OA.

5.4 Osteoarthritic changes in the subchondral bone

Cartilage degradation may be attributed to increased stiffness and rigidity of the underlying subchondral bone (Radin and Rose, 1986). Subchondral bone modifications include formation of bone marrow lesions (BML) and osteophytosis. BML are associated with disease progression and increased risk of total knee replacement (Scher et al., 2008, Tanamas et al., 2010b, Raynauld et al., 2011). Histologically, BML are characterised as replacement of subchondral bone marrow by fibrovascular tissue, in addition to manifestations of necrosis, bone marrow bleeding, trabecular micro fractures and bone marrow oedema (BME) (Zanetti et al., 2000, Eriksen and Ringe, 2011). Osteophytes are cartilaginous and osseous protrusions that develop along the joint margin and are a hallmark feature of OA that can be visualised by radiographs (Nagaosa et al., 2000), or by direct visualisation of the dissected knee.

5.5 Synovial inflammation in knee osteoarthritis

OA is an active disease process, and often perceived to be mechanically driven (Felson, 2013); however inflammation has been increasingly recognised as an important contributor to the disease process (Sellam and Berenbaum, 2010). Synovial inflammation is characterised by hypertrophy and hyperplasia of the synovial lining, in addition to increased cellularity and increased inflammatory infiltrate (Haywood et al., 2003). Synovitis has been observed in both early and late disease (Haywood et al., 2003, Benito et al., 2005, Atukorala et al., 2014). Products of cartilage degradation and/or inflammatory cytokines may induce synoviocytes to release proteolytic enzymes and pro-inflammatory mediators, which could drive the inflammatory response (Rosenthal, 2011). Furthermore, crystals within the joint may contribute to synovitis and cartilage degradation through the production of pro-inflammatory mediators such as nitric oxide (NO), matrix metalloproteinase 13 (MMP-13) and prostaglandin E2 (PGE(2))(Liu et al., 2009).

5.6 Histological grading of OA pathology

Various histological grading systems have been developed to assess the severity of osteoarthritic pathology in several tissue types of the knee joint. Grading of OA pathology, however, usually focuses on articular cartilage and have been developed logically, rather than empirically, and have used samples obtained at total knee replacement (TKR, end stage OA).

Several histopathological grading systems have been developed to measure the severity of OA changes in the articular cartilage. The histologic-histochemical grading system was developed by Mankin and colleagues and is currently the most widely applied grading system (Mankin et al., 1971). The score is favoured due to ease of application. The grading system was initially developed by assessing femoral heads obtained at OA joint replacement surgery, but has since been applied to other joints and used in both human and animal studies. Criticism has arisen regarding the utility of the grading system in early OA (Ostergaard et al., 1999). The system uses a 14-point score which encompasses articular surface integrity (0-6 points), tidemark integrity (0-1 point), proteoglycan staining (0-4 points) and chondrocyte morphology (0-3 points). A total score is derived through the addition of all 4 components; a score of 0 represents normal cartilage, whereas a score of 14 indicates the most severe cartilage pathology. One of the possible criticisms of Mankin score is centred on the lack of weighted contribution of each component to the total score. The scoring is not clearly related to the relative importance of each component. The cartilage component accounts for almost half of the total score, whereas tidemark breaching contributes to only a small proportion of the total score. Furthermore, the relevance of the each component to OA pathogenesis has not yet been assessed (Aigner, 2012).

Several groups have attempted to modify the Mankin score. One modified score takes into account chondrocyte cloning as a separate parameter (Armstrong et al., 1994). Another group omitted evaluation of tidemark integrity due to the absence of calcified cartilage and subchondral bone on equine specimens, in addition to compressing cartilage surface integrity scores to a 4-point scale, although the modified Mankin score did not correlate with

macroscopic scores (Thomas et al., 2007). Histological and macroscopic scores should be complementary measures of structural severity (Walsh et al., 2009). In this study evaluation of tidemark integrity was included as vascular channels breaching the tidemark has previously been associated with OA, both in a previous chapter within this thesis (chapter 3), and within the literature (Suri et al., 2007, Walsh et al., 2007).

More recently the OARSI working group redefined histopathological assessment of the articular cartilage with the aim of producing a more useful measure of pathology (Pritzker et al., 2006). The OARSI score describes both the extent (0 [no OA activity] to 4 [>50% involvement]) and severity (0 [normal cartilage architecture] to 6 [subchondral bone remodelling]) of articular cartilage pathology. Several studies have demonstrated a strong association between the Mankin and OARSI histopathological scores (Custers et al., 2007, Pearson et al., 2011, Pauli et al., 2012). Inclusion of the extent of pathology is commendable; however there are several limitations of the OARSI method. The score assumes a pathological sequence of events in OA where cartilage pathology precedes subchondral bone pathology; grades 1 to 4 examine articular cartilage changes, whereas grades 5 to 6 include subchondral bone alterations. This sequence of progression may not be relevant to all cases of knee OA. Furthermore, there are multiple criteria within each grade boundary and contradictory observations may occur (Pearson et al., 2011).

Histological aspects of synovial inflammation are characterised as hypercellularity and hyperplasia of the synovial lining cells, increased cellularity and inflammatory cell infiltrate. Various histological grading systems have been developed to examine synovial inflammation. Haywood and colleagues described a scoring system based on a simple 3-point score which encompasses the degree of synovial lining hyperplasia, cellularity and inflammatory infiltrate within each grade boundary (Haywood et al., 2003). A score of 0 indicates no synovitis, 1 mild synovitis, 2 moderate synovitis and 3 severe synovitis. Krenn and colleagues have developed a 9-point based score which assess each of the three histological features of synovitis (lining

hyperplasia, cellularity and inflammatory infiltrate) separately (Krenn et al., 2002, Krenn et al., 2006).

Meniscal degeneration can be assessed by examining the orientation and appearance of meniscal collagen bundles, in addition to chondrocyte morphology. A grading system has been developed to assess meniscal degeneration; 0 (collagen bundles closely set and normal distribution of chondrocytes) to 2 (severe meniscal degeneration; severe clefts to collagen bundles and cyst formation, with areas of chondrocyte hypocellularity) (Copenhaver W, 1978, Ishihara et al., 2009).

Histological evaluation of osteoarthritic alteration in the knee joint should consider that OA is a multi-tissue disease driven by both mechanical and inflammatory factors (Loeser et al., 2012). It is therefore of potential value to develop a histological scoring system that fully encompasses all aspects of joint disease, not merely cartilage pathology. This scoring system would improve assessment of OA severity by providing a global measure of pathology in the joint.

The measurement characteristics of a well-functioning scoring system, where total scores are derived from the summation of individual item scores (such as the Mankin scoring system) can be explored using Rasch analysis. Rasch analysis is a psychometric tool used to validate newly developed outcome scales or reform existing ones, and has not previously been used for histological methods in OA. Various prerequisites are required in order for the scale to fit the Rasch model. The score should have unidimensional properties, i.e., there should be one underlying measurement construct where each parameter should be measuring the same aspect of OA severity. Rasch analysis allows for examination of the scoring structure of each histological feature. In Rasch analysis terms each histological feature (i.e., cartilage surface integrity, chondrocyte morphology, proteoglycan loss and tidemark breaching) is referred to as an “item”. Rasch analysis also assesses the overall fit of the items to the Rasch model. Furthermore, one of the properties of the Rasch model is independence of the items, when this is failed response dependency occurs. Each item should not be dependent upon a response to a subsequent item.

The Rasch model has previously been applied to assess the internal construct validity of several ordinal based questionnaires used within OA research and clinical practice (Davis et al., 2003, Moreton et al., 2012, Moreton et al., 2014). Furthermore, the Oxford knee score (Ko et al., 2009), and the ordinal magnetic resonance imaging (MRI) score for knee OA (Conaghan et al., 2006) have been fitted to the Rasch model. However, evaluation of internal construct validity of histological measurement systems for use within knee OA has been not been reported.

5.7 Histological phenotypes in knee OA

Patients with knee OA often have varied clinical presentations, suggesting the existence of distinct clinical phenotypes within the heterogeneous population of patients with the disease (Driban et al., 2010). Identifying homogenous subgroups of patients based on OA phenotypes may ultimately result in important changes in the classification of patients with OA. Furthermore, subgrouping patients will allow for stratification of treatments, by targeting treatments that are most likely to modify key aspects of disease progression or symptoms according to the patient subgroup being treated.

Latent class analysis (LCA) is a statistical modelling tool that can be used to identify phenotypes or subgroups of patients that share similar characteristics within a large data pool (Nylund et al., 2007). Homogeneous psychological phenotypes of knee OA patients have previously been identified (Cruz-Almeida et al., 2013). However classifications based on histopathological characteristics are limited. It is unclear whether discrete pathological features occur concurrently, or are specific to separate pathological subgroups.

5.8 Objectives

1. To optimise the fit of the 4-item Mankin score to the Rasch model.

2. To extend the Mankin score to develop a validated weighted histopathological score that better reflects OA as a multi-tissue disease.

3. To define histopathological features of mild/early OA.

4. To investigate whether discrete pathological features occur concurrently, or are specific to separate pathological subgroups.

METHODS

General methodology is given in chapter 2. Patient selection and sample processing are stated in sections 2.1.5, 2.1.6 and 2.2, respectively. Histological and macroscopic grading is detailed in sections 2.5 and 2.7, respectively. Image analysis is described in section 2.6.

5.9 Study subgroups

The study subgroups are detailed in figure 5.2. Histological scores were documented for the medial tibial plateau and synovia of 486 cases, of these 343 were from tissue donated at post-mortem examination and 143 tissue samples were obtained at the time of total knee replacement (TKR) surgery for symptomatic OA. Histological meniscal scores were recorded for 182 post-mortem cases, but were not available for TKR cases.

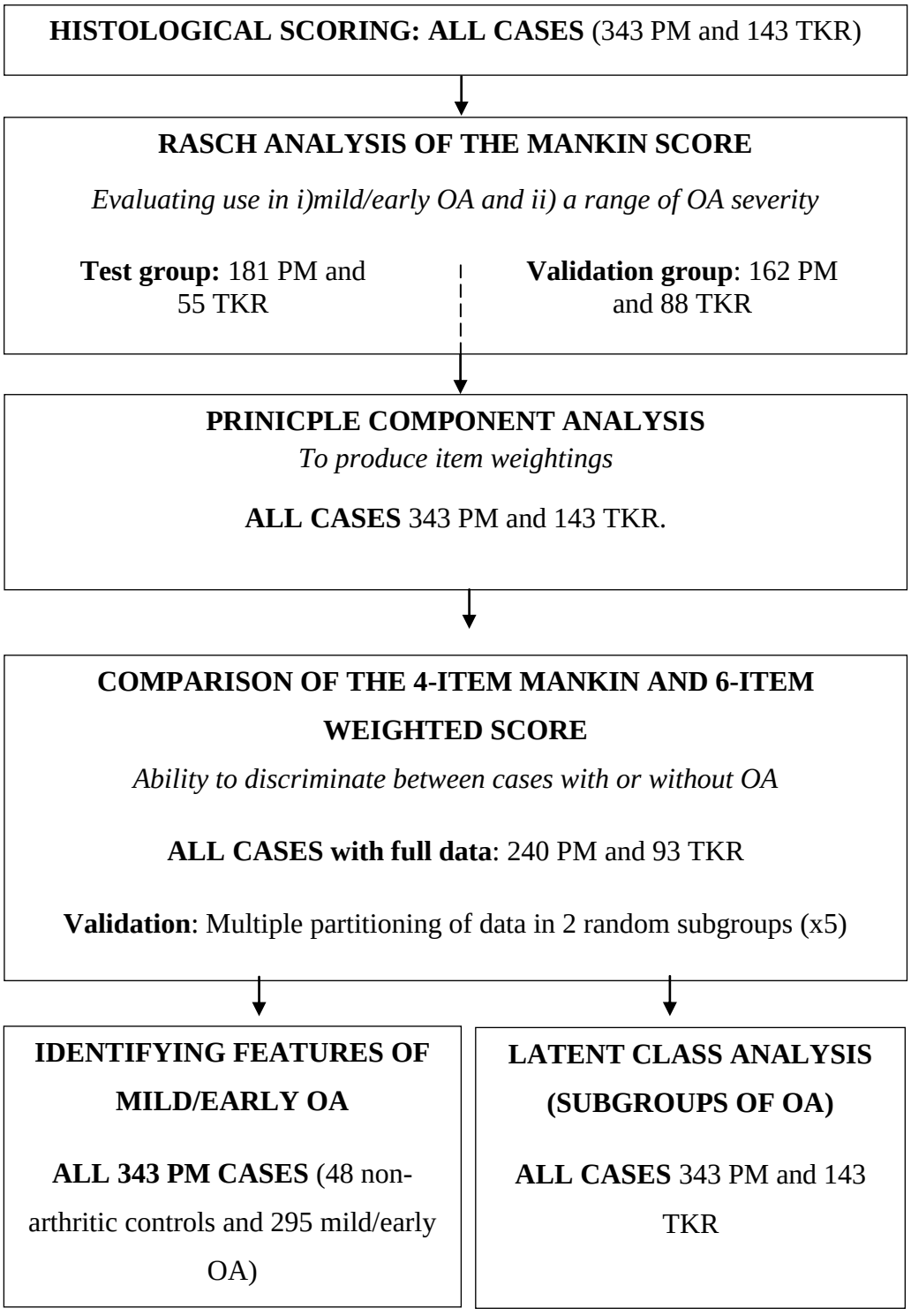


Figure 5.2: Flowchart detailing the overall study designs including numbers of PM and TKR cases that were required at each step.

Initially histological scores were documented for 486 cases (343 PM and 143 TKR). Rasch analysis was first applied to a test group, and was subsequently validated on a different set of PM and TKR cases. Rasch rescaled items were used in subsequent

analyses. Principle components analysis (PCA) was performed using histological scores from all 486 cases, to produce item weightings for developing the histological weighted score. Scores for synovitis and subchondral bone marrow replacement were included in the PCA. The 6-item weighted score was compared with the original 4-item Mankin score. Cases with a full set of histological scores for the 6-items were used in the analysis. The ability for both scores to distinguish between OA and non-OA cases was compared. Multiple partitioning of the data was used for validation purposes. If pathological features of OA are irreversible, early features would be more prevalent than late features. The prevalence of each pathological feature in the medial tibial plateau or synovium was investigated in the PM group. Second, to identify features of mild/early OA, the PM cases were classified as non-arthritic controls based on history and macroscopic examination of joint surfaces, the remaining PM cases were classified as mild/early OA. Histological scores were compared between groups. Latent class analysis was conducted to determine subgroups based on histological criteria using the 486 cases.

5.10 Histological scoring methods

The histological score developed by Mankin and colleagues (Mankin et al., 1971) was used to assess the severity of cartilage pathology in the PM and TKR samples (as described in chapter 2, section 2.5.1). This score was then subjected to Rasch analysis. One of the properties of the Rasch model is independence of the items, when this is failed response dependency occurs. From this perspective the Mankin score is more adaptable to the Rasch model than the OARSI histological score, as the Mankin score considers the score of each histological item to be independent of other items. For example, the score allocated to the amount of proteoglycan loss does not influence the score allocated to chondrocyte morphology. In contrast, the OARSI score assesses multiple components within each grade boundary; this scoring structure would not be represented in Rasch analysis. For this reason the Rasch analysis was applied only to the Mankin histopathological score.

Synovial inflammation was scored using the system developed by Haywood and colleagues (Haywood et al., 2003) as described in chapter 2, section 2.5.2. This score was chosen over the score developed by Krenn and colleagues (Krenn et al., 2002) as it has previously been shown to be a complementary measure of OA structural severity (Walsh et al., 2009).

5.11 Statistical analysis

5.11.1 Rasch analysis of the Mankin scoring system

Rasch analysis was conducted to assess the validity of the Mankin histopathological scoring system. Two analyses were performed using:

i. **Test group** of 181 PM and 55 TKR cases.

ii. **Validation group** of 162 PM and 88 TKR cases. This group consisted of a different set of cases to the test group.

The Mankin score was analysed in two stages. First, in order to examine the measurement qualities of the score for use in mild or early OA, histological

scores from only PM cases were analysed. It was anticipated that mild histological changes in the medial tibial plateaux would be observed in this group. Following this Rasch analysis was performed on all PM and TKR cases representing the full range of OA pathological change from normal to end stage.

Key fit statistics were examined which included person and item fit to the model. In these analyses "person" refers to the PM or TKR case histologically assessed and "item" refers to each histological feature. Rasch also aimed to analyse scale unidimensionality, scoring structure, absence of item dependency and targeting of the Mankin score. The person separation index (PSI) was used to measure internal consistency of the Mankin score, a value of at least 0.7 was considered acceptable (Ayele et al., 2014).

The Spearman-Brown Prophecy formula was used to calculate the number of items needed in Rasch analysis to achieve PSI value of 0.7 (Linacre).

$$T = \frac{C * RT * (1 - RC)}{((1 - RT) * RC)}$$

Where T = Target number of items, C = Current number of items, RT = Target person reliability and RC = current person reliability.

A basic Rasch analysis was conducted to determine whether the new weighted histological score was unidimensional.

5.11.2 Principle components analysis

Principle component analysis (PCA) was used to determine the contributions of each histological parameter to the principle component, using the Rasch rescaled dataset. Histological scores for synovial inflammation and subchondral bone marrow replacement were included in PCA. PCA analysis was conducted on all 343 PM and 143 TKR cases. A one-factor forced PCA determined the correlations between the histological variables and the principle component. The factor loadings were used to inform weightings of each variable in order to give a final maximum score of 10. For each variable the PCA weighting was multiplied by the maximum score for that variable (e.g.,

0.78 x 6 for cartilage surface integrity). Summation of these scores revealed a weighted scale with a possible range of 0 to 10.23. For ease of use, the score was transformed to a scale of 0 to 10. Each weighting was multiplied by a transformation factor of 0.977 (i.e., 10.23/10 = 0.977). The weightings were used in subsequent analyses to weight the 6-item score.

5.11.3 Receiver operating characteristic (ROC) analysis

The original 4-item Mankin and 6-item weighted score were compared for their ability to discriminate between OA and non-OA specimens. Specimens were considered as non-OA or OA based on two different factors:

i. If the cases had evidence of osteophytes (hallmark feature of OA).

ii. If the cases had undergone total knee replacement for symptomatic OA.

For each case the total Mankin score (range 0 to 14) and total weighted score (range 0 to 10) were calculated. Only cases with a full set of histological scores for cartilage pathology, synovitis and subchondral bone marrow replacement were included in the analysis. The total Mankin score and weighted score were compared, and areas under the curves (AUC) for discriminating between non-OA and OA specimens were calculated using receiver operating characteristic (ROC) curves. This analysis was conducted using all PM and TKR cases with a full set of histological data (total n = 333; 240 PM and 93 TKR cases). Validation analysis consisted of randomly splitting the whole dataset of 333 cases into two subgroups. This process was repeated a further four times, to produce ten random subgroup datasets in which to validate the scoring systems on.

Further analyses were conducted to assess the discriminative ability of the weighted score to distinguish between symptomatic and asymptomatic cases. This analysis was conducted using histopathological scores from asymptomatic chondropathy and symptomatic chondropathy cases described in chapter 3. Additionally, the use of the weighted score in cases with mild/early OA was assessed.

5.11.4 Latent class analysis

Latent class analysis was performed to determine histological subgroups using histological data collected from all 343 PM and 143 TKR cases. Additional analysis examined histological subgroups in mild/early OA and TKR cases separately. Detailed methodology for latent class analysis is described in chapter 2, section 2.13.6.

RESULTS

5.12 Histological features of osteoarthritis

Patient demographics are reported in table 5.1. Histological appearance of the medial tibial plateaux and synovia was as previously reported in chapter 3. Articular cartilage displayed varying degrees of loss of cartilage surface integrity; from mild clefts to the articular surface to deep clefts and severe cartilage loss. Proteoglycan content ranged from normal to severe loss. In the majority of cases examined the synovium was normal; however in some cases mild, moderate or severe inflammation was observed. Subchondral bone marrow spaces contained normal fatty tissue in the majority of cases, whereas in some cases this was replaced by fibrovascular tissue. Channels were frequently observed breaching the tidemark between calcified and non-calcified cartilage.

Table 5.1: Clinical demographics of study groups.

	Rasch analysis§		Post-mortem cases			TKR cases	ROC analysis¥				All cases‡
	Test	Validation	Non-arthritic controls	Mild/Early OA	All PM cases δ	All TKR cases	TKR-	TKR+	OST -	OST+	
N	181 PM & 55 TKR	162 PM & 88 TKR	48	295	343	143	240	95	196	139	**343 PM & 143 TKR**
Age	65 (55-71)	66 (60-75)	54 (43-66)	66 (60-73)	65 (58-72)	68 (60-74)	66 (59-73)	68 (59-75)	65 (59-72)	68 (60-77)	**66 (59-73)**
Male (%)	57	52	60	58	58	46	55	46	57	48	**54**
Macroscopic chondropathy (0-400)	91 (58-130)	121 (92-168) †	48 (28-71)	107 (81-156)	97 (67-142) ¶	NA	99 (69-145)¶¶	228 (185-248)¶¶	93 (65-121)¶¶	165 (112-211)¶¶	**101 (71-156)**
Cases with osteophytes (%)	42	41	0	21	18	100	19	100	0	100	**41**

§. Rasch analysis was first conducted on a test group of PM and TKR cases, followed by validation on a second group of cases.

‡The complete dataset of histological data recorded from 486 cases was used in principle components analysis and latent class analysis

¶Macroscopic chondropathy scores were available for 261/343 PM cases. Data expressed as median (IQR) unless otherwise stated.

¶¶Macroscopic chondropathy scores were available for 203/240 TKR-, 12/95 TKR+, 159/196 OST- and 55/139 OST+ cases.

† Macroscopic data available for 78/162 (48%) PM cases in the validation group

δAll PM cases includes both non-arthritic controls and mild/early OA cases.

¥For comparison of area under the receiver operating characteristic curve (AUC) cases were classified according to whether they had sought a total knee replacement (TKR+) compared to those that had not (TKR-), or whether their knees did (OST+), or did not (OST-) have osteophytes. Cases in these four groups overlapped with cases included in the 'All PM' and 'All TKR' columns. Only cases with full sets of histopathological data were included in the AUC comparison analysis.

Preliminary analyses confirmed associations of histological features with OA. In univariate analyses cartilage integrity, chondrocyte appearance, proteoglycan loss, tidemark breaching, subchondral bone marrow replacement and synovitis were each significantly increased in TKR compared to PM cases (table 5.2).

Table 5.3 shows univariate associations between histological and macroscopic features of OA. Macroscopic chondropathy score was significantly associated with each histological parameter in the medial tibial plateaux and synovium (r = 0.2- 0.44, $P < 0.05$). Further details on macroscopic chondropathy scoring are given in chapter 2, section 2.7. Age was associated with macroscopic chondropathy score, cartilage surface integrity, chondrocyte morphology, osteophytosis and tidemark breaching, but association of age with synovitis, proteoglycan depletion or bone marrow replacement did not reach statistical significance (r values 0.07 to 0.09). Female gender was weakly associated with chondrocyte morphology, synovitis and osteophyte presence (r values 0.09 to 0.12, $P = 0.01$to 0.05).

Table 5.2: Histological characteristics of PM and TKR cases

Histological parameter	PM cases (n=343)	TKR cases (n =143)	*P* value
Cartilage surface integrity	3 (2-4)	4 (4-4)	≤ 0.001
Tidemark breached (% of cases)	52	70	≤ 0.001
Chondrocyte morphology	2 (0-3)	2 (2-3)	0.002
Proteoglycan loss	1 (1-2)	1(1-2)	≤ 0.001
Subchondral bone marrow replacement (% of cases)	14	42	≤ 0.001
Synovitis	0 (0-0)	1 (0-2.5)	≤ 0.001
Meniscal pathology†	1 (1-2)	NA	NA

Data displayed as median (IQR) unless otherwise stated. Tidemark breaching is expressed as a percentage of those cases in which cartilage integrity permitted assessment (PM group n =319, End-stage OA group n =121). Statistical significance accepted when $P<0.05$.NA = not available. †Meniscus scores were recorded for 168 PM cases.

Table 5.3: Associations between macroscopic chondropathy scores, histologic score, ages and gender.

	Macroscopic chondropathy	Cartilage	Tidemark	Chondrocytes	Proteoglycan	Bone marrow replacement	Synovitis	Osteophytes	Meniscus†	Age
Cartilage	**.385****									
Tidemark	**.233****	**.098***								
Chondrocytes	**.239****	**.277****	.094							
Proteoglycan	**.231****	**.286****	-.019	.044						
Bone marrow replacement	**.246****	**.286****	.081	.044	**.096***					
Synovitis	**.289****	**.247****	.071	.070	**.128***	**.216****				
Osteophytes	**.439****	**.401****	**.202****	**.143****	**.192****	**.247****	**.400****			
Meniscus†	**.228****	**.166***	0.076	-0.02	**.225****	-.013	.071	.076		
Age	**.536****	**.207****	**.144****	**.204****	.085	.069	.089	**.156****	**.200****	
Gender	.079	.050	-.024	**.112***	-.015	.009	**.120***	**.089***	0.081	.034

Associations are expressed as Spearman's rank correlation coefficients. Osteophytes were visualised on the dissected knee (PM cases) or by radiographs (TKR cases). Significant associations in bold. $*P < 0.05$, $**P<0.01$.

† Meniscus scores were not available for TKR cases. Score were recorded for 168 PM cases.

5.13 Rasch analysis of the Mankin scoring system

5.13.1 Test group; early or mild OA

Rasch analysis was first conducted on a test group of cases (n = 181 PM cases and 55 TKR cases). Results are reported in table 5.4. The use of the Mankin score in PM cases indicated moderate fit to the Rasch model (table 5.4, initial analysis). However the person separation index (PSI) was poor (0.44, ideal value > 0.7). There was no evidence of DIF for gender. Two out of the 180 t-tests were significant which represented 1.1% of the total tests indicating scale unidimensionality. The mean location of person-item threshold distribution was -0.81 (SD = 1) suggesting the sample was located slightly below the average of the scale.

One item (tidemark) displayed slight misfit (fit residual > 2.5), and another item (chondrocyte morphology) displayed disordered thresholds. Response option '1' (chondrocyte hypercellularity) had a low probability of selection such that there was no point along the continuum of Mankin scores that it was the most likely option to be selected. Different rescoring options were explored, whereby response option '1' (chondrocyte hypercellularity) was merged with either response '2' (chondrocyte cloning), or response '0' (normal chondrocyte appearance). The chondrocyte scale was rescored from the original 4-point scale (0123) to a 3-point scale (0112 or 0012, accordingly). Rescoring improved fit (table 5.4, analysis 2 and 3, respectively) and solved the disordered thresholds although the PSI was still low (0.42 and 0.44, respectively). Each rescored scale was unidimensional (1.1% significant t-tests) and there was no evidence of DIF for gender. The mean location of person-item threshold was -0.83 (SD 1.09, figure 5.3A) and -0.86 (SD 1.11) for the 0112 and 0012 chondrocyte rescore, respectively.

5.13.2 Test group; normal to end-stage OA

In the initial analysis of the Mankin score using the full range of OA cases (normal to end-stage OA) item misfit and disordered thresholds for chondrocyte morphology were observed (figure 5.4A). There was no evidence of DIF for gender. The scale was unidimensional (1.7% significant t-tests). The

Mankin score was reasonably targeted (mean -0.45, SD 1.08, figure 5.3B). Rescoring of response options for chondrocyte morphology (table 5.4, analysis 5&6) resolved the disordered thresholds (figure 5.4 B&C) and misfit but resulted in misfit of the cartilage item (fit residual < -2.5). The scale remained unidimensional; for the 0112 chondrocyte rescore option there were no significant t-tests. For the 0012 rescore, two out of the 234 t-tests were significant (0.08 %). Targeting remained reasonable for both the 0012 and 0012 rescore (mean -0.48, SD 1.17, and -0.55 SD 1.20, respectively).

Overall fit was improved following chondrocyte rescoring in the mild/early OA cases and when scoring cases with a range of OA severities. Therefore, Rasch compressed chondrocyte scores were used in subsequent analyses. The scoring option that merged chondrocyte hypercellularity with chondrocyte cloning was selected, rather than with normal chondrocytes, as the former option better represent chondrocyte hypercellularity as a pathological alteration in OA. In TKR cases, 1/55 (2%) displayed normal chondrocyte morphology, whereas chondrocyte cloning was observed in 22/55 (46%) of cases.

5.13.3 Validation group

Rasch analysis on the validation group (n = 162 PM cases and 88 TKR cases) revealed similar results as the test group (table 5.5). Chondrocyte scoring was initially disordered. Overall fit was improved following rescoring, using the 0012 or 0112 options. There was no evidence of DIF for gender, and the score was unidimensional. PSI remained low (0.44-0.56). Rasch transformed scales for chondrocyte scoring (0 = normal, 1 = hypercellular or cloned chondrocytes, 2 = hypercellular chondrocytes) were used in subsequent analyses where appropriate.

5.13.4 Spearman-Brown Prophecy formula

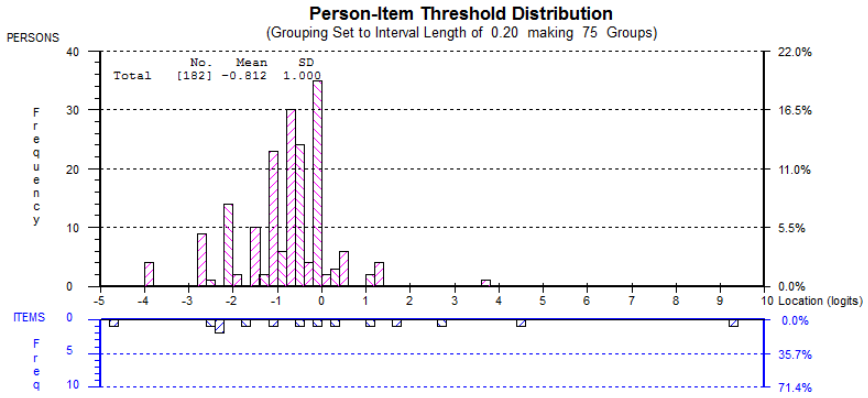
Based on the PSI values listed in tables 5.4 and 5.5, the Spearman-Brown Prophecy formula was used to calculate the number of items needed in each analysis to achieve a PSI value of 0.7.

An example calculation is given below for the initial analysis of the Mankin score in ‘mild/early OA’ (analysis 1, table 5.4) where PSI was 0.44.

$$Number\ of\ items\ needed = \frac{4 * 0.7 * (1 - 0.44)}{((1 - 0.7) * 0.44)} = \mathbf{12}$$

In this analysis 12 items would be needed to increase the PSI value from 0.44 to 0.7. The Spearman-Brown Prophecy formula was subsequently applied to each analysis presented in table 5.4 and 5.5. The number of items needed for each analysis ranged from 8-13 (table 5.4 & 5.5).

A



B

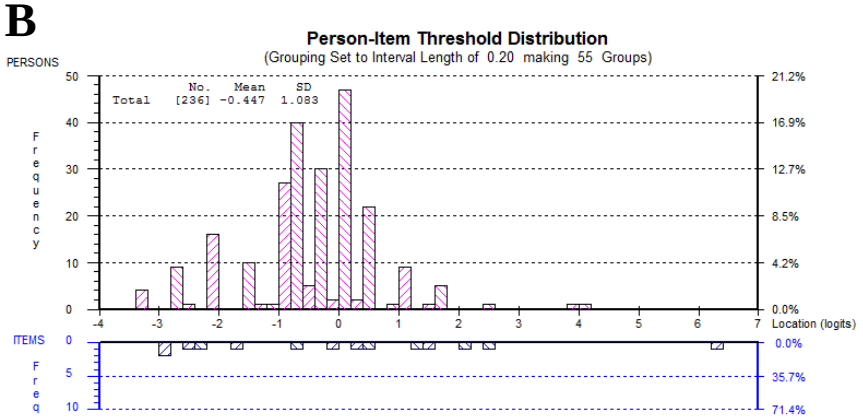


Figure 5.3: Person item-threshold distributions for the Rasch transformed Mankin score.

Person item-threshold distributions in mild/early OA **(A)**, and in full range of OA severity **(B).** The upper part of the histogram illustrates the distribution of persons in each analysis. The lower part represents the distribution of the 4 items. For a well targeted measurement scale the distribution of persons and items should mirror each other.

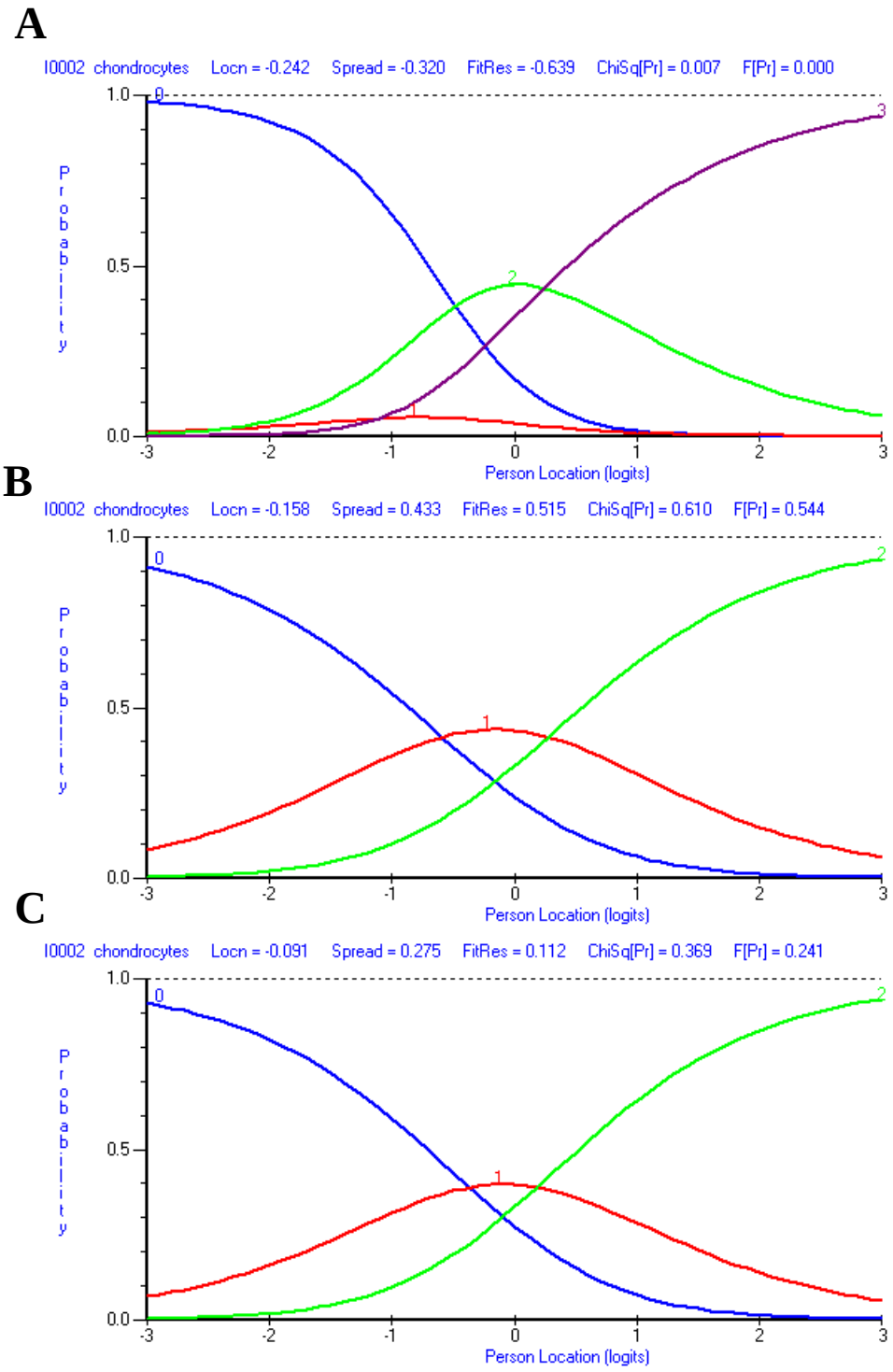


Figure 5.4: Category probability curves for chondrocyte morphology scores.

Category probability curves showing disordered thresholds for initial analysis **(A)**, and ordered thresholds after rescoring chondrocyte morphology 0112 where chondrocyte hypercellularity was rescored as chondrocyte cloning **(B)**, and rescoring 0012 where chondrocyte hypercellularity was rescored as normal chondrocytes **(C).**

Table 5.4: Rasch analysis of the Mankin scoring system on initial test group.

Analysis	Item fit residual mean (S.D.)	Person fit residual mean (S.D.)	χ^2 (P value)	PSI	No of items needed for PSI of 0.7¶
Post-mortem cases only (early/mild OA, n = 181)					
1. Initial	0.62 (1.46)	-0.20 (0.76)	15.63 (0.05)	0.44	12
2. Rescore item 2 (0112)†	0.60 (1.80)	-0.21 (0.80)	9.1 (0.34)	0.42	13
3. Rescore item 2 (0012)‡	0.53 (1.80)	-0.21 (0.77)	10.51 (0.23)	0.44	12
Post-mortem plus total knee replacement cases (range of OA severity, n = 236)					
4. Initial	0.08 (1.83)	-0.22 (0.77)	19.54 (0.08)	0.55	8
5. Rescore item 2 (0112)†	0.02 (2.20)	-0.24 (0.83)	7.04 (0.86)	0.53	10
6. Rescore item 2 (0012)‡	-0.04 (2.23)	-0.24 (0.82)	10.28 (0.59)	0.55	8
Ideal values	*0 (1)*	*0 (1)*	*P > 0.05*	*>0.7*	

†Rescoring item 2 (chondrocyte morphology scores) by merging 'chondrocyte hypercellularity' with 'chondrocyte cloning' (i.e. 0112). ‡Rescoring item 2 (chondrocyte morphology scores) by merging 'chondrocyte hypercellularity' with 'normal chondrocytes' (i.e. 0012). ¶Spearman-Brown Prophecy formula used to calculate the number of items needed in each analysis to achieve a person separation index (PSI) value of 0.7, calculations were based on current PSI values.

Table 5.5: Rasch analysis of the Mankin scoring system on validation group.

Analysis	Item fit residual mean (S.D.)	Person fit residual mean (S.D.)	χ^2 (P value)	PSI	No. of items needed for PSI of 0.7¶
Post-mortem cases only (early/mild OA, n = 162)					
1. Initial	0.65 (2.90)	-0.14 (0.68)	6.75 (0.56)	0.56	9
2. Rescore item 2 (0112)†	0.75 (2.97)	-0.13 (0.70)	5.41(0.71)	0.54	8
3. Rescore item 2 (0012)‡	0.65 (2.90)	-0.15 (0.72)	5.73 (0.67)	0.54	8
Post-mortem plus total knee replacement cases (range of OA severity, n = 250)					
4. Initial	0.43 (3.3)	-0.22 (0.73)	11.40 (0.5)	0.44	12
5. Rescore item 2 (0112)†	0.62 (3.8)	-0.20 (0.78)	8.42 (0.75)	0.44	12
6. Rescore item 2 (0012)‡	0.61 (3.7)	-0.22 (0.81)	7.57 (0.82)	0.45	11
Ideal values	*0 (1)*	*0 (1)*	*P > 0.05*	*>0.7*	

†Rescoring chondrocyte morphology scores by merging 'chondrocyte hypercellularity' with 'chondrocyte cloning'. ‡Rescoring chondrocyte morphology by merging 'chondrocyte hypercellularity' with 'normal chondrocytes'. ¶Spearman-Brown Prophecy formula used to calculate the number of items needed in each analysis to achieve a PSI value of 0.7, calculations were based on current PSI values.

5.14 Principle components analysis

Based on the assumption that each histological item represented an aspect of OA pathology, a one-factor forced PCA was used determine associations between each of the 6 histological variables and the principle component. A scoring formula was generated comprising the sum of each item multiplied by its respective PCA weightings, transformed by a constant x0.977 in order to give a possible score range of 0 to 10;

Weighted OA 6-item score = (0.76 x cartilage integrity) + (0.51 x proteoglycan depletion) + (0.53 x synovitis) + (0.50 x chondrocyte morphology) + (0.48 x subchondral bone marrow replacement) + (0.33 x tidemark integrity).

In an additional analysis, PCA derived weightings were determined on the dataset using the original Mankin scoring structure for chondrocyte morphology (i.e., 4-point scale, 0123). These weightings were used in subsequent analyses to determine whether any differences in the discriminative abilities of the weighted OA and Mankin score were affected by compressing the chondrocyte scores. Weightings are illustrated in table 5.7. The weighting for each variable was multiplied by the maximum score for each variable to produce a scale of 0 to 10.91 Scores were transformed to a scale of 0 to 10 using a transformation factor of 9.216 (i.e., 10/10.91).

Weighted OA score (original chondrocytes) = (0.72 x cartilage integrity) + (0.47 x proteoglycan depletion) + (0.49 x synovitis) + (0.53 x chondrocyte morphology) + (0.44 x subchondral bone marrow replacement) + (0.32 x tidemark integrity).

Table 5.6: Weightings for each histological variable derived from principle components analysis using Rasch transformed* chondrocyte morphology scoring.

Histological variable	PCA factor loading	Transformed coefficients (scale 0 to 10)	Maximum score (0-10)
Cartilage (0-6)	0.783	0.76	4.56
Synovitis (0-3)	0.544	0.53	1.59
Proteoglycan (0-4)	0.521	0.51	2.04
Chondrocytes (0-2)*	0.505	0.50	1
Subchondral bone marrow replacement (0-1)	0.488	0.48	0.48
Tidemark (0-1)	0.344	0.33	0.33

*Rasch rescaled chondrocyte scores were used in PCA. Relative coefficient scores were transformed to a produce a scale of 0 to10, using 0.977 as the transformation factor. Abbreviations; PCA = principle components analysis

Table 5.7: Weightings for each histological variable derived from principle components analysis using uncompressed original chondrocyte scoring.

Histological variable	PCA factor loading	Transformed coefficients (scale 0 to 10)	Maximum score (0-10)
Cartilage (0-6)	0.780	0.72	4.32
Synovitis (0-3)	0.531	0.49	1.47
Proteoglycan (0-4)	0.518	0.47	1.88
Chondrocytes (0-3)†	0.580	0.53	1.59
Subchondral bone marrow replacement (0-1)	0.482	0.44	0.44
Tidemark (0-1)	0.344	0.32	0.32

Original Mankin chondrocyte scores were used in PCA. Relative coefficient scores were transformed to a produce a scale of 0 to10, using 0.9216 as the transformation factor. Abbreviations; PCA = principle components analysis †Original chondrocyte morphology scores

5.15 Rasch analysis

A basic Rasch analysis was conducted to on the weighted OA score to check for unidimensionality when including the two additional items (synovial inflammation and subchondral bone marrow replacement) in the 6-item score. Both in the test and validation analyses of all PM and TKR cases, the scores remained unidimensional (no. of t tests significant was 2.15% and 3.24%, respectively). Furthermore the PSI was increased slightly compared to the 4-item score both in the initial analysis of the test (0.58 vs. 0.55) and validation group (0.52 vs. 0.44).

5.16 Discriminative abilities of the Mankin and weighted score

The ability of the Mankin and weighted score to distinguish between cases with end-stage OA from PM cases, and between cases with or without osteophytes was examined using AUC.

5.16.1 Distinguishing cases with end-stage OA from post-mortem cases

In the initial analysis of the whole dataset which excluded cases with missing data, 28% of cases had end-stage OA (i.e., had sought TKR surgery). The weighted 6-item score had a larger AUC (0.85, 95% confidence interval (C.I) 0.80-0.90) in its ability to distinguish cases with end-stage OA from PM cases compared with the original Mankin scoring system (0.75, 95% C.I 0.69 – 0.80, P <0.0001) (figure 5.5 C vs. A). Optimal cut-offs for the Mankin score were >8 (sensitivity = 69%; specificity = 65%), and for the weighted score were > 4.68 (sensitivity = 77%; specificity = 80%), using both the Youden index and (0,1) method. In each of the 10 validation analyses, the weighted score was better than the Mankin score at distinguishing between cases with end-stage OA and PM cases (table 5.8).

5.16.2 Distinguishing between knees with or without osteophytes

In the whole dataset 41% of cases had osteophytes. The weighted 6-item score had a larger AUC (0.79, 95% C.I 0.74-0.84) compared to the original 4-item Mankin scoring system (0.73, 95% C.I 0.68 – 0.79, P = 0.0001) for distinguishing between knees with or without osteophytes (fig. 5.5 D vs B). Optimal cut-offs for Mankin score were >8 (sensitivity=65%;

specificity=70%), and for the weighted score were > 4.68 (sensitivity=64%; specificity=83%) for the Youden index and > 4.63 (sensitivity=65%; specificity =82%) for the (0,1) method. AUC for the weighted score was numerically greater than for the Mankin score in each of the 10 validation datasets, but the difference did not reach statistical significance in 3 datasets (*P* = 0.05 to 0.07, table 5.8).

5.16.3 Mankin vs uncompressed weighted score

Using uncompressed scores (i.e., original) scores for chondrocyte morphology produced similar results for AUCS (table 5.8). The weighted un-compressed 6-item score had a larger AUC (0.84, 95% confidence interval (C.I) 0.79-0.89) in its ability to differentiate cases with end-stage OA from PM cases compared with the original Mankin scoring system (0.75, 95% C.I 0.69 – 0.80, P <0.0001) (figure 5.5E vs. A, respectively). Optimal cut-offs for the Mankin score were >8 (sensitivity =69%; specificity = 65%), and for the weighted score were > 4.99 (sensitivity = 77%; specificity = 80%), using both the Youden index and (0,1) method.

Moreover, the uncompressed weighted score was better than the Mankin score at discriminating between cases with or without osteophytes (AUC 0.79 vs. 0.73, *P*<0.0001, figure 5.5F vs. B, respectively). The Rasch derived compression of chondrocyte scoring made little difference to the AUC values. Optimal cut-offs for the Mankin score were >8 (sensitivity =65%; specificity = 70%), and for the weighted score were > 4.68 (sensitivity = 64%; specificity = 83%) for the Youden method and > 4.63 (sensitivity 65%; specificity 82%) for the (0,1) method.

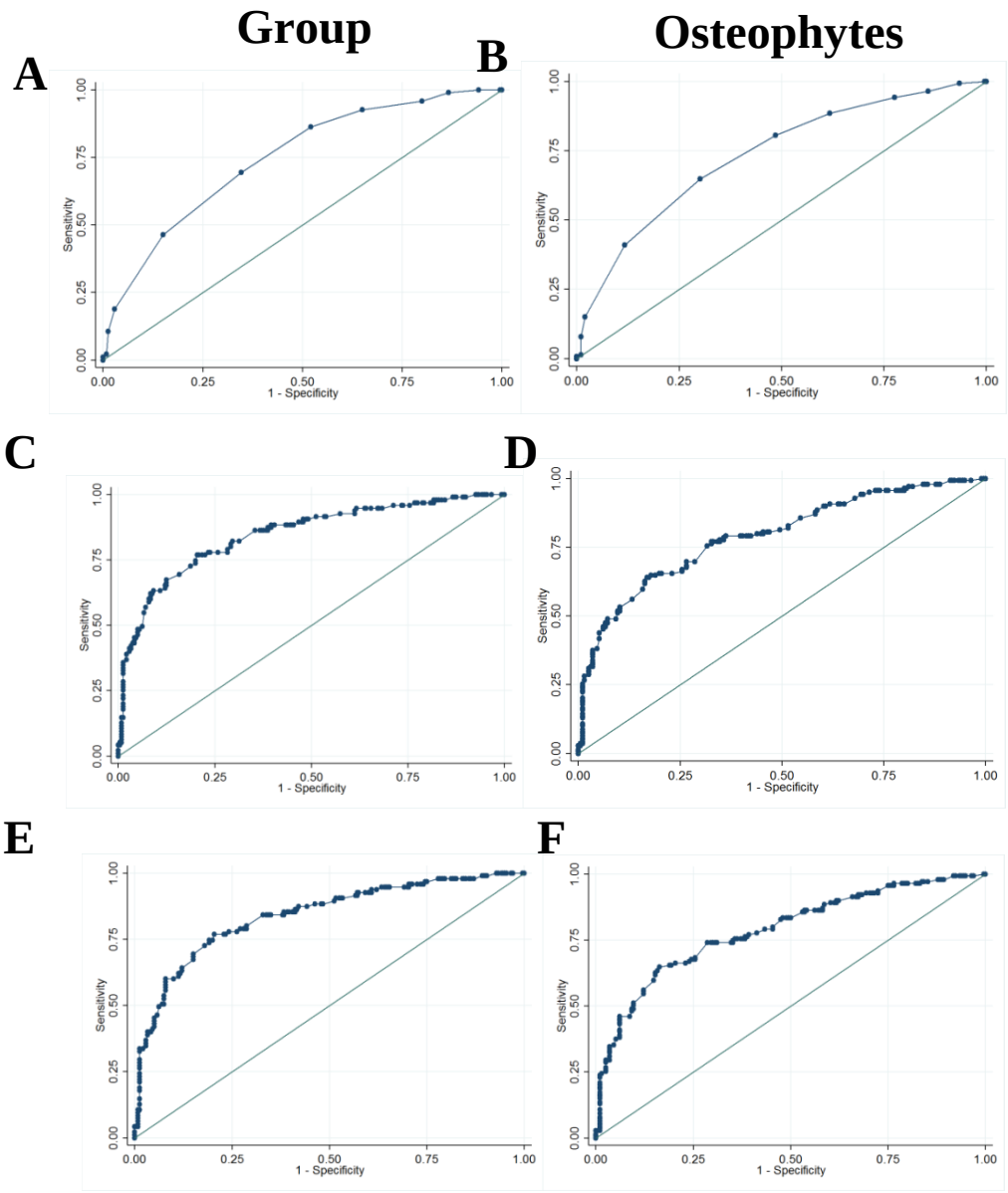


Figure 5.5 Comparison of area under receiver operating characteristic (ROC) curves for the Mankin and weighted scores (compressed and original/uncompressed chondrocyte morphology scores).

Areas under ROC curve were 0.75 for the Mankin score **(A)**, 0.85 for the compressed weighted score **(C)** and 0.84 for the uncompressed weighted score **(E)** in distinguishing between cases with end-stage OA from PM cases. Areas under ROC curve were 0.73 for the Mankin score **(B),** 0.79 for the compressed weighted score **(D),** 0.79 for the uncompressed weighted score **(F)** in distinguishing between knees with or without osteophytes. Results are reported for the whole dataset. The diagonal line represents level of prediction by chance alone.

Table 5.8: Comparison of the abilities of the original Mankin scoring system and weighted OA score to distinguish between cases with end-stage OA and PM cases, and between those with or without osteophytes.

Dataset	% of cases		Distinguishing between cases with end-stage OA and PM cases			Distinguishing between cases with or without osteophytes		
	TKR	Ost	Mankin AUC (95% CI)	Weighted compressed AUC (95% CI)¶	Weighted uncompressed AUC (95% CI)δ	Mankin score AUC (95% CI)	Weighted score AUC (95% CI)¶	Weighted uncompressed AUC (95% CI)δ
Whole dataset	28	41	0.76 (0.71-0.81)	**0.85 (0.80-0.90)§**	**0.84 (0.79-0.89)§**	0.75 (0.70-0.80)	**0.80 (0.75-0.85)§**	**0.79 (0.74-0.84)§**
Validation subgroups								
1	30	40	0.76 (0.68-0.84)	**0.86 (0.79-0.93)§**	**0.85 (0.78-0.92)§**	0.71 (0.63-0.79)	**0.80 (0.73-0.87)§**	**0.78 (0.71-0.86)§**
2	33	47	0.75 (0.67-0.82)	**0.86 (0.80-0.92)§**	**0.85 (0.79-0.91)§**	0.76 (0.69-0.83)	**0.84 (0.78-0.90)‡**	**0.83 (0.77-0.89)§**
3	23	36	0.74 (0.65-0.83)	**0.83 (0.74-0.91)†**	**0.81 (0.73-0.90)†**	0.70 (0.62-0.78)	0.74 (0.66-0.82)	0.74 (0.66-0.82)
4	30	41	0.75 (0.67-0.82)	**0.84 (0.77-0.90)§**	**0.83 (0.76-0.90) §**	0.71 (0.63-0.79)	**0.78 (0.71-0.85)‡**	**0.77 (0.70-0.85)‡**
5	26	42	0.75 (0.67-0.83)	**0.85 (0.78-0.93)§**	**0.85 (0.77-0.93)§**	0.76 (0.69-0.83)	0.80 (0.73-0.87)	0.80 (0.73-0.87)
6	35	48	0.76 (0.69-0.84)	**0.85 (0.79-0.91)§**	**0.84 (0.77-0.90)§**	0.78 (0.71-0.85)	**0.82 (0.76-0.88)***	**0.82 (0.75-0.88) †**
7	22	35	0.73 (0.64-0.82)	**0.85 (0.77-0.92)§**	**0.84 (0.76-0.92)§**	0.69 (0.61-0.77)	**0.76 (0.68-0.84)†**	**0.76 (0.68-0.84)†**
8	33	47	0.75 (0.67-0.82)	**0.86 (0.80-0.92)§**	**0.85 (0.79-0.91)§**	0.76 (0.69-0.83)	**0.84 (0.78-0.90)‡**	**0.83 (0.77-0.89) §**
9	29	40	0.75 (0.67-0.82)	**0.86 (0.79-0.92)§**	**0.85 (0.78-0.92)§**	0.74 (0.67-0.82)	**0.82 (0.75-0.89)‡**	**0.81 (0.74-0.88)‡**
10	29	43	0.75 (0.67-0.83)	**0.83 (0.76-0.91) ‡**	**0.83 (0.76-0.90) ‡**	0.72 (0.65-0.80)	0.76 (0.69-0.84)	0.76 (0.69-0.84)
Mean (S.D)			*0.75 (0.009)*	*0.85 (0.01)*	*0.84 (0.01)*	*0.73 (0.03)*	*0.80 (0.04)*	*0.79 (0.03)*

Abbreviations TKR = total knee replacement cases (end-stage OA), OST= osteophytes present. AUC = area under the curve.

¶ Weighted compressed AUC refers to weighted score where chondrocytes were Rasch transformed and scored as 0 = normal, 1 = hypercellular or cloning, 2 = hypocellular.

δ Weighted uncompressed AUC refers to weighted score where original chondrocyte scoring was maintained; 0 = normal, 1 = hypercellular, 2 = cloning, 3 = hypocellular.

*P<0.05 vs Mankin AUC, †P<0.01 vs Mankin AUC ‡P<0.001 vs Mankin AUC, §P ≤0.0001 vs Mankin AUC.

5.16.4 Distinguishing between cases with or without pain

The performance of the weighted score and original Mankin score for classifying cases as asymptomatic or symptomatic was assessed. The scores were tested using histological data collected from the asymptomatic and symptomatic chondropathy study groups described in chapter 3. Complete histological data were available for 23/29 (79%) of asymptomatic chondropathy and 18/29 (62%) of symptomatic chondropathy cases. The weighted score had larger AUC values than the original Mankin (0.82 [95% CI 0.68-0.95] vs. 0.68 [95% CI 0.53-0.84]), but the difference did not reach statistical significance (P= 0.08, figure 5.6). Optimal cut-offs for Mankin score were >8 (sensitivity=78%; specificity=52%) for the Youden index method, and cut-off >9 (sensitivity= 67%, specificity =61%) for the (0,1) method. For the weighted score optimal cut-offs were > 5.37 (sensitivity=72%; specificity=83%).

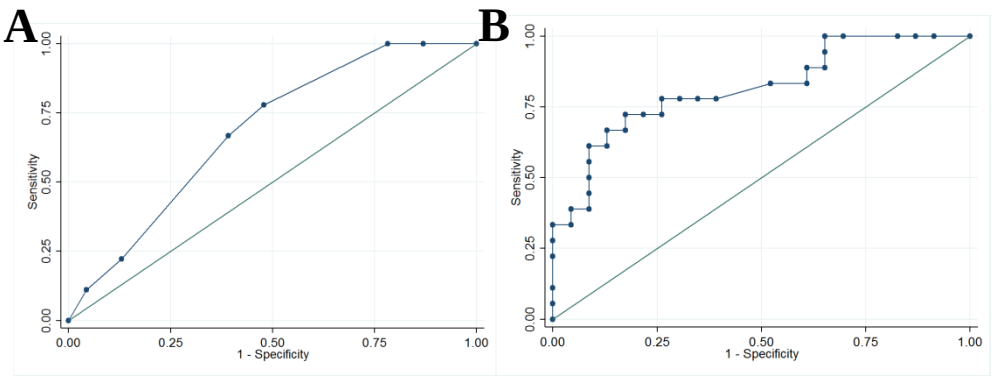


Figure 5.6: Comparison of area under receiver operating characteristic (ROC) curves for the Mankin and weighted score.

Areas under ROC curve were 0.68 for the Mankin score **(A)** and 0.82 for the weighted score **(B)** in discriminating between symptomatic and asymptomatic cases. The diagonal line represents level of prediction by chance alone.

5.16.5 The use of the weighted score in mild/early OA

Utility of the weighted score for use in mild/early OA was examined using PM cases with full histological data (n = 254). Of these, 42 (17%) were classified as non-arthritic controls based on history and macroscopic examination of joint surfaces. The remaining 212 (83%) of cases were classified as 'mild/early OA' cases. The ability of the Mankin and weighted score to distinguish between cases classified as mild/early OA or non-arthritic controls and between PM knees with or without osteophytes was compared.

The weighted score was no better than the Mankin score at classifying cases as mild/early OA or non-arthritic controls (AUC 0.68 [95% CI 0.59-0.77] vs. 0.66 [0.57-0.76], *P* = 0.43, figure 5.7 C vs. A). Optimal cut-offs for Mankin score were >5 (sensitivity=82%; specificity=40%) for the Youden index and >7 (sensitivity = 54%; specificity =67%) for the (0,1) method. For the weighted score optimal cut-offs were > 3.07 (sensitivity=76%; specificity= 50%) for the

Youden index and cut-off > 3.29 (sensitivity = 69%; specificity = 55%) for the (0,1) method.

Moreover, the weighted score was no better than the Mankin score at distinguishing between PM knees with or without osteophytes (AUC 0.64 [0.55 -0.73] vs. 0.65 [0.56-0.74], *P* = 0.50, figure 5.7 D vs B). Optimal cut-offs for Mankin score were >8 (sensitivity=53%; specificity=70%), and for the weighted score were > 4.36 (sensitivity=56%; specificity=68%).

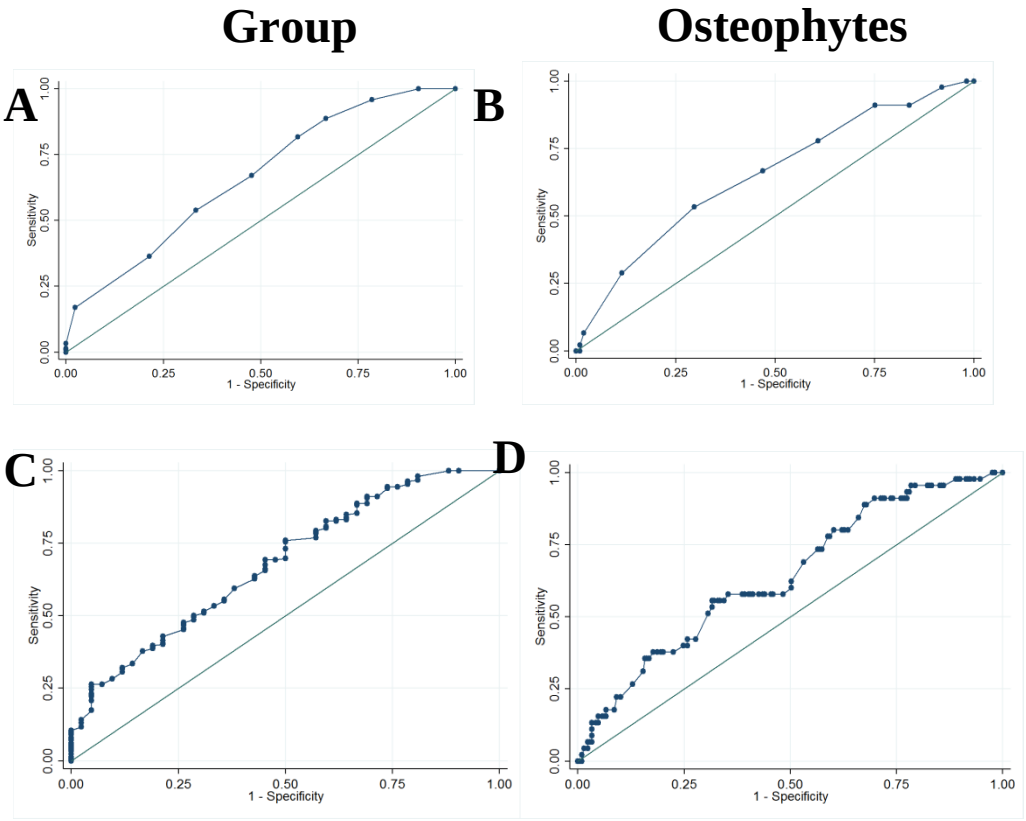


Figure 5.7: Comparison of area under receiver operating characteristic (ROC) curves for the Mankin and weighted score in mild/early OA.

Areas under ROC curve were 0.66 for the Mankin score **(A)** and 0.68 for the weighted score **(C)** in distinguishing between PM cases who were classified as mild/early OA from non-arthritic controls. Areas under ROC curve were 0.65 for the Mankin score **(B)** and 0.64 for the weighted score **(D)** in distinguishing between PM knees with or without osteophytes. The diagonal line represents level of prediction by chance alone.

5.16.6 Correlations between histopathological and macroscopic scores

The relationship between the both Mankin and weighted histopathological scores and macroscopic chondropathy scores were examined (table 5.9). Both the total Mankin score (range 0 to 14) and total weighted score (range 0 to 10) were associated with macroscopic score, and were highly correlated with each other.

Table 5.9: Associations of the Mankin and weighted score with macroscopic chondropathy score.

	Total Mankin score	Total weighted score
Macroscopic chondropathy score	0.424**	0.451**
Total weighted score	0.921**	

Associations are expressed as Spearman's rank correlation coefficients. ***P*<0.01

5.17 Identifying the earliest features of knee osteoarthritis

If pathological features of OA are irreversible, early features would be more prevalent than late features. The prevalence of each pathological feature in the medial tibial plateau or synovium was investigated in the PM group (figure 5.8).

The majority of PM cases had at least mild cartilage surface irregularities (87%, cartilage score ≥ 2) and mild proteoglycan loss (91%, proteoglycan score ≥1). Of the PM cases where histologic meniscal degradation was assessed, the majority of cases (80%) showed evidence of at least mild meniscal degeneration (meniscal score ≥1), and 29% severe damage (meniscal score =2). Alteration in chondrocyte morphology (chondrocyte score ≥ 1) was observed in 64% of PM cases. Breaching of the tidemark by channels originating in the subchondral bone was a feature of just over half (52%) of PM cases. Just under one fifth (18%) of PM cases had osteophytes either in the

tibial plateaux, femoral condyle or patella. Only 15% of PM cases displayed histological evidence of synovitis. Mild, moderate and severe synovitis was a feature of 12%, 3%, and 0.3% of PM cases, respectively. Subchondral bone marrow spaces usually contained fatty marrow tissue, but in 14% of cases this was replaced by fibrovascular tissue.

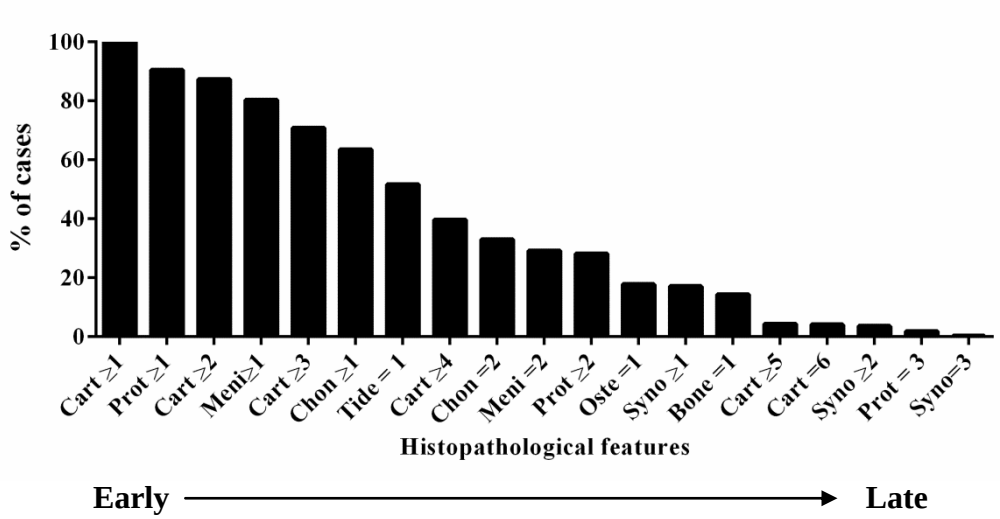


Figure 5.8: Histogram of the commonest pathological features observed in knee tissue collected from 343 post-mortem cases.

The histopathological features towards the left side of the histogram indicate features which may be normal or earlier features of OA as they were most commonly observed. Features towards the right of the histogram may be later features of OA. Cumulative scores are plotted for each variable. Abbreviations: cart = cartilage surface integrity, prot = proteoglycan loss, meni = meniscal degradation, chon = chondrocyte morphology, tide = tidemark breached, oste = osteophytes present, syno = synovial inflammation, bone = subchondral bone marrow replacement by fibrovascular tissue. Chondrocyte scores have been compressed. The different histopathological measures are displayed on the x-axis. Cumulative percentages for each histological measure are given, for example cart ≥ 1 indicates the percentage of cases that had a cartilage surface integrity score of 1 or above (i.e., between 1 and 6), cart ≥ 2 indicates the percentage of cases that were scored between 2 and 6, etc. Histological meniscus scores were recorded for 168/343 (49%) PM cases.

In order to further investigate which features might characterise early OA, histological scores were compared between non-arthritic controls and early OA

cases (figure 5.9). PM cases were classified as non-arthritic controls, or mild/early OA cases based on macroscopic appearance and history, and histological scores compared between groups. Histological features were considered "early" if histological severity scores differed significantly between non-arthritic control and early OA groups. In order to identify later features of OA, histological scores from both PM groups were also compared with TKR cases (end-stage OA). Non-arthritic controls were significantly younger than early OA and end-stage OA cases (table 5.1).

Each item subscore was higher in end-stage OA cases compared to early OA groups. Furthermore, tidemark breaching was observed more frequently in the early OA group (55%) than in non-arthritic controls (30 %) (P = 0.02). Significant differences in synovitis, bone marrow replacement and other cartilage parameters were restricted to the end stage OA group. Subchondral bone marrow replacement was more common in end-stage OA compared to early OA cases (42% vs. 16%, respectively, P<0.01).

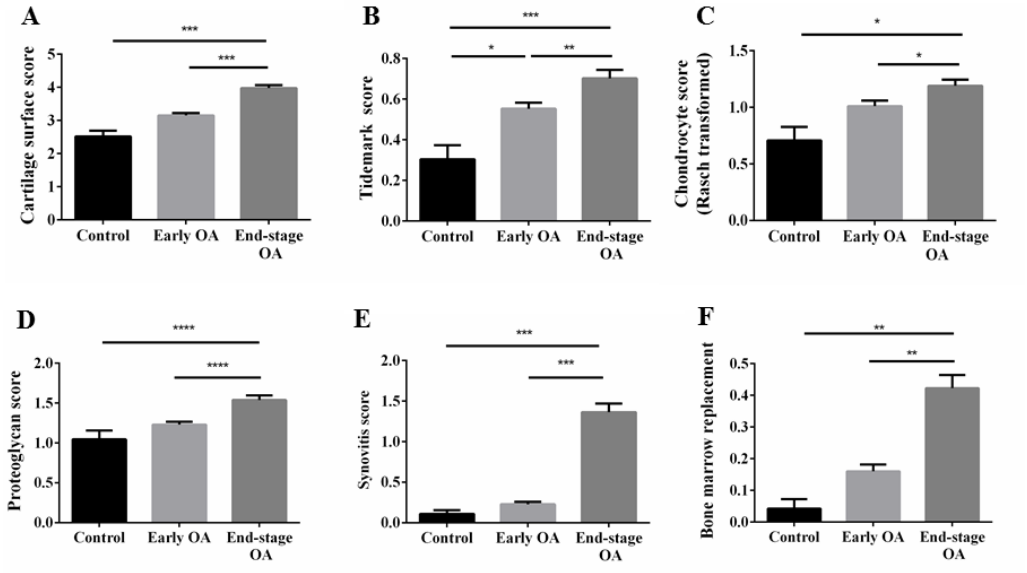


Figure 5.9: Histograms illustrating histopathological differences between non-arthritic controls, mild/early OA and end-stage OA cases.

For cartilage surface irregularity scores **(A)**, tidemark breaching **(B)**, Rasch compressed chondrocyte morphology scores **(C)**, proteoglycan scores **(D)**, synovitis scores **(E)** and subchondral bone marrow replacement by fibrovascular tissue **(F)**. Data presented as mean (+S.E.M). Differences between groups were compared using a

multinomial regression analysis adjusted for age and gender. *P<0.05 **P<0.01 ****P<0.0001.

5.18 Latent class analysis

5.18.1 Whole dataset

A 3-class model was identified as the best fitting solution by LCA analysis. The fit indices determined by the LMR and BLRT test revealed that the 3-class model was a better fit than the 2-class model, but the 4-class model was no better than the 3-class model. Lower Akaike Information Criteria (AIC) and sample size adjusted Bayesian Information criteria (SSAdj. BIC) values for the 3-class model compared to the 2-class model indicated better fit (table 5.10). Entropy values for the 2-class model were similar to the 3-class model and above 0.8 (0.929 vs. 0.921). Overall 449/486 cases (92%) could be assigned to a particular class with a probability of at least 0.8.

Class 1 was the largest class, with 343 (71%) members, class 2 had 69 (14%) members and class 3 had 74 (15%) members. Both PM and TKR cases were assigned to each latent class. The majority of PM cases classified as non-arthritic controls were allocated to class 1 (90%); the remaining 10% were allocated to class 2. Demographic, macroscopic and histopathological characteristics were compared between the classes (table 5.11). Classes did not significantly differ by age or gender.

Table 5.10: Latent class models fit indices in whole dataset.

Model	AIC¶	SS.Adj BIC¶	Entropy†	BLRT (*P-value*)	LRM (*P-value*)	Classes
1-class	5715.04	5728.19	NA	NA	NA	1: n = 486 (100%)
2-class	5379.17	5399.41	0.929	0.000	0.000	1: n = 414 (85%),
						2: n = 72 (15%)
3-class	5104.84	5132.17	0.921	0.0081	0.0089	1: n = 343 (71%)
						2: n =69 (14%)
						3: n = 74 (15%)
4-class	5093.18	5127.6	0.783	0.14	0.15	1: n = 70 (14%)
						2: n = 231 (48%)
						3: n = 107 (22%)
						4: n =78 (16%)

Fit indices determined by LMR and BLRT tests indicate that the 3-class model was a better fit than the 2-class model, but the 4-class model was no better than the 3-class model. Abbreviations; AIC = Akaike Information Criteria, SS Adj. BIC = Sample size adjusted Bayesian Information Criterion ¶Lower AIC and SSAdj. BIC values indicate better fit. †Entropy values >0.8 indicate good fit.

5.18.2 Class 1: No synovitis, mild structural change

Class 1 was formed of 84% PM cases and 16% TKR cases. Cases were characterised by an absence of synovitis, and lower macroscopic and histological indices of OA (cartilage surface loss and subchondral bone marrow replacement by fibrovascular tissue), compared to class 2 or 3 (table 5.11).

5.18.3 Class 2: Mild synovitis and moderate structural change

Class 2 comprised of 59% PM and 41% TKR cases. Cases were characterised by more severe cartilage surface integrity loss, higher chondropathy scores, and were more likely to osteophytes than those assigned to class 1 (table 5.11) . Furthermore, all cases within this class showed evidence of mild (grade 1) synovial inflammation. The presence of subchondral bone marrow replacement by fibrovascular tissue was increased compared to class 1 (33% vs. 16%, respectively $P = 0.007$), but was not significantly less than cases in class 3.

5.18.4 Class 3: Moderate or severe synovitis, severe structural change

Class 3 comprised mainly of TKR cases (81%) and were more likely to display osteophytes than cases within class 2 (table 5.11). Generally, histopathological features in this group were more severe than seen in class 1 and 2. Cartilage surface integrity loss, the presence of subchondral bone marrow replacement and macroscopic chondropathy score were all significantly increased compared to class 1, but were not significantly different compared to class 2. Severity of synovitis was increased compared to class 2. The presence of tidemark breaching, alterations in chondrocyte morphology and proteoglycan score but did not reach statistical significance.

Table 5.11: Clinical characteristics of the 3 latent classes.

	Classes		
	1	**2**	**3**
N	343	69	74
% TKR	16	41	81
Age	65 (58-72)	68 (62-76)	67 (61-74)
% male	57	55	43
% osteophytes	30	**51†**	**85¥**
Macroscopic chondropathyδ	96 (66-135)	**134 (91-190)†**	**203 (169-243)‡**
Cartilage surface integrity (0-6)	3 (2-4)	**4 (3-4) †**	**4 (3-4)‡**
Chondrocyte morphology (0-2)	1 (0-2)	1 (0-2)	1 (1-2)
Proteoglycan loss (0-4)	1 (1-2)	1 (1-2)	1 (1-2)
Tidemark breaching (% of cases)	55	61	66
Synovitis (0-3)	0 (0-0)	1 (1-1)	**2 (2-3)§**
Subchondral bone marrow replacement (% of cases)	16	**33†**	**41‡**

Data presented as median (interquartile range) unless otherwise stated,δ Macroscopic chondropathy scores available for 221 (64%) of class 1, 42 (61%) class 2 and 12 (16%) of class 3 cases. † $P \leq 0.01$ versus class 1, ‡ $P \leq 0.001$ versus class 1, § $P \leq 0.001$ versus class 2, ¥ $P \leq 0.0001$ versus class 1 and 2.

5.18.5 Clinical characteristics of TKR cases

Clinical information was available for 143 TKR cases (table 5.12), but was limited for PM cases which precluded such analysis in these cases. Classes did not significantly differ by symptom duration, previous surgery or fracture, morning or inactivity stiffness, warmth, effusion or synovial thickening detected by clinical examination, nor the presence of Heberden's nodes (table 5.12). Cases assigned to class 3 were more likely to have had surgery on their right knee (77%) than were those in classes 1 (58%) or 2 (46%).

5.18.6 Analgesic use

No significant differences were found between classes in the percentages of cases who were or were not using any analgesic medication prior surgery *(P* = 0.653). More cases in class 3 reported taking paracetamol (72%) compared to class 1 (47.3%, *P* = 0.02), and more cases in class 1 reported taking anti-neuropathic medications (20%) compared to class 3 (5%, *P* = 0.03). NSAID and opiate use did not differ significantly between classes (figure 5.10).

Table 5.12: Clinical characteristics defining the 3 latent classes in total knee replacement cases.

		Classes			
		1 (n=55)	**2 (n=28)**	**3 (n=60)**	**P value**
Symptoms onset in joint	5 yrs +	95	100	95	0.467
Previous surgery or fracture to biopsied joint	None	76	75	82	0.678
	Athroscopy	24	21	18	
	Fracture	0	4	0	
Morning stiffness in biopsied joint	< 30 mins	96	89	88	0.264
	30 mins – 1hr	4	11	10	
	2hrs +	0	0	2	
Inactivity stiffness in biopsied joint	N/A	0	3	0	0.063
	< 30 mins	96	93	87	
	30 mins – 1hr	4	4	12	
	2hrs +	0	0	2	
Increased warmth in biopsied joint	(% yes)	95	100	92	0.287
Effusion in biopsied joint	(% yes)	78	96	77	0.069
Synovial thickening in biopsied joint	(% yes)	76	89	73	0.240
Herberden's nodes	(% with at least one)	9	18	10	0.499
Laterality	(% right knee)	58	46	77	0.013

All data are presented as % unless otherwise stated.

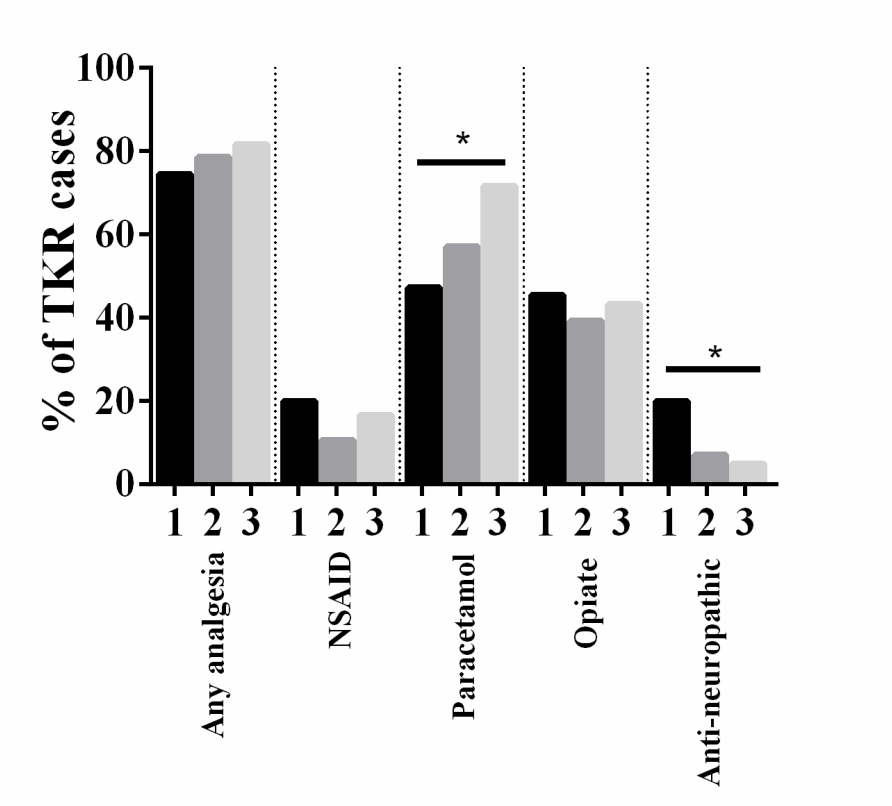


Figure 5.10: Analgesic uses of TKR cases within each latent class.

Percentage of TKR cases who took any analgesia, non-steroidal anti-inflammatories (NSAIDs), paracetamol, opiates or anti-neuropathic medication. *P<0.05 (class 1 vs. 3).

Table 5.13: Classification of analgesic medications used by TKR patients.

Category	Medications
NSAID	Ibuprofen (oral and topical), Diclofenac, Celecoxib, naproxen, celebrex, lodine
Paracetamol	Paracetamol, co-dydramol, kapake, allopurinol, dihydrocodeine,
Opiate	Tramadol, MST, co-codamol, co-dyramol, kapake, dihydrocodiene, oramorph, zomorph
Anti-neuropathic	Doxepin, gabapentin, amitriptyline, clomipramine, felodipine

Abbreviations: NSAID = non-steroidal anti-inflammatory.

5.18.7 Mild/Early OA

In secondary analyses LCA was applied to discrete subsets of cases (i.e, PM and TKR cases, separately). LCA using PM cases only (n = 343) indicated that the 1-class model was the best fitting solution. The fit indices determined by the LMR and BLRT test revealed that the 2-class model was not a better fit than the 1-class model, although the AIC values and SS.Adj BIC were slightly improved (table 5.14).

5.18.8 End-stage OA

Similarly, LCA using only TKR cases (n = 143) indicated that the 1-class model was the best fit. For the 2-class model the LMR and BLRT *P* values did not reach statistical significance, indicating that the 1-class model was the best fit. The AIC and SS.Adj BIC values were improved on the 2-class model, compared to the 1-class (table 5.14).

Table 5.14: Latent class models fit indices in PM cases and TKR cases, separately only

Model	AIC¶	SS.Adj BIC¶	Entropy†	BLRT	LRM	Classes
PM cases only (n =343)						
1-class	3611.84	3620.49	NA	NA	NA	1: n = 343 (100%)
2-class	3312.31	3325.62	0.927	0.380	0.374	1: n = 291 (85%),
						2: n = 52 (15%)
TKR cases only (n=143)						
1-class	1683.39	1680.77	NA	NA	NA	1: n = 143 (100%)
2-class	1641.08	1637.05	0.893	0.22	0.21	1: n = 76 (53%)
						2: n = 67 (47%)

Abbreviations; AIC = Akaike Information Criteria, SS Adj. BIC = Sample size adjusted Bayesian Information Criterion ¶Lower AIC and SSAdj. BIC values indicate better fit. †Entropy values >0.8 indicate good fit

5.19 Summary of results

- Cartilage integrity, chondrocyte appearance, proteoglycan loss, tidemark breaching, subchondral bone marrow replacement and synovitis are all significantly associated with OA.

- Rasch analysis indicated misfit of the Mankin score to the Rasch model. Chondrocyte morphology showed evidence of disordered thresholds, which was resolved by compressing scores for chondrocyte 'hypercellularity' and 'cloning'. The person separation index (PSI) which is a measure of reliability was low (< 0.7) for the Mankin score.

- The weighted score was better than the Mankin score for distinguishing end-stage OA from PM cases (AUC values 0.85 vs. 0.75, respectively, $P< 0.0001$) and between knees with or without osteophytes (AUC 0.79 vs.0.73, $P = 0.0001$).

- Significant increases in tidemark breaching were seen in the early OA group, compared to non-arthritic controls, whereas significant differences in synovitis, bone marrow replacement and other cartilage parameters were restricted to the end stage OA group.

- Latent class analysis identified three histological subgroups, each comprised of PM and TKR cases. Latent class analysis identified a subgroup of people with mild chondropathy and absence of synovitis, and for 2 subgroups with established chondropathy distinguished by the severity of synovitis.

DISCUSSION

This chapter attempted to address some of the limitations of Mankin's logically derived histological scoring method for OA, by improving its measurement and classification properties and addressing the multi-tissue nature of this disease. These data suggest that loss of tidemark integrity may be a feature of early OA, whereas synovitis is more common in severe and established disease.

Latent class analysis identified 3 latent classes based on histopathological characteristics, which might correspond to mild chondropathy with no synovitis, and established/severe chondropathy distinguished by the severity of synovitis. This study was unable to demonstrate a range of latent class groups of unequivocally normal knees suggests that, in this study population, the high prevalence of early OA pathology precludes a pathological classification of disease onset. Future research might better aim to prevent progression to symptomatic disease, rather than to prevent the development of early OA.

OA is a multi-tissue disease (Loeser et al., 2012) whereas histopathological scoring systems often focus on pathology in one tissue type only, most commonly the articular cartilage (Mankin et al., 1971, Pritzker et al., 2006). Standardised scoring systems are needed to address the severity of OA histopathology in human tissue specimens. The histological score developed by Mankin (Mankin et al., 1971) is widely used but is subject to limitations (Ostergaard et al., 1999, Pritzker et al., 2006). Evaluation of internal construct validity of the Mankin score using Rasch analysis has not previously been reported.

Overall the Mankin score was reasonably well targeted and the items were unidimensional. Unidimensionality suggests that each individual item score when summed together is measuring a single construct or trait (in this case OA severity), which is essential for a well-functioning scoring system.

This study is the first to examine the scoring structure of the individual Mankin components. Chondrocyte morphology scoring was disordered, a score of '1' (chondrocyte hypercellularity) was rarely observed. Two rescore options where chondrocyte hypercellularity scores were compressed with normal chondrocyte

scoring (score of 0), or with chondrocyte cloning (score of 2) were explored, both compressions improved overall fit to the Rasch model. The latter compression was used in subsequent analyses as it better represents chondrocyte hypercellularity as a pathological alteration in OA, rather than a normal feature. The rationale was logically derived (there is no clear pathological reason why scores "1, hypercellularity" and "2, cloning" should be ordered). Chondrocyte hypercellularity and cloning may therefore not represent incremental OA severity, but rather be parallel processes in cartilage samples with similar chondropathy.

The use of the Mankin score in mild/early OA was first examined using knee tissue obtained at PM. PM donors had died from an unrelated illness, and mild changes in the articular cartilage were anticipated, since prevalence of OA is associated with ageing (Felson et al., 1987). The Mankin grading system displayed limitations as a measurement tool in cases with mild/early knee OA, which is likely to be because the score was developed using specimens with severe OA. This finding is consistent with previous work, where the scoring system displayed poor discrimination in cases with mild/moderate OA (Ostergaard et al., 1999).

The person separation index (PSI) which informs the ability of the scoring system to differentiate between cases was lower than the acceptable value of 0.7 in all analyses (Shea et al., 2009). These findings suggest that the Mankin score may not be sensitive enough to distinguish between different severities of pathology. Furthermore, the fit indices may be unreliable due to a low PSI (Ayele et al., 2014). PSI may be increased by adding more items to the scale or a wider range of scores by increasing the person sample. The Spearman-Brown Prophecy formula was used to calculate the number of items in the 4-item Mankin score needed to achieve an acceptable measure of reliability. Between 8-13 items were needed to improve PSI to an acceptable level. For the weighted score an additional 2 items were added to the 4 Mankin components which slightly improved the PSI, although this was still poor. Rasch analysis of the 6-item scale confirmed unidimensionality.

In order to extend the Mankin score to develop a validated histopathological score that reflects OA as a multi-tissue disease, scores for synovitis and subchondral bone marrow replacement were included. The rationale behind the weighting given to each structural feature in the Mankin score is unclear in the original publication and the relevance each of feature to OA pathogenesis has not yet been assessed. PCA was used to determine the potential value of structural changes in the pathology of OA. Cartilage surface integrity and synovitis were the highest loading components, suggesting a larger contribution to OA pathology classification.

OA is a multi-tissue disease (Loeser et al., 2012) and this works adds new insights into the importance of considering tissue types other than articular cartilage when measuring OA changes in the knee joint. The weighted scoring system is a useful measure of joint disease, and by including scores for subchondral bone and synovium pathology is more sensitive to OA changes within the joint, compared to previous standard cartilage assessment alone. Indeed, previous researchers have used modified versions of the Mankin score (Armstrong et al., 1994, Thomas et al., 2007). However, this work extends previous research findings by first assessing the scoring structure of the current Mankin system, and secondly by developing a histological score that better represents OA as a multi-tissue disease. Moreover the histological score was correlated to macroscopic chondropathy scores, which implies both are complementary measures for assessing OA structural severity.

All histological scores tested displayed limitations as measurement tools. The weighted score was no better than the Mankin score at distinguishing between early OA and non-arthritic controls cases, or in distinguishing between symptomatic and asymptomatic cases. Although the weighted score had a larger AUC for the latter comparison, it did not quite reach statistical significance. It is possible that the study may have had insufficient power to detect differences between groups. Further work would be required to better understand the critical pathological features that characterise mild/early OA or reflect clinically important disease progression.

Focal cartilage loss is a key feature of knee OA (Loeser et al., 2012). In this study the majority of tissue sections obtained from PM donations showed at least mild evidence of clefts in the superficial cartilage layer. These findings suggest that mild loss of cartilage surface integrity may be a feature of normal ageing. Cartilage surface loss is an established feature of OA; however it is difficult to determine the stage at which cartilage loss transitions from a normal feature of ageing, to a pathological feature in OA. Moreover there was no significant difference in histological scores for loss of cartilage surface integrity between non-arthritic controls and early OA cases. These results again imply at least mild scores are an earlier feature of the disease. Moreover significant increases in loss of cartilage surface integrity were one of the defining features distinguishing between classes 1 (no synovitis, mild chondropathy) and 2 (mild synovitis, moderate chondropathy). These results suggest that cartilage loss is an important contributor to OA pathology, in particular during the transition from mild to moderate disease.

Tidemark breaching may be an earlier feature of OA, and might contribute less to diagnostic classification than do other aspects of chondropathy and synovitis. Significant increases in tidemark breaching were seen in the early OA group, compared to non-arthritic controls. Indeed, these findings are consistent with results in chapter 3, where tidemark breaching was greater in PM cases with high chondropathy (asymptomatic chondropathy) compared to non-arthritic controls. Loss of tidemark integrity has previously been associated with end-stage disease and symptoms (Mapp et al., 2010). However tidemark breaching alone may not be a defining feature of OA. Additional factors that may occur later in the disease, such as accompanying vascular and neuronal growth, may mediate an association of tidemark breaching to pathology and symptoms (Walsh et al., 2010).

Subchondral bone remodelling is associated with symptoms in OA (Felson et al., 2001, Felson et al., 2007). Results from this study suggest that remodelling may occur later in the disease, since significant changes in subchondral bone marrow replacement were seen in the TKR group compared to early OA cases. Moreover, osteophytes, a hallmark feature of OA (Altman et al., 1986) were

only present in 18% of PM cases, suggesting that they be a later feature of the disease (Pottenger et al., 1990). These findings suggest various aspects of chondropathy occur before subchondral bone remodelling (Bobinac et al., 2003), although this is in contrast to literature hypothesising a role for subchondral changes in the earliest stages of OA (Radin and Rose, 1986). BML, which are associated with histological subchondral bone marrow lesions (Zanetti et al., 2000), might be an early feature, occurring before the development of radiographic OA(Roemer et al., 2013). , Furthermore osteophytes might sometimes be a feature of preclinical disease.

It is possible that other indices of subchondral bone remodelling may play a more important role in the early stages of OA. Osteoclasts and osteoblasts are involved in subchondral bone resorption and formation, respectively. Inhibition of osteoclasts using zoledronate treatment prevented osteoclast-mediated resorption of the calcified cartilage in an animal model of OA (Strassle et al., 2010), suggesting that subchondral bone remodelling may be an important feature of early OA. Future work could address the importance and abundance of osteoclasts and osteoblasts in patients with early stage OA.Meniscal pathology scores were not collected for all PM cases. Of the cases where the meniscus was assessed, 80% showed evidence of at least mild meniscal pathology, implying that meniscal pathology to a degree may be normal or an early feature of knee OA. This work supports previous imaging studies that have suggested degenerative meniscal damage may be a feature of early OA (Englund et al., 2003). Indeed, meniscal tears detected by imaging are highly prevalent in the general population, and incidence increases with age (Englund et al., 2008). Histopathological appearances of meniscal degeneration were also associated with age in this study. Meniscal pathology is a frequent finding in patients with knee OA (Englund et al., 2009) and is strongly associated with disease progression (Berthiaume et al., 2005).

Synovitis is an important characteristic of knee OA (Sellam and Berenbaum, 2010, Wenham and Conaghan, 2010). Incorporating histological scores for these features alongside chondropathy improved ability to distinguish OA from non-OA cases. Synovitis might be a later feature of OA that distinguishes

between cases with moderate and severe OA, In support severe synovial inflammation was present in only 31% of OA cases collected at the time of TKR in one study, suggesting it could be a later feature (Haywood et al., 2003). In contrast, work by Benito and colleagues have suggested synovitis may be an early feature of OA, since inflammation was increased in early OA cases compared to end-stage OA (TKR cases) (Benito et al., 2005). The early OA patients in the study by Benito all fulfilled ACR criteria for knee OA(Altman et al., 1986), had knee pain less than 1 year and had arthroscopic manifestations of OA. Different pathological features of OA often coincide and structural change may have developed before symptom onset. It is difficult to prove whether synovitis precedes or is the result of other tissue changes in the joint, such as chondropathy.

Additionally, recent work by Atukorala et al demonstrated that synovitis, as detected through non-contrast enhanced MRI, is a strong predictor of incidence radiographic knee OA (Atukorala et al., 2014) which implies synovial changes may occur early in the disease. However the patient cohort in the study by Atukorala and colleagues included patients with knee OA, or those who were at high risk of developing OA. It is possible that findings may not be relevant in the general population. Furthermore, alterations in other tissue structures were not measured. Again, it is difficult to prove whether synovitis precedes or is a consequence of pathology derived from other areas of the joint, which may have more relevance in early OA.

In addition to disease progression, synovitis has also been associated with symptoms in OA (Hill et al., 2007, Baker et al., 2010). However, LCA identified a small homogenous subgroup of TKR patients characterised by mild chondropathy and absence of synovitis. Furthermore, the use of anti-neuropathic medication was increased in these cases, suggesting OA symptoms may be mediated by central mechanisms, rather than peripheral joint changes in this group. Following TKR surgery, approximately 20% of patients still have persistent pain, consistent with neuropathic pain (Wylde et al., 2011). Further work would be necessary to determine whether these TKR cases had a poor

outcome following surgery, which would strongly suggest a key role for central sensitisation in mediating knee pain in these patients.

LCA also identified 2 other groups of cases with established chondropathy, distinguished by the severity of synovitis. It is likely that these subgroups represent different degrees of OA severity or different stages of a homogenous pathology. Since age is similar between all 3 classes it is likely that the 3 subgroups identified from LCA represent 'mild', 'moderate' and 'severe' disease, rather than 'early', 'middle' and 'late' OA. Lack of differences in clinical characteristics between the classes may indicate that pathological subgroups cannot be determined by standard clinical characteristics alone. These findings suggest that people within each subgroup may have similar clinical characteristics, consistent with a hidden heterogeneity in OA.

Identifying homogenous subgroups of patients based on OA histopathological phenotypes may ultimately result in important changes in the classification of patients with OA. Furthermore, subgrouping patients will allow for stratification of treatments, by focusing on those which are most likely to modify disease progression and improve outcomes. Availability of pain measures for TKR cases would be beneficial to determine associations between aspects of pain and pathology, and to confirm whether pain phenotypes exist across the groups. This study is necessarily subject to a number of limitations, these are explained in detail in the following chapter (chapter 6, section 6.2.2).

5.20 Conclusions

There are no discrete boundaries between early OA pathology and normal changes within the joint. Synovitis and subchondral marrow replacement by fibrovascular tissue are important characteristics of knee OA and might occur later in the disease. Incorporating histological scores for these features alongside chondropathy improved ability to distinguish OA from non-OA cases. Loss of tidemark integrity may be an early feature of OA, but might contribute less to diagnostic classification than do chondropathy and synovitis. Further work is necessary to determine whether early OA transitions to later OA.

LCA identified 3 histopathological subgroups; a mild subgroup characterised by mild histopathological changes and absence of synovitis, and 2 subgroups with established OA distinguished by the severity of synovitis. Identifying subgroups of patients based on OA histopathological phenotypes will allow for targeted treatments to improve disease outcomes and modify disease progression. Moreover better understanding of pathological processes in early disease is needed to inform further modifications that might improve targeting across the range of OA, including non-TKR populations.

CHAPTER 6: CONCLUSIONS AND FUTURE DIRECTIONS

Arthritic disease is a major source of pain and disability in the middle aged to elderly population, and it places a major economic burden on society (Bitton, 2009). Osteoarthritis (OA) is the most common type of arthritis and the knee joint is one of the most commonly affected sites. OA was previously regarded as a disease primarily of the articular cartilage, it is now clear that all tissues within the joint are affected by OA (Loeser et al., 2012). Pathological features are typified by articular cartilage degradation, with an accompanying remodelling of the subchondral bone. In addition to synovial inflammation, which is a recognised feature in both early (Benito et al., 2005) and late stage disease (Haywood et al., 2003), and meniscal changes (Ashraf et al., 2011).

Pain is the predominant symptom of OA, and although joint pathology contributes to pain, the relationship between structural pathology and pain is not entirely clear (Bedson and Croft, 2008). The major aim of this thesis was to better understand the role of joint pathology in OA pain.

Elucidating the earliest intrinsic tissue changes in OA is extremely challenging, since structural change may develop in the absence of symptoms. Furthermore OA is a heterogeneous disease, and the sequence of disease progression is widely debated. Secondary objectives of this thesis were to determine the earliest features of OA and to classify subgroups of patients based on histopathological characteristics.

In this thesis evidence is presented to suggest that symptomatic OA is mediated by specific structural alterations in the joint, whereas other changes may be coincidental. In particular, synovial inflammation and in addition the up-regulation of pro-nociceptive and inflammatory molecules appear to contribute to symptomatic OA.

6.1 KEY FINDINGS FROM THIS THESIS

The main findings that have arisen from this thesis are listed below:

- A range of histopathological features in the synovium and medial tibial plateaux were associated with OA, however not all were associated with symptoms. Synovitis, increased synovial NGF immunoreactivity, chondrocyte changes and loss of cartilage surface integrity were associated with symptoms. Better understanding of the structural features associated with symptoms is crucial to developing targeted analgesic treatments.

- This work has identified new potential therapeutic targets within the synovium that may play a key role in symptomatic OA. Of these, chemokine ligand 2/monocyte chemoattractant protein-1 (CCL2/MCP1) may have a particular importance in symptomatic OA.

- OA is a disease of the whole joint. Incorporating histological scores for synovitis and subchondral bone marrow replacement in addition to aspects of chondropathy improved histological classification of OA and non-OA specimens compared to previous scoring systems.

- Synovitis is a key feature of knee OA. It is associated with symptoms, and appears to occur later in the disease. Moreover severity of synovitis is a key feature in distinguishing between 2 groups of established OA cases. Identifying subgroups of patients based on OA histopathological phenotypes will allow for the development of targeted treatments to improve disease outcomes and modify disease progression.

6.1.1 Histological and molecular features associated with symptomatic osteoarthritis

The relevance of structural changes to OA symptoms have been difficult to determine (Dieppe et al., 1997, Bedson and Croft, 2008). Radiographs are often weakly correlated with OA symptoms, and are insensitive to detect discrete histological or molecular changes within the joint that may directly mediate

pain in OA patients. Possible associations of structural features with OA symptoms have been determined through imaging studies (Hill et al., 2007, Felson et al., 2007); however studies of associations with histopathology have been limited.

This thesis provides evidence for a key contribution of histological synovitis to symptomatic OA. This finding supports imaging studies that demonstrate an association between synovial changes and OA knee pain (Baker et al., 2010, Hill et al., 2007, Zhang et al., 2011b). Moreover synovial changes detected by MRI are associated with histological evidence of synovitis (Loeuille et al., 2005). In addition to contributing to symptoms, synovitis is associated with increased chondropathy and may also predict structural damage in OA (Ayral et al., 2005, Walsh et al., 2009). Since pathological features typically coincide in OA, it is difficult to determine the specific cause of pain. Work presented within this thesis showed that synovitis is associated with symptomatic OA independent of the severity of chondropathy.

The characteristics of synovitis that might mediate an association with symptomatic OA were explored. Macrophage infiltration was increased in OA as previously reported (Benito et al., 2005) but the presence of macrophage infiltration alone may not be sufficient to explain pain.

The nociceptive roles of NGF are increasingly being recognised, and NGF is elevated in rheumatoid arthritis and spondyloarthritis (Halliday et al., 1998, Barthel et al., 2009). Indeed clinical trials to inhibit NGF have shown promise in reducing OA knee pain (Lane et al., 2010, Sanga et al., 2013), indicating a causal link between NGF and symptoms. The data presented in this thesis support a key association of elevated synovial NGF immunoreactivity with symptomatic OA. Synovial fibroblasts, and to a lesser extent, synovial macrophages were found to be an important source of NGF. NGF may mediate pain in the synovium through acting on sensory nerves or through the release of other pro-inflammatory mediators (Manni et al., 2003).

Microarray analysis identified a number of additional potential targets for developing new analgesic treatments. A recent study has identified differences in gene expression patterns between normal and inflamed areas of the

synovium from 12 OA patients (Lambert et al., 2014). Lambert and colleagues also detected an up-regulation (1.7) fold of chemokine ligand 2/monocyte chemoattractant protein-1 (CCL2/MCP-1) in inflamed areas of synovium compared to non-inflamed areas. The work reported in this thesis extends these findings by identifying gene expression patterns which are associated with pain in OA patients, compared to asymptomatic PM donors with similar structural severity of OA.

One of the potential therapeutic targets identified from this work was CCL2/MCP1. CCL2/MCP1 is released from synovial fibroblasts (Eisinger et al., 2012) and might contribute to pain through recruiting and activing other inflammatory cells to sites of inflammation (Voscopoulos and Lema, 2010). One of the mechanisms by which CCL2 might mediate pain during inflammation is through activation of the TRPV1 receptor (Spicarova et al., 2014). CCL2 mediates its effects through its receptor CCR2, which is also activated by CCL8. Since CCL8 was also upregulated and associated with pain it is possible that the CCL2/CCL8/CCR2 axis may be an important pathway contributing to symptomatic OA. Mice that are deficient in the CCR2 receptor do not develop movement provoked pain (Miller et al., 2012), further suggesting that activation of CCR2 receptors is an important event in pain pathogenesis. Therapeutic strategies to block the CCR2 receptor may provide novel therapeutic strategies to alleviate OA knee pain.

6.1.2 Histological features of early and mild osteoarthritis and subgroups

The histological Mankin score is widely used to assess OA structural pathology. Although additional grading systems have been developed to improve histological assessment (Pritzker et al., 2006) they are limited by their focus on articular cartilage pathology. This thesis describes methodology development to improve OA histological classification. Including scores for synovitis and subchondral bone replacement in addition to determining relevant weightings for each component improved OA classification compared to the Mankin score. Subchondral bone remodelling and synovitis are being increasingly recognised as important contributors to OA pathogenesis and symptoms (Li et al., 2013, Sellam and Berenbaum, 2010), and should be

considered when assessing structural pathology of the whole joint. The score developed is a useful measure to assess OA histopathology and should be considered in future histopathological studies.

The sequence of OA progression has widely been debated, it is unknown whether OA develops in a temporal manner, or whether multiple pathologies eventually converge to facilitate total joint failure. It is likely that different phenotypes of OA patients exist. Identifying homogenous subgroups of OA patients is currently an important goal within the research field. Classifying patients based on specific phenotypic characteristics would allow for targeted therapies by focusing on those which are most likely to modify disease progression and improve outcomes. A recent review (Driban et al., 2010) has highlighted potential clinical stratification systems for classifying OA patients. Indeed, OA patients can be stratified according to mechanism of onset, by the severity of symptoms, or therapeutic response to treatment. However stratifying OA cases based on severity and patterns of histopathology has not previously been reported.

Three classes were identified from LCA. LCA provides evidence for the existence of a mild chondropathy group with no synovitis, moderate chondropathy group, with mild synovitis and severe chondropathy group with moderate/synovitis. These subgroups are more likely to represent mild to severe disease, rather than early to late since age was not different between groups. Synovitis is an important characteristic defining differences between groups and appears to be associated with more severe structural changes (Ayral et al., 2005, Walsh et al., 2009).

The use of anti-neuropathic medication in TKR cases was greater in cases with ‘mild OA’ compared to those with ‘severe OA’ (20% vs. 5%, respectively). This indicates potential differences in pain processing between groups, where the pain experienced by TKR cases in the ‘mild OA’ class may be partly attributed to alterations in central pain processing. These pilot findings should be validated on a larger sample. Furthermore collection of pain measures is essential to identify potential associations between pain mechanisms and histopathological classifications.

Defining early OA is extremely challenging. Moreover there is limited access to study joint tissue from people with 'early OA' whose pain is less than that which would lead them to undergo joint replacement. OA is associated with ageing, therefore access to joint tissue donated from PM donors who had died from an unrelated illness, and were mostly middle aged to elderly, is of value.

Histological comparisons revealed that tidemark breaching might be an earlier feature of OA than previously recognised (Walsh et al., 2007). It is possible that growth of blood vessels and nerves into the articular cartilage occur later in the disease (Wojtys et al., 1990, Mapp et al., 2010, Walsh et al., 2010). Histological aspects of chondropathy (loss of surface integrity, chondrocyte abnormalities and proteoglycan loss) were commonly detected features in PM cases, suggesting that these features may be early features of OA. In contrast, synovitis and subchondral bone remodelling may have more relevance in the later stages of disease.

6.2 LIMITATIONS

The results presented in this thesis provide evidence for the importance of synovial inflammation in mediating pain in OA, in addition to distinguishing between different subgroups of OA phenotypes. The studies reported are however necessarily subject to a number of limitations.

6.2.1 Histological and molecular associations of symptomatic OA

The study assumes the asymptomatic chondropathy cases were in less pain than the symptomatic chondropathy group, as they had not sought help for knee pain in the last year of life. Clinical data acquisition in PM cases relies on case notes, where knee pain may not have been reported, and from interviews with bereaved relatives, who may not have been aware of symptoms.

Histological analysis was performed on only one section of osteochondral tissues per case obtained from the mid-coronal section of the middle third of the medial tibial plateaux, a key weight-bearing site. It is possible that different structural associations with symptoms may occur at other sites within the joint. Furthermore, the symptomatic chondropathy cases all had end-stage OA

(sought TKR) and different structural features may be associated with early OA pain.

The study design avoided confounding by age in characterisation of features associated with OA, but it was not possible to simultaneously match for sex. Matching for chondropathy severity precluded age matching between symptomatic and asymptomatic chondropathy groups, even when using a source repository containing samples from > 1700 cases. However, age differences were adjusted for in the analyses.

The number of cases included in the molecular study design was determined by the availability of fresh synovial tissue for asymptomatic and symptomatic chondropathy cases with matched chondropathy. It was however not possible to match for age or sex. Age was significantly greater in the asymptomatic group, and was inversely correlated with the expression of 5 out of 92 target genes; interleukin -1 converting enzyme (CASP1), interleukin-1 receptor (IL-1R1), peroxisome proliferator-activated receptor-alpha (PPAR), tumour necrosis factor (TNF) and the ligand of receptor activator of nuclear factor (RANKL/TNFSF11). In other words expression of these 5 genes decreased as the age of the PM cases increased, and these 5 genes were significantly different between groups. Gene expression of CASP1, TNF and RANKL were significantly increased in the symptomatic chondropathy group. It is possible that these differences may be partly attributed to the age-related decline of these 3 genes observed in post-mortem tissue.

One of the major concerns with comparing knee tissue obtained from PM donors with that obtained at TKR is the potential of biased results due to post-mortem decay. Tissues obtained at PM were not collected until 24-48 hours after death; the tissue may have undergone natural decay in the body before fixation. The time, in hours, between death and tissue collection is referred to as the "post-mortem delay". In the histological associations study, NGF and macrophage immunohistochemical parameters were stable with a range of post mortem delay or ex vivo incubation of tissues. Protein abundance did not appear to significantly decrease with increasing PM delay. In general synovial gene expression patterns in this study appeared to be stable with increased post

mortem delay. Although for one gene, CCL4, expression may be partly affected by post mortem delay, since reduction in CCL4 expression was associated with increasing PM delay interval.

Gene expression patterns were identified using microarray analysis, however many of the fold changes in gene expression between groups were quite small (< 2). These findings therefore need to be validated, ways of which are discussed in section 6.3.

6.2.2 Osteoarthritis as a multi-tissue disease and features of early knee osteoarthritis

In order to identify early features of OA PM cases were classified as 'early OA' if they did not fit the criteria to be classified as non-arthritic controls. It is likely that not all of the early OA PM cases had 'early OA' and some of the histopathological changes observed may be attributed to normal ageing. However since the prevalence of OA strongly increases with age, and 21% of early OA cases had osteophytes, (the hallmark diagnostic criteria for OA) it is likely that some of these cases did have early or preclinical signs of the disease. The study design was cross-sectional (i.e., the data was collected at one time point), and will also include some people who are normal and not osteoarthritic when characterising early features of OA.

In LCA each PM and TKR case was given a probability of membership to each group. Cases were allocated to the class which they had the highest probability of membership. The class allocations therefore are not discrete entities and this should be considered when considering differences between the classes. Nevertheless, 449/486 cases (92%) could be assigned to a particular class with a probability of at least 0.8.

There was disparity in the number of classes identified when using the whole dataset combining PM and TKR cases (3 classes), and when analysing PM and TKR cases separately (both 1-class models). These differences may be attributed to a larger and more heterogeneous sample population when using the whole dataset (i.e., wider range of histology scores). Within the PM group, a range of structural changes are observed and the same is true for the TKR

group. It is likely that the range of severity within each group is not wide enough to detect large enough differences to represent homogenous subgroups.

The weighted score included scores for synovitis and subchondral bone marrow replacement to better reflect OA as a multi-tissue disease. One of the limitations of the score is the need for synovial tissue in addition to tibial plateaux. Indeed, at TKR synovial tissue is not always routinely collected. Therefore this would limit calculation of an overall OA severity score.

6.3 FUTURE DIRECTIONS

This study presents an important contribution to better understanding the role of joint pathology in OA pain, and has shown promise in identifying discrete subgroups of OA patients based on histological characteristics. Further work is required to confirm and validate these findings.

Tidemark breaching has previously been associated with pain and OA progression. Work in this thesis suggests that the presence of tidemark breaching may be an early feature of OA and breaching alone might not be associated with symptoms. Instead, progressive blood vessel and nerve growth into the usually aneural and avascular articular cartilage may mediate an association with pain. However asymptomatic and symptomatic cases matched for macroscopic chondropathy had a very restricted range of OA stage, it is possible that tidemark breaching may be associated with pain in patients with more severe degrees of chondropathy. Further work would be required to determine the time course and mechanisms by which channels breaching the tidemark may predispose to pain.

Imaging studies have associated subchondral bone marrow lesions with symptomatic OA (Felson et al., 2001, Torres et al., 2006, Szebenyi et al., 2006). Magnetic resonance detected lesions have been associated with fibrovascular marrow replacement (Zanetti et al., 2000). However as reported in this thesis, bone marrow replacement was not significantly associated with pain, even though it was twice as common in the symptomatic chondropathy group as it was in the asymptomatic chondropathy group. It is likely that this study had insufficient power to detect differences in this parameter between

groups. Future work should investigate the specific structural and biochemical features of bone marrow lesions which may mediate an association with pain. For example, a microarray analysis of differentially expressed genes in the bone marrow of symptomatic chondropathy cases would provide a useful insight into associations of gene expression patterns with pain.

There may be more relevant parameters of subchondral bone remodelling that better associate with symptomatic OA. Osteoclasts are partially responsible for subchondral bone turnover and inhibition of osteoclasts appear to inhibit pain behaviour in an animal model of OA (Sagar et al., 2013), suggesting a role of osteoclasts in mediating OA pain. Associations between osteoclasts and symptomatic OA could be addressed in future studies by comparing osteoclast activation in the subchondral bone of asymptomatic and symptomatic chondropathy cases.

The weighted score is a useful measure of OA pathology, and provides new insights into the multi-tissue nature of OA. In future work the score could be translated for use in animal studies of OA to measure disease modifying effects of new treatments. Moreover, it could be used to examine associations between OA severity and other indices of OA such as symptoms, genetic factors etc.

The weighted score improved OA classification but had limitations for use in mild/early OA. This issue could be addressed by developing a new score through determining factor loadings from histological scores derived from mild/early OA cases. These cases would be those PM cases that did not fit the criteria to be classified as non-arthritic controls, or from those cases allocated to latent class 1, characterised by mild structural pathology. Moreover, the score was not significantly better at discriminating between symptomatic and asymptomatic cases with similar chondropathy, possibly due to lack of power. Increasing numbers of asymptomatic and symptomatic chondropathy cases, or increasing the range of chondropathy in future studies may improve classification of asymptomatic and symptomatic specimens.

The most robust way to define histopathological characteristics of early OA would be to measure histopathological features serially to see if cases transition from early to late stage OA. This approach would be difficult to employ in human studies, but could be addressed using animal models with slow progressing OA. Time course experiments could be conducted to determine key histopathological signatures at different time points in order to identify the stage at which the first signs of pathology begin to appear.

The majority of animal models used within OA research are induced chemically or surgically which reflects post-traumatic human OA. Age is a major risk factor for OA (Felson et al., 1987), yet the majority of studies are performed on younger animals. Designing research studies which directly compare young and old animals would provide an interesting and novel insight into the contributing mechanism underlying the association of age to OA pathogenesis. Moreover this would allow for characterisation of early features of the disease.

Latent class analysis revealed a small subgroup of symptomatic TKR cases with mild structural severity and absence of synovitis. It is possible that the pain experienced by these patients may be mediated by alterations in central pain processing, which is associated with poor outcome following TKR surgery (Wylde et al., 2011). The Oxford knee score (OKS) is a 12-item patient reported outcome measure (PROM) developed to assess function and pain. OKS are collected pre-operatively and post-operatively in routine clinical practice in the UK. Associations between histopathological features and outcomes measured by pre and post-operative OKS have not yet been explored. It would be useful to compare post-operative OKS between OA patients with 'mild OA' compared to those with 'severe OA' to determine whether the latent class predicts surgery outcome. Elucidating the key structural features that predict pre and post-operative knee pain would help refine strategies for developing structure-modifying treatments, and individualising patient care by focusing on those treatments which are most likely to improve outcomes.

This thesis has identified potentially important novel molecular targets which may associate synovitis with OA knee pain. Further work is required to validate these results. First, results should be confirmed using individual TaqMan assays. Second, differential expression of the genes should be confirmed at the protein level using techniques such as Western blotting. An additional analysis should include replicating the experiment using a different set of cases with matched chondropathy. Furthermore the addition of a non-arthritic control group would be valuable to determine gene expression levels in normal samples.

6.4 CONCLUDING REMARKS

Pain is the predominant symptom of knee OA, and is the main determinant for patients to seek medical assistance. The link between structural pathology in the joint and pain experienced is not completely understood. All structures within the joint are affected in OA, but not all features may directly contribute to pain. Current modalities to access structural pathology, such as radiographs, MRI and arthroscopy are limited in their ability to identify the specific cellular and molecular determinants of pain.

The findings outlined in this thesis provide evidence for a key role for synovial inflammation in contributing to symptoms in knee OA. In particular up-regulation of pro-nociceptive and inflammatory mediators in the synovium of patients before they have had a knee replacement may partly explain symptoms in OA. Inhibition of these molecular targets may therefore have the potential to provide analgesic relief and structure modifying treatments to OA patients.

Nevertheless the existence of a subgroup of TKR cases characterised by absence of synovial inflammation suggest that analgesic therapies that target inflammation would not be beneficial to all OA patients. Further work is crucial to confirm the existence of phenotypic subgroups and to identify histological signatures that predict poor outcome to TKR surgery. Determining OA phenotypes based on histopathological characteristics may result in important changes in classification of OA patients. This would lead to stratified and individualised treatment, which would ultimately improve outcomes and modify disease progression.

Further studies are essential to confirm molecular associations with symptomatic OA are also observed at the protein level. Moreover determining histopathological predictors of post-operative knee pain would be an extremely useful measure for determining which patients will do well, or have poor outcomes following surgery.

CHAPTER 7: REFERENCES

Abdi, H. & Williams, L. J. 2010. "Principal component analysis". Wiley Interdisciplinary Reviews: Computational Statistics, 2**,** 433-459.

Abramova, T. O., Redina, O. E., Smolenskaya, S. E. & Markel, A. L. 2013. "Elevated expression of the Ephx2 mRNA in the kidney of hypertensive ISIAH rats". Molecular Biology, 47**,** 821-826.

Ackerman, I. N. & Osborne, R. H. 2012. "Obesity and increased burden of hip and knee joint disease in Australia: results from a national survey". BMC Musculoskelet Disord, 13**,** 254.

Adamopoulos, I. E., Danks, L., Itonaga, I., Locklin, R. M., Sabokbar, A., Ferguson, D. J. & Athanasou, N. A. 2006. "Stimulation of osteoclast formation by inflammatory synovial fluid". Virchows Arch, 449**,** 69-77.

Aigner, T., Vornehm, S. I., Zeiler, G., Dudhia, J., Von Der Mark, K. & Bayliss, M. T. 1997. "Suppression of cartilage matrix gene expression in upper zone chondrocytes of osteoarthritic cartilage". Arthritis Rheum, 40**,** 562-9.

Aigner, T. 2012. "Osteoarthritis histopathology grading criteria – a never ending story?". Osteoarthritis and Cartilage, 20**,** 469-470.

Akaike, H. 1974. "A new look at the statistical model identification". Automatic Control, IEEE Transactions on, 19**,** 716-723.

Akobeng, A. K. 2007. "Understanding diagnostic tests 3: Receiver operating characteristic curves". Acta Paediatr, 96**,** 644-7.

Alexander, W. S. 2002. "Suppressors of cytokine signalling (SOCS) in the immune system". Nat Rev Immunol, 2**,** 410-6.

Aloe, L., Tuveri, M. A., Carcassi, U. & Levi-Montalcini, R. 1992. "Nerve growth factor in the synovial fluid of patients with chronic arthritis". Arthritis Rheum, 35**,** 351-5.

Altman, D. G. & Bland, J. M. 1994. "Diagnostic tests 3: receiver operating characteristic plots". BMJ, 309**,** 188.

Altman, R., Asch, E., Bloch, D., Bole, G., Borenstein, D., Brandt, K., Christy, W., Cooke, T. D., Greenwald, R., Hochberg, M. & Et Al. 1986. "Development of criteria for the classification and reporting of osteoarthritis. Classification of osteoarthritis of the knee. Diagnostic and Therapeutic Criteria Committee of the American Rheumatism Association". Arthritis Rheum, 29**,** 1039-49.

Altman, R. D. 1980. "Musculoskeletal manifestations of Paget's disease of bone". Arthritis Rheum, 23**,** 1121-7.

Amadesi, S., Grant, A. D., Cottrell, G. S., Vaksman, N., Poole, D. P., Rozengurt, E. & Bunnett, N. W. 2009. "Protein kinase D isoforms are expressed in rat and mouse primary sensory neurons and are activated by agonists of protease-activated receptor 2". J Comp Neurol, 516**,** 141-56.

Andersen, C. L., Jensen, J. L. & Ørntoft, T. F. 2004. "Normalization of Real-Time Quantitative Reverse Transcription-PCR Data: A Model-Based Variance Estimation Approach to Identify Genes Suited for

Normalization, Applied to Bladder and Colon Cancer Data Sets". Cancer Research, 64**,** 5245-5250.

Andrich D, Lyne A, Sheridan B & G, L. 2003. "RUMM2020". Perth, Australia: RUMM Laboratory.

Antonov, J., Goldstein, D. R., Oberli, A., Baltzer, A., Pirotta, M., Fleischmann, A., Altermatt, H. J. & Jaggi, R. 2005. "Reliable gene expression measurements from degraded RNA by quantitative real-time PCR depend on short amplicons and a proper normalization". Lab Invest, 85**,** 1040-50.

Antony, B., Ding, C., Stannus, O., Cicuttini, F. & Jones, G. 2011. "Association of baseline knee bone size, cartilage volume, and body mass index with knee cartilage loss over time: a longitudinal study in younger or middle-aged adults". J Rheumatol, 38**,** 1973-80.

Arita, M., Ohira, T., Sun, Y. P., Elangovan, S., Chiang, N. & Serhan, C. N. 2007. "Resolvin E1 selectively interacts with leukotriene B4 receptor BLT1 and ChemR23 to regulate inflammation". J Immunol, 178**,** 3912-7.

Armstrong, S., Read, R. & Ghosh, P. 1994. "The effects of intraarticular hyaluronan on cartilage and subchondral bone changes in an ovine model of early osteoarthritis". J Rheumatol, 21**,** 680-8.

Asfaha, S., Cenac, N., Houle, S., Altier, C., Papez, M. D., Nguyen, C., Steinhoff, M., Chapman, K., Zamponi, G. W. & Vergnolle, N. 2007. "Protease-activated receptor-4: a novel mechanism of inflammatory pain modulation". Br J Pharmacol, 150**,** 176-85.

Ashraf, S., Wibberley, H., Mapp, P. I., Hill, R., Wilson, D. & Walsh, D. A. 2011. "Increased vascular penetration and nerve growth in the meniscus: a potential source of pain in osteoarthritis". Ann Rheum Dis, 70**,** 523-9.

Ashraf, S., Mapp, P. I., Burston, J., Bennett, A. J., Chapman, V. & Walsh, D. A. 2014. "Augmented pain behavioural responses to intra-articular injection of nerve growth factor in two animal models of osteoarthritis". Ann Rheum Dis, 73**,** 1710-8.

Asparouhov, T. & Muthen, B. 2012. *Using Mplus TECH11 and TECH14 to test the number of latent classes. MPlus webnotes: No. 14.* [Online]. Available: https://www.statmodel.com/examples/webnotes/webnote14.pdf [Accessed Oct 2014].

Athanasou, N. A. 1995. "Synovial macrophages". Annals of the Rheumatic Diseases, 54**,** 392-394.

Attur, M. G., Patel, R. N., Abramson, S. B. & Amin, A. R. 1997. "Interleukin-17 up-regulation of nitric oxide production in human osteoarthritis cartilage". Arthritis Rheum, 40**,** 1050-3.

Atukorala, I., Kwoh, C. K., Guermazi, A., Roemer, F. W., Boudreau, R. M., Hannon, M. J. & Hunter, D. J. 2014. "Synovitis in knee osteoarthritis: a precursor of disease?". Annals of the Rheumatic Diseases.

Ayele, D. G., Zewotir, T. & Mwambi, H. 2014. "Using Rasch modeling to re-evaluate rapid malaria diagnosis test analyses". Int J Environ Res Public Health, 11**,** 6681-91.

Ayoub, S. S., Yazid, S. & Flower, R. J. 2008. "Increased susceptibility of annexin-A1 null mice to nociceptive pain is indicative of a spinal antinociceptive action of annexin-A1". Br J Pharmacol, 154**,** 1135-42.

Ayral, X., Gueguen, A., Listrat, V., Bahuaud, J., Beaufils , P. & Beguin, J. 1994. "Simplified arthroscopy scoring system for chondropathy of the knee (revised SFA score)". Rev Rhum [Engl Ed], 61**,** 88-90.

Ayral, X., Pickering, E. H., Woodworth, T. G., Mackillop, N. & Dougados, M. 2005. "Synovitis: a potential predictive factor of structural progression of medial tibiofemoral knee osteoarthritis – results of a 1 year longitudinal arthroscopic study in 422 patients". Osteoarthritis and Cartilage, 13**,** 361-367.

Bajaj, P., Bajaj, P., Graven-Nielsen, T. & Arendt-Nielsen, L. 2001. "Osteoarthritis and its association with muscle hyperalgesia: an experimental controlled study". Pain, 93**,** 107-14.

Baker, K., Grainger, A., Niu, J., Clancy, M., Guermazi, A., Crema, M., Hughes, L., Buckwalter, J., Wooley, A., Nevitt, M. & Felson, D. T. 2010. "Relation of synovitis to knee pain using contrast-enhanced MRIs". Ann Rheum Dis, 69**,** 1779-83.

Baldwin, A. S., Jr. 1996. "The NF-kappa B and I kappa B proteins: new discoveries and insights". Annu Rev Immunol, 14**,** 649-83.

Bancroft, J. & Stevens, A. (eds.) 1996. *Theory and Practice of Histological Techniques*: Churchill Livingstone.

Banda, M. J. & Werb, Z. 1981. "Mouse macrophage elastase. Purification and characterization as a metalloproteinase". Biochem J, 193**,** 589-605.

Barland, P., Novikoff, A. B. & Hamerman, D. 1962. "Electron microscopy of the human synovial membrane". J Cell Biol, 14**,** 207-20.

Barthel, C., Yeremenko, N., Jacobs, R., Schmidt, R. E., Bernateck, M., Zeidler, H., Tak, P. P., Baeten, D. & Rihl, M. 2009. "Nerve growth factor and receptor expression in rheumatoid arthritis and spondyloarthritis". Arthritis Res Ther, 11**,** R82.

Bassiouni, H. M. 2010. "Bone marrow lesions in the knee: the clinical conundrum". Int J Rheum Dis, 13**,** 196-202.

Bedson, J. & Croft, P. R. 2008. "The discordance between clinical and radiographic knee osteoarthritis: a systematic search and summary of the literature". BMC Musculoskelet Disord, 9**,** 116.

Ben-Av, P., Crofford, L. J., Wilder, R. L. & Hla, T. 1995. "Induction of vascular endothelial growth factor expression in synovial fibroblasts by prostaglandin E and interleukin-1: a potential mechanism for inflammatory angiogenesis". FEBS Letters, 372**,** 83-87.

Benito, M. J., Veale, D. J., Fitzgerald, O., Van Den Berg, W. B. & Bresnihan, B. 2005. "Synovial tissue inflammation in early and late osteoarthritis". Ann Rheum Dis, 64**,** 1263-7.

Benjamini, Y. & Hochberg, Y. 1995. "Controlling the False Discovery Rate: A Practical and Powerful Approach to Multiple Testing". Journal of the Royal Statistical Society. Series B (Methodological), 57**,** 289-300.

Berberat, J. E., Nissi, M. J., Jurvelin, J. S. & Nieminen, M. T. 2009. "Assessment of interstitial water content of articular cartilage with T1 relaxation". Magn Reson Imaging, 27**,** 727-32.

Berthiaume, M. J., Raynauld, J. P., Martel-Pelletier, J., Labonte, F., Beaudoin, G., Bloch, D. A., Choquette, D., Haraoui, B., Altman, R. D., Hochberg,

M., Meyer, J. M., Cline, G. A. & Pelletier, J. P. 2005. "Meniscal tear and extrusion are strongly associated with progression of symptomatic knee osteoarthritis as assessed by quantitative magnetic resonance imaging". Ann Rheum Dis, 64**,** 556-63.

Bhattacharyya, T., Gale, D., Dewire, P., Totterman, S., Gale, M. E., Mclaughlin, S., Einhorn, T. A. & Felson, D. T. 2003. "The clinical importance of meniscal tears demonstrated by magnetic resonance imaging in osteoarthritis of the knee". J Bone Joint Surg Am, 85-A**,** 4-9.

Binch, A., Cross, A. & Le Maitre, C. 2014. " The regulation of nerve and blood vessel ingrowth in aneural and avascular intervertebral disc and articular cartilage". OA Arthritis, 2**,** 4.

Binshtok, A. M., Wang, H., Zimmermann, K., Amaya, F., Vardeh, D., Shi, L., Brenner, G. J., Ji, R. R., Bean, B. P., Woolf, C. J. & Samad, T. A. 2008. "Nociceptors are interleukin-1beta sensors". J Neurosci, 28**,** 14062-73.

Bitton, R. 2009. "The economic burden of osteoarthritis". Am J Manag Care, 15**,** S230-5.

Black, R. A. 2002. "Tumor necrosis factor-alpha converting enzyme". Int J Biochem Cell Biol, 34**,** 1-5.

Bobinac, D., Spanjol, J., Zoricic, S. & Maric, I. 2003. "Changes in articular cartilage and subchondral bone histomorphometry in osteoarthritic knee joints in humans". Bone, 32**,** 284-90.

Boisclair, Y. R., Wang, J., Shi, J., Hurst, K. R. & Ooi, G. T. 2000. "Role of the suppressor of cytokine signaling-3 in mediating the inhibitory effects of interleukin-1beta on the growth hormone-dependent transcription of the acid-labile subunit gene in liver cells". J Biol Chem, 275**,** 3841-7.

Bondeson, J., Wainwright, S. D., Lauder, S., Amos, N. & Hughes, C. E. 2006. "The role of synovial macrophages and macrophage-produced cytokines in driving aggrecanases, matrix metalloproteinases, and other destructive and inflammatory responses in osteoarthritis". Arthritis Res Ther, 8**,** R187.

Boureau, F., Schneid, H., Zeghari, N., Wall, R. & Bourgeois, P. 2004. "The IPSO study: ibuprofen, paracetamol study in osteoarthritis. A randomised comparative clinical study comparing the efficacy and safety of ibuprofen and paracetamol analgesic treatment of osteoarthritis of the knee or hip". Ann Rheum Dis, 63**,** 1028-34.

Brown, M. T., Murphy, F. T., Radin, D. M., Davignon, I., Smith, M. D. & West, C. R. 2012. Tanezumab reduces osteoarthritic knee pain: results of a randomized, double-blind, placebo-controlled phase III trial. *J Pain.* United States: 2012 American Pain Society. Published by Elsevier Inc.

Bruno, M. A. & Cuello, A. C. 2006. "Activity-dependent release of precursor nerve growth factor, conversion to mature nerve growth factor, and its degradation by a protease cascade". Proc Natl Acad Sci U S A, 103**,** 6735-40.

Buckingham, J. C. & Flower, R. J. 1997. "Lipocortin 1: a second messenger of glucocorticoid action in the hypothalamo-pituitary-adrenocortical axis". Mol Med Today, 3**,** 296-302.

Buckland-Wright, C. 2004. "Subchondral bone changes in hand and knee osteoarthritis detected by radiography". Osteoarthritis Cartilage, 12 Suppl A**,** S10-9.

Buckland-Wright, J. C., Macfarlane, D. G., Jasani, M. K. & Lynch, J. A. 1994. "Quantitative microfocal radiographic assessment of osteoarthritis of the knee from weight bearing tunnel and semiflexed standing views". J Rheumatol, 21**,** 1734-41.

Buckland-Wright, J. C., Macfarlane, D. G., Lynch, J. A. & Jasani, M. K. 1995. "Quantitative microfocal radiography detects changes in OA knee joint space width in patients in placebo controlled trial of NSAID therapy". J Rheumatol, 22**,** 937-43.

Buckland-Wright, J. C., Lynch, J. A. & Macfarlane, D. G. 1996. "Fractal signature analysis measures cancellous bone organisation in macroradiographs of patients with knee osteoarthritis". Ann Rheum Dis, 55**,** 749-55.

Buckland-Wright, J. C., Lynch, J. A. & Dave, B. 2000. "Early radiographic features in patients with anterior cruciate ligament rupture". Ann Rheum Dis, 59**,** 641-6.

Buckwalter, J. A., Mankin, H. J. & Grodzinsky, A. J. 2005. "Articular cartilage and osteoarthritis". Instr Course Lect, 54**,** 465-80.

Bullock, C. M., Wookey, P., Bennett, A., Mobasheri, A., Dickerson, I. & Kelly, S. 2014. "Peripheral calcitonin gene-related peptide receptor activation and mechanical sensitization of the joint in rat models of osteoarthritis pain". Arthritis Rheumatol, 66**,** 2188-200.

Bulstra, S. K., Drukker, J., Kuijer, R., Buurman, W. A. & Van Der Linden, A. J. 1993. "Thionin staining of paraffin and plastic embedded sections of cartilage". Biotech Histochem, 68**,** 20-8.

Burr, D. B. 2004. "Anatomy and physiology of the mineralized tissues: role in the pathogenesis of osteoarthrosis". Osteoarthritis Cartilage, 12 Suppl A**,** S20-30.

Burry, R. W. 2011. "Controls for immunocytochemistry: an update". J Histochem Cytochem, 59**,** 6-12.

Burston, J. J., Sagar, D. R., Shao, P., Bai, M., King, E., Brailsford, L., Turner, J. M., Hathway, G. J., Bennett, A. J., Walsh, D. A., Kendall, D. A., Lichtman, A. & Chapman, V. 2013. "Cannabinoid CB2 receptors regulate central sensitization and pain responses associated with osteoarthritis of the knee joint". PLoS One, 8**,** e80440.

Busch-Dienstfertig, M. & González-Rodríguez, S. 2013. "IL-4, JAK-STAT signaling, and pain". JAK-STAT, 2**,** e27638.

Calvo, E., Palacios, I., Delgado, E., Ruiz-Cabello, J., Hernandez, P., Sanchez-Pernaute, O., Egido, J. & Herrero-Beaumont, G. 2001. "High-resolution MRI detects cartilage swelling at the early stages of experimental osteoarthritis". Osteoarthritis Cartilage, 9**,** 463-72.

Campbell, D. J. 2001. "The kallikrein-kinin system in humans". Clin Exp Pharmacol Physiol, 28**,** 1060-5.

Carney, S. L., Billingham, M. E., Muir, H. & Sandy, J. D. 1984. "Demonstration of increased proteoglycan turnover in cartilage explants from dogs with experimental osteoarthritis". J Orthop Res, 2**,** 201-6.

Caterina, M. J., Schumacher, M. A., Tominaga, M., Rosen, T. A., Levine, J. D. & Julius, D. 1997. "The capsaicin receptor: a heat-activated ion channel in the pain pathway". Nature, 389**,** 816-24.

Cavanaugh, D. J., Chesler, A. T., Braz, J. M., Shah, N. M., Julius, D. & Basbaum, A. I. 2011. "Restriction of transient receptor potential

vanilloid-1 to the peptidergic subset of primary afferent neurons follows its developmental downregulation in nonpeptidergic neurons". J Neurosci, 31, 10119-27.

Chao, M. V. & Hempstead, B. L. 1995. "p75 and Trk: A two-receptor system". Trends in Neurosciences, 18, 321-326.

Chen, B., Deng, Y., Tan, Y., Qin, J. & Chen, L.-B. 2014a. "Association between severity of knee osteoarthritis and serum and synovial fluid interleukin 17 concentrations". Journal of International Medical Research, 42, 138-144.

Chen, J. J., Huang, J. F., Du, W. X. & Tong, P. J. 2014b. "Expression and significance of MMP3 in synovium of knee joint at different stage in osteoarthritis patients". Asian Pac J Trop Med, 7, 297-300.

Chen, L., Lv, F. & Pei, L. 2013. "Annexin 1: A glucocorticoid-inducible protein that modulates inflammatory pain". Eur J Pain.

Chevalier, X., Goupille, P., Beaulieu, A. D., Burch, F. X., Bensen, W. G., Conrozier, T., Loeuille, D., Kivitz, A. J., Silver, D. & Appleton, B. E. 2009. "Intraarticular injection of anakinra in osteoarthritis of the knee: A multicenter, randomized, double-blind, placebo-controlled study". Arthritis Care & Research, 61, 344-352.

Christensen, R., Astrup, A. & Bliddal, H. 2005. "Weight loss: the treatment of choice for knee osteoarthritis? A randomized trial". Osteoarthritis and Cartilage, 13, 20-27.

Chung, C. D., Liao, J., Liu, B., Rao, X., Jay, P., Berta, P. & Shuai, K. 1997. "Specific inhibition of Stat3 signal transduction by PIAS3". Science, 278, 1803-5.

Cicuttini, F. M., Jones, G., Forbes, A. & Wluka, A. E. 2004. "Rate of cartilage loss at two years predicts subsequent total knee arthroplasty: a prospective study". Ann Rheum Dis, 63, 1124-7.

Claes, S., Vereecke, E., Maes, M., Victor, J., Verdonk, P. & Bellemans, J. 2013. "Anatomy of the anterolateral ligament of the knee". J Anat, 223, 321-8.

Clark, J. M. 1990. "The structure of vascular channels in the subchondral plate". J Anat, 171, 105-15.

Clockaerts, S., Bastiaansen-Jenniskens, Y. M., Feijt, C., Verhaar, J. a. N., Somville, J., De Clerck, L. S. & Van Osch, G. J. V. M. 2011. "Peroxisome proliferator activated receptor alpha activation decreases inflammatory and destructive responses in osteoarthritic cartilage". Osteoarthritis and Cartilage, 19, 895-902.

Cohen, S. B., Proudman, S., Kivitz, A. J., Burch, F. X., Donohue, J. P., Burstein, D., Sun, Y. N., Banfield, C., Vincent, M. S., Ni, L. & Zack, D. J. 2011. "A randomized, double-blind study of AMG 108 (a fully human monoclonal antibody to IL-1R1) in patients with osteoarthritis of the knee". Arthritis Res Ther, 13, R125.

Collins, C. E., La, D. T., Yang, H.-T., Massin, F., Gibot, S., Faure, G. & Stohl, W. 2009. "Elevated synovial expression of triggering receptor expressed on myeloid cells 1 in patients with septic arthritis or rheumatoid arthritis". Annals of the Rheumatic Diseases, 68, 1768-1774.

Conaghan, P. G., Tennant, A., Peterfy, C. G., Woodworth, T., Stevens, R., Guermazi, A., Genant, H., Felson, D. T. & Hunter, D. 2006.

"Examining a whole-organ magnetic resonance imaging scoring system for osteoarthritis of the knee using Rasch analysis". Osteoarthritis and Cartilage, 14, Supplement 1**,** 116-121.

Coons, A. H. & Kaplan, M. H. 1950. "Localization of antigen in tissue cells; improvements in a method for the detection of antigen by means of fluorescent antibody". J Exp Med, 91**,** 1-13.

Copenhaver W, K. D., Wood Rl 1978. "The Connective tissues: Cartilage and Bone In: Wilfred M, Douglas EK, Richard LW ed. Bailey's textbook of histolgy", Philadelphia, Williams & Wilkins.

Cotofana, S., Buck, R., Wirth, W., Roemer, F., Duryea, J., Nevitt, M., Eckstein, F. & Osteoarthritis Initiative Investigators, G. 2012. "Cartilage thickening in early radiographic knee osteoarthritis: A within-person, between-knee comparison". Arthritis Care & Research, 64**,** 1681-1690.

Cruz-Almeida, Y., King, C. D., Goodin, B. R., Sibille, K. T., Glover, T. L., Riley, J. L., Sotolongo, A., Herbert, M. S., Schmidt, J., Fessler, B. J., Redden, D. T., Staud, R., Bradley, L. A. & Fillingim, R. B. 2013. "Psychological Profiles and Pain Characteristics of Older Adults With Knee Osteoarthritis". Arthritis Care & Research, 65**,** 1786-1794.

Cuellar, J. M., Scuderi, G. J., Cuellar, V. G., Golish, S. R. & Yeomans, D. C. 2009. "Diagnostic utility of cytokine biomarkers in the evaluation of acute knee pain". J Bone Joint Surg Am, 91**,** 2313-20.

Custers, R. J., Creemers, L. B., Verbout, A. J., Van Rijen, M. H., Dhert, W. J. & Saris, D. B. 2007. "Reliability, reproducibility and variability of the traditional Histologic/Histochemical Grading System vs the new OARSI Osteoarthritis Cartilage Histopathology Assessment System". Osteoarthritis Cartilage, 15**,** 1241-8.

Dai, J., Agelan, A., Yang, A., Zuluaga, V., Sexton, D., Colman, R. W. & Wu, Y. 2012. "Role of plasma kallikrein-kinin system activation in synovial recruitment of endothelial progenitor cells in experimental arthritis". Arthritis Rheum, 64**,** 3574-82.

Dai, Y., Moriyama, T., Higashi, T., Togashi, K., Kobayashi, K., Yamanaka, H., Tominaga, M. & Noguchi, K. 2004. "Proteinase-activated receptor 2-mediated potentiation of transient receptor potential vanilloid subfamily 1 activity reveals a mechanism for proteinase-induced inflammatory pain". J Neurosci, 24**,** 4293-9.

Dai, Y., Wang, S., Tominaga, M., Yamamoto, S., Fukuoka, T., Higashi, T., Kobayashi, K., Obata, K., Yamanaka, H. & Noguchi, K. 2007. "Sensitization of TRPA1 by PAR2 contributes to the sensation of inflammatory pain". J Clin Invest, 117**,** 1979-87.

Dauer, D. J., Ferraro, B., Song, L., Yu, B., Mora, L., Buettner, R., Enkemann, S., Jove, R. & Haura, E. B. 2005. "Stat3 regulates genes common to both wound healing and cancer". Oncogene, 24**,** 3397-408.

Davies-Tuck, M. L., Wluka, A. E., Wang, Y., English, D. R., Giles, G. G. & Cicuttini, F. 2009. "The natural history of bone marrow lesions in community-based adults with no clinical knee osteoarthritis". Ann Rheum Dis, 68**,** 904-8.

Davies, D. V. & Edwards, D. A. 1948. "The blood supply of the synovial membrane and intra-articular structures". Ann R Coll Surg Engl, 2**,** 142-46.

Davis, A. M., Badley, E. M., Beaton, D. E., Kopec, J., Wright, J. G., Young, N. L. & Williams, J. I. 2003. "Rasch analysis of the Western Ontario McMaster (WOMAC) Osteoarthritis Index: results from community and arthroplasty samples". J Clin Epidemiol, 56**,** 1076-83.

Dawes, J. M., Kiesewetter, H., Perkins, J. R., Bennett, D. L. & Mcmahon, S. B. 2013. "Chemokine expression in peripheral tissues from the monosodium iodoacetate model of chronic joint pain". Mol Pain, 9**,** 57.

De Andres, M. C., Imagawa, K., Hashimoto, K., Gonzalez, A., Goldring, M. B., Roach, H. I. & Oreffo, R. O. 2011. "Suppressors of cytokine signalling (SOCS) are reduced in osteoarthritis". Biochem Biophys Res Commun, 407**,** 54-9.

De Lange-Brokaar, B. J., Ioan-Facsinay, A., Van Osch, G. J., Zuurmond, A. M., Schoones, J., Toes, R. E., Huizinga, T. W. & Kloppenburg, M. 2012. "Synovial inflammation, immune cells and their cytokines in osteoarthritis: a review". Osteoarthritis Cartilage, 20**,** 1484-99.

Delozier, T. C., Kissling, G. E., Coulter, S. J., Dai, D., Foley, J. F., Bradbury, J. A., Murphy, E., Steenbergen, C., Zeldin, D. C. & Goldstein, J. A. 2007. "Detection of human CYP2C8, CYP2C9, and CYP2J2 in cardiovascular tissues". Drug Metab Dispos, 35**,** 682-8.

Denes, A., Lopez-Castejon, G. & Brough, D. 2012. "Caspase-1: is IL-1 just the tip of the ICEberg[quest]". Cell Death Dis, 3**,** e338.

Deval, E., Noël, J., Lay, N., Alloui, A., Diochot, S., Friend, V., Jodar, M., Lazdunski, M. & Lingueglia, E. 2008. "ASIC3, a sensor of acidic and primary inflammatory pain". The EMBO Journal, 27**,** 3047-3055.

Dickenson, A. H. 2002. "Gate control theory of pain stands the test of time". Br J Anaesth, 88**,** 755-7.

Didenko, V. V. 2001. "DNA probes using fluorescence resonance energy transfer (FRET): designs and applications". Biotechniques, 31**,** 1106-16, 1118, 1120-1.

Dieppe, P. A., Cushnaghan, J. & Shepstone, L. 1997. "The Bristol 'OA500' study: progression of osteoarthritis (OA) over 3 years and the relationship between clinical and radiographic changes at the knee joint". Osteoarthritis Cartilage, 5**,** 87-97.

Dieppe, P. A. & Lohmander, L. S. 2005. "Pathogenesis and management of pain in osteoarthritis". The Lancet, 365**,** 965-973.

Dougados, M., Ayral, X., Listrat, V., Gueguen, A., Bahuaud, J., Beaufils, P., Beguin, J. A., Bonvarlet, J. P., Boyer, T., Coudane, H. & Et Al. 1994. "The SFA system for assessing articular cartilage lesions at arthroscopy of the knee". Arthroscopy, 10**,** 69-77.

Doya, H., Ohtori, S., Fujitani, M., Saito, T., Hata, K., Ino, H., Takahashi, K., Moriya, H. & Yamashita, T. 2005. "c-Jun N-terminal kinase activation in dorsal root ganglion contributes to pain hypersensitivity". Biochemical and Biophysical Research Communications, 335**,** 132-138.

Driban, J. B., Sitler, M. R., Barbe, M. F. & Balasubramanian, E. 2010. "Is osteoarthritis a heterogeneous disease that can be stratified into subsets?". Clin Rheumatol, 29**,** 123-31.

Duncan, R., Peat, G., Thomas, E., Hay, E., Mccall, I. & Croft, P. 2007. "Symptoms and radiographic osteoarthritis: not as discordant as they are made out to be?". Annals of the Rheumatic Diseases, 66**,** 86-91.

Eisinger, K., Bauer, S., Schaffler, A., Walter, R., Neumann, E., Buechler, C., Muller-Ladner, U. & Frommer, K. W. 2012. "Chemerin induces CCL2 and TLR4 in synovial fibroblasts of patients with rheumatoid arthritis and osteoarthritis". Exp Mol Pathol, 92**,** 90-6.

Endres, M., Andreas, K., Kalwitz, G., Freymann, U., Neumann, K., Ringe, J., Sittinger, M., Haupl, T. & Kaps, C. 2010. "Chemokine profile of synovial fluid from normal, osteoarthritis and rheumatoid arthritis patients: CCL25, CXCL10 and XCL1 recruit human subchondral mesenchymal progenitor cells". Osteoarthritis Cartilage, 18**,** 1458-66.

Englund, M., Roos, E. M. & Lohmander, L. S. 2003. "Impact of type of meniscal tear on radiographic and symptomatic knee osteoarthritis: A sixteen-year followup of meniscectomy with matched controls". Arthritis & Rheumatism, 48**,** 2178-2187.

Englund, M., Niu, J., Guermazi, A., Roemer, F. W., Hunter, D. J., Lynch, J. A., Lewis, C. E., Torner, J., Nevitt, M. C., Zhang, Y. Q. & Felson, D. T. 2007. "Effect of meniscal damage on the development of frequent knee pain, aching, or stiffness". Arthritis Rheum, 56**,** 4048-54.

Englund, M., Guermazi, A., Gale, D., Hunter, D. J., Aliabadi, P., Clancy, M. & Felson, D. T. 2008. "Incidental Meniscal Findings on Knee MRI in Middle-Aged and Elderly Persons". New England Journal of Medicine, 359**,** 1108-1115.

Englund, M., Guermazi, A. & Lohmander, L. S. 2009. "The meniscus in knee osteoarthritis". Rheum Dis Clin North Am, 35**,** 579-90.

Enslen, H., Raingeaud, J. & Davis, R. J. 1998. "Selective activation of p38 mitogen-activated protein (MAP) kinase isoforms by the MAP kinase kinases MKK3 and MKK6". J Biol Chem, 273**,** 1741-8.

Eriksen, E. F. & Ringe, J. D. 2011. "Bone marrow lesions: a universal bone response to injury?". Rheumatol Int.

Fehrenbacher, J. C., Burkey, T. H., Nicol, G. D. & Vasko, M. R. 2005. "Tumor necrosis factor alpha and interleukin-1beta stimulate the expression of cyclooxygenase II but do not alter prostaglandin E2 receptor mRNA levels in cultured dorsal root ganglia cells". Pain, 113**,** 113-22.

Felson, D. T., Naimark, A., Anderson, J., Kazis, L., Castelli, W. & Meenan, R. F. 1987. "The prevalence of knee osteoarthritis in the elderly. The Framingham Osteoarthritis Study". Arthritis Rheum, 30**,** 914-8.

Felson, D. T., Anderson, J. J., Naimark, A., Walker, A. M. & Meenan, R. F. 1988. "Obesity and knee osteoarthritis. The Framingham Study". Ann Intern Med, 109**,** 18-24.

Felson, D. T., Lawrence, R. C., Dieppe, P. A., Hirsch, R., Helmick, C. G., Jordan, J. M., Kington, R. S., Lane, N. E., Nevitt, M. C., Zhang, Y., Sowers, M., Mcalindon, T., Spector, T. D., Poole, A. R., Yanovski, S. Z., Ateshian, G., Sharma, L., Buckwalter, J. A., Brandt, K. D. & Fries, J. F. 2000. "Osteoarthritis: New Insights. Part 1: The Disease and Its Risk Factors". Annals of Internal Medicine, 133**,** 635-646.

Felson, D. T., Chaisson, C. E., Hill, C. L., Totterman, S. M., Gale, M. E., Skinner, K. M., Kazis, L. & Gale, D. R. 2001. "The association of bone marrow lesions with pain in knee osteoarthritis". Ann Intern Med, 134**,** 541-9.

Felson, D. T., Mclaughlin, S., Goggins, J., Lavalley, M. P., Gale, M. E., Totterman, S., Li, W., Hill, C. & Gale, D. 2003. "Bone marrow edema

and its relation to progression of knee osteoarthritis". Ann Intern Med, 139, 330-6.
Felson, D. T., Niu, J., Guermazi, A., Roemer, F., Aliabadi, P., Clancy, M., Torner, J., Lewis, C. E. & Nevitt, M. C. 2007. "Correlation of the development of knee pain with enlarging bone marrow lesions on magnetic resonance imaging". Arthritis Rheum, 56, 2986-92.
Felson, D. T. 2009. "Developments in the clinical understanding of osteoarthritis". Arthritis Res Ther, 11, 203.
Felson, D. T. 2013. "Osteoarthritis as a disease of mechanics". Osteoarthritis Cartilage, 21, 10-5.
Fenn, S., Datir, A. & Saifuddin, A. 2009. "Synovial recesses of the knee: MR imaging review of anatomical and pathological features". Skeletal Radiol, 38, 317-28.
Fernandes, J., Tardif, G., Martel-Pelletier, J., Lascau-Coman, V., Dupuis, M., Moldovan, F., Sheppard, M., Krishnan, B. R. & Pelletier, J. P. 1999. "In vivo transfer of interleukin-1 receptor antagonist gene in osteoarthritic rabbit knee joints: prevention of osteoarthritis progression". Am J Pathol, 154, 1159-69.
Fernandes, J. C., Martel-Pelletier, J. & Pelletier, J. P. 2002. "The role of cytokines in osteoarthritis pathophysiology". Biorheology, 39, 237-46.
Ferreira, S. H., Cunha, F. Q., Lorenzetti, B. B., Michelin, M. A., Perretti, M., Flower, R. J. & Poole, S. 1997. "Role of lipocortin-1 in the anti-hyperalgesic actions of dexamethasone". Br J Pharmacol, 121, 883-8.
Ferrell, W. R., Lockhart, J. C., Kelso, E. B., Dunning, L., Plevin, R., Meek, S. E., Smith, A. J., Hunter, G. D., Mclean, J. S., Mcgarry, F., Ramage, R., Jiang, L., Kanke, T. & Kawagoe, J. 2003. "Essential role for proteinase-activated receptor-2 in arthritis". J Clin Invest, 111, 35-41.
Finbloom, D. S. & Winestock, K. D. 1995. "IL-10 induces the tyrosine phosphorylation of tyk2 and Jak1 and the differential assembly of STAT1 alpha and STAT3 complexes in human T cells and monocytes". J Immunol, 155, 1079-90.
Fischer, M., Mak, S. & Mcnaughton, P. 2010. "Sensitisation of Nociceptors – What are Ion Channels Doing?". The Open Pain Journal, 3, 82-96.
Fleige, S. & Pfaffl, M. W. 2006. "RNA integrity and the effect on the real-time qRT-PCR performance". Mol Aspects Med, 27, 126-39.
Flower, R. J. 1988. "Eleventh Gaddum memorial lecture. Lipocortin and the mechanism of action of the glucocorticoids". Br J Pharmacol, 94, 987-1015.
Franses, R. E., Mcwilliams, D. F., Mapp, P. I. & Walsh, D. A. 2010. "Osteochondral angiogenesis and increased protease inhibitor expression in OA". Osteoarthritis Cartilage, 18, 563-71.
Franz, T., Hasler, E. M., Hagg, R., Weiler, C., Jakob, R. P. & Mainil-Varlet, P. 2001. "In situ compressive stiffness, biochemical composition, and structural integrity of articular cartilage of the human knee joint". Osteoarthritis Cartilage, 9, 582-92.
Galasso, O., Familiari, F., De Gori, M. & Gasparini, G. 2012. "Recent Findings on the Role of Gelatinases (Matrix Metalloproteinase-2 and -9) in Osteoarthritis". Advances in Orthopedics, 2012, 7.
Garcia Del Cano, G., Montana, M., Aretxabala, X., Gonzalez-Burguera, I., Lopez De Jesus, M., Barrondo, S. & Salles, J. 2014. "Nuclear

phospholipase C-beta1 and diacylglycerol LIPASE-alpha in brain cortical neurons". Adv Biol Regul, 54**,** 12-23.
Gardner, E. 1948. "The innervation of the knee joint". The Anatomical Record, 101**,** 109-130.
Garnero, P., Peterfy, C., Zaim, S. & Schoenharting, M. 2005. "Bone marrow abnormalities on magnetic resonance imaging are associated with type II collagen degradation in knee osteoarthritis: a three-month longitudinal study". Arthritis Rheum, 52**,** 2822-9.
Gelber, A. C., Hochberg, M. C., Mead, L. A., Wang, N. Y., Wigley, F. M. & Klag, M. J. 2000. "Joint injury in young adults and risk for subsequent knee and hip osteoarthritis". Ann Intern Med, 133**,** 321-8.
Ghosh, A. K. & Vaughan, D. E. 2012. "PAI-1 in tissue fibrosis". J Cell Physiol, 227**,** 493-507.
Ginty, D. D. & Segal, R. A. 2002. "Retrograde neurotrophin signaling: Trk-ing along the axon". Current Opinion in Neurobiology, 12**,** 268-274.
Goldring, M. B. 2000. "The role of the chondrocyte in osteoarthritis". Arthritis & Rheumatism, 43**,** 1916-1926.
Goldring, M. B. & Marcu, K. B. 2009. "Cartilage homeostasis in health and rheumatic diseases". Arthritis Res Ther, 11**,** 224.
Goldring, M. B. & Otero, M. 2011. "Inflammation in osteoarthritis". Curr Opin Rheumatol, 23**,** 471-8.
Goulding, N. J., Dixey, J., Morand, E. F., Dodds, R. A., Wilkinson, L. S., Pitsillides, A. A. & Edwards, J. C. 1995. "Differential distribution of annexins-I, -II, -IV, and -VI in synovium". Ann Rheum Dis, 54**,** 841-5.
Goulston, L. M., Kiran, A., Javaid, M. K., Soni, A., White, K. M., Hart, D. J., Spector, T. D. & Arden, N. K. 2011. "Does obesity predict knee pain over fourteen years in women, independently of radiographic changes?". Arthritis Care Res (Hoboken), 63**,** 1398-406.
Grotle, M., Hagen, K. B., Natvig, B., Dahl, F. A. & Kvien, T. K. 2008. "Prevalence and burden of osteoarthritis: results from a population survey in Norway". J Rheumatol, 35**,** 677-84.
Grubbs, F. 1969. "Procedures for Detecting Outlying Observations in Samples". Technometrics, 11**,** 1-21.
Ha, J., Choi, H.-S., Lee, Y., Kwon, H.-J., Song, Y. W. & Kim, H.-H. 2010. "CXC Chemokine Ligand 2 Induced by Receptor Activator of NF-κB Ligand Enhances Osteoclastogenesis". The Journal of Immunology, 184**,** 4717-4724.
Haider, S. & Pal, R. 2013. "Integrated analysis of transcriptomic and proteomic data". Curr Genomics, 14**,** 91-110.
Halliday, D. A., Zettler, C., Rush, R. A., Scicchitano, R. & Mcneil, J. D. 1998. "Elevated nerve growth factor levels in the synovial fluid of patients with inflammatory joint disease". Neurochem Res, 23**,** 919-22.
Hammaker, D. & Firestein, G. S. 2010. "“Go upstream, young man”: lessons learned from the p38 saga". Annals of the Rheumatic Diseases, 69**,** i77-i82.
Hanley, J. A. & Mcneil, B. J. 1982. "The meaning and use of the area under a receiver operating characteristic (ROC) curve". Radiology, 143**,** 29-36.
Hannan, M. T., Felson, D. T. & Pincus, T. 2000. "Analysis of the discordance between radiographic changes and knee pain in osteoarthritis of the knee". J Rheumatol, 27**,** 1513-7.

Haringman, J. J., Smeets, T. J., Reinders-Blankert, P. & Tak, P. P. 2006. "Chemokine and chemokine receptor expression in paired peripheral blood mononuclear cells and synovial tissue of patients with rheumatoid arthritis, osteoarthritis, and reactive arthritis". Ann Rheum Dis, 65**,** 294-300.

Harirforoosh, S. & Jamali, F. 2009. "Renal adverse effects of nonsteroidal anti-inflammatory drugs". Expert Opin Drug Saf, 8**,** 669-81.

Hassan, H. & Walsh, D. A. 2014. "Central pain processing in osteoarthritis: implications for treatment". Pain Manag, 4**,** 45-56.

Hawker, G. A., Stewart, L., French, M. R., Cibere, J., Jordan, J. M., March, L., Suarez-Almazor, M. & Gooberman-Hill, R. 2008. "Understanding the pain experience in hip and knee osteoarthritis--an OARSI/OMERACT initiative". Osteoarthritis Cartilage, 16**,** 415-22.

Haywood, L. & Walsh, D. A. 2001. "Vasculature of the normal and arthritic synovial joint". Histol Histopathol, 16**,** 277-84.

Haywood, L., Mcwilliams, D. F., Pearson, C. I., Gill, S. E., Ganesan, A., Wilson, D. & Walsh, D. A. 2003. "Inflammation and angiogenesis in osteoarthritis". Arthritis Rheum, 48**,** 2173-7.

Heijink, A., Gomoll, A. H., Madry, H., Drobnic, M., Filardo, G., Espregueira-Mendes, J. & Van Dijk, C. N. 2012. "Biomechanical considerations in the pathogenesis of osteoarthritis of the knee". Knee Surg Sports Traumatol Arthrosc, 20**,** 423-35.

Helyes, Z., Sándor, K., Borbély, É., Tékus, V., Pintér, E., Elekes, K., Tóth, D. M., Szolcsányi, J. & Mcdougall, J. J. 2010. "Involvement of transient receptor potential vanilloid 1 receptors in protease-activated receptor-2-induced joint inflammation and nociception". European Journal of Pain, 14**,** 351-358.

Hernandez-Molina, G., Guermazi, A., Niu, J., Gale, D., Goggins, J., Amin, S. & Felson, D. T. 2008a. "Central bone marrow lesions in symptomatic knee osteoarthritis and their relationship to anterior cruciate ligament tears and cartilage loss". Arthritis Rheum, 58**,** 130-6.

Hernandez-Molina, G., Neogi, T., Hunter, D. J., Niu, J., Guermazi, A., Reichenbach, S., Roemer, F. W., Mclennan, C. E. & Felson, D. T. 2008b. "The association of bone attrition with knee pain and other MRI features of osteoarthritis". Ann Rheum Dis, 67**,** 43-7.

Herova, M., Schmid, M., Gemperle, C. & Hersberger, M. 2015. "ChemR23, the Receptor for Chemerin and Resolvin E1, Is Expressed and Functional on M1 but Not on M2 Macrophages". J Immunol, 194**,** 2330-7.

Hill, C. L., Gale, D. G., Chaisson, C. E., Skinner, K., Kazis, L., Gale, M. E. & Felson, D. T. 2001. "Knee effusions, popliteal cysts, and synovial thickening: association with knee pain in osteoarthritis". J Rheumatol, 28**,** 1330-7.

Hill, C. L., Hunter, D. J., Niu, J., Clancy, M., Guermazi, A., Genant, H., Gale, D., Grainger, A., Conaghan, P. & Felson, D. T. 2007. "Synovitis detected on magnetic resonance imaging and its relation to pain and cartilage loss in knee osteoarthritis". Ann Rheum Dis, 66**,** 1599-603.

Holland, N. T., Smith, M. T., Eskenazi, B. & Bastaki, M. 2003. "Biological sample collection and processing for molecular epidemiological studies". Mutat Res, 543**,** 217-34.

Holness Cl & Simmons, D. 1993. "Molecular cloning of CD68, a human macrophage marker related to lysosomal glycoproteins". Blood, 81**,** 1607-13.

Honorati, M. C., Bovara, M., Cattini, L., Piacentini, A. & Facchini, A. 2002. "Contribution of interleukin 17 to human cartilage degradation and synovial inflammation in osteoarthritis". Osteoarthritis Cartilage, 10**,** 799-807.

Horvath, C. M. 2004. "The Jak-STAT pathway stimulated by interferon gamma". Sci STKE, 2004**,** tr8.

Hsu, S. M., Raine, L. & Fanger, H. 1981. "Use of avidin-biotin-peroxidase complex (ABC) in immunoperoxidase techniques: a comparison between ABC and unlabeled antibody (PAP) procedures". Journal of Histochemistry & Cytochemistry, 29**,** 577-80.

Hudelmaier, M., Glaser, C., Hohe, J., Englmeier, K. H., Reiser, M., Putz, R. & Eckstein, F. 2001. "Age-related changes in the morphology and deformational behavior of knee joint cartilage". Arthritis Rheum, 44**,** 2556-61.

Hunter, D. J., March, L. & Sambrook, P. N. 2003. "The association of cartilage volume with knee pain". Osteoarthritis and Cartilage, 11**,** 725-729.

Hunter, D. J., Zhang, Y., Niu, J., Goggins, J., Amin, S., Lavalley, M. P., Guermazi, A., Genant, H., Gale, D. & Felson, D. T. 2006a. "Increase in bone marrow lesions associated with cartilage loss: a longitudinal magnetic resonance imaging study of knee osteoarthritis". Arthritis Rheum, 54**,** 1529-35.

Hunter, D. J., Zhang, Y. Q., Tu, X., Lavalley, M., Niu, J. B., Amin, S., Guermazi, A., Genant, H., Gale, D. & Felson, D. T. 2006b. "Change in joint space width: hyaline articular cartilage loss or alteration in meniscus?". Arthritis Rheum, 54**,** 2488-95.

Hunter, D. J., Zhang, Y. Q., Niu, J. B., Tu, X., Amin, S., Clancy, M., Guermazi, A., Grigorian, M., Gale, D. & Felson, D. T. 2006c. "The association of meniscal pathologic changes with cartilage loss in symptomatic knee osteoarthritis". Arthritis Rheum, 54**,** 795-801.

Hunter, D. J., Mcdougall, J. J. & Keefe, F. J. 2008. "The Symptoms of Osteoarthritis and the Genesis of Pain". Rheumatic Disease Clinics of North America, 34**,** 623-643.

Hunter, D. J., Guermazi, A., Roemer, F., Zhang, Y. & Neogi, T. 2013. "Structural correlates of pain in joints with osteoarthritis". Osteoarthritis Cartilage, 21**,** 1170-8.

Huo, L. W., Ye, Y. L., Wang, G. W. & Ye, Y. G. 2015. "Fractalkine (CX3CL1): A Biomarker Reflecting Symptomatic Severity in Patients With Knee Osteoarthritis". J Investig Med.

Ishihara, G., Kojima, T., Saito, Y. & Ishiguro, N. 2009. "Roles of metalloproteinase-3 and aggrecanase 1 and 2 in aggrecan cleavage during human meniscus degeneration". Orthop Rev (Pavia), 1**,** e14.

Ishijima, M., Nakamura, T., Shimizu, K., Hayashi, K., Kikuchi, H., Soen, S., Omori, G., Yamashita, T., Uchio, Y., Chiba, J., Ideno, Y., Kubota, M., Kurosawa, H. & Kaneko, K. 2014. "Intra-articular hyaluronic acid injection versus oral non-steroidal anti-inflammatory drug for the treatment of knee osteoarthritis: a multi-center, randomized, open-label, non-inferiority trial". Arthritis Res Ther, 16**,** R18.

Isomaki, P., Alanara, T., Isohanni, P., Lagerstedt, A., Korpela, M., Moilanen, T., Visakorpi, T. & Silvennoinen, O. 2007. "The expression of SOCS is altered in rheumatoid arthritis". Rheumatology (Oxford), 46**,** 1538-46.

Isozaki, T., Kasama, T., Takahashi, R., Odai, T., Wakabayashi, K., Kanemitsu, H., Nohtomi, K., Takeuchi, H. T., Matsukura, S. & Tezuka, M. 2008. "Synergistic induction of CX3CL1 by TNF alpha and IFN gamma in osteoblasts from rheumatoid arthritis: involvement of NF-kappa B and STAT-1 signaling pathways". J Inflamm Res, 1**,** 19-28.

Izquierdo, E., Canete, J. D., Celis, R., Del Rey, M. J., Usategui, A., Marsal, S., Sanmarti, R., Criado, G. & Pablos, J. L. 2011. "Synovial fibroblast hyperplasia in rheumatoid arthritis: clinicopathologic correlations and partial reversal by anti-tumor necrosis factor therapy". Arthritis Rheum, 63**,** 2575-83.

James, C. G., Appleton, C. T., Ulici, V., Underhill, T. M. & Beier, F. 2005. "Microarray analyses of gene expression during chondrocyte differentiation identifies novel regulators of hypertrophy". Mol Biol Cell, 16**,** 5316-33.

Javaid, M. K., Lynch, J. A., Tolstykh, I., Guermazi, A., Roemer, F., Aliabadi, P., Mcculloch, C., Curtis, J., Felson, D., Lane, N. E., Torner, J. & Nevitt, M. 2010. "Pre-radiographic MRI findings are associated with onset of knee symptoms: the most study". Osteoarthritis Cartilage, 18**,** 323-8.

Ji, R.-R., Samad, T. A., Jin, S.-X., Schmoll, R. & Woolf, C. J. 2002. "p38 MAPK Activation by NGF in Primary Sensory Neurons after Inflammation Increases TRPV1 Levels and Maintains Heat Hyperalgesia". Neuron, 36**,** 57-68.

Ji, R. R., Xu, Z. Z., Wang, X. & Lo, E. H. 2009. "Matrix metalloprotease regulation of neuropathic pain". Trends Pharmacol Sci, 30**,** 336-40.

Jiang, L., Tian, W., Wang, Y., Rong, J., Bao, C., Liu, Y., Zhao, Y. & Wang, C. 2012. "Body mass index and susceptibility to knee osteoarthritis: a systematic review and meta-analysis". Joint Bone Spine, 79**,** 291-7.

Jung, T. & Wickrama, K. a. S. 2008. "An Introduction to Latent Class Growth Analysis and Growth Mixture Modeling". Social and Personality Psychology Compass, 2**,** 302-317.

Kaneko, S., Satoh, T., Chiba, J., Ju, C., Inoue, K. & Kagawa, J. 2000. "Interleukin-6 and interleukin-8 levels in serum and synovial fluid of patients with osteoarthritis". Cytokines Cell Mol Ther, 6**,** 71-9.

Kapoor, M., Martel-Pelletier, J., Lajeunesse, D., Pelletier, J. P. & Fahmi, H. 2011. "Role of proinflammatory cytokines in the pathophysiology of osteoarthritis". Nat Rev Rheumatol, 7**,** 33-42.

Kawasaki, Y., Xu, Z. Z., Wang, X., Park, J. Y., Zhuang, Z. Y., Tan, P. H., Gao, Y. J., Roy, K., Corfas, G., Lo, E. H. & Ji, R. R. 2008. "Distinct roles of matrix metalloproteases in the early- and late-phase development of neuropathic pain". Nat Med, 14**,** 331-6.

Kellgren, J. H. & Lawrence, J. S. 1957. "Radiological Assessment of Osteo-Arthrosis". Annals of the Rheumatic Diseases, 16**,** 494-502.

Khasabov, S. G., Rogers, S. D., Ghilardi, J. R., Peters, C. M., Mantyh, P. W. & Simone, D. A. 2002. "Spinal Neurons that Possess the Substance P Receptor Are Required for the Development of Central Sensitization". The Journal of Neuroscience, 22**,** 9086-9098.

Kidd, B. L., Photiou, A. & Inglis, J. J. 2004. "The role of inflammatory mediators on nociception and pain in arthritis". Novartis Found Symp, 260**,** 122-33; discussion 133-8, 277-9.

King, D. F. & King, L. A. 1986. "A brief historical note on staining by hematoxylin and eosin". Am J Dermatopathol, 8**,** 168.

Kishimoto, T. 2006. "Interleukin-6: discovery of a pleiotropic cytokine". Arthritis Res Ther, 8 Suppl 2**,** S2.

Kiviranta, I., Jurvelin, J., Tammi, M., Saamanen, A. M. & Helminen, H. J. 1985. "Microspectrophotometric quantitation of glycosaminoglycans in articular cartilage sections stained with Safranin O". Histochemistry, 82**,** 249-55.

Knoop, J., Van Der Leeden, M., Thorstensson, C. A., Roorda, L. D., Lems, W. F., Knol, D. L., Steultjens, M. P. & Dekker, J. 2011. "Identification of phenotypes with different clinical outcomes in knee osteoarthritis: data from the Osteoarthritis Initiative". Arthritis Care Res (Hoboken), 63**,** 1535-42.

Ko, Y., Lo, N. N., Yeo, S. J., Yang, K. Y., Yeo, W., Chong, H. C. & Thumboo, J. 2009. "Rasch analysis of the Oxford Knee Score". Osteoarthritis Cartilage, 17**,** 1163-9.

Koch, A. E., Kunkel, S. L., Shah, M. R., Fu, R., Mazarakis, D. D., Haines, G. K., Burdick, M. D., Pope, R. M. & Strieter, R. M. 1995. "Macrophage Inflammatory Protein-Iβ: A C-C Chemokine in Osteoarthritis". Clinical Immunology and Immunopathology, 77**,** 307-314.

Kohler, G. & Milstein, C. 1975. "Continuous cultures of fused cells secreting antibody of predefined specificity". Nature, 256**,** 495-497.

Korb, A., Tohidast-Akrad, M., Cetin, E., Axmann, R., Smolen, J. & Schett, G. 2006. "Differential tissue expression and activation of p38 MAPK alpha, beta, gamma, and delta isoforms in rheumatoid arthritis". Arthritis Rheum, 54**,** 2745-56.

Kornaat, P. R., Bloem, J. L., Ceulemans, R. Y., Riyazi, N., Rosendaal, F. R., Nelissen, R. G., Carter, W. O., Hellio Le Graverand, M. P. & Kloppenburg, M. 2006. "Osteoarthritis of the knee: association between clinical features and MR imaging findings". Radiology, 239**,** 811-7.

Kornaat, P. R., Kloppenburg, M., Sharma, R., Botha-Scheepers, S. A., Le Graverand, M. P., Coene, L. N., Bloem, J. L. & Watt, I. 2007. "Bone marrow edema-like lesions change in volume in the majority of patients with osteoarthritis; associations with clinical features". Eur Radiol, 17**,** 3073-8.

Kou, S. & Wu, Y. 2014. "Meta-analysis of tumor necrosis factor alpha -308 polymorphism and knee osteoarthritis risk". BMC Musculoskelet Disord, 15**,** 373.

Krenn, V., Morawietz, L., Haupl, T., Neidel, J., Petersen, I. & Konig, A. 2002. "Grading of chronic synovitis--a histopathological grading system for molecular and diagnostic pathology". Pathol Res Pract, 198**,** 317-25.

Krenn, V., Morawietz, L., Burmester, G. R., Kinne, R. W., Mueller-Ladner, U., Muller, B. & Haupl, T. 2006. "Synovitis score: discrimination between chronic low-grade and high-grade synovitis". Histopathology, 49**,** 358-64.

Kubista, M., Andrade, J. M., Bengtsson, M., Forootan, A., Jonák, J., Lind, K., Sindelka, R., Sjöback, R., Sjögreen, B., Strömbom, L., Ståhlberg, A. &

Zoric, N. 2006. "The real-time polymerase chain reaction". Molecular Aspects of Medicine, 27**,** 95-125.

Kuroda, K. & Tajima, S. 2004. "HSP47 is a useful marker for skin fibroblasts in formalin-fixed, paraffin-embedded tissue specimens". J Cutan Pathol, 31**,** 241-6.

Kuziora, M., Liu, Z., Higgs, B., Brohawn, P., Lehmann, K. & Pilataxi, F. 2013. "A Subset Of Osteoarthritis Individuals Has Elevated IL-6 Pathway Activation Associated With Worse Symptoms. [abstract]". Arthritis Rheum, 65 Suppl 10:150.

Lambert, C., Dubuc, J.-E., Montell, E., Vergés, J., Munaut, C., Noël, A. & Henrotin, Y. 2014. "Gene Expression Pattern of Cells From Inflamed and Normal Areas of Osteoarthritis Synovial Membrane". Arthritis & Rheumatology, 66**,** 960-968.

Lane, N. E., Schnitzer, T. J., Birbara, C. A., Mokhtarani, M., Shelton, D. L., Smith, M. D. & Brown, M. T. 2010. "Tanezumab for the treatment of pain from osteoarthritis of the knee". N Engl J Med, 363**,** 1521-31.

Lawand, N. B., Willis, W. D. & Westlund, K. N. 1997. "Blockade of joint inflammation and secondary hyperalgesia by L-NAME, a nitric oxide synthase inhibitor". Neuroreport, 8**,** 895-9.

Le, A. P. & Friedman, W. J. 2012. "Matrix metalloproteinase-7 regulates cleavage of pro-nerve growth factor and is neuroprotective following kainic acid-induced seizures". J Neurosci, 32**,** 703-12.

Lee, E. Y., Lee, Z. H. & Song, Y. W. 2013. "The interaction between CXCL10 and cytokines in chronic inflammatory arthritis". Autoimmun Rev, 12**,** 554-7.

Lee, K.-M., Kang, B.-S., Lee, H.-L., Son, S.-J., Hwang, S.-H., Kim, D.-S., Park, J.-S. & Cho, H.-J. 2004. "Spinal NF-kB activation induces COX-2 upregulation and contributes to inflammatory pain hypersensitivity". European Journal of Neuroscience, 19**,** 3375-3381.

Lee, R., Kermani, P., Teng, K. K. & Hempstead, B. L. 2001. "Regulation of cell survival by secreted proneurotrophins". Science, 294**,** 1945-8.

Lee, Y., Rodriguez, C. & Dionne, R. A. 2005. "The role of COX-2 in acute pain and the use of selective COX-2 inhibitors for acute pain relief". Curr Pharm Des, 11**,** 1737-55.

Lee, Y. C., Lu, B., Bathon, J. M., Haythornthwaite, J. A., Smith, M. T., Page, G. G. & Edwards, R. R. 2011. "Pain sensitivity and pain reactivity in osteoarthritis". Arthritis Care Res (Hoboken), 63**,** 320-7.

Levi-Montalcini, R. & Hamburger, V. 1951. "Selective growth stimulating effects of mouse sarcoma on the sensory and sympathetic nervous system of the chick embryo". J Exp Zool, 116**,** 321-61.

Levi-Montalcini, R. 1987. "The nerve growth factor 35 years later". Science, 237**,** 1154-62.

Levi-Montalcini, R. 1990. "A role for nerve growth factor in nervous, endocrine and immune systems.". Prog Neurol Endocrinol Immunol, 1**,** 1-10.

Li, G., Yin, J., Gao, J., Cheng, T. S., Pavlos, N. J., Zhang, C. & Zheng, M. H. 2013. "Subchondral bone in osteoarthritis: insight into risk factors and microstructural changes". Arthritis Res Ther, 15**,** 223.

Li, J., Simone, D. A. & Larson, A. A. 1999. "Windup leads to characteristics of central sensitization". Pain, 79**,** 75-82.

Li, L., Yan, Y., Xu, H., Qu, T. & Wang, B. 2011. "Selection of reference genes for gene expression studies in ultraviolet B-irradiated human skin fibroblasts using quantitative real-time PCR". BMC Mol Biol, 12**,** 8.

Li, L. & Jiang, B. E. 2015. "Serum and synovial fluid chemokine ligand 2/monocyte chemoattractant protein 1 concentrations correlates with symptomatic severity in patients with knee osteoarthritis". Ann Clin Biochem, 52**,** 276-82.

Lichtman, J. W. & Conchello, J. A. 2005. "Fluorescence microscopy". Nat Methods, 2**,** 910-9.

Lin, J., Li, G., Den, X., Xu, C., Liu, S., Gao, Y., Liu, H., Zhang, J., Li, X. & Liang, S. 2010. "VEGF and its receptor-2 involved in neuropathic pain transmission mediated by P2X2/3 receptor of primary sensory neurons". Brain Research Bulletin, 83**,** 284-291.

Linacre, J. M. *Reliability and separation of measures* [Online]. Available: http://www.winsteps.com/winman/reliability.htm [Accessed 22.01 2015].

Liu, L., Ishijima, M., Futami, I., Kaneko, H., Kubota, M., Kawasaki, T., Matsumoto, T., Kurihara, H., Ning, L., Xu, Z., Ikeda, H., Takazawa, Y., Saita, Y., Kimura, Y., Xu, S., Kaneko, K. & Kurosawa, H. 2010. "Correlation between synovitis detected on enhanced-magnetic resonance imaging and a histological analysis with a patient-oriented outcome measure for Japanese patients with end-stage knee osteoarthritis receiving joint replacement surgery". Clin Rheumatol, 29**,** 1185-90.

Liu, Y. Z., Jackson, A. P. & Cosgrove, S. D. 2009. "Contribution of calcium-containing crystals to cartilage degradation and synovial inflammation in osteoarthritis". Osteoarthritis Cartilage, 17**,** 1333-40.

Livak, K. J. & Schmittgen, T. D. 2001. "Analysis of Relative Gene Expression Data Using Real-Time Quantitative PCR and the 2−ΔΔCT Method". Methods, 25**,** 402-408.

Livshits, G., Zhai, G., Hart, D. J., Kato, B. S., Wang, H., Williams, F. M. & Spector, T. D. 2009. "Interleukin-6 is a significant predictor of radiographic knee osteoarthritis: The Chingford Study". Arthritis Rheum, 60**,** 2037-45.

Lo, G. H., Hunter, D. J., Zhang, Y., Mclennan, C. E., Lavalley, M. P., Kiel, D. P., Mclean, R. R., Genant, H. K., Guermazi, A. & Felson, D. T. 2005. "Bone marrow lesions in the knee are associated with increased local bone density". Arthritis Rheum, 52**,** 2814-21.

Lo, Y., Mendell, N. R. & Rubin, D. B. 2001. "Testing the number of components in a normal mixture". Biometrika, 88**,** 767-778.

Loeser, R. F., Goldring, S. R., Scanzello, C. R. & Goldring, M. B. 2012. "Osteoarthritis: a disease of the joint as an organ". Arthritis Rheum, 64**,** 1697-707.

Loeuille, D., Chary-Valckenaere, I., Champigneulle, J., Rat, A. C., Toussaint, F., Pinzano-Watrin, A., Goebel, J. C., Mainard, D., Blum, A., Pourel, J., Netter, P. & Gillet, P. 2005. "Macroscopic and microscopic features of synovial membrane inflammation in the osteoarthritic knee: correlating magnetic resonance imaging findings with disease severity". Arthritis Rheum, 52**,** 3492-501.

Lohmander, L. S., Hoerrner, L. A. & Lark, M. W. 1993. "Metalloproteinases, tissue inhibitor, and proteoglycan fragments in knee synovial fluid in human osteoarthritis". Arthritis Rheum, 36**,** 181-9.

Lohmander, L. S., Ostenberg, A., Englund, M. & Roos, H. 2004. "High prevalence of knee osteoarthritis, pain, and functional limitations in female soccer players twelve years after anterior cruciate ligament injury". Arthritis Rheum, 50**,** 3145-52.

Ma, W. & Quirion, R. 2008. "Does COX2-dependent PGE2 play a role in neuropathic pain?". Neuroscience Letters, 437**,** 165-169.

Macfarlane, S. R., Seatter, M. J., Kanke, T., Hunter, G. D. & Plevin, R. 2001. "Proteinase-activated receptors". Pharmacol Rev, 53**,** 245-82.

Madry, H., Luyten, F. P. & Facchini, A. 2012. "Biological aspects of early osteoarthritis". Knee Surg Sports Traumatol Arthrosc, 20**,** 407-22.

Mahmoud, R. K., El-Ansary, A. K., El-Eishi, H. H., Kamal, H. M. & El-Saeed, N. H. 2005. "Matrix metalloproteinases MMP-3 and MMP-1 levels in sera and synovial fluids in patients with rheumatoid arthritis and osteoarthritis". Ital J Biochem, 54**,** 248-57.

Makris, E. A., Hadidi, P. & Athanasiou, K. A. 2011. "The knee meniscus: structure-function, pathophysiology, current repair techniques, and prospects for regeneration". Biomaterials, 32**,** 7411-31.

Malfait, A. M., Tortorella, M., Thompson, J., Hills, R., Meyer, D. M., Jaffee, B. D., Chinn, K., Ghoreishi-Haack, N., Markosyan, S. & Arner, E. C. 2009. "Intra-articular injection of tumor necrosis factor-α in the rat: an acute and reversible in vivo model of cartilage proteoglycan degradation". Osteoarthritis and Cartilage, 17**,** 627-635.

Mandelbaum, B. R., Browne, J. E., Fu, F., Micheli, L., Mosely, J. B., Erggelet, C., Minas, T. & Peterson, L. 1998. "Articular Cartilage Lesions of the Knee". The American Journal of Sports Medicine, 26**,** 853-861.

Manicone, A. M. & Mcguire, J. K. 2008. "Matrix metalloproteinases as modulators of inflammation". Semin Cell Dev Biol, 19**,** 34-41.

Mankin, H. J., Dorfman, H., Lippiello, L. & Zarins, A. 1971. "Biochemical and metabolic abnormalities in articular cartilage from osteo-arthritic human hips. II. Correlation of morphology with biochemical and metabolic data". J Bone Joint Surg Am, 53**,** 523-37.

Manni, L., Lundeberg, T., Fiorito, S., Bonini, S., Vigneti, E. & Aloe, L. 2003. "Nerve growth factor release by human synovial fibroblasts prior to and following exposure to tumor necrosis factor-alpha, interleukin-1 beta and cholecystokinin-8: the possible role of NGF in the inflammatory response". Clin Exp Rheumatol, 21**,** 617-24.

Mantyh, P. W., Koltzenburg, M., Mendell, L. M., Tive, L. & Shelton, D. L. 2011. "Antagonism of nerve growth factor-TrkA signaling and the relief of pain". Anesthesiology, 115**,** 189-204.

Mapp, P. I., Kidd, B. L., Gibson, S. J., Terry, J. M., Revell, P. A., Ibrahim, N. B. N., Blake, D. R. & Polak, J. M. 1990. "Substance P-, calcitonin gene-related peptide-and C-flanking peptide of neuropeptide Y-immunoreactive fibres are present in normal synovium but depleted in patients with rheumatoid arthritis". Neuroscience, 37**,** 143-153.

Mapp, P. I. 1995. "Innervation of the synovium". Ann Rheum Dis, 54**,** 398-403.

Mapp, P. I., Walsh, D. A., Bowyer, J. & Maciewicz, R. A. 2010. "Effects of a metalloproteinase inhibitor on osteochondral angiogenesis, chondropathy and pain behavior in a rat model of osteoarthritis". Osteoarthritis Cartilage, 18**,** 593-600.

Mapp, P. I. & Walsh, D. A. 2012. "Mechanisms and targets of angiogenesis and nerve growth in osteoarthritis". Nat Rev Rheumatol, 8**,** 390-8.

Martel-Pelletier, J., Pelletier, J. P. & Fahmi, H. 2003. "Cyclooxygenase-2 and prostaglandins in articular tissues". Semin Arthritis Rheum, 33**,** 155-67.

Mcalindon, T. E., Bannuru, R. R., Sullivan, M. C., Arden, N. K., Berenbaum, F., Bierma-Zeinstra, S. M., Hawker, G. A., Henrotin, Y., Hunter, D. J., Kawaguchi, H., Kwoh, K., Lohmander, S., Rannou, F., Roos, E. M. & Underwood, M. 2014. "OARSI guidelines for the non-surgical management of knee osteoarthritis". Osteoarthritis Cartilage, 22**,** 363-88.

Mcdougall, J. J. 2006. "Arthritis and pain. Neurogenic origin of joint pain". Arthritis Res Ther, 8**,** 220.

Mcdougall, J. J., Zhang, C., Cellars, L., Joubert, E., Dixon, C. M. & Vergnolle, N. 2009. "Triggering of proteinase-activated receptor 4 leads to joint pain and inflammation in mice". Arthritis Rheum, 60**,** 728-37.

Mckelvey, L., Shorten, G. D. & O'keeffe, G. W. 2013. "Nerve growth factor-mediated regulation of pain signalling and proposed new intervention strategies in clinical pain management". Journal of Neurochemistry, 124**,** 276-289.

Mcquibban, G. A., Butler, G. S., Gong, J. H., Bendall, L., Power, C., Clark-Lewis, I. & Overall, C. M. 2001. "Matrix metalloproteinase activity inactivates the CXC chemokine stromal cell-derived factor-1". J Biol Chem, 276**,** 43503-8.

Mcquibban, G. A., Gong, J. H., Wong, J. P., Wallace, J. L., Clark-Lewis, I. & Overall, C. M. 2002. "Matrix metalloproteinase processing of monocyte chemoattractant proteins generates CC chemokine receptor antagonists with anti-inflammatory properties in vivo". Blood, 100**,** 1160-7.

Meini, S. & Maggi, C. A. 2008. "Knee osteoarthritis: a role for bradykinin?". Inflamm Res, 57**,** 351-61.

Melzack, R. & Wall, P. D. 1965. "Pain mechanisms: a new theory". Science, 150**,** 971-9.

Mendell, L. M. 1966. "Physiological properties of unmyelinated fiber projection to the spinal cord". Exp Neurol, 16**,** 316-32.

Merskey, H. & Bogduk, N. 1994. "Classification of Chronic Pain ". ISAP Press, Seattle**,** 209-214.

Messier, S. P., Loeser, R. F., Miller, G. D., Morgan, T. M., Rejeski, W. J., Sevick, M. A., Ettinger, W. H., Jr., Pahor, M. & Williamson, J. D. 2004. "Exercise and dietary weight loss in overweight and obese older adults with knee osteoarthritis: the Arthritis, Diet, and Activity Promotion Trial". Arthritis Rheum, 50**,** 1501-10.

Messner, K. & Gao, J. 1998. "The menisci of the knee joint. Anatomical and functional characteristics, and a rationale for clinical treatment". J Anat, 193 (Pt 2)**,** 161-78.

Milgram, J. W. 1983. "Morphologic alterations of the subchondral bone in advanced degenerative arthritis". Clin Orthop Relat Res**,** 293-312.

Miller, R. E., Tran, P. B., Das, R., Ghoreishi-Haack, N., Ren, D., Miller, R. J. & Malfait, A.-M. 2012. "CCR2 chemokine receptor signaling mediates pain in experimental osteoarthritis". Proceedings of the National Academy of Sciences, 109**,** 20602-20607.

Miller, R. E., Tran, P. B., Ishihara, S., Miller, R. J. & Malfait, A. M. 2014. "Damps provide a link between joint tissue damage and pain through direct activation of TLR4 expressed by sensory neurons". Osteoarthritis and Cartilage, 22, Supplement**,** S416-S417.

Milz, S. & Putz, R. 1994. "Quantitative morphology of the subchondral plate of the tibial plateau". J Anat, 185 (Pt 1)**,** 103-10.

Minashima, T., Campbell, K. & Kirsch, T. 2013. "Annexins: novel therapeutic targets for the treatment of osteoarthritis?". J Am Acad Orthop Surg, 21**,** 256-7.

Mitchell, N. S. & Shepard, N. 1978. "Changes in proteoglycan and collagen in cartilage in rheumatoid arthritis". J Bone Joint Surg Am, 60**,** 342-8.

Moens, U., Kostenko, S. & Sveinbjornsson, B. 2013. "The Role of Mitogen-Activated Protein Kinase-Activated Protein Kinases (MAPKAPKs) in Inflammation". Genes (Basel), 4**,** 101-33.

Moochhala, S. M. & Sawynok, J. 1984. "Hyperalgesia produced by intrathecal substance P and related peptides: desensitization and cross desensitization". Br J Pharmacol, 82**,** 381-8.

Moore, K. W., De Waal Malefyt, R., Coffman, R. L. & O'garra, A. 2001. "Interleukin-10 and the interleukin-10 receptor". Annu Rev Immunol, 19**,** 683-765.

Moreton, B. J., Wheeler, M., Walsh, D. A. & Lincoln, N. B. 2012. "Rasch analysis of the intermittent and constant osteoarthritis pain (ICOAP) scale". Osteoarthritis Cartilage, 20**,** 1109-15.

Moreton, B. J., Tew, V., Das Nair, R., Wheeler, M., Walsh, D. A. & Lincoln, N. B. 2014. "Pain phenotype in people with knee osteoarthritis; classification and measurement properties of painDETECT and S-LANSS in a cross-sectional study". Arthritis Care & Research**,** n/a-n/a.

Moses, M. A., Sudhalter, J. & Langer, R. 1990. "Identification of an inhibitor of neovascularization from cartilage". Science, 248**,** 1408-10.

Moses, M. A., Wiederschain, D., Wu, I., Fernandez, C. A., Ghazizadeh, V., Lane, W. S., Flynn, E., Sytkowski, A., Tao, T. & Langer, R. 1999. "Troponin I is present in human cartilage and inhibits angiogenesis". Proc Natl Acad Sci U S A, 96**,** 2645-50.

Mueller, O., Lightfoot, S. & Schroeder, A. 2004. "RNA integrity number (RIN)—standardization of RNA quality control". Agilent Application Note**,** Publication 5989-1165EN 1-8.

Mullis, K. B. & Faloona, F. A. 1987. "Specific synthesis of DNA in vitro via a polymerase-catalyzed chain reaction". Methods Enzymol, 155**,** 335-50.

Murata, M., Yudoh, K. & Masuko, K. 2008. "The potential role of vascular endothelial growth factor (VEGF) in cartilage: how the angiogenic factor could be involved in the pathogenesis of osteoarthritis?". Osteoarthritis Cartilage, 16**,** 279-86.

Murphy, G., Knauper, V., Atkinson, S., Butler, G., English, W., Hutton, M., Stracke, J. & Clark, I. 2002. "Matrix metalloproteinases in arthritic disease". Arthritis Res, 4 Suppl 3**,** S39-49.

Muthen, B. & Muthen, L. K. 2000. "Integrating person-centered and variable-centered analyses: growth mixture modeling with latent trajectory classes". Alcohol Clin Exp Res, 24**,** 882-91.

Muthuri, S. G., Mcwilliams, D. F., Doherty, M. & Zhang, W. 2011. "History of knee injuries and knee osteoarthritis: a meta-analysis of observational studies". Osteoarthritis Cartilage, 19**,** 1286-93.

Myers, S. L., Brandt, K. D., Ehlich, J. W., Braunstein, E. M., Shelbourne, K. D., Heck, D. A. & Kalasinski, L. A. 1990. "Synovial inflammation in patients with early osteoarthritis of the knee". J Rheumatol, 17**,** 1662-9.

Nagaosa, Y., Mateus, M., Hassan, B., Lanyon, P. & Doherty, M. 2000. "Development of a logically devised line drawing atlas for grading of knee osteoarthritis". Ann Rheum Dis, 59**,** 587-95.

Neame, R. L., Muir, K., Doherty, S. & Doherty, M. 2004. "Genetic risk of knee osteoarthritis: a sibling study". Ann Rheum Dis, 63**,** 1022-7.

Neumann, S., Doubell, T. P., Leslie, T. & Woolf, C. J. 1996. "Inflammatory pain hypersensitivity mediated by phenotypic switch in myelinated primary sensory neurons". Nature, 384**,** 360-4.

Neziri, A. Y., Haesler, S., Petersen-Felix, S., Muller, M., Arendt-Nielsen, L., Manresa, J. B., Andersen, O. K. & Curatolo, M. 2010. "Generalized expansion of nociceptive reflex receptive fields in chronic pain patients". Pain, 151**,** 798-805.

Nico, B., Mangieri, D., Benagiano, V., Crivellato, E. & Ribatti, D. 2008. "Nerve growth factor as an angiogenic factor". Microvasc Res, 75**,** 135-41.

Njr. 2015. *National Joint Registry StatsOnline* [Online]. Available: http://www.njrcentre.org.uk/njrcentre/Healthcareproviders/Accessingthedata/StatsOnline/NJRStatsOnline/tabid/179/Default.aspx [Accessed 01.05.15.

Nolan, G. P., Fujita, T., Bhatia, K., Huppi, C., Liou, H. C., Scott, M. L. & Baltimore, D. 1993. "The bcl-3 proto-oncogene encodes a nuclear I kappa B-like molecule that preferentially interacts with NF-kappa B p50 and p52 in a phosphorylation-dependent manner". Mol Cell Biol, 13**,** 3557-66.

Norling, L. V. & Perretti, M. 2013. "The role of omega-3 derived resolvins in arthritis". Curr Opin Pharmacol, 13**,** 476-81.

Nwosu, L. N., Mapp, P. I., Chapman, V. & Walsh, D. A. 2015. "Blocking the Tropomyosin receptor kinase A (TrkA) receptor inhibits pain behaviour in two rat models of osteoarthritis.". Annals of Rheumatic Diseases (under review).

Nylund, K., Asparouhov, T. & Muthen, B. 2007. "Deciding on the Number of Classes in Latent Class Analysis and Growth Mixture Modeling: A Monte Carlo Simulation Study". Structural Equation Modeling, 14**,** 535-569.

Nystedt, S., Ramakrishnan, V. & Sundelin, J. 1996. "The Proteinase-activated Receptor 2 Is Induced by Inflammatory Mediators in Human Endothelial Cells: COMPARISON WITH THE THROMBIN RECEPTOR". Journal of Biological Chemistry, 271**,** 14910-14915.

Odell, I. D. & Cook, D. 2013. "Immunofluorescence Techniques". J Invest Dermatol, 133**,** e4.

Oegema, T. R., Jr., Carpenter, R. J., Hofmeister, F. & Thompson, R. C., Jr. 1997. "The interaction of the zone of calcified cartilage and subchondral bone in osteoarthritis". Microsc Res Tech, 37**,** 324-32.

Ofman, J. J., Maclean, C. H., Straus, W. L., Morton, S. C., Berger, M. L., Roth, E. A. & Shekelle, P. 2002. "A metaanalysis of severe upper gastrointestinal complications of nonsteroidal antiinflammatory drugs". J Rheumatol, 29**,** 804-12.

Orita, S., Koshi, T., Mitsuka, T., Miyagi, M., Inoue, G., Arai, G., Ishikawa, T., Hanaoka, E., Yamashita, K., Yamashita, M., Eguchi, Y., Toyone, T., Takahashi, K. & Ohtori, S. 2011. "Associations between proinflammatory cytokines in the synovial fluid and radiographic grading and pain-related scores in 47 consecutive patients with osteoarthritis of the knee". BMC Musculoskelet Disord, 12**,** 144.

Ostergaard, K., Andersen, C. B., Petersen, J., Bendtzen, K. & Salter, D. M. 1999. "Validity of histopathological grading of articular cartilage from osteoarthritic knee joints". Ann Rheum Dis, 58**,** 208-13.

Oxford English Dictionary. *Phenotype. Oxford English Dictionary* [Online]. Available: http://www.oed.com/view/Entry/142359?rskey=0K7CuB&result=1#eid [Accessed July 2014].

Paik, S., Kim, C.-Y., Song, Y.-K. & Kim, W.-S. 2005. "Technology Insight: application of molecular techniques to formalin-fixed paraffin-embedded tissues from breast cancer". Nat Clin Prac Oncol, 2**,** 246-254.

Pallant, J. F. & Tennant, A. 2007. "An introduction to the Rasch measurement model: An example using the Hospital Anxiety and Depression Scale (HADS)". British Journal of Clinical Psychology, 46**,** 1-18.

Pandey, S. 2010. "Hybridoma technology for production of monoclonal antibodies". International Jounral of Pharmaceutical Sciences Review and Research, 1**,** 88-94.

Papadopoulos, E. J., Fitzhugh, D. J., Tkaczyk, C., Gilfillan, A. M., Sassetti, C., Metcalfe, D. D. & Hwang, S. T. 2000. "Mast cells migrate, but do not degranulate, in response to fractalkine, a membrane-bound chemokine expressed constitutively in diverse cells of the skin". Eur J Immunol, 30**,** 2355-61.

Park, S. H., Goo, J. M. & Jo, C. H. 2004. "Receiver operating characteristic (ROC) curve: practical review for radiologists". Korean J Radiol, 5**,** 11-8.

Parks, W. C., Wilson, C. L. & Lopez-Boado, Y. S. 2004. "Matrix metalloproteinases as modulators of inflammation and innate immunity". Nat Rev Immunol, 4**,** 617-29.

Pauli, C., Whiteside, R., Heras, F. L., Nesic, D., Koziol, J., Grogan, S. P., Matyas, J., Pritzker, K. P. H., D'lima, D. D. & Lotz, M. K. 2012. "Comparison of cartilage histopathology assessment systems on human knee joints at all stages of osteoarthritis development". Osteoarthritis and Cartilage, 20**,** 476-485.

Pearson, R. G., Kurien, T., Shu, K. S. & Scammell, B. E. 2011. "Histopathology grading systems for characterisation of human knee osteoarthritis--reproducibility, variability, reliability, correlation, and validity". Osteoarthritis Cartilage, 19**,** 324-31.

Peat, G., Mccarney, R. & Croft, P. 2001. "Knee pain and osteoarthritis in older adults: a review of community burden and current use of primary health care". Ann Rheum Dis, 60**,** 91-7.

Peat, G., Thomas, E., Duncan, R., Wood, L., Hay, E. & Croft, P. 2006. "Clinical classification criteria for knee osteoarthritis: performance in the general population and primary care". Ann Rheum Dis, 65**,** 1363-7.

Pei, L., Zhang, J., Zhao, F., Su, T., Wei, H., Tian, J., Li, M. & Shi, J. 2011. "Annexin 1 exerts anti-nociceptive effects after peripheral inflammatory pain through formyl-peptide-receptor-like 1 in rat dorsal root ganglion". Br J Anaesth, 107**,** 948-58.

Pelletier, J. P., Caron, J. P., Evans, C., Robbins, P. D., Georgescu, H. I., Jovanovic, D., Fernandes, J. C. & Martel-Pelletier, J. 1997. "In vivo suppression of early experimental osteoarthritis by interleukin-1 receptor antagonist using gene therapy". Arthritis Rheum, 40**,** 1012-9.

Perretti, M. & D'acquisto, F. 2009. "Annexin A1 and glucocorticoids as effectors of the resolution of inflammation". Nat Rev Immunol, 9**,** 62-70.

Pesesse, L., Sanchez, C. & Henrotin, Y. 2011. "Osteochondral plate angiogenesis: a new treatment target in osteoarthritis". Joint Bone Spine, 78**,** 144-9.

Pessler, F., Ogdie, A. R., Mayer, C. T., Kretzschmar, W. W., Dai, L., Elsaman, A. M., Einhorn, E., Krenn, V. & Schumacher, H. R. 2014. "Amyloid arthropathy associated with multiple myeloma: polyarthritis without synovial infiltration of CD20+ or CD38+ cells". Amyloid, 21**,** 28-34.

Pezet, S. & Mcmahon, S. B. 2006. "Neurotrophins: mediators and modulators of pain". Annu Rev Neurosci, 29**,** 507-38.

Phan, C. M., Link, T. M., Blumenkrantz, G., Dunn, T. C., Ries, M. D., Steinbach, L. S. & Majumdar, S. 2006. "MR imaging findings in the follow-up of patients with different stages of knee osteoarthritis and the correlation with clinical symptoms". Eur Radiol, 16**,** 608-18.

Pickens, S. R., Chamberlain, N. D., Volin, M. V., Gonzalez, M., Pope, R. M., Mandelin, A. M., 2nd, Kolls, J. K. & Shahrara, S. 2011. "Anti-CXCL5 therapy ameliorates IL-17-induced arthritis by decreasing joint vascularization". Angiogenesis, 14**,** 443-55.

Pincus, T., Koch, G. G., Sokka, T., Lefkowith, J., Wolfe, F., Jordan, J. M., Luta, G., Callahan, L. F., Wang, X., Schwartz, T., Abramson, S. B., Caldwell, J. R., Harrell, R. A., Kremer, J. M., Lautzenheiser, R. L., Markenson, J. A., Schnitzer, T. J., Weaver, A., Cummins, P., Wilson, A., Morant, S. & Fort, J. 2001. "A randomized, double-blind, crossover clinical trial of diclofenac plus misoprostol versus acetaminophen in patients with osteoarthritis of the hip or knee". Arthritis Rheum, 44**,** 1587-98.

Piperno, M., Reboul, P., Hellio Le Graverand, M. P., Peschard, M., Annefeld, M., Richard, M. & Vignon, E. 1998. "Osteoarthritic cartilage fibrillation is associated with a decrease in chondrocyte adhesion to fibronectin". Osteoarthritis Cartilage, 6**,** 393-9.

Poole, C. A. 1997. "Articular cartilage chondrons: form, function and failure". J Anat, 191 (Pt 1)**,** 1-13.

Poole, D. P., Amadesi, S., Veldhuis, N. A., Abogadie, F. C., Lieu, T., Darby, W., Liedtke, W., Lew, M. J., Mcintyre, P. & Bunnett, N. W. 2013.

"Protease-activated receptor 2 (PAR2) protein and transient receptor potential vanilloid 4 (TRPV4) protein coupling is required for sustained inflammatory signaling". J Biol Chem, 288**,** 5790-802.

Pottenger, L. A., Phillips, F. M. & Draganich, L. F. 1990. "The effect of marginal osteophytes on reduction of varus-valgus instability in osteoarthritic knees". Arthritis Rheum, 33**,** 853-8.

Pritzker, K. P., Gay, S., Jimenez, S. A., Ostergaard, K., Pelletier, J. P., Revell, P. A., Salter, D. & Van Den Berg, W. B. 2006. "Osteoarthritis cartilage histopathology: grading and staging". Osteoarthritis Cartilage, 14**,** 13-29.

Radin, E. L. & Rose, R. M. 1986. "Role of subchondral bone in the initiation and progression of cartilage damage". Clin Orthop Relat Res**,** 34-40.

Raingeaud, J., Whitmarsh, A. J., Barrett, T., Derijard, B. & Davis, R. J. 1996. "MKK3- and MKK6-regulated gene expression is mediated by the p38 mitogen-activated protein kinase signal transduction pathway". Mol Cell Biol, 16**,** 1247-55.

Ralphs, J. & Benjamin, M. 1994. "The joint capsule: structure, composition, ageing and disease ". Journal of Anatomy, 184**,** 503-590.

Rang, H. P., Bevan, S. & Dray, A. 1991. "Chemical activation of nociceptive peripheral neurones". Br Med Bull, 47**,** 534-48.

Rawlings, J. S., Rosler, K. M. & Harrison, D. A. 2004. "The JAK/STAT signaling pathway". Journal of Cell Science, 117**,** 1281-1283.

Raychaudhuri, S. P., Raychaudhuri, S. K., Atkuri, K. R. & Herzenberg, L. A. 2011. "Nerve growth factor: A key local regulator in the pathogenesis of inflammatory arthritis". Arthritis Rheum, 63**,** 3243-52.

Raynauld, J. P., Buckland-Wright, C., Ward, R., Choquette, D., Haraoui, B., Martel-Pelletier, J., Uthman, I., Khy, V., Tremblay, J. L., Bertrand, C. & Pelletier, J. P. 2003. "Safety and efficacy of long-term intraarticular steroid injections in osteoarthritis of the knee: a randomized, double-blind, placebo-controlled trial". Arthritis Rheum, 48**,** 370-7.

Raynauld, J. P., Martel-Pelletier, J., Haraoui, B., Choquette, D., Dorais, M., Wildi, L. M., Abram, F. & Pelletier, J. P. 2011. "Risk factors predictive of joint replacement in a 2-year multicentre clinical trial in knee osteoarthritis using MRI: results from over 6 years of observation". Ann Rheum Dis, 70**,** 1382-8.

Reboul, P., Pelletier, J. P., Tardif, G., Cloutier, J. M. & Martel-Pelletier, J. 1996. "The new collagenase, collagenase-3, is expressed and synthesized by human chondrocytes but not by synoviocytes. A role in osteoarthritis". J Clin Invest, 97**,** 2011-9.

Reichenbach, S., Guermazi, A., Niu, J., Neogi, T., Hunter, D. J., Roemer, F. W., Mclennan, C. E., Hernandez-Molina, G. & Felson, D. T. 2008. "Prevalence of bone attrition on knee radiographs and MRI in a community-based cohort". Osteoarthritis Cartilage, 16**,** 1005-10.

Reichenberger, E., Aigner, T., Von Der Mark, K., Stoss, H. & Bertling, W. 1991. "In situ hybridization studies on the expression of type X collagen in fetal human cartilage". Dev Biol, 148**,** 562-72.

Ricciotti, E. & Fitzgerald, G. A. 2011. "Prostaglandins and Inflammation". Arteriosclerosis, thrombosis, and vascular biology, 31**,** 986-1000.

Rigoglou, S. & Papavassiliou, A. G. 2013. "The NF-kappaB signalling pathway in osteoarthritis". Int J Biochem Cell Biol, 45**,** 2580-4.

Roemer, F. W., Zhang, Y., Niu, J., Lynch, J. A., Crema, M. D., Marra, M. D., Nevitt, M. C., Felson, D. T., Hughes, L. B., El-Khoury, G. Y., Englund, M. & Guermazi, A. 2009a. "Tibiofemoral joint osteoarthritis: risk factors for MR-depicted fast cartilage loss over a 30-month period in the multicenter osteoarthritis study". Radiology, 252**,** 772-80.

Roemer, F. W., Guermazi, A., Javaid, M. K., Lynch, J. A., Niu, J., Zhang, Y., Felson, D. T., Lewis, C. E., Torner, J. & Nevitt, M. C. 2009b. "Change in MRI-detected subchondral bone marrow lesions is associated with cartilage loss: the MOST Study. A longitudinal multicentre study of knee osteoarthritis". Ann Rheum Dis, 68**,** 1461-5.

Roemer, F. W., Kwoh, C. K., Hannon, M. J., Boudreau, R., Hunter, D. J., Eckstein, F., Wang, Z., Grago, J. & Guermazi, A. 2013. "OP0153 Subchondral Bone Marrow Lesions Predict Incident Radiographic Osteoarthritis". Annals of the Rheumatic Diseases, 72**,** A104.

Roman-Blas, J. A. & Jimenez, S. A. 2006. "NF-kappaB as a potential therapeutic target in osteoarthritis and rheumatoid arthritis". Osteoarthritis Cartilage, 14**,** 839-48.

Rommel, C., Camps, M. & Ji, H. 2007. "PI3K delta and PI3K gamma: partners in crime in inflammation in rheumatoid arthritis and beyond?". Nat Rev Immunol, 7**,** 191-201.

Rosenthal, A. K. 2011. "Crystals, inflammation, and osteoarthritis". Curr Opin Rheumatol, 23**,** 170-3.

Rundhaug, J. 2005. "Matrix metalloproteinases and angiogenesis". Journal of cellular and molecular medicine, 9**,** 2267-2285.

Russell, F. A. & Mcdougall, J. J. 2009. "Proteinase activated receptor (PAR) involvement in mediating arthritis pain and inflammation". Inflamm Res, 58**,** 119-26.

Ruth, J. H., Volin, M. V., Haines, G. K., 3rd, Woodruff, D. C., Katschke, K. J., Jr., Woods, J. M., Park, C. C., Morel, J. C. & Koch, A. E. 2001. "Fractalkine, a novel chemokine in rheumatoid arthritis and in rat adjuvant-induced arthritis". Arthritis Rheum, 44**,** 1568-81.

Sadouk, M. B., Pelletier, J. P., Tardif, G., Kiansa, K., Cloutier, J. M. & Martel-Pelletier, J. 1995. "Human synovial fibroblasts coexpress IL-1 receptor type I and type II mRNA. The increased level of the IL-1 receptor in osteoarthritic cells is related to an increased level of the type I receptor". Lab Invest, 73**,** 347-55.

Sagar, D. R., Ashraf, S., Xu, L., Burston, J. J., Menhinick, M. R., Poulter, C. L., Bennett, A. J., Walsh, D. A. & Chapman, V. 2013. "Osteoprotegerin reduces the development of pain behaviour and joint pathology in a model of osteoarthritis". Annals of the Rheumatic Diseases.

Saha, N., Moldovan, F., Tardif, G., Pelletier, J.-P., Cloutier, J.-M. & Martel-Pelletier, J. 1999. "Interleukin-1β–converting enzyme/caspase-1 in human osteoarthritic tissues: Localization and role in the maturation of interleukin-1β and interleukin-18". Arthritis & Rheumatism, 42**,** 1577-1587.

Sampey, A. V., Hutchinson, P. & Morand, E. F. 2000. "Annexin I and dexamethasone effects on phospholipase and cyclooxygenase activity in human synoviocytes". Mediators Inflamm, 9**,** 125-32.

Sanchez, C., Deberg, M. A., Piccardi, N., Msika, P., Reginster, J. Y. & Henrotin, Y. E. 2005. "Subchondral bone osteoblasts induce phenotypic

changes in human osteoarthritic chondrocytes". Osteoarthritis Cartilage, 13, 988-97.

Sandell, L. J. & Aigner, T. 2001. "Articular cartilage and changes in arthritis. An introduction: cell biology of osteoarthritis". Arthritis Res, 3, 107-13.

Sanga, P., Katz, N., Polverejan, E., Wang, S., Kelly, K. M., Haeussler, J. & Thipphawong, J. 2013. "Efficacy, safety, and tolerability of fulranumab, an anti-nerve growth factor antibody, in the treatment of patients with moderate to severe osteoarthritis pain". Pain, 154, 1910-9.

Scaife, S., Brown, R., Kellie, S., Filer, A., Martin, S., Thomas, A. M. C., Bradfield, P. F., Amft, N., Salmon, M. & Buckley, C. D. 2004. "Detection of differentially expressed genes in synovial fibroblasts by restriction fragment differential display". Rheumatology, 43, 1346-1352.

Scanzello, C. R., Umoh, E., Pessler, F., Diaz-Torne, C., Miles, T., Dicarlo, E., Potter, H. G., Mandl, L., Marx, R., Rodeo, S., Goldring, S. R. & Crow, M. K. 2009. "Local cytokine profiles in knee osteoarthritis: elevated synovial fluid interleukin-15 differentiates early from end-stage disease". Osteoarthritis and Cartilage, 17, 1040-1048.

Schaible, H. G. & Grubb, B. D. 1993. "Afferent and spinal mechanisms of joint pain". Pain, 55, 5-54.

Scheiman, J. M. 2013. "The use of proton pump inhibitors in treating and preventing NSAID-induced mucosal damage". Arthritis Res Ther, 15 Suppl 3, S5.

Schelbergen, R. F., De Munter, W., Van Den Bosch, M. H., Lafeber, F. P., Sloetjes, A., Vogl, T., Roth, J., Van Den Berg, W. B., Van Der Kraan, P. M., Blom, A. B. & Van Lent, P. L. 2014. "Alarmins S100A8/S100A9 aggravate osteophyte formation in experimental osteoarthritis and predict osteophyte progression in early human symptomatic osteoarthritis". Ann Rheum Dis.

Scher, C., Craig, J. & Nelson, F. 2008. "Bone marrow edema in the knee in osteoarthrosis and association with total knee arthroplasty within a three-year follow-up". Skeletal Radiol, 37, 609-17.

Schett, G., Tohidast-Akrad, M., Smolen, J. S., Schmid, B. J., Steiner, C. W., Bitzan, P., Zenz, P., Redlich, K., Xu, Q. & Steiner, G. 2000. "Activation, differential localization, and regulation of the stress-activated protein kinases, extracellular signal-regulated kinase, c-JUN N-terminal kinase, and p38 mitogen-activated protein kinase, in synovial tissue and cells in rheumatoid arthritis". Arthritis Rheum, 43, 2501-12.

Schmidt, R., Schmelz, M., Forster, C., Ringkamp, M., Torebjork, E. & Handwerker, H. 1995. "Novel classes of responsive and unresponsive C nociceptors in human skin". J Neurosci, 15, 333-41.

Schmittgen, T. D. & Livak, K. J. 2008. "Analyzing real-time PCR data by the comparative CT method". Nat. Protocols, 3, 1101-1108.

Schnell, S. A., Staines, W. A. & Wessendorf, M. W. 1999. "Reduction of lipofuscin-like autofluorescence in fluorescently labeled tissue". J Histochem Cytochem, 47, 719-30.

Schönbeck, U., Mach, F. & Libby, P. 1998. "Generation of Biologically Active IL-1β by Matrix Metalloproteinases: A Novel Caspase-1-Independent

Pathway of IL-1β Processing". The Journal of Immunology, 161**,** 3340-3346.
Schroeder, A., Mueller, O., Stocker, S., Salowsky, R., Leiber, M., Gassmann, M., Lightfoot, S., Menzel, W., Granzow, M. & Ragg, T. 2006. "The RIN: an RNA integrity number for assigning integrity values to RNA measurements". BMC Mol Biol, 7**,** 3.
Sclove, S. 1987. "Application of model-selection criteria to some problems in multivariate analysis". Psychometrika, 52**,** 333-343.
Seedhom, B. B., Dowson, D. & Wright, V. 1974. "Proceedings: Functions of the menisci. A preliminary study". Ann Rheum Dis, 33**,** 111.
Seibel, M. J., Duncan, A. & Robins, S. P. 1989. "Urinary hydroxy-pyridinium crosslinks provide indices of cartilage and bone involvement in arthritic diseases". J Rheumatol, 16**,** 964-70.
Seibert, K. & Masferrer, J. L. 1994. "Role of inducible cyclooxygenase (COX-2) in inflammation". Receptor, 4**,** 17-23.
Seidel, M. F., Herguijuela, M., Forkert, R. & Otten, U. 2010. "Nerve growth factor in rheumatic diseases". Semin Arthritis Rheum, 40**,** 109-26.
Sellam, J. & Berenbaum, F. 2010. "The role of synovitis in pathophysiology and clinical symptoms of osteoarthritis". Nat Rev Rheumatol, 6**,** 625-35.
Serhan, C. N., Chiang, N. & Van Dyke, T. E. 2008. "Resolving inflammation: dual anti-inflammatory and pro-resolution lipid mediators". Nat Rev Immunol, 8**,** 349-61.
Setton, L. A., Mow, V. C., Muller, F. J., Pita, J. C. & Howell, D. S. 1994. "Mechanical properties of canine articular cartilage are significantly altered following transection of the anterior cruciate ligament". J Orthop Res, 12**,** 451-63.
Shane Anderson, A. & Loeser, R. F. 2010. "Why is osteoarthritis an age-related disease?". Best Pract Res Clin Rheumatol, 24**,** 15-26.
Shao, W. H., Del Prete, A., Bock, C. B. & Haribabu, B. 2006. "Targeted disruption of leukotriene B4 receptors BLT1 and BLT2: a critical role for BLT1 in collagen-induced arthritis in mice". J Immunol, 176**,** 6254-61.
Sharif, M., George, E. & Dieppe, P. A. 1995. "Correlation between synovial fluid markers of cartilage and bone turnover and scintigraphic scan abnormalities in osteoarthritis of the knee". Arthritis Rheum, 38**,** 78-81.
Shea, T., Tennant, A. & Pallant, J. 2009. "Rasch model analysis of the Depression, Anxiety and Stress Scales (DASS)". BMC Psychiatry, 9**,** 21.
Shen, X., Hong, F., Nguyen, V. A. & Gao, B. 2000. "IL-10 attenuates IFN-alpha-activated STAT1 in the liver: involvement of SOCS2 and SOCS3". FEBS Lett, 480**,** 132-6.
Shepstone, L., Rogers, J., Kirwan, J. & Silverman, B. 2000. "Distribution of distal femoral osteophytes in a human skeletal population". Ann Rheum Dis, 59**,** 513-20.
Shi, S. R., Key, M. E. & Kalra, K. L. 1991. "Antigen retrieval in formalin-fixed, paraffin-embedded tissues: an enhancement method for immunohistochemical staining based on microwave oven heating of tissue sections". Journal of Histochemistry & Cytochemistry, 39**,** 741-8.

Shim, S. S. & Leung, G. 1986. "Blood supply of the knee joint. A microangiographic study in children and adults". Clin Orthop Relat Res**,** 119-25.

Shu, S., Ju, G. & Fan, L. 1988. "The glucose oxidase-DAB-nickel method in peroxidase histochemistry of the nervous system". Neuroscience Letters, 85**,** 169-171.

Silvestri, T., Pulsatelli, L., Dolzani, P., Facchini, A. & Meliconi, R. 2006. "Elevated serum levels of soluble interleukin-4 receptor in osteoarthritis". Osteoarthritis Cartilage, 14**,** 717-9.

Simao, A. P., Mendonca, V. A., De Oliveira Almeida, T. M., Santos, S. A., Gomes, W. F., Coimbra, C. C. & Lacerda, A. C. 2014. "Involvement of BDNF in knee osteoarthritis: the relationship with inflammation and clinical parameters". Rheumatol Int.

Sivilotti, L. & Woolf, C. J. 1994. "The contribution of GABAA and glycine receptors to central sensitization: disinhibition and touch-evoked allodynia in the spinal cord". J Neurophysiol, 72**,** 169-79.

Smith, M. D., Triantafillou, S., Parker, A., Youssef, P. P. & Coleman, M. 1997. "Synovial membrane inflammation and cytokine production in patients with early osteoarthritis". J Rheumatol, 24**,** 365-71.

Smith, M. D. 2011. "The normal synovium". Open Rheumatol J, 5**,** 100-6.

Soren, A., Cooper, N. S. & Waugh, T. R. 1988. "The nature and designation of osteoarthritis determined by its histopathology". Clin Exp Rheumatol, 6**,** 41-6.

Sowers, M. F., Hayes, C., Jamadar, D., Capul, D., Lachance, L., Jannausch, M. & Welch, G. 2003. "Magnetic resonance-detected subchondral bone marrow and cartilage defect characteristics associated with pain and X-ray-defined knee osteoarthritis". Osteoarthritis Cartilage, 11**,** 387-93.

Sowers, M. R. & Karvonen-Gutierrez, C. A. 2010. "The evolving role of obesity in knee osteoarthritis". Curr Opin Rheumatol, 22**,** 533-7.

Spector, T. D. & Cooper, C. 1993. "Radiographic assessment of osteoarthritis in population studies: whither Kellgren and Lawrence?". Osteoarthritis Cartilage, 1**,** 203-6.

Spector, T. D., Cicuttini, F., Baker, J., Loughlin, J. & Hart, D. 1996. "Genetic influences on osteoarthritis in women: a twin study". BMJ, 312**,** 940-3.

Spector, T. D., Nandra, D., Hart, D. J. & Doyle, D. V. 1997. "Is hormone replacement therapy protective for hand and knee osteoarthritis in women?: The Chingford Study". Ann Rheum Dis, 56**,** 432-4.

Spicarova, D., Adamek, P., Kalynovska, N., Mrozkova, P. & Palecek, J. 2014. "TRPV1 receptor inhibition decreases CCL2-induced hyperalgesia". Neuropharmacology, 81**,** 75-84.

Srinivasan, R., Wolfe, D., Goss, J., Watkins, S., De Groat, W. C., Sculptoreanu, A. & Glorioso, J. C. 2008. "Protein kinase C epsilon contributes to basal and sensitizing responses of TRPV1 to capsaicin in rat dorsal root ganglion neurons". Eur J Neurosci, 28**,** 1241-54.

Standring, S. (ed.) 2005. *Gray's Anatomy. The Anatomical Basis of Clinical Practice*: Elsevier Churchill Livingstone.

Stannus, O., Jones, G., Cicuttini, F., Parameswaran, V., Quinn, S., Burgess, J. & Ding, C. 2010. "Circulating levels of IL-6 and TNF-alpha are associated with knee radiographic osteoarthritis and knee cartilage loss in older adults". Osteoarthritis Cartilage, 18**,** 1441-7.

Stannus, O. P., Jones, G., Blizzard, L., Cicuttini, F. M. & Ding, C. 2012. "Associations between serum levels of inflammatory markers and change in knee pain over 5 years in older adults: a prospective cohort study". Ann Rheum Dis.

Starr, R., Willson, T. A., Viney, E. M., Murray, L. J., Rayner, J. R., Jenkins, B. J., Gonda, T. J., Alexander, W. S., Metcalf, D., Nicola, N. A. & Hilton, D. J. 1997. "A family of cytokine-inducible inhibitors of signalling". Nature, 387**,** 917-21.

Steinhoff, M., Vergnolle, N., Young, S. H., Tognetto, M., Amadesi, S., Ennes, H. S., Trevisani, M., Hollenberg, M. D., Wallace, J. L., Caughey, G. H., Mitchell, S. E., Williams, L. M., Geppetti, P., Mayer, E. A. & Bunnett, N. W. 2000. "Agonists of proteinase-activated receptor 2 induce inflammation by a neurogenic mechanism". Nat Med, 6**,** 151-8.

Strassle, B. W., Mark, L., Leventhal, L., Piesla, M. J., Jian Li, X., Kennedy, J. D., Glasson, S. S. & Whiteside, G. T. 2010. "Inhibition of osteoclasts prevents cartilage loss and pain in a rat model of degenerative joint disease". Osteoarthritis Cartilage, 18**,** 1319-28.

Sun, J.-M., Sun, L.-Z., Liu, J., Su, B.-H. & Shi, L. 2013. "Serum Interleukin-15 Levels Are Associated with Severity of Pain in Patients with Knee Osteoarthritis". Disease Markers, 35**,** 4.

Sun, Y., Yu, H., Zheng, D., Cao, Q., Wang, Y., Harris, D. & Wang, Y. 2011. "Sudan black B reduces autofluorescence in murine renal tissue". Arch Pathol Lab Med, 135**,** 1335-42.

Suokas, A. K., Walsh, D. A., Mcwilliams, D. F., Condon, L., Moreton, B., Wylde, V., Arendt-Nielsen, L. & Zhang, W. 2012. "Quantitative sensory testing in painful osteoarthritis: a systematic review and meta-analysis". Osteoarthritis Cartilage, 20**,** 1075-85.

Suri, S., Gill, S. E., Massena De Camin, S., Wilson, D., Mcwilliams, D. F. & Walsh, D. A. 2007. "Neurovascular invasion at the osteochondral junction and in osteophytes in osteoarthritis". Ann Rheum Dis, 66**,** 1423-8.

Swales, C. & Athanasou, N. A. 2010. "(i) The pathobiology of osteoarthritis". Orthopaedics and Trauma, 24**,** 399-404.

Swan, A., Heywood, B., Chapman, B., Seward, H. & Dieppe, P. 1995. "Evidence for a causal relationship between the structure, size, and load of calcium pyrophosphate dihydrate crystals, and attacks of pseudogout". Ann Rheum Dis, 54**,** 825-30.

Swann, D. A., Bloch, K. J., Swindell, D. & Shore, E. 1984. "The lubricating activity of human synovial fluids". Arthritis Rheum, 27**,** 552-6.

Szebenyi, B., Hollander, A. P., Dieppe, P., Quilty, B., Duddy, J., Clarke, S. & Kirwan, J. R. 2006. "Associations between pain, function, and radiographic features in osteoarthritis of the knee". Arthritis Rheum, 54**,** 230-5.

Tak, P. P. & Firestein, G. S. 2001. "NF-kappaB: a key role in inflammatory diseases". J Clin Invest, 107**,** 7-11.

Tamiya, T., Kashiwagi, I., Takahashi, R., Yasukawa, H. & Yoshimura, A. 2011. "Suppressors of Cytokine Signaling (SOCS) Proteins and JAK/STAT Pathways: Regulation of T-Cell Inflammation by SOCS1 and SOCS3". Arteriosclerosis, Thrombosis, and Vascular Biology, 31**,** 980-985.

Tanamas, S., Hanna, F. S., Cicuttini, F. M., Wluka, A. E., Berry, P. & Urquhart, D. M. 2009. "Does knee malalignment increase the risk of development and progression of knee osteoarthritis? A systematic review". Arthritis Rheum, 61**,** 459-67.

Tanamas, S. K., Wluka, A. E., Pelletier, J. P., Martel-Pelletier, J., Abram, F., Wang, Y. & Cicuttini, F. M. 2010a. "The association between subchondral bone cysts and tibial cartilage volume and risk of joint replacement in people with knee osteoarthritis: a longitudinal study". Arthritis Res Ther, 12**,** R58.

Tanamas, S. K., Wluka, A. E., Pelletier, J. P., Pelletier, J. M., Abram, F., Berry, P. A., Wang, Y., Jones, G. & Cicuttini, F. M. 2010b. "Bone marrow lesions in people with knee osteoarthritis predict progression of disease and joint replacement: a longitudinal study". Rheumatology (Oxford), 49**,** 2413-9.

Tang, C. H., Hsu, C. J. & Fong, Y. C. 2010. "The CCL5/CCR5 axis promotes interleukin-6 production in human synovial fibroblasts". Arthritis Rheum, 62**,** 3615-24.

Tennant, A. & Conaghan, P. G. 2007. "The Rasch measurement model in rheumatology: What is it and why use it? When should it be applied, and what should one look for in a Rasch paper?". Arthritis Care & Research, 57**,** 1358-1362.

Thomas, C. M., Fuller, C. J., Whittles, C. E. & Sharif, M. 2007. "Chondrocyte death by apoptosis is associated with cartilage matrix degradation". Osteoarthritis Cartilage, 15**,** 27-34.

Thompson, S. W., Woolf, C. J. & Sivilotti, L. G. 1993. "Small-caliber afferent inputs produce a heterosynaptic facilitation of the synaptic responses evoked by primary afferent A-fibers in the neonatal rat spinal cord in vitro". J Neurophysiol, 69**,** 2116-28.

Tiseo, P. J., Kivitz, A. J., Ervin, J. E., Ren, H. & Mellis, S. J. 2014. "Fasinumab (REGN475), an antibody against nerve growth factor for the treatment of pain: Results from a double-blind, placebo-controlled exploratory study in osteoarthritis of the knee". Pain, 155**,** 1245-52.

Torres, L., Dunlop, D. D., Peterfy, C., Guermazi, A., Prasad, P., Hayes, K. W., Song, J., Cahue, S., Chang, A., Marshall, M. & Sharma, L. 2006. "The relationship between specific tissue lesions and pain severity in persons with knee osteoarthritis". Osteoarthritis Cartilage, 14**,** 1033-40.

Uchino, M., Izumi, T., Tominaga, T., Wakita, R., Minehara, H., Sekiguchi, M. & Itoman, M. 2000. "Growth factor expression in the osteophytes of the human femoral head in osteoarthritis". Clin Orthop Relat Res**,** 119-25.

Valdes, A. M., Hart, D. J., Jones, K. A., Surdulescu, G., Swarbrick, P., Doyle, D. V., Schafer, A. J. & Spector, T. D. 2004. "Association study of candidate genes for the prevalence and progression of knee osteoarthritis". Arthritis & Rheumatism, 50**,** 2497-2507.

Valdes, A. M., De Wilde, G., Doherty, S. A., Lories, R. J., Vaughn, F. L., Laslett, L. L., Maciewicz, R. A., Soni, A., Hart, D. J., Zhang, W., Muir, K. R., Dennison, E. M., Wheeler, M., Leaverton, P., Cooper, C., Spector, T. D., Cicuttini, F. M., Chapman, V., Jones, G., Arden, N. K. & Doherty, M. 2011. "The Ile585Val TRPV1 variant is involved in risk of painful knee osteoarthritis". Ann Rheum Dis, 70**,** 1556-61.

Valdes, A. M., Suokas, A. K., Doherty, S. A., Jenkins, W. & Doherty, M. 2014. "History of knee surgery is associated with higher prevalence of neuropathic pain-like symptoms in patients with severe osteoarthritis of the knee". Semin Arthritis Rheum, 43**,** 588-92.

Van Der Esch, M., Knoop, J., Hunter, D. J., Klein, J. P., Van Der Leeden, M., Knol, D. L., Reiding, D., Voorneman, R. E., Gerritsen, M., Roorda, L. D., Lems, W. F. & Dekker, J. 2013. "The association between reduced knee joint proprioception and medial meniscal abnormalities using MRI in knee osteoarthritis: results from the Amsterdam osteoarthritis cohort". Osteoarthritis and Cartilage, 21**,** 676-681.

Van Lent, P. L. E. M., Blom, A. B., Schelbergen, R. F. P., Slöetjes, A., Lafeber, F. P. J. G., Lems, W. F., Cats, H., Vogl, T., Roth, J. & Van Den Berg, W. B. 2012. "Active involvement of alarmins S100A8 and S100A9 in the regulation of synovial activation and joint destruction during mouse and human osteoarthritis". Arthritis & Rheumatism, 64**,** 1466-1476.

Vandenabeele, P., Declercq, W., Beyaert, R. & Fiers, W. 1995. "Two tumour necrosis factor receptors: structure and function". Trends in Cell Biology, 5**,** 392-399.

Vandesompele, J., De Preter, K., Pattyn, F., Poppe, B., Van Roy, N., De Paepe, A. & Speleman, F. 2002. "Accurate normalization of real-time quantitative RT-PCR data by geometric averaging of multiple internal control genes". Genome Biol, 3**,** RESEARCH0034.

Viera, A. & Garrett, J. 2005. "Understanding Interobserver Agreement: The Kappa Statistic". Family Medicine, 37**,** 360-363.

Vogl, T., Gharibyan, A. L. & Morozova-Roche, L. A. 2012. "Pro-Inflammatory S100A8 and S100A9 Proteins: Self-Assembly into Multifunctional Native and Amyloid Complexes". Int J Mol Sci, 13**,** 2893-917.

Voscopoulos, C. & Lema, M. 2010. "When does acute pain become chronic?". Br J Anaesth, 105 Suppl 1**,** i69-85.

Vuong, Q. H. 1989. "Likelihood Ratio Tests for Model Selection and Non-Nested Hypotheses". Econometrica, 57**,** 307-333.

Walker, J. G., Ahern, M. J., Coleman, M., Weedon, H., Papangelis, V., Beroukas, D., Roberts-Thomson, P. J. & Smith, M. D. 2006. "Expression of Jak3, STAT1, STAT4, and STAT6 in inflammatory arthritis: unique Jak3 and STAT4 expression in dendritic cells in seropositive rheumatoid arthritis". Ann Rheum Dis, 65**,** 149-56.

Walsh, D. A., Bonnet, C. S., Turner, E. L., Wilson, D., Situ, M. & Mcwilliams, D. F. 2007. "Angiogenesis in the synovium and at the osteochondral junction in osteoarthritis". Osteoarthritis and Cartilage, 15**,** 743-751.

Walsh, D. A., Yousef, A., Mcwilliams, D. F., Hill, R., Hargin, E. & Wilson, D. 2009. "Evaluation of a Photographic Chondropathy Score (PCS) for pathological samples in a study of inflammation in tibiofemoral osteoarthritis". Osteoarthritis Cartilage, 17**,** 304-12.

Walsh, D. A., Mcwilliams, D. F., Turley, M. J., Dixon, M. R., Franses, R. E., Mapp, P. I. & Wilson, D. 2010. "Angiogenesis and nerve growth factor at the osteochondral junction in rheumatoid arthritis and osteoarthritis". Rheumatology (Oxford), 49**,** 1852-61.

Wang, Z., Qiu, Y., Lu, J. & Wu, N. 2013. "Connective tissue growth factor promotes interleukin-1beta-mediated synovial inflammation in knee osteoarthritis". Mol Med Rep, 8**,** 877-82.
Wenham, C. Y. & Conaghan, P. G. 2010. "The role of synovitis in osteoarthritis". Ther Adv Musculoskelet Dis, 2**,** 349-59.
White, F. A., Jung, H. & Miller, R. J. 2007. "Chemokines and the pathophysiology of neuropathic pain". Proceedings of the National Academy of Sciences, 104**,** 20151-20158.
White, F. A., Feldman, P. & Miller, R. J. 2009. "Chemokine signaling and the management of neuropathic pain". Mol Interv, 9**,** 188-95.
Wilkinson, C. E., Carr, A. J. & Doherty, M. 2005. "Does increasing the grades of the knee osteoarthritis line drawing atlas alter its clinimetric properties?". Ann Rheum Dis, 64**,** 1467-73.
Wise, B. L., Niu, J., Zhang, Y., Wang, N., Jordan, J. M., Choy, E. & Hunter, D. J. 2010. "Psychological factors and their relation to osteoarthritis pain". Osteoarthritis and Cartilage, 18**,** 883-887.
Wojdasiewicz, P., Poniatowski, L. A., Kotela, A., Deszczynski, J., Kotela, I. & Szukiewicz, D. 2014a. "The Chemokine CX3CL1 (Fractalkine) and its Receptor CX3CR1: Occurrence and Potential Role in Osteoarthritis". Arch Immunol Ther Exp (Warsz).
Wojdasiewicz, P., Poniatowski, L. A. & Szukiewicz, D. 2014b. "The Role of Inflammatory and Anti-Inflammatory Cytokines in the Pathogenesis of Osteoarthritis". Mediators Inflamm, 2014**,** 561459.
Wojtys, E. M., Beaman, D. N., Glover, R. A. & Janda, D. 1990. "Innervation of the human knee joint by substance-P fibers". Arthroscopy, 6**,** 254-63.
Woolf, A. P., B 2003. "Burden of musculoskeletal conditions". Bulletin of the World Health Organisation, 81**,** 646-656.
Woolf, C. J. 1983. "Evidence for a central component of post-injury pain hypersensitivity". Nature, 306**,** 686-688.
Woolf, C. J. & King, A. E. 1990. "Dynamic alterations in the cutaneous mechanoreceptive fields of dorsal horn neurons in the rat spinal cord". J Neurosci, 10**,** 2717-26.
Woolf, C. J. & Thompson, S. W. 1991. "The induction and maintenance of central sensitization is dependent on N-methyl-D-aspartic acid receptor activation; implications for the treatment of post-injury pain hypersensitivity states". Pain, 44**,** 293-9.
Woolf, C. J. 1996. "Phenotypic modification of primary sensory neurons: the role of nerve growth factor in the production of persistent pain". Philos Trans R Soc Lond B Biol Sci, 351**,** 441-8.
Woolf, C. J. & Salter, M. W. 2000. "Neuronal plasticity: increasing the gain in pain". Science, 288**,** 1765-9.
Woolf, C. J. 2011. "Central sensitization: implications for the diagnosis and treatment of pain". Pain, 152**,** S2-15.
Wylde, V., Hewlett, S., Learmonth, I. D. & Dieppe, P. 2011. "Persistent pain after joint replacement: prevalence, sensory qualities, and postoperative determinants". Pain, 152**,** 566-72.
Yasukawa, H., Misawa, H., Sakamoto, H., Masuhara, M., Sasaki, A., Wakioka, T., Ohtsuka, S., Imaizumi, T., Matsuda, T., Ihle, J. N. & Yoshimura, A. 1999. "The JAK-binding protein JAB inhibits Janus tyrosine kinase activity through binding in the activation loop". EMBO J, 18**,** 1309-20.

Zanetti, M., Bruder, E., Romero, J. & Hodler, J. 2000. "Bone marrow edema pattern in osteoarthritic knees: correlation between MR imaging and histologic findings". Radiology, 215**,** 835-40.

Zhang, J. M. & An, J. 2007. "Cytokines, inflammation, and pain". Int Anesthesiol Clin, 45**,** 27-37.

Zhang, N., Inan, S., Cowan, A., Sun, R., Wang, J. M., Rogers, T. J., Caterina, M. & Oppenheim, J. J. 2005a. "A proinflammatory chemokine, CCL3, sensitizes the heat- and capsaicin-gated ion channel TRPV1". Proc Natl Acad Sci U S A, 102**,** 4536-41.

Zhang, W., Doherty, M., Peat, G., Bierma-Zeinstra, M. A., Arden, N. K., Bresnihan, B., Herrero-Beaumont, G., Kirschner, S., Leeb, B. F., Lohmander, L. S., Mazieres, B., Pavelka, K., Punzi, L., So, A. K., Tuncer, T., Watt, I. & Bijlsma, J. W. 2010. "EULAR evidence-based recommendations for the diagnosis of knee osteoarthritis". Ann Rheum Dis, 69**,** 483-9.

Zhang, W., Mcwilliams, D. F., Ingham, S. L., Doherty, S. A., Muthuri, S., Muir, K. R. & Doherty, M. 2011a. "Nottingham knee osteoarthritis risk prediction models". Annals of the Rheumatic Diseases, 70**,** 1599-1604.

Zhang, X., Huang, J. & Mcnaughton, P. A. 2005b. "NGF rapidly increases membrane expression of TRPV1 heat-gated ion channels". EMBO J, 24**,** 4211-23.

Zhang, Y., Nevitt, M., Niu, J., Lewis, C., Torner, J., Guermazi, A., Roemer, F., Mcculloch, C. & Felson, D. T. 2011b. "Fluctuation of knee pain and changes in bone marrow lesions, effusions, and synovitis on magnetic resonance imaging". Arthritis Rheum, 63**,** 691-9.

Zhang, Z. J., Cao, D. L., Zhang, X., Ji, R. R. & Gao, Y. J. 2013. "Chemokine contribution to neuropathic pain: respective induction of CXCL1 and CXCR2 in spinal cord astrocytes and neurons". Pain, 154**,** 2185-97.

Zhuang, Z. Y., Xu, H., Clapham, D. E. & Ji, R. R. 2004. "Phosphatidylinositol 3-kinase activates ERK in primary sensory neurons and mediates inflammatory heat hyperalgesia through TRPV1 sensitization". J Neurosci, 24**,** 8300-9.

Zoricic, S., Maric, I., Bobinac, D. & Vukicevic, S. 2003. "Expression of bone morphogenetic proteins and cartilage-derived morphogenetic proteins during osteophyte formation in humans". J Anat, 202**,** 269-77.

Zou, Y., Li, Y., Lu, L., Lin, Y., Liang, W., Su, Z., Wang, X., Yang, H., Wang, J., Yu, C., Huo, L. & Ye, Y. 2013. "Correlation of fractalkine concentrations in serum and synovial fluid with the radiographic severity of knee osteoarthritis". Ann Clin Biochem, 50**,** 571-5.

CHAPTER 8 : APPENDIX

8.1 PATIENT CONSENT FORMS

8.1.1 Post-mortem tissue

1 copy to be retained by research participant, 1 copy to be retained by Investigator, 1 copy to be retained in hospital notes

Brief Title: Collection of spine and joint tissues for research into human disease

Full study title: A study of the molecular mechanisms of various human diseases using post mortem spine and joint tissues

Principal (Chief) Investigator and Study Doctor: Professor David Walsh
(Sherwood Forest Hospitals NHS Foundation Trust and University of Nottingham)
Sponsors: Sherwood Forest Hospitals NHS Foundation Trust and University of Nottingham

CONSENT FORM
To confirm agreement with each of the statements below, please initial in the box

1. Have you read and understood and had time to consider the information sheet (Version 6 dated 01-05-2014) and had the opportunity to ask questions?	
2. Have all your questions been answered satisfactorily?	
3. Do you agree to donate tissues from your relative's knees and a sample of spinal cord? These tissues will be used to identify changes that accompany disease and to help us to develop new drugs that could prevent these changes in patients.	
4. Do you understand that tissue obtained in this study may be stored for more than 15 years?	
5. Do you understand and agree that data relating to the donated samples may be stored electronically?	
6. Do you agree that some tissue could be used in research that includes the use of laboratory animals? (OPTIONAL)	
7. Do you agree to allow us to record some information about your relative's medical problems from their medical records?	
8. Do you understand that you are free to withdraw from the study at any time, without having to give a reason?	
9. Are you aware of any objection to tissue removal that your relative raised during his/her lifetime, which may indicate that they would not have wished to take part in this research?	
10. Do you agree that some tissue and data may be provided to other academic centres and commercial companies to use for research?	
11. Do you understand that you and your relative's personal data such as name, address, telephone number will **not** be provided to the University of Nottingham or Nottingham University Hospitals NHS Trust, **nor** to third parties, and that we treat all information obtained on you in the strictest confidence?	
12. Do you understand that donated samples are not sold, but costs are recovered on a non-profit-making basis and that you will not gain financially in any way from this donation?	

Name of the deceased relative……

Name of person giving consent……Relationship to deceased……

Signature…… Date……..

……
Name of Witness Signature of Witness Date

I, (Name of person taking consent, block letters) ..... have explained

the nature and the purpose of the study to .....

Signed: .....Date: .....

Investigator's Signature:.....Date: .....

Version 6 01-05-2014 Page 1 of 1

8.1.2 Surgical tissue

1 copy to be retained by research participant, 1 copy to be retained by Investigator, 1 copy to be retained in hospital notes

Sherwood Forest Hospitals NHS

NHS Foundation Trust

King's Mill Hospital
Mansfield Road
Sutton in Ashfield
Nottinghamshire
NG17 4JL

Study Title: Molecular mechanisms of human joint disease
Principal (Chief) Investigator and Study Doctor: Professor David Walsh
(Sherwood Forest Hospitals NHS Foundation Trust and University of Nottingham)
Sponsor: Sherwood Forest Hospitals NHS Foundation Trust

PATIENT CONSENT FORM (Joint surgery)
To confirm agreement with each of the statements below, please initial in the box

1. Have you read, understood and had time to consider the Patient Information Sheet (v. 5, dated 21/01/2014 and had the opportunity to ask questions?	
2. Have all your questions been answered satisfactorily?	
3. Do you agree to donate joint tissue that would normally be removed as part of the operation? This tissue will be used to identify changes in the joint that accompany arthritis and to help us to develop new drugs that could prevent these changes in other patients.	
4. Do you agree to donate a small sample of joint tissue additional to tissue that would normally be removed as part of the operation?	
5. Do you agree to allow a member of our research team to briefly examine your knees and other joints for the presence of arthritis and ask you some simple questions concerning your joints and any symptoms that you have experienced?	
6. Do you agree to allow a member of our research team to take a blood sample from an arm vein? You may also be asked to attend the radiology department at Sherwood Forest Hospitals NHS Foundation Trust to have some X-rays taken of your joints. (OPTIONAL)	
7. Do you agree to allow a member of our research team to record some information about your joint problem from your medical records?	
8. Do you understand and agree that data relating to your donated samples may be stored electronically?	
9. Do you agree that some tissue could be used in research that includes the use of laboratory animals? (OPTIONAL)	
10. Do you understand that you can stop the study at any time, without having to give a reason, and without prejudice to your further treatment?	
11. Do you agree that some tissue and data may be provided to other academic centres and commercial companies to use for research?	
12. Do you understand that your personal data such as name, address, telephone number will **not** be provided to the University of Nottingham or Nottingham University Hospitals NHS Trust, **nor** to third parties, and that we treat all information obtained on you in the strictest confidence?	
13. Do you understand that donated samples are not sold, but costs are recovered on a non-profit-making basis and that you will not gain financially in any way from this donation?	

Signed: ..... Date: .....

Name (Block capitals).....

I, (Name of person taking consent, block letters) ..... have explained the nature and the purpose of the study to ..... and believe that he/she understands what the study involves.

Signed: ..... Date: .....

Researcher: ..... Date: .....

8.1 PATIENT INFORMATION SHEET

8.1.1 Post-mortem tissue

1 copy to be retained by research participant, 1 copy to be retained by Investigator

Brief Title: Collection of spine and joint tissues for research into human disease

Full study title: A study of the molecular mechanisms of various human diseases using post mortem spine and joint tissues

Principal (Chief) Investigator and Study Doctor	Professor David Walsh Sherwood Forest Hospitals NHS Foundation Trust University of Nottingham
Sponsors	Sherwood Forest Hospitals NHS Foundation Trust, University of Nottingham

INFORMATION SHEET

We appreciate this isn't an easy time for you, and are grateful for any time that you are spending having this research explained to you. You are being asked for permission for samples of tissue to be removed from the knees and spine of your relative who has recently died, and for those tissues and relevant information about your relative to be stored and used for medical research. Before you decide if you want to take part it is important for you to understand why Sherwood Forest Hospitals NHS Foundation Trust, Nottingham University Hospitals NHS Trust and the University of Nottingham are doing the study, how your relative's information and tissue will be used, what the study will involve and the potential benefits and risks. Take your time to read the following information and discuss it with the doctor or a member of the research team. If you are willing for your relative's tissue to be donated you will be asked to sign a consent form and will be given a copy of this information sheet to keep.

DO I NEED TO TAKE PART? NO IT IS ENTIRELY VOLUNTARY.

Participation in this study is voluntary and entirely up to you. You do not have to donate the tissue if you don't want to. If you decide that you do not want your relative to provide tissue for the study, you don't have to give a reason for this. It won't be held against you in any way. If you do decide to take part you will be given this information sheet and consent form to sign and keep. If you decide to take part you are still free to withdraw at a later date

You can withdraw your consent for tissue collection, without giving any reasons, up to the time of that collection, by phoning the study contacts on 01623 672533. You can withdraw your consent for the continued retention and use of the tissue and information about your relativeeven after they have been collected, without giving any reasons, by phoning that same number. We will still use the data from any analyses that have already been conducted. It will be the responsibility of the Sponsors to ensure that all that remains of the samples from your relative are destroyed. If you withdraw your consent, no specific data about your relative will be used again, except where the data are required by regulatory authorities to ensure validity of the Study.

WHY IS THIS STUDY BEING DONE?

Many diseases (such as arthritis for example) cause unpleasant symptoms and can prevent sufferers from carrying out everyday activities. In many cases available treatments could be improved upon, and often do not cure the disease. More research is needed to find new and improved treatments for these diseases.

Researchers at Sherwood Forest Hospitals NHS Foundation Trust, Nottingham University Hospitals NHS Trust and the Arthritis Research UK Pain Centre at the University of Nottingham, are carrying out research to identify molecules (the body's chemicals) that cause disease and symptoms, such as arthritis pain. It is not yet known what causes many diseases, although some research has provided clues about what is important. We are looking for differences in tissues from patients who have had diseases compared with "normal" tissues from people without the disease. These differences may be seen as the presence or absence of molecules that are important for tissue damage in and around the joints, and which can affect pain signals through the spinal cord. This study provides tissues and information to the Nottingham Health Sciences Biobank (NHSB) which may share this material with other researchers in order to further advance medical knowledge.

WHAT ARE WE ASKING YOU TO DO?

If you are willing for your relative to be included in our research, and you are unaware of any objection to tissue removal that your relative may have raised during his/her lifetime, then we would ask you a few questions about your relative's health and any joint problems you think they may have had. Later, we would remove bone and other tissues from both knees. The procedure used for removing tissues is similar to that used in total knee joint replacement surgery. About 4 cm (1½ inches) of bone, cartilage and soft tissue will be removed from each knee. No skin will be removed, and the skin will be closed after tissues have been removed, leaving stitches for about 45 cm (18 inches) down the front of each knee.

If you are willing, we may also remove spinal tissues (bone, nerves and joint tissues). The tissues that would not be helpful for our research would then be put back and the skin will be closed, leaving stitches for about 40 cm (16 inches) down the midline of the lower back, just above the pelvis (hip girdle). The collected tissues will be accepted as a gift from you on behalf of your relative

We would also ask for permission to access your relative's clinical notes for other information that may be helpful to the research ("Study Data"), for example, medical history and medicines that have been prescribed.

WHAT ARE THE BENEFITS OF TAKING PART?

Agreeing for us to use joint and spinal tissues and Study Data from your relative means that you may possibly help people with diseases in the future, as our research findings may be used to develop new treatments. There will be no direct personal gain from participation. There will be no payment for taking part in this study.

HOW WILL THE STUDY DATA AND SAMPLES BE USED?

The Investigator and the Study Sponsors may use the Study Data and the tissue samples for administration purposes, research and development of pharmaceutical products, diagnostics and/or medical aids, statistical analysis, the approval, registration and marketing processes relating to their products/study medication, carrying out safety and efficacy evaluations, and for teaching, training and audit.

Tissues may be used to measure the amounts of molecules that can cause disease and symptoms. Some molecules may be extracted from the tissue to help us to identify them. Some tissues may be used to test how they respond to new medicines. It may be appropriate for genetic tests to be carried out in order to determine whether genetic makeup has any connection with disease. These tissues may also be used to form experimental cell lines which are a useful model for testing new therapies. Only if you agree, the samples that you donate can be used in research using laboratory animals..

Overall, it is hoped that these studies will help us to treat and diagnose illness in other patients in the future. However, the samples that you donate will not themselves be used to treat or diagnose illness in other patients. Whilst there is no specific expiry for the use of these data or tissues, samples that are no longer required for research will be disposed of by the research team in a legal and sensitive manner.

WHO WILL USE THE DATA AND SAMPLES THAT I HAVE DONATED?

Samples and Study Data will be stored for at least 15 years. They will be stored, processed and used for investigations at Sherwood Forest Hospitals NHS Foundation Trust, Nottingham University Hospitals NHS Trust and in the Arthritis Research UK Pain Centre at the University of Nottingham. The researchers with whom we may share your data and samples could be located outside of the European Union. Please be aware that Data Protection laws may be different in these countries. None the less, the researchers will only be allowed to use your data in the way described here and for research approved by the ethics committee. The researchers are responsible for handling your data in accordance with applicable Data Protection law(s) in force in their countries.

Special precautions are taken to ensure the research study is carried out with a high degree of confidentiality. A code that is specific to your relative will be used to label the samples and Study Data and identify all results that are recorded. The coding of all information is to ensure that the results are kept confidential by keeping your relative's identity and the results separate, whilst retaining a link that would enable us to identify the samples should you request they be destroyed.

Samples and Study Data shared with Sponsors and collaborators outside Sherwood Forest Hospitals NHS Foundation Trust will not include your relative's name or address. Only the Study Doctor and his staff at Sherwood Forest Hospitals NHS Foundation Trust have access to the code key with which it is possible to connect the Study Data to your relative. However, any of the personal data that are available to the Study Doctor, may be reviewed at the Sherwood Forest Hospitals NHS Foundation Trust site by the Sponsors and/or their representatives, their contractors, regulatory authorities, or other supervisory bodies. The purpose of these reviews is to assure the proper conduct of the study and/or the quality of the Study Data. Please note, the results of the study may be published in medical literature, but your identity and that of your relative will not be revealed.

IS THERE ANY RESEARCH THAT THE DONATED SAMPLES AND DATA WILL NOT BE USED FOR?

The Nottingham Health Science Biobank (NHSB) Access Committee, comprising your Study Doctor, NHSB senior staff, professional researchers and service providers as well as lay persons, will look at applications for access to donated tissues and data according to the Human Tissue Act regulations and the NHSB Tissue Access Policy. Only if the project fits within the ethical approval would tissues or data be made available. The samples that you donate will **not** be used for research that involves reproductive cloning, research into termination of pregnancy, non-clinical research such as testing cosmetic products, or for transplantation purposes. When we provide samples to researchers they are obliged to only use the samples for the research they said they would do. They will be bound by a strict agreement to ensure this.

WHAT RIGHTS DO I HAVE TO THE RESULTS OF THE RESEARCH?

Any information derived directly or indirectly from this research, as well as any patents, diagnostic tests, drugs, or biological products developed directly or indirectly as a result of this research, are the sole property of the Study Sponsors (and their successors, licensees, and assigns). This property may be used for commercial purposes. It is intended that you have no right to this property or to any share of the profits that may be earned directly or indirectly as a result of this research. However, in signing this form and donating the samples for research, you do not give up any rights that you would otherwise have.

FUTURE CONTACT

There is no planned future contact. You will not have direct access to the research data. However, if you have an interest in knowing how the tissue donation has contributed to advances in research you may contact the Study Doctor in the future, who will be pleased to provide you with a summary.

WHO CAN I CONTACT IF I HAVE ANY QUESTIONS ABOUT THIS STUDY?

If you have any further questions about this study, or wish to contact the Study Sponsors, please discuss this in the first instance with:
Professor **David Walsh** (Principal (Chief) Investigator and Study Doctor)

Telephone 01623 672533

If you wish to complain about any aspect of the way you have been treated during the course of the study you can do so using the normal NHS complaints procedure. The number to ring for the Complaints and Litigation Department is 01623 672222.

Thank you for taking the time to read this invitation

8.1.2 Surgical tissue

1 copy to be retained by research participant, 1 copy to be retained by Investigator

Study Title: Molecular mechanisms of human joint disease

Principal (Chief) Investigator and Study Doctor	Professor David Walsh Sherwood Forest Hospitals NHS Foundation Trust University of Nottingham
Sponsor	Sherwood Forest Hospitals NHS Foundation Trust

PATIENT INFORMATION SHEET (Joint surgery)

You are being invited to take part in this research study. Before you decide if you want to take part it is important for you to understand why Sherwood Forest Hospitals NHS Foundation Trust and Nottingham University Hospitals NHS Trust are doing the study, how your information will be used, what the study will involve and the potential benefits, risks and possible discomforts. If you are willing to take part you will be asked to sign a consent form and will be given a copy to keep.

WHY IS THIS STUDY BEING DONE?

Arthritis causes pain, and can prevent sufferers from carrying out everyday activities. Operations may help some people. Available treatments can often control the pain and help the disease, even though they cannot cure arthritis. More research is needed to find new treatments that can cure arthritis.

Researchers at Sherwood Forest Hospitals NHS Foundation Trust, Nottingham University Hospitals NHS Trust and University of Nottingham are carrying out research to identify molecules that cause arthritis. It is not yet known what causes arthritis, although some research has provided clues about what is important. One approach to finding a cure is to identify changes in the joint that accompany arthritis and then develop new drugs that can prevent these changes. We are looking for changes in tissues from the joints of patients who have had different types of arthritis for different lengths of time. It is anticipated that about 200 participants like you will take part in this research study each year. This study provides tissues and information to the Nottingham Health Sciences Biobank (NHSB) which may share this material with other researchers in order to further advance medical knowledge.

WHAT ARE WE ASKING YOU TO DO?

Your surgeon has recommended that you have an operation on your joint to help with the treatment of your joint pain. Some samples of joint tissue are always removed as a normal part of your operation. If you are willing to take part in our research, your surgeon will provide us with some of those joint tissues. Your surgeon may also collect some very small samples (up to 4, each about the size of a pea) of your joint tissues during your operation specifically for our research.

Members of our research team have been specially trained for this study, and they may briefly examine your knees and other joints for the presence of arthritis. They may ask you some simple questions concerning your joints and any symptoms that you have experienced, and you may be asked to fill in some questionnaires about your pain and how you cope with pain. Members of our research team may take a blood sample from an arm vein, and you may be asked to attend the radiology department at King's Mill Hospital to have radiographs (X-rays) taken of the joint that will be operated on, if these have not been done recently. We shall also ask you about, and record from your medical records, information that could be relevant to your joint problem ("Study Data").

DO I NEED TO TAKE PART?

NO. IT IS ENTIRELY VOLUNTARY. It is up to you to decide whether or not to take part. If you do decide to take part you will be given this information sheet and consent form to sign and keep. If you decide to take part you are still free to withdraw at any time. If you choose not to take part, now or in the future, you will not be disadvantaged in any way, including medical treatment and care you are entitled to receive. You will be told if any new findings occur during the study that may affect your willingness to take part.

If you withdraw your consent, the Study Sponsor will arrange to have your samples destroyed, and we shall no longer use your Study Data or share them with others. The only exceptions to this, where the Study Sponsor may continue to use your Study Data or Samples even if you withdraw consent are:

- They may share your Study Data with regulatory authorities where this is required to ensure validity of the Study.
- They may continue to use uncoded information that was shared with them before you withdrew your consent, where that information cannot be linked to you personally.
- They are not obliged to destroy results of research that has already been performed.

If you agree to donate your samples for this study, they may be used for research within 24 hours, because some types of research require fresh samples. Please note that the link between you and the coded samples you have donated and the associated medical data will be kept for at least 15 years after donation. After this time it will not be possible to remove your samples or data from the repository, even if you withdraw from the study, as the link will be broken and so the samples and data can no longer be traced.

WHAT ARE THE RISKS IF I TAKE PART?

Joint tissue will be removed during your routine surgical operation. The side effects from sampling of joint tissues are rare. The operation you are having is sometimes followed by pain in the joint. There may rarely be a very small increase in pain, on the following day, if your joint tissues have been sampled during the operation. Pain killers are available for all patients following joint surgery.

WHAT ARE THE BENEFITS OF MY TAKING PART?

Taking part in this study means that you may possibly help other arthritis sufferers in the future, as information about the changes that occur in painful or arthritic joints may be used to develop new treatments for arthritis. There will be no direct personal gain from your participation. You will not be paid for taking part in this study.

HOW WILL MY STUDY DATA AND SAMPLES BE USED?

The investigator and the Study Sponsor may use your Study Data and samples for administration purposes, research and development of pharmaceutical products, diagnostics and/or medical aids, statistical analysis, the approval, registration and marketing processes relating to its products/study medication, carrying out safety and efficacy evaluations, and for teaching, training and audit.

Joint tissues may be stained to measure the amounts of molecules that can cause inflammation. Some molecules may be extracted from the tissue to help us to identify them. Some tissues may be used to test how they respond to new medicines. Blood samples may be used to measure markers of your joint disease.

The studies that we are doing are not intended to suggest any clinical diagnosis or treatment for your joint disease. It is not the purpose of this research to provide you with test results. However, occasionally research on joint tissues can reveal unexpected information about the cause of your joint pain. In that event, the information may be passed to your doctor and the samples that have been taken from your joint may be made available for further tests to help with your treatment. Other than this, and as required by law, Study Data, samples or results with which you could be identified, will not be made available to anyone else now or in the future. You have the right to request information about any personal data that the Study Doctor may hold about you. You also have the right to request that any inaccuracies in your personal data be corrected. If you wish to make a request, then please contact the Study Doctor.

Overall, it is hoped that these studies will help us to treat and diagnose illness in other patients in the future. However, the samples that you donate will not themselves be used to treat or diagnose illness in other patients. It may be appropriate for genetic tests to be carried out in order to determine whether genetic makeup has any connection with disease. These tissues may also be used to form experimental cell lines which are a useful model for testing new therapies. Only if you agree, the samples that you donate can be used in research using laboratory animals.

IS THERE ANY RESEARCH THAT MY DATA AND SAMPLES WILL NOT BE USED FOR?

The Nottingham Health Science Biobank (NHSB) Access Committee, comprising your Study Doctor, NHSB senior staff, professional researchers and service providers as well as lay persons, will look at applications for access to your data or tissues according to the Human Tissue Act regulations and the NHSB Tissue Access Policy. Only if the project fits within the ethical approval would your data or tissues be made available. Your tissue will **not** be used for research that involves reproductive cloning, research into termination of pregnancy, non-clinical research such as testing cosmetic products, or for transplantation purposes. When we provide samples to researchers they are obliged to only use the samples for the research they said they would do. They will be bound by a strict agreement to ensure this.

WHO WILL USE THE DATA AND SAMPLES THAT I HAVE DONATED?

The samples and associated personal medical data ("Study Data") that you donate will be stored, processed and used for investigations at Sherwood Forest Hospitals NHS Foundation Trust, Nottingham University Hospitals NHS Trust and University of Nottingham.

Special precautions are taken to ensure the research study is carried out with a high degree of confidentiality. A code that is specific to you will be allocated if you agree to participate in the study and will be used to label your samples and Study Data and identify all results that are

recorded. The coding of all information resulting from you taking part in the study is to ensure that the results are kept confidential by keeping your identity and the results separate. Samples and Study Data will be stored for at least 15 years.

Samples and Study Data shared with collaborators outside Sherwood Forest Hospitals NHS Trust will **not** include your name, address or social security number. Only the Study Doctor and his staff at Sherwood Forest Hospitals NHS Foundation Trust have access to the code key with which it is possible to connect your Study Data to you. However, any of your personal data that are available to the Study Doctor, may be reviewed at the Sherwood Forest Hospitals NHS Foundation Trust site by the Sponsor and/or their representatives, their contractors, regulatory authorities, the Independent Ethics Committee or other supervisory bodies. The purpose of these reviews is to assure the proper conduct of the study and/or the quality of your Study Data. Please note, the results of the study may be published in medical literature, but your identity will not be revealed.

WHAT RIGHTS DO I HAVE TO THE RESULTS OF THE RESEARCH?

Any information derived directly or indirectly from this research, as well as any patents, diagnostic tests, drugs, or biological products developed directly or indirectly as a result of this research, are the sole property of the Study Sponsor (and their successors, licensees, and assigns) and may be used for commercial purposes. It is intended that you have no right to this property or to any share of the profits that may be earned directly or indirectly as a result of this research. However, in signing this form and donating the samples for research, you do not give up any rights that you would otherwise have as a participant in research.

WHO CAN I CONTACT IF I HAVE ANY QUESTIONS ABOUT THIS STUDY?

If you have any further questions about this study, or wish to contact the Study Sponsor, please discuss this in the first instance with:

Professor David Walsh, Principal (Chief) Investigator and Study Doctor
Telephone 01623 672533

It is unlikely that anything will go wrong with your treatment or care but if you wish to complain about any aspect of the way you have been treated during the course of the study you can do so using the normal NHS complaints procedure. Each hospital has a leaflet outlining the procedure that you can follow if you would like to make a complaint.

The number to ring for the Complaints and Litigation Department is 01623 672366

Thank you for taking the time to read this invitation.

This document must be kept in the investigator's study file and retained for a minimum period of 15 years after completion of the study.

Arthritis Research UK | pain centre

The University of Nottingham
UNITED KINGDOM · CHINA · MALAYSIA

Director: Prof D A Walsh
Deputy Director: Professor V Chapman

Arthritis Research UK Pain Centre
Academic Rheumatology
Clinical Sciences Building
Nottingham City Hospital
NG5 1PB
Tel: +44 (0)115 82 31766
Fax: +44 (0)115 82 31757
www.nottingham.ac.uk/PainCentre

5 December, 2012

East Midlands - Nottingham Research Ethics Committee 1
The Old Chapel
Royal Standard Place
Nottingham
NG1 6FS

Full title: **A research project to develop an articular repository for studies on molecular mechanisms of human arthritis**

REC Ref: **05/Q2403/24**

Dear Sir/Madam,

Please find enclosed a substantial amendment to the NHS REC Research Tissue Bank (RTB) ethics application for the above named study.

The amendment concerns a change in sponsorship arrangements following AstraZeneca's decision to withdraw from the repository collaboration for new recruitment of sample and data collection. As a result, the Sherwood Forest Hospitals NHS Foundation Trust will be the sole sponsor of this tissue repository. The Sherwood Forest Hospitals NHS Foundation Trust will continue to work in collaboration with the University of Nottingham, and tissue samples will be stored and used for research within the University of Nottingham subject to a separate Material Transfer Agreement between the Trust and the University that ensures compliance with conditions of ethical approval.

Following the above change in sponsorship, new tissue and data acquired in this repository will no longer be routinely dispatched to, or shared with, AstraZeneca, and therefore AstraZeneca will not have any sponsorship responsibility for new sample and data collection. However, some tissue and data acquired prior to the sponsorship change will remain under the custodianship of AstraZeneca, subject to same prior legal and contractual obligations.

Arthritis Research UK Pain Centre Management Group:
Prof D. Auer, Prof V. Chapman, Prof M. Doherty, Dr S. Kelly, Prof N. Lincoln, Prof B. Scammell, Dr D.A. Walsh, Dr W. Zhang

The study protocol HTASP/D/003, Patient Information Sheets and Patient Consent Forms have been revised using track-changes to reflect the altered collaborative and contractual arrangements with AstraZeneca. The enclosed IRAS substantial amendment form provides a summary of changes including an annotated list of revisions to the 2005 NHS REC application (ref. 05/Q2403/24, dated 21/01/2005) following AstraZeneca's decision to cease sponsorship for new sample and data.

No changes have been made to patient recruitment and informed consent procedures, or how the tissue samples and data are collected, processed, stored, used and disposed by the Sherwood Forest Hospitals NHS Foundation Trust and the University of Nottingham.

The Sherwood Forest Hospitals NHS Foundation Trust has agreed to continue as the sponsor of the tissue repository, and we are in the process of securing the signature of Dr Samuel Kemp from the Trust's Research & Development office.

If you have any questions or queries regarding this application, please do not hesitate to contact me.

Yours sincerely

Prof David Walsh
Consultant Rheumatologist
Chief Investigator

8.2 Antibodies

8.2.1 Primary antibodies

Antigen	Clone	Clonality	Code	Source	Dilution
CD68	PG-M1	Monoclonal	IS613	Dako UK Ltd. Cambridge, UK	1.200 (IHC), 1:20 (IF)
NGF	EP1320Y	Monoclonal	ab52918	Abcam, Cambridge, UK	1.200 (IHC), 1:20 (IF)
HSP47	M16.10A1	Monoclonal	ADI-SPA-470-F	Enzo Life Sciences, Exeter, UK.	1:80 (IF)

Abbreviations: IHC, immunohistochemistry, IF, immunofluorescence.

8.2.2 Secondary antibodies

Description	Antigen	Donor	Code	Label	Source	Dilution
Biotinylated Anti-Rabbit IgG, Affinity Purified	Rabbit IgG	Goat	BA-1000	Biotinylated	Vector Laboratories Ltd. Peterborough, UK	1.100
Biotinylated Anti-Mouse IgG, Affinity Purified	Mouse	Horse	BA-2000	Biotinylated	Vector Laboratories Ltd. Peterborough, UK	1:100
Texas Red Anti-Mouse IgG, Affinity Purified	Mouse IgG	Horse	TI-2000	Texas Red	Vector Laboratories Ltd. Peterborough, UK	1:200
Fluorescein Anti-Rabbit IgG, Affinity Purified	Rabbit IgG	Goat	FI-1000	Fluorescein	Vector Laboratories Ltd. Peterborough, UK	1:200

8.3 RNA CONCENTRATIONS

The volume of DEPC water needed to dilute each sample to 100 ng/µl was calculated.

$V1 = (C2 \times V2)/ C1$

Where;

V_1 = Volume of RNA needed.

V_2 = Volume (50µl).

C_1 = RNA concentration.

C_2 = Concentration wanted (100µl).

Sample code	**260:280 ratio**	**Nanodrop conc (**ng/µl)	**RNA (V1: 100 x 50/ nanodrop)**	**DEPC water (50-V1)**
1	2.03	445.59	11.22107767	38.77892233
2	2.03	200.68	24.91528802	25.08471198
3	2.01	219.75	22.75312856	27.24687144
4	2.03	304.16	16.43871647	33.56128353
5	2.02	299.04	16.72017121	33.27982879
6	1.98	245.48	20.36825811	29.63174189
7	2.00	110.74	45.15080368	4.849196316
8	2.01	151.82	32.93373732	17.06626268
9	1.98	375.44	13.31770722	36.68229278
10	2.04	314.29	15.90887397	34.09112603
11	2.07	224.68	22.25387217	27.74612783
12	2.06	348.91	14.33034307	35.66965693
13	2.10	278.92	17.92628711	32.07371289
14	1.93	441.25	11.33144476	38.66855524
15	2.01	340.66	14.67739095	35.32260905
16	2.04	189.83	26.33935627	23.66064373
17	2.00	182.33	27.4228048	22.5771952
18	2.08	861.96	5.800733213	44.19926679
19	1.97	1396.77	3.579687422	46.42031258
20#	2.02	88.37	56.58028743	-6.580287428
21*	1.95	16.4	304.8780488	-254.8780488
22	2.04	391.22	12.78053269	37.21946731
23	2.09	561.71	8.901390397	41.0986096
24	2.02	152.45	32.79763857	17.20236143
Positive control (liver)	2.05	1744.21	2.866627298	47.1333727

Concentration (88.37 ng/µl) was too low to dilute to 100 ng/µl. For reverse transcription 500ng (5µl of 100ng/µl) of diluted RNA was mixed with 15.7µl and 3µl of random primers to give a final volume of 23.7µl. Therefore for sample 20 5.7µl of

undiluted RNA (500/88.37) was mixed with 15µl of water and 3µl of random primers to give a final end product of 23.7µl.

*RNA concentration for sample 21 was too low.

8.4 MICROFLUIDIC CARD ASSAY SELECTION

Table 8.1 Assay section for each gene included in the microfluidic cards.

Assay ID	Gene Symbol(s)	Gene Name(s)	RefSeq(s)	Amplicon Length
Hs00174179_m1	ACE	Angiotensin I converting enzyme	NM_152830.2;NM_001178057.1;NM_000789.3	74
Hs01060665_g1	ACTB	Beta actin	NM_001101.3	63
Hs00234224_m1	ADAM17	ADAM metallopeptidase domain 17	NM_003183.4	90
Hs00167549_m1	ANXA1	Annexin I	NM_000700.1	66
Hs00241762_m1	ANXA6	Annexin A6	NM_001155.4;NM_001193544.1	70
Hs00245097_m1	ASIC3	Acid-sensing (proton-gated) ion channel 3	NM_020321.3;NR_046401.1;NM_004769.3;NM_020322.3	71
Hs00180403_m1	BCL3	B-cell CLL/lymphoma 3	NM_005178.4	60
Hs03805848_m1	BDNF	Brain-derived neurotrophic factor	NM_001143809.1	103
Hs00354832_m1	CASP1	Caspase 1	NM_033292.3;NM_033293.3;NM_033294.3;NM_001223.4;NM_001257118.1;NM_001257119.1	77
Hs00234140_m1	CCL2	Chemokine (C-C motif) ligand 2	NM_002982.3	101

Hs00234142_m1	CCL3	Chemokine (C-C motif) ligand 3	NM_002983.2	53
Hs99999148_m1	CCL4	Chemokine (C-C motif) ligand 4	-	94
Hs00982282_m1	CCL5	Chemokine (C-C motif) ligand 5	NM_001278736.1;NM_002985.2	70
Hs00271615_m1	CCL8	Chemokine (C-C motif) ligand 8	NM_005623.2	107
Hs03063327_m1	CMKLR1	Chemokine-like receptor 1	NM_004072.2;NM_001142343.1	54
Hs00361490_m1	CNR2	Cannabinoid receptor 2 (macrophage)	NM_001841.2	65
Hs00170014_m1	CTGF	Connective tissue growth factor	NM_001901.2	60
Hs01080388_m1	CTSK	Cathepsin K	NM_000396.3	124
Hs00171086_m1	CX3CL1	Chemokine (C-X3-C motif) ligand 1	NM_002996.3	72
Hs00236937_m1	CXCL1	Chemokine (C-X-C motif) ligand 1	NR_046035.1;NM_001511.3	70
Hs99999049_m1	CXCL10	Chemokine (C-X-C motif) ligand 10	-	73
Hs00236966_m1	CXCL2	Chemokine (C-X-C motif) ligand 2	NM_002089.3	68
Hs00171085_m1	CXCL5	Chemokine (C-X-C motif) ligand 5	NM_002994.4	90
Hs00237017_m1	CXCL6	Chemokine (C-X-C motif) ligand 6	NM_002993.3	98
Hs00356035_m1	CYP2J2	Cytochrome P450, family 2, subfamily J, polypeptide 2	NM_000775.2	58

Hs00157403_m1	EPHX2	Epoxide hydrolase 2, cytoplasmic	NM_001979.5;NM_001256482.1;NM_001256483.1;NM_001256484.1	83
Hs00608346_m1	F2RL1	Coagulation factor II (thrombin) receptor-like 1	NM_005242.4	119
Hs01006385_g1	F2RL3	Coagulation factor II (thrombin) receptor-like 3	NM_003950.2	121
Hs99999140_m1	FOS	FBJ murine osteosarcoma viral oncogene homolog	NM_005252.3	77
Hs00265954_m1	FPR2	Formyl peptide receptor 2	NM_001462.3	73
Hs99999905_m1	GAPDH	-	-	0
Hs00609297_m1	HMBS	Hydroxymethylbilane synthase	NM_000190.3;NM_001258208.1	64
Hs00174143_m1	IFNG	interferon, gamma	NM_000619.2	79
Hs00174086_m1	IL10	Interleukin 10	NM_000572.2	119
Hs00542571_m1	IL15	Interleukin 15	NM_172175.2	76
Hs00174383_m1	IL17A	Interleukin 17A	NM_002190.2	80
Hs01555410_m1	IL1B	Interleukin 1, beta	NM_000576.2	91
Hs00168392_m1	IL1R1	Interleukin 1 receptor, type I	NM_000877.2	66
Hs00929862_m1	IL4	Interleukin 4	NM_000589.3	70

Hs00166237_m1	IL4R	Interleukin 4 receptor	NM_001257406.1;NM_001257407.1;NM_000418.3;NM_001257997.1	70
Hs00174131_m1	IL6	Interleukin 6	NM_000600.3	95
Hs99999034_m1	IL8	Interleukin 8	NM_000584.3	81
Hs99999141_s1	JUN	Jun proto-oncogene	NM_002228.3	64
Hs00176676_m1	KDR	Kinase insert domain receptor (a type III receptor tyrosine kinase)	NM_002253.2	84
Hs01086545_m1	KLK1	Kallikrein 1	NM_002257.3	82
Hs00609525_m1	LTB4R	Leukotriene B4 receptor	NM_181657.3	74
Hs00177127_m1	MAP2K3	Mitogen-activated protein kinase kinase 3	NM_002756.4;NM_145109.2	62
Hs00992389_m1	MAP2K6	Mitogen-activated protein kinase kinase 6	NM_002758.3	68
Hs01051152_m1	MAPK14	Mitogen-activated protein kinase 14	NM_139014.2;NM_001315.2;NM_139012.2;NM_139013.2	91
Hs01116946_m1	MAPKAPK2	Mitogen-activated protein kinase-activated protein kinase 2	NM_004759.4;NM_032960.3	121
Hs00233958_m1	MMP1	Matrix metallopeptidase 1 (interstitial collagenase)	NM_001145938.1;NM_002421.3	133
Hs00159178_m1	MMP12	Matrix metallopeptidase 12 (macrophage elastase)	NM_002426.4	62

Hs01548727_m1	MMP2	Matrix metallopeptidase 2 (gelatinase A, 72kDa gelatinase, 72kDa type IV collagenase)	NM_004530.4;NM_001127891.1	65
Hs00968305_m1	MMP3	Matrix metallopeptidase 3 (stromelysin 1, progelatinase)	NM_002422.3	126
Hs01042795_m1	MMP7	Matrix metallopeptidase 7 (matrilysin, uterine)	NM_002423.3	71
Hs00957562_m1	MMP9	Matrix metallopeptidase 9 (gelatinase B, 92kDa gelatinase, 92kDa type IV collagenase)	NM_004994.2	67
Hs00231653_m1	NFKB1	Nuclear factor of kappa light polypeptide gene enhancer in B-cells 1	NM_003998.3;NM_001165412.1	73
Hs00153283_m1	NFKBIA	Nuclear factor of kappa light polypeptide gene enhancer in B-cells inhibitor, alpha	NM_020529.2	68
Hs01113193_m1	NGF	Nerve growth factor (beta polypeptide)	NM_002506.2	86
Hs00609977_m1	NGFR	Nerve growth factor receptor	NM_002507.3	140
Hs01075529_m1	NOS2	Nitric oxide synthase 2, inducible	NM_000625.4	67
Hs00167166_m1	NOS3	Nitric oxide synthase 3 (endothelial cell)	NM_000603.4	80
Hs00176787_m1	NTRK1	Neurotrophic tyrosine kinase, receptor, type 1	NM_001007792.1;NM_001012331.1;NM_002529.3	68

Hs00180666_m1	PIAS3	Protein inhibitor of activated STAT, 3	NM_006099.3	102
Hs00180679_m1	PIK3CA	Phosphatidylinositol-4,5-bisphosphate 3-kinase, catalytic subunit alpha	NM_006218.2	104
Hs00178872_m1	PIK3CB	Phosphatidylinositol-4,5-bisphosphate 3-kinase, catalytic subunit beta	NM_001256045.1;NM_006219.2	85
Hs00908666_m1	PIK3CD	Phosphatidylinositol-4,5-bisphosphate 3-kinase, catalytic subunit delta	NM_005026.3	64
Hs00939828_m1	PLAT	Plasminogen activator, tissue	-	55
Hs00248563_m1	PLCB1	Phospholipase C, beta 1 (phosphoinositide-specific)	NM_182734.2;NM_015192.3	61
Hs00947536_m1	PPARA	Peroxisome proliferator-activated receptor alpha	NM_001001928.2;NM_005036.4	62
Hs00178455_m1	PRKCE	Protein kinase C, epsilon	NM_005400.2	91
Hs00177037_m1	PRKD1	Protein kinase D1	NM_002742.2	82
Hs00212828_m1	PRKD2	Protein kinase D2	NM_001079881.1;NM_001079882.1;NM_016457.4;NM_001079880.1	73
Hs00178657_m1	PRKD3	Protein kinase D3	NM_005813.3	67
Hs00377726_m1	PTGS1	Prostaglandin-endoperoxide synthase 1 (prostaglandin G/H synthase and cyclooxygenase)	NM_080591.2;NM_000962.3;NM_001271367.1;NM_001271164.1;NM_001271166.1;NM_001271368.1;	60

			NM_001271165.1	
Hs00153133_m1	PTGS2	Prostaglandin-endoperoxide synthase 2 (prostaglandin G/H synthase and cyclooxygenase)	NM_000963.2	75
Hs00161209_g1	RARRES2	Retinoic acid receptor responder (tazarotene induced) 2	NM_002889.3	114
Hs00153294_m1	RELA	V-rel avian reticuloendotheliosis viral oncogene homolog A	NM_001145138.1;NM_001243985.1;NM_021975.3;NM_001243984.1	71
Hs00374263_m1	S100A8	S100 calcium binding protein A8	NM_002964.4	70
Hs00610058_m1	S100A9	S100 calcium binding protein A9	NM_002965.3	83
Hs01126603_m1	SERPINE1	Serpin peptidase inhibitor, clade E (nexin, plasminogen activator inhibitor type 1), member 1	NM_000602.4	75
Hs00864158_g1	SOCS1	Suppressor of cytokine signaling 1	NM_003745.1	145
Hs01000485_g1	SOCS3	Suppressor of cytokine signaling 3	NM_003955.4	111
Hs00234829_m1	STAT1	Signal transducer and activator of transcription 1	NM_007315.3;NM_139266.2	79
Hs01047580_m1	STAT3	Signal transducer and activator of transcription 3 (acute-phase response factor)	NM_003150.3;NM_139276.2;NM_213662.1	87
Hs00174974_m1	TG	Thyroglobulin	NM_003235.4	69

Hs00174128_m1	TNF	Tumor necrosis factor	NM_000594.3	80
Hs00900358_m1	TNFRSF11B	Tumor necrosis factor receptor superfamily, member 11b	NM_002546.3	74
Hs00243519_m1	TNFSF11	Tumor necrosis factor (ligand) superfamily, member 11	NM_003701.3	71
Hs00218624_m1	TREM1	Triggering receptor expressed on myeloid cells 1	NM_018643.3	80
Hs00175798_m1	TRPA1	Transient receptor potential cation channel, subfamily A, member 1	NM_007332.2	124
Hs00218912_m1	TRPV1	Transient receptor potential cation channel, subfamily V, member 1	NM_018727.5;NM_080705.3;NM_080704.3;NM_080706.3	94
Hs01099348_m1	TRPV4	Transient receptor potential cation channel, subfamily V, member 4	NM_147204.2;NM_001177433.1;NM_021625.4;NM_001177428.1;NM_001177431.1	65
Hs00177464_m1	TYK2	Tyrosine kinase 2	NM_003331.4	80
Hs00824723_m1	UBC	Ubiquitin C	NM_021009.5	71
Hs00903129_m1	VEGFA	Vascular endothelial growth factor A	NM_003376.5;NM_001171624.1	65

8.5 LATENT CLASS ANALYSIS

8.5.1 Input syntax

The syntax used for the LCA when analysing the whole dataset is displayed below.

```
TITLE:  LCA;

DATA:
  FILE IS "Z:\Validating weighted score\Latent class analysis\Master PM and TKR\All2.csv";
VARIABLE:

 NAMES ARE id cart tide chond prot bone syn ost;

  USEVARIABLES cart tide chond prot bone syn;
  CATEGORICAL tide bone;

  missing are all (-999);

  CLASSES = GRP(3);
    idvariable are id;



ANALYSIS:
  TYPE = MIXTURE;
  STARTS = 0;
  OPTSEED = 789985;
      PROCESSORS = 4(STARTS);
      LRTSTARTS = 0 0 100 20;


 MODEL:
      %OVERALL%
       cart WITH chond prot syn;
       cart WITH prot syn;
       cart WITH syn;


OUTPUT: TECH1 TECH11 TECH14;

SAVEDATA:
    SAVE = CPROBABILITIES;
    FILE = FINAL3GRPS.csv;
```

8.6 MATERIALS AND REAGENTS

1-bromo-3-chloro-propane (BCP)	Sigma Aldrich, Poole, UK
Acetic acid	VWR Ltd, Lutterworth,UK
AffinityScript Multiple Temperature RT	Agilent Technologies, CA, USA
AffinityScript RT Buffer	Agilent Technologies, CA, USA
Albumin, Bovine serum (A7030)	Sigma Aldrich, Poole, UK
Ammonium Chloride	VWR Ltd, Lutterworth,UK
Beta-D-glucose	Sigma Aldrich, Poole, UK
Citric Acid	Sigma Aldrich, Poole, UK
Coverslips	VWR Ltd, Lutterworth,UK
Deoxynucleotide triphosphates (dNTPs)	Promega, Southampton, UK
DePeX	VWR Ltd, Lutterworth,UK
Diaminobenzidine	Sigma Aldrich, Poole, UK
Diammonium Nickel II sulphate	Sigma Aldrich, Poole, UK
Disodium phosphate heptahydrate	Sigma Aldrich, Poole, UK
EDTA	Sigma Aldrich, Poole, UK
Eosin (1%)	Raymond A Lamb, Eastbourne, UK
Ethanol	Sigma Aldrich, Poole, UK
Fast Green (F7258)	Sigma Aldrich, Poole, UK
Glucose oxidase Apergillus Niger (G2133)	Sigma Aldrich, Poole, UK
Glycerol (G2025)	Sigma Adrich, Poole, UK
Goat serum	Sigma Aldrich, Poole, UK
Hematoxylin	Sigma Aldrich, Poole, UK
Haematoxylin (Mayers)	Raymond A Lamb, Eastbourne, UK
Horse serum (H1270)	Sigma Aldrich, Poole, UK
Hydrochloric Acid	VWR Ltd, Lutterworth,UK
Iron (III) Chloride	Sigma Aldrich, Poole, UK
Isopropanol	Sigma Aldrich, Poole, UK

KS300 image analysis software	AxioVision
Mayers Haematoxylin	Raymond A Lamb, Eastbourne, UK
Monosodium Phosphate Monohydrate	Sigma Aldrich, Poole, UK
Paraformaldehyde (158127)	Sigma Aldrich, Poole, UK
Pepsin (porcine gastric mucosa)	Sigma Aldrich, Poole, UK
Phosphate Buffered Saline pH 7.4	VWR Ltd, Lutterworth,UK
Picric Acid (2%, saturated)	VWR Ltd, Lutterworth,UK
Polysine microscope adhesion slides	Fisher Scientific, Loughborough, UK
Polyvinylpyrrolidone (PVP40)	Sigma Aldrich, Poole, UK
Random primers	Promega, Southampton, UK
RNase block ribonuclease inhibitor	Promega, Southampton, UK
Safranin-O (S8884)	Sigma Aldrich, Poole, UK
Sodium Azide	Sigma Aldrich, Poole, UK
Sodium Citrate Tribasic	Sigma Aldrich, Poole, UK
Sodium hydroxide pellets	Fisher Scientific, Loughborough, UK
Sucrose	Sigma Aldrich, Poole, UK
Sudan black B (199664)	Sigma Aldrich, Poole, UK
TriReagent	Sigma Aldrich, Poole, UK
Tris base	Sigma Aldrich, Poole, UK
Vectastain® *Elite* ABC Kit (PK6100)	Vector Laboratories Ltd. Peterborough, UK
Xylene	Sigma Aldrich, Poole, UK
Zeiss Axioscop-50 microscope	Carl Zeiss, Ltd. Welwyn Garden City, UK

8.7 SOLUTIONS AND BUFFERS

Acetic Acid	4 ml	Glacial Acetic Acid
	396 ml	Distilled water
Acid Alcohol	5 ml	1M Hydrochloric Acid
	350 ml	Ethanol (IMS)
	145 ml	Distilled water
Citrate buffer	0.265g	Citric acid
	2.57g	Sodium citrate
	1L	Distilled water
Decalcification fluid	2.5 L	Distilled water
(pH 6.95)	250 g	EDTA (10%)
	187.5 g	PVP (7.5%)
	3.35 g	Tris base
Fast Green solution	0.1 g	Fast Green
	500 ml	Distilled water
Goat blocking buffer	0.01 g	BSA
	700 µl	Goat serum
	2 ml	0.1M PBS
	17.3 ml	Distilled water
Horse blocking buffer	0.01 g	BSA
	700 µl	Horse serum
	2 ml	0.1M PBS
	17.3 ml	Distilled water
Hydrochloric Acid (1M)	0.5 ml	Hydrochloric Acid (37%)
	4.5 ml	Distilled water
Paraformaldehyde (16%)	160 g	Paraformaldehyde powder
(pH 7)	1 L	Distilled water
PBS (0.1M) (pH 7.4)	70.1 g	Sodium Chloride
	4.4 g	Sodium dihydrogen Orthophosphate
	12.8 g	Di-sodium hydrogen Orthophosphate

	2 g	Potassium Chloride
Phosphate Buffer (0.2M)	7.41 g	Monosodium Phosphate Monohydrate
	39.2 g	Disodium Phosphate heptahydrate
	1 L	Distilled water
PBS sucrose (pH 7.4)	375 g	Sucrose
	0.25 g	Sodium Azide
	2.5 L	0.01M PBS
Safranin-O solution	0.4 g	Safranin-O
	400 ml	Distilled water
Sodium Acetate (0.1M)	5.64 g	Sodium Acetate Trihydrate
	3.51 ml	Glacial Acetic Acid
	1 L	Distilled water
Sodium Acetate (0.2M)	25.77 g	Sodium Acetate Trihydrate
	0.6 ml	Glacial Acetic Acid
	1 L	Distilled water
Sudan Black B (1%)	1g	Sudan Black
	100ml	70 % ethanol (IMS)
Weigert's Haematoxylin		
Reagent A	2 g	Haematoxylin
	200 ml	Ethanol (IMS)
	10 ml	Distilled water
Reagent B	8 ml	Ferric chloride solution (2.9g in 19ml distilled water)

Weigert's Haematoxylin is made by mixing together an equal amount of Reagent A with Reagent B

Zamboni's fixative (pH 7.3)	250 ml	Paraformaldehyde solution (16%)
	150 ml	Saturated Picric Acid
	500 ml	0.2M phosphate buffer
	100 ml	Distilled water